

AD-A087 858

WILLIAMS COLL WILLIAMSTOWN MASS
COASTAL STORM MODEL.(U)
APR 76 W T FOX, R A DAVIS
TR-14

F/O 4/2

N00014-69-C-0151
NI

UNCLASSIFIED

1 of 2

2007-08-28

①

B. S.

13. 2. 1961

ADA 087858



✓
WITH *2/1/1948*

Approved for public release;
Distribution is unlimited.

DGC FILE COPY,

COASTAL STORM MODEL

by

William T. Fox

and

Richard A. Davis, Jr.

Technical Report No. 14, April 30, 1976

of

ONR Task No. 388-092/10-18-68(414)

Contract N00014-69-C-0151 ✓

Office of Naval Research



Williams College

Williamstown, Massachusetts

This report has been made possible through support and sponsorship by the United States Department of the Navy, Office of Naval Research, under ONR Task Number 388-092, Contract N00014-69-C-0151. Reproduction in whole or in part is permitted for any purpose by the United States Government.

DISTRIBUTION STATEMENT A

Approved for public release;
Distribution Unlimited

ABSTRACT

A mathematical simulation model of a coastal storm has been programmed to forecast or hindcast wave and longshore current conditions at a coastal site. Storm parameters for the model are based on the size, shape intensity and path of the storm as derived from weather maps. An elliptical form is used to model the size and shape of the storm which are controlled by varying the length and orientation of the major and minor axes. Storm intensity is a function of the barometric pressure gradient which is modeled by an inverted normal curve through the storm center. The storm path is based on actual storm positions for the hindcast mode, and on projected positions assuming constant speed and direction for the forecast mode. The location, shoreline orientation and nearshore bottom slope provide input data for each coastal site.

For each storm position, the geostrophic wind speed and direction are computed at the shore site as a function of barometric pressure gradient and latitude. The geostrophic wind is converted into surface wind speed and direction by applying corrections for frictional effects over land and sea. The surface wind speed, fetch and duration are used to compute the wave period, breaker height and breaker angle at the shore site. The longshore current velocity is computed as a function of wave period, breaker height and angle and nearshore bottom slope.

The model was tested by comparing hindcast output with observed data for several coastal locations. Forecasts were made for actual storms and for hypothetical circular and elliptical shaped storms.

Accession For	
NTIS GRA&I	<input checked="" type="checkbox"/>
EDC TAB	<input type="checkbox"/>
Unannounced	<input type="checkbox"/>
Justification	
By	
Distribution/	
Availability Codes	
Dist	Avail and/or special
A	

TABLE OF CONTENTS

INTRODUCTION.....	1
Previous Work.....	2
COMPUTER PROGRAMS - COASTAL STORM MODELS.....	5
Program STORM.....	5
Main Program - Input and Output Options.....	6
Subroutine LOCAT.....	11
Subroutine ELIPS.....	14
Subroutine WIND.....	17
Subroutine DECAY.....	24
Subroutine ETIME.....	25
Subroutine FETCH.....	27
Subroutine WAVES.....	33
Subroutine TIDES.....	36
Subroutine SURF.....	39
Subroutine ENRGY.....	43
Subroutine ARCTA.....	43
HINDCAST ANALYSIS WITH COASTAL STORM MODEL.....	44
Hindcast Tests of Models.....	44
Stevensville, Michigan, July 1969.....	44
Additional Hindcast Examples.....	49
FORECAST ANALYSIS WITH COASTAL STORM MODEL.....	54
Short-term Forecasts.....	54
Circular Storm Test.....	54
Barometric Pressure.....	58
Wind Speed and Direction.....	60
Wave Period and Breaker Height.....	64
Breaker Angles and Longshore Current Velocity.....	65
Elliptical Storm Test.....	71
CONCLUSIONS.....	79
REFERENCES CITED.....	80
APPENDIX A - Coastal Storm Programs.....	84
APPENDIX B - Hindcast Storm Data and Output.....	99
APPENDIX C - Forecast Storm Data and Output.....	115

LIST OF FIGURES

Figure 1.	Location map of field sites designated by project year.....	3
2.	A. Map coordinate system (X-Y) for locating storm center and shore site, and B. Storm coordinate system (X1-Y1) with origin at storm center and X axis parallel to the shore.....	13
3.	Location of the shore site (X1,Y1) within a storm ellipse (AB) and on a minor ellipse (A1,B1).....	15
4.	Orientation of the frictional force near the surface of the earth (Godske, et al, 1957, p. 453).....	19
5.	Angle between surface and geostrophic winds and ratio of surface to geostrophic wind speed.....	23
6.	Case 1 - storm fetch when the distance from center of storm X is less than 1/3 storm radius, R.....	29
7.	Case 2 - storm fetch when the distance from center of storm X is less than 0.4444 and greater than 1/3 storm radius, R.....	30
8.	Case 3 - storm fetch when the distance from center of storm X is greater than 0.4444 storm radius, R.....	31
9.	Deepwater wave forecasting curves as a function of wind speed, fetch length and wind duration based on the S.M.B. method.....	35
10.	Observed and hindcast curves for barometric pressure, wind velocity, longshore current and breaker height at Stevensville, Michigan, July 26-30, 1969.....	47
11.	Observed and hindcast curves for Holland, Michigan, July 3-5, 1970.....	50
12.	Observed and hindcast curves for Holland, Michigan, July 18-20, 1970.....	51
13.	Observed and hindcast curves for Sheboygan, Wisconsin, July 16-18, 1972.....	52
14.	Observed and hindcast curves for Sheboygan, Wisconsin, July 22-26, 1972.....	53
15.	Map of storm tracks and time-distance plot of barometric pressure for a circular storm.....	57

Figure 16.	Time-distance plot of barometric pressure and pressure profiles 200 km north, over the site, and 200 km south of the site.....	59
17.	Time-distance plot of surface wind speed and three profiles of wind speed in a circular storm.....	59
18.	Time-distance plots of A - surface wind speed, B - wind direction, C - onshore wind, and D - alongshore wind in a circular storm.....	63
19.	Time-distance plot of breaker height and three profiles of breaker height in a circular storm.....	67
20.	Time-distance plot of longshore current and three profiles of longshore current in a circular storm.....	67
21.	Time-distance plot of A - wave period, B - breaker height, C - breaker angle, and D - longshore current in a circular storm.....	69
22.	Time-distance plot of barometric pressure in an elliptical storm.....	73
23.	Time-distance plot of A - surface wind speed, B - wind direction, C - onshore wind and D - alongshore wind in an elliptical storm.....	75
24.	Time-distance plot of A - wave period, B - breaker height, C - breaker angle and D - longshore current in an elliptical storm.....	77

ACKNOWLEDGEMENTS

We would like to acknowledge the cooperation and financial assistance of the Geography Programs, Office of Naval Research. We would also like to express our appreciation to the 30 undergraduate and graduate students from Williams College, University of South Florida, Western Michigan University, University of Texas and Oregon State University who participated in various aspects of the field projects which provided a foundation for the coastal storm model.

Thomas Getz of Williams College developed some of the sub-routines and provided significant input in the theory and application of the computer simulation model. Douglas Rosen of the University of South Florida assisted in drafting several of the illustrations. Annie Laliberte typed and proofread the manuscript.

COASTAL STORM MODEL

INTRODUCTION

Coastal storms which provide a combination of high winds, pounding waves and rapid longshore currents are a major cause of destructive erosion along beaches and cliffs. Beaches which are generally composed of sand or cobbles are subject to sudden changes during storms. During one storm at Chesil Bank near Abbotsbury, England, the crest of a shingle beach was cut back 1.53 meters in 3 hours (Lewis, 1931). During a severe storm in July 1969 at Stevensville, Michigan, the beach and bluff were eroded back over 5.5 meters when the waves reached a height of 2 meters (Fox and Davis, 1970b). On the Oregon coast, a beach was stripped of a 2 meter thick blanket of sand and the wave cut terrace was exposed when the waves reached heights of 8 meters during late November storms (Fox and Davis, 1974).

For any operation involving the coastal zone, it is essential to make predictions of wave and current conditions during a coastal storm. General wave forecasts on a worldwide grid are available from the National Weather Service and Fleet Numerical Weather Center. These forecasts provide accurate predictions of wave conditions on the open ocean, but do not provide detailed enough predictions for the coastal zone. Therefore, a computer simulation model was developed to fill the gap between wave predictions on the open ocean and surf predictions along the coast.

The coastal storm model utilizes an ellipse to simulate a map of barometric pressure. The shape of the storm can be modified by varying the length and orientation of the major and minor axes of the ellipse. The intensity of the storm is controlled by increasing or decreasing the range in barometric pressure. The actual storm track and dimensions are read in as data for hindcasting wave and current conditions. For making forecasts, the size, shape and intensity of the storm are provided as input data for the model. In forecasting, the storm path is plotted by assuming a constant azimuth and velocity.

One of the initial steps in developing a coastal storm model is determination of the barometric pressure gradient at any point on the ground surface under the storm. The pressure gradient is then used in conjunction with the latitude to calculate the geostrophic wind speed, which in turn is used to compute the surface wind speed, wave height and longshore current velocity. In the model, it is assumed that a profile of barometric pressure along the major or minor axis of the storm ellipse can be represented by an inverted normal curve. By rotating the normal curve around the ellipse and taking the derivative, it is possible to calculate the pressure gradient at any point on the ground. From that point on, conventional methods are employed for determining the geostrophic wind speed, surface wind speed, wave height and longshore current velocity.

PREVIOUS WORK

The coastal storm model is based on a series of detailed field studies which extended from 1969 through 1975. The studies included the analysis and synthesis time-series data on barometric pressure, wind speed and direction, wave period and height and longshore current velocity for 15 days to 1 year. Topographic profiles across the beach and nearshore area were used to construct topographic maps and maps of erosion and deposition. The sites in the study are plotted by date in Figure 1 and included in the following list along with references for each study.

1969	Stevensville, Michigan	Fox and Davis, 1970a, 1970b
1970	Holland, Michigan	Fox and Davis, 1971a Davis and Fox, 1971
1971-2	Mustang Island, Texas	Davis and Fox, 1972c Davis and Fox, 1975
1972	Sheboygan, Wisconsin	Fox and Davis, 1972
1973	Cedar Island, Virginia	Davis and Fox, 1974a
1973-4	South Beach, Oregon	Fox and Davis, 1974
1974	Zion, Illinois	Davis and Fox, 1974b
1974	South Haven, Michigan	Davis and Fox, 1974b
1975	Plum Island, Massachusetts	

The models have evolved from a geometric model called the area-time prism (Davis and Fox, 1972a) through a conceptual model (Davis and Fox, 1972b) to a process-response model for Lake Michigan (Fox and Davis, 1971b and 1973). The simulation model developed for Lake Michigan was limited to the local geographic area where the storms moved directly onshore to the north of the study area. The proposed coastal storm model is an outgrowth of the earlier model but is more generalized with broader application under a wider range of storm conditions and shoreline orientations.

Several different types of computer models have been proposed for the coastal environment. Probabilistic models were developed to reproduce gross coastal features such as a recurved spit on the south coast of England (McCallagh and King, 1970) and the Mississippi River Delta (McCammon, 1971). A markov process was used to simulate the sequence of bar formation and migration across a beach

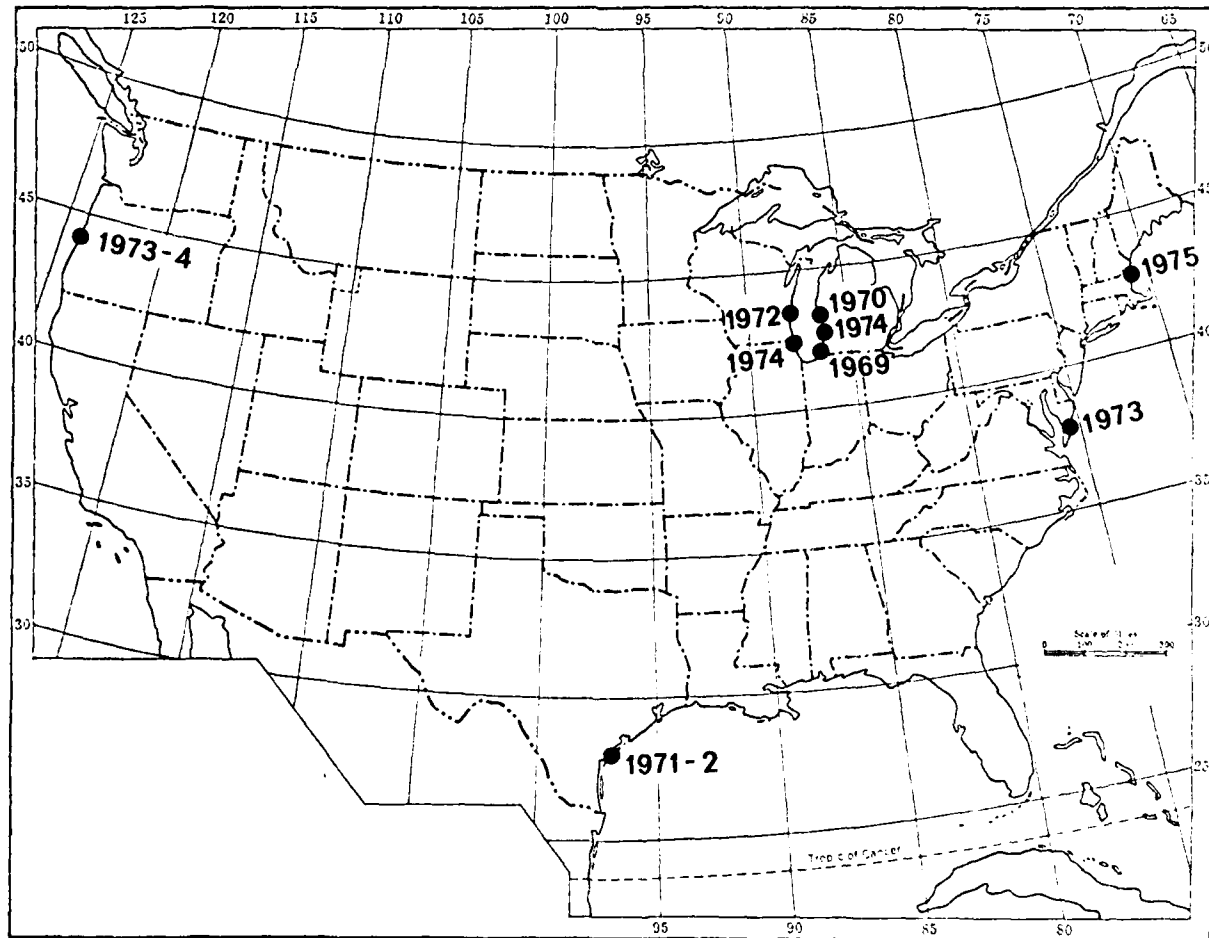


Figure 1. Location map of field sites designated by project year.

(Sonu and van Beek, 1971). A deterministic model resembling a wave tank experiment was proposed to simulate the interaction between a prograding delta and waves (Komar, 1973). A statistical model with a relatively simple beach topography to compute breaker height, longshore current velocity and wave setup (Collins, 1971) was followed by a more deterministic approach to model the nearshore circulation patterns employing monochromatic waves and more complex beach topographies (Noda, et al, 1974). An explicit finite difference model for predicting time-dependent, wave induced nearshore circulation was developed by Birkemeier and Dalrymple (1976).

On a larger scale, Resio and Hayden (1973) proposed an integrated storm model which combines three scales of atmospheric motion, large scale, synoptic scale and small scale into an estimation of a winter wave-surge climate for the mid-Atlantic coast. At a similar scale, Goldsmith, et al (1974) developed a wave climate model for the mid-Atlantic coast by using Dobson's (1967) wave refraction program to project offshore waves into the coastal zone.

The coastal storm model proposed in this report provides a link between the large-scale, seasonal wave-climate models and the dynamic surf zone models. By tracking a storm across a shoreline, the wave parameters which are output from the storm model furnish input for the surf zone models. Therefore, the proposed storm model could be combined with other computer models to provide an integrated process model for the coastal zone.

COMPUTER PROGRAMS - COASTAL STORM MODEL

Program STORM

Program STORM is a mathematical simulation model which has been programmed for the computer to forecast or hindcast wave conditions at a coastal site during a storm. The actual storm as represented by the isobars on a weather map is modeled by an elliptical storm with major and minor axes at right angles and passing through the center of the low. The size, shape, intensity and path of the storm as determined from weather maps are used to generate the surface wind pattern, wave height and period, and longshore current velocity as the storm moves across the coast.

The computer program is divided into a main program, STORM, and a series of 11 subroutines. The main program is used to read in the data, call the various subroutines for computing the wind, wave and current conditions, print out the predictions at one hour intervals. All the input and output is handled by the main program while the calculations are carried out by the various subroutines. In this way, any portion of the model can be independently tested by using a small main program to call each subroutine individually. Therefore, if any problem arises in the main program, it can be narrowed down to a particular subroutine, and that subroutine can be tested under a variety of conditions without using the main program. Also, if a portion of the simulation model is to be incorporated into another program, any of the individual subroutines can be removed and used separately with the appropriate calling arguments.

The theory and mechanics of the program will be explained in detail starting with the MAIN program and proceeding through each of the subroutines as they are called by the MAIN program. The program was written in FORTRAN IV for an 8k IBM 1130 at Williams College. A full listing of the programs with appropriate comment cards is included in Appendix A. A second version of the MAIN program was written for the Xerox 530 which includes a graphics package for a 29 inch plotter. The graphics package is used to plot barometric pressure, surface wind, onshore wind, alongshore wind, breaker height, wave period and longshore current.

Main Program - Input and Output Options

The main program is used to read the input data for the storm and shoreline conditions, call the various subroutines and print out the results at one hour intervals. A listing of the input cards is included in Appendix I with a description of each of the input variables. The program is dimensioned to make predictions up to 130 hours or 5 days and 10 hours. If a longer prediction is desired, it is necessary to increase the dimension of U(130) and V(130) to the required number of hours. In the model, 130 hours was selected because of core limitations on the 8k IBM 1130. For most of the storms, the 130 hour limitation was not a serious constriction, however, a larger dimension statement would be helpful in some cases.

The first two data cards are used to read in the title, starting time, date and input/output options. The title used for the location of the shore site can be up to 80 spaces long filling card 1. On the second card, the starting hour, ISTRT, is included in columns 1 and 2 followed by the date, DAY, in columns 3 to 22. The starting time is read in as an interger and must be right justified. If ISTRT is read in as 0, the program will terminate. For the input option, INAUT, in column 23, a 0 is used for metric units and a 1 is used for nautical units including nautical miles, knots, and feet per second. The output option, NAUT, in column 24 is separate from the input option but uses the same code, 0 for metric units and 1 for nautical units. Although metric units are becoming the standard and are now required for scientific reports, it may be desirable at times to have the input or output in nautical units. With separate input and output options, it is possible to have the input in metric or nautical units and convert to the other units with the output.

The first 3 columns of card 3 are used to select the major options for the program. For the first option, INOPT, a 1 in column 1 will call the hindcasting mode, while a 2 in column 1 will call the forecasting mode. The hindcasting mode is used when storm positions are available at six hour intervals. The hourly positions of the storm are determined by a linear interpolation between the 6-hour positions. For the forecasting mode, the initial position of the storm along with a constant velocity and azimuth are used to calculate successive positions at 1-hour intervals. The variables for the hindcasting and forecasting modes are read in on card 6. The second option on card 3 is the tide prediction option, IFTID. If a 0 is punched in column 2, the tide prediction option is suppressed and card 4 is not included in the data set. The tide option is omitted for a non-tidal body of water, such as the Great Lakes. Where tide data are available from the tide tables or from observations, a 1 is punched in column 2, and the tide data are included on card 4. The longshore current equation for the simulation run is selected in option 3, LSCOP. Four different longshore current equations are included, (1) Fox and Davis (1972), (2) Longuet-Higgins (1970), (3)

Coastal Engineering Research Center (1973), and (4) Komar and Inman (1970). The longshore current equations are called in subroutines SURF and their differences will be discussed under that subroutine.

The number of storm positions, NX, are punched in columns 4 to 6 of card 3, for 6-hour intervals in the hindcasting mode, and for 1-hour intervals in the forecasting mode. For example, if the hindcasting mode is used, and 3 days of data are included, the initial position and 4 positions for each day would give a total of 13 for NX. For the forecasting mode, a 3 day forecast would use a 73 for NX, 1 for the initial position, and 72 for the 72 hour forecast. The maximum value for NX is 22 for the hindcast mode and 130 for the forecast mode.

The average basin fetch in kilometers, BNFCH, is punched in columns 7 to 12 on card 3. The average basin fetch is used as the limiting fetch in determining the wave height and period from the wind speed. Where the basin fetch is smaller than the maximum storm axis, the waves are fetch limited. However, where the fetch is significantly larger than the storm size, the average basin fetch will not be a limiting factor in determining the wave parameters. The basin fetch is considered in an offshore direction from the shore site. In the case of a large ocean, the approximate width of the ocean can be used as the basin fetch.

In columns 13 to 17 of card 3, the time interval between storm positions TINT is normally set at 1.0. The time interval refers to the printout spacing for the forecast modes. For the hindcast mode, the values are read in at 6-hour intervals, and the results are printed out at 1-hour intervals.

The minimum barometric pressure in millibars, PMIN, taken at the center of the low pressure cell is punched in columns 18 to 24 on card 3. Usually, the minimum barometric pressure is interpolated within the smallest isobar. Thus, if the smallest isobar is 1004, and the isobar spacing is 4 millibars, the minimum pressure would be estimated at 1002 millibars. The pressure at the largest encircling isobar, PMAXR, is used to determine the intensity of the storm. If the storm is circular or oval shaped, the largest isobar which encloses the storm center is used for PMAXR and punched in columns 25 to 31 of card 3. If, however, the storm has a wave form extending down from the north, a line is drawn along the storm path through the storm center to the margins of the storm. The largest isobar which the line crosses on both sides of the storm is then considered the largest encircling isobar, PMAXR. In the program, the largest encircling isobar is defined as 2 standard deviations away from the center of the storm. Therefore, the total storm radius would be 1.5 times the radius of the largest encircling isobar. The

pressure range would be 1.145 times the range within the largest encircling isobar. The latitude at the shore site, SLAT, punched in columns 32 to 36 is used in subroutine WIND to compute the geostrophic wind speed.

The geographic size of the storm is defined in terms of an ellipse with a major half-axis and minor half-axis corresponding to radius of a circle. The major half-axis, AR, of the storm ellipse measured when the storm is closest to the study site is punched in columns 37 to 42. If the storm ellipse is asymmetrical, the longest half-axis on the side toward the shore location is used as the major half-axis. The minor half-axis, BR, is measured at right angles to the major half-axis through the center of the low. The major and minor half-axes are measured from the center of the low to the largest encircling isobar PMAXR. The minor half-axis, BR, is punched in columns 43 to 48 on card 3.

The orientation of the major half axis EAZ is punched in columns 49 to 54 of card 3. The orientation of the major axis is measured in degrees from true north to the northern end of the major axis ranging from -90° on the west to 90° on the east. For a front or trough related to a low pressure system, the major axis is usually several times longer than the minor axis and the orientation of the major axis lies along the line of the front. In a circular or oval storm, the major axis is usually 1 to 1.5 times as long as the minor axis. The major and minor half axis are measured when the center of the storm is at its nearest position to the shore study site.

Variables for hourly tide prediction are contained on card 4. The spring tide range in meters, ST, is punched in columns 0 to 5 and the neap tide range, TN, in columns 6 to 10. The spring and neap tide ranges and the time of the last spring high tide are available in the tide tables which are published annually by N.O.A.A. In making the hourly predictions for the model, it is necessary to punch the number of days since the last spring tide, TDAY, in columns 11 to 15. The hour of the last spring high tide, THR, preceding the start of the run is punched in columns 16 to 20. The tidal form number, FN, punched in columns 21 to 25 is used to reproduce a semi-diurnal, mixed-semidiurnal, mixed-diurnal or diurnal tide with the right spacing and tidal beat. The nearshore bottom slope at low tide, SLPLO, is punched in columns 26 to 32 and the slope at high tide, SLPHI, is punched in columns 33 to 39. The nearshore bottom slope which varies with tidal elevation is used for computing long-shore current velocity in subroutine SURF. The preferred method of determining bottom slope is to fit a linear surface to the nearshore map at low tide, and repeat the process at high tide. The linear slope should extend to a depth of at least twice the breaker height. For the high tide range, the foreshore slope and low tide terrace should be included in the slope calculation. Where it is not possible to fit a linear surface because of lack of data, it is possible

to get an approximation of the nearshore slope by measuring the depth at some predetermined distance from the shore at low tide and at high tide. By dividing the depth by the distance, a good approximation of nearshore slope can be estimated for low and high tides. The nearshore slope is an initial factor for the determination of the longshore current velocity, so care should be taken in estimating nearshore slope at low and high tide. It also should be pointed out that nearshore bars have a significant influence on nearshore currents and must be considered in making an estimate of the nearshore slope. The final variable on the tide prediction card is the mean tide level, TMEAN, which is the difference between mean sea level and mean low tide as reported in the annual tide tables.

Data for the shore site location including geographic coordinates, onshore direction, average bottom slope and offshore island option are punched on card 5. The shore site location is given in a X and Y coordinate system where the X-axis runs east-west with positive X in the east direction, and the Y-axis north-south with positive Y in the north direction. The X-Y coordinate system is measured in kilometers with the origin located at the southwest of the study site. In practice, a piece of 10 to the inch rectangular grid graph paper is laid over the weather map with the Y axis parallel to the longitude line nearest the study site. The origin of the graph paper is placed several inches to the southwest of the shore location so that the X-axis runs east-west and the Y-axis runs north-south parallel to the latitude and longitude lines through the study site. The X and Y coordinates are read off the map in inches and converted to kilometers before they are used in the program. The X coordinate, ULOC, is punched in columns 1 to 7 and the Y coordinate, VLOC, is punched in columns 8 to 14 on card 5.

The orientation of the shoreline given by the onshore azimuth, SHAZ, and the average nearshore bottom slope, SLOPE, are punched on columns 15 to 21 and 22 to 38 respectively. The onshore direction measured in degrees in a clockwise direction from north is used to give the orientation of the shoreline. Since the storm is considered a regional feature, it is necessary to give the regional orientation for the shoreline. An east-west shoreline with land to the north would give a 0 azimuth. If a shoreline is running north-south with the land to the east and water to the west, the shoreline azimuth would be 90 degrees. Similarly, if the shoreline is running north-south with the land on the west and the water on the east, the onshore azimuth would be 270 degrees.

An option is available with the program for an offshore island which is not influenced by a large continental land mass. When a 0 is punched in column 30 of card 5, the offshore island option is suppressed and a normal continental coast or barrier island is assumed.

For a coast backed by land, land corrections are used in computing the surface wind speed when the wind blows offshore. Therefore, when the island option is used and a 1 is punched in column 30 of card 5, the wind is assumed to be blowing from the sea in all directions and the land correction is not used. For a barrier island which lies roughly parallel to the coast, the island option is not used because an offshore wind blows over land for a long distance before it hits the lagoon and barrier island.

The storm positions for the hindcasting and forecasting modes are punched on card 6. For option 1, the hindcasting mode, the X and Y coordinates are punched in columns 1 to 7 and 8 to 14 respectively. The X and Y coordinates are from the rectangular grid discussed for the shore site location on card 5. The coordinates for the storm are given for the initial storm position and at successive 6 hour intervals, with one pair of coordinates per card. The number of pairs of coordinates is specified by NX, the number of storm positions on card 3. For the forecasting mode, option 2, the storm positions are determined at 1 hour intervals from the storm velocity, storm azimuth and initial X and Y coordinates. The storm velocity, SVEL, in columns 1 to 7, is given in kilometers per hour. Reasonable storm velocities would vary from about 25 to 75 kilometers per hour for a slow to fast moving storm. In the forecasting mode, it is not possible to vary the storm velocity, so the initial storm velocity must be maintained for the entire forecast run. The storm azimuth or path is measured in degrees clockwise from north. As with the storm velocity, it is not possible to vary the storm azimuth in the middle of a forecast run. An azimuth of 0 degrees would have the storm moving due north, and a 90 degree azimuth would have the storm heading east. In the forecast mode, the initial X and Y coordinates for the storm are punched in columns 15 to 21 and 22 to 28 respectively. It is possible to make a map for each predicted variable by making a series of runs with different initial coordinates.

It is possible to run a series of models for different coastal situations by including a new data set for each model starting with the title card. To terminate the run, two blank cards are included at the back of the data deck. Since the second card of the new data set is blank, ISTRT is read in as 0 and the program will finish.

Different versions of the main program are used for making forecasts directly from the console, and for printing a map using the forecast mode. Listing of the programs are included in Appendix A along with explanations of the input options.

Subroutine LOCAT

As a storm moves across a coastline, subroutine LOCAT is used to determine the position of the coastal site relative to the storm center for each increment of time. In preparing the input data for the program, the location of the coastal site and a sequence of storm positions are plotted on a rectangular grid referred to as the map coordinate system. For the map coordinate system, the X axis points east, the Y points heading north and the origin is located to the southwest of the initial storm position. When the shore location and storm positions are plotted on a weather map, the coordinates are measured in kilometers or nautical miles, whichever are the most convenient units for the project.

In computing the geostrophic wind speed, it is necessary to determine the gradient in barometric pressure at the coastal site. Therefore, a storm coordinate system is established with the origin at the center of the storm, the X1 axis parallel to the shore, the Y1 axis perpendicular to the shore, and the positive Y1 direction heading onshore. When facing the land from the sea, the positive X1 direction is along the shore to the right, and the negative X1 direction is to the left (Figure 2). Each time the storm moves, the origin of the storm coordinate system is also moved to the new location for the center of the storm. However, the orientation of the X1 and Y1 axes remains the same with the X1 axis parallel to the shore and the Y1 axis at right angles to the coast.

In the storm model, the units for the X1, Y1 coordinate system are converted from kilometers or nautical miles to storm radii by dividing by the radius of the storm. In an elliptical storm, the length of the major half axis is used in place of the storm radius.

In subroutine LOCAT, ULOC and VLOC are the map coordinates for the coastal site, and UST and VST are the map coordinates for the storm center (Figure 2). Vectors are computed parallel to the X axis ($U = UST - ULOC$) and parallel to the Y axis ($V = VLOC - VST$). The resultant vector ($Z^2 = U^2 + V^2$) gives the map distance from the storm center to the coastal site. The counterclockwise angle (ANG) between the positive X axis and the Z vector is computed by the arc-tangent subroutine ARCTA. The onshore azimuth (SHAZ) is the onshore direction normal to the shoreline measured in a clockwise direction from north. The angle A ($A = ANG - SHAZ$) is used for converting coordinates from the map system to the storm system. The shore position is then determined in the storm coordinate system for distances along the X1 axis ($X1 = -Z * \cos(A)$) and along the Y1 axis ($Y1 = Z * \sin(A)$).

A third coordinate system is set up for dealing with an elliptical storm. In the elliptical coordinate system, the P axis lies along the major half-axis and the Q axis lies along the minor half-

axis. The distances, P and Q, within the storm ellipse are used to locate the shore site relative to the center of the ellipse. The orientation of the storm ellipse is given by the ellipse azimuth (EAZ) which is the azimuth of the major half-axis plus or minus 90 degrees from true north.

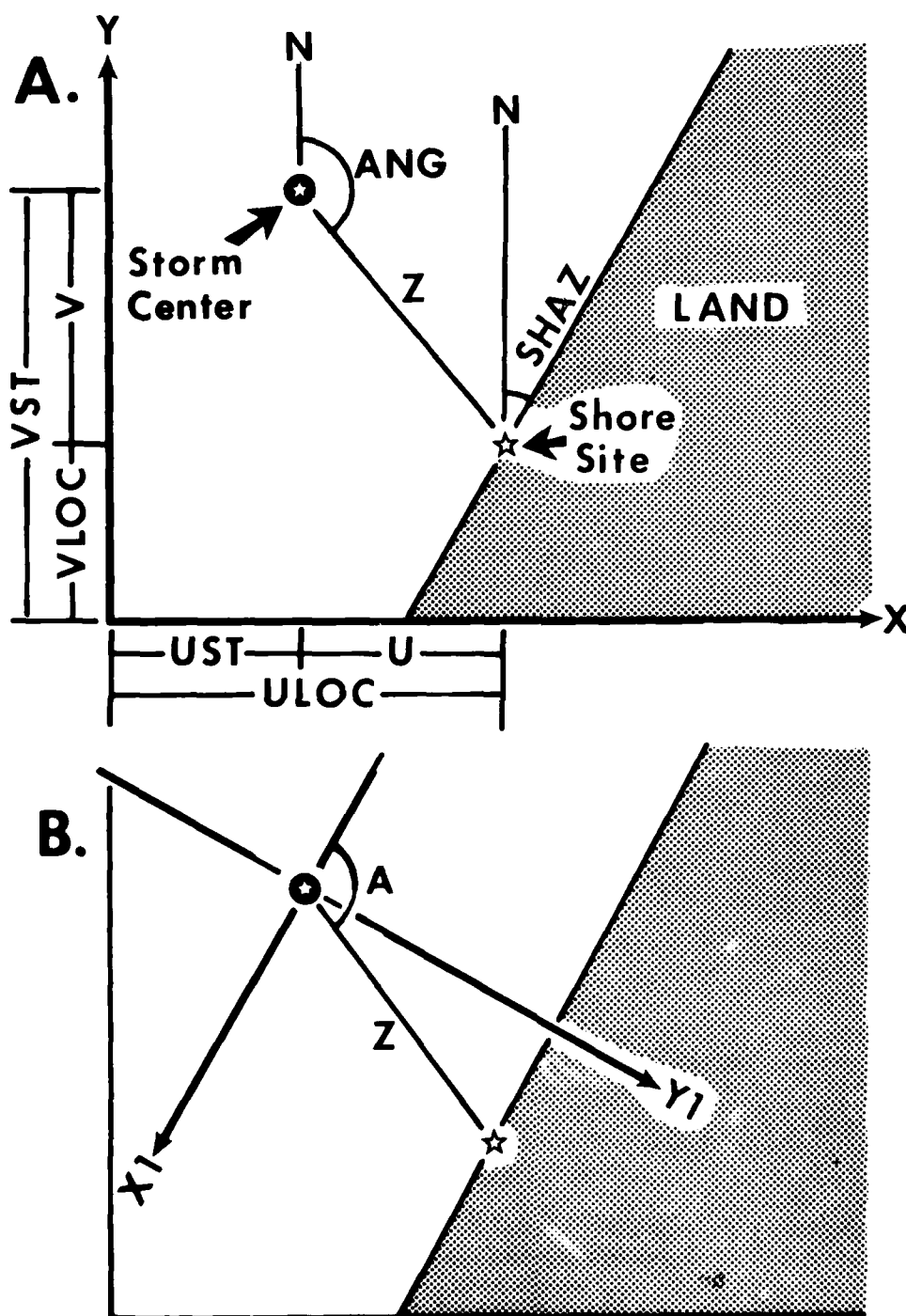


Figure 2. A. Map coordinate system (X-Y) for locating storm center and shore site, and B. Storm coordinate system (X_1-Y_1) with origin at storm center and X axis parallel to the shore.

Subroutine ELIPS

The wind angle and barometric pressure gradient at any position within an elliptical storm are determined by subroutine ELIPS. A is the length of the major half axis, B is the length of the minor half axis and EAZ is the angle from true north to the path of the major half axis. The shore site is located at point X₁, Y₁ within the storm ellipse. To determine the pressure gradient, a second ellipse is plotted with axes A₁ and B₁ which passes through point X₁, Y₁. The second ellipse has the same axial ratio B/A and the same origin as the storm ellipse (Figure 3). The tangent to an ellipse is defined by equation 1.

$$\frac{X_1 X}{a^2} + \frac{Y_1 Y}{b^2} = 1 \quad (1)$$

therefore, the intersection of the tangent to the ellipse with the X axis can be found by equation 2.

$$X = \frac{a^2}{X_1} - \frac{a^2 Y_1 Y}{b^2 X_1} \quad (2)$$

Equation 3 is used to generate the line normal to the tangent

$$X = X_0 + \frac{b^2 X_1}{a^2 Y_1} Y. \quad (3)$$

The intersection of the line normal to the tangent and the A axis is found by equation 4.

$$X_0 = X - \frac{b^2 X_1}{a^2 Y_1} Y \quad (4)$$

which in terms of the point X₁, Y₁ would be

$$X_0 = X_1 - \frac{b^2}{a^2} Y_1 \quad (5)$$

The distance X₀ is measured from the center of the ellipse to the point where the line normal to the tangent through X₁, Y₁ intersects the A axis. The point X₂, Y₂ is the intersection of the line normal to the tangent at X₁, Y₁ and the path of the ellipse.

To determine the gradient of the barometric pressure, it is assumed that the pressure gradient follows a normal curve along

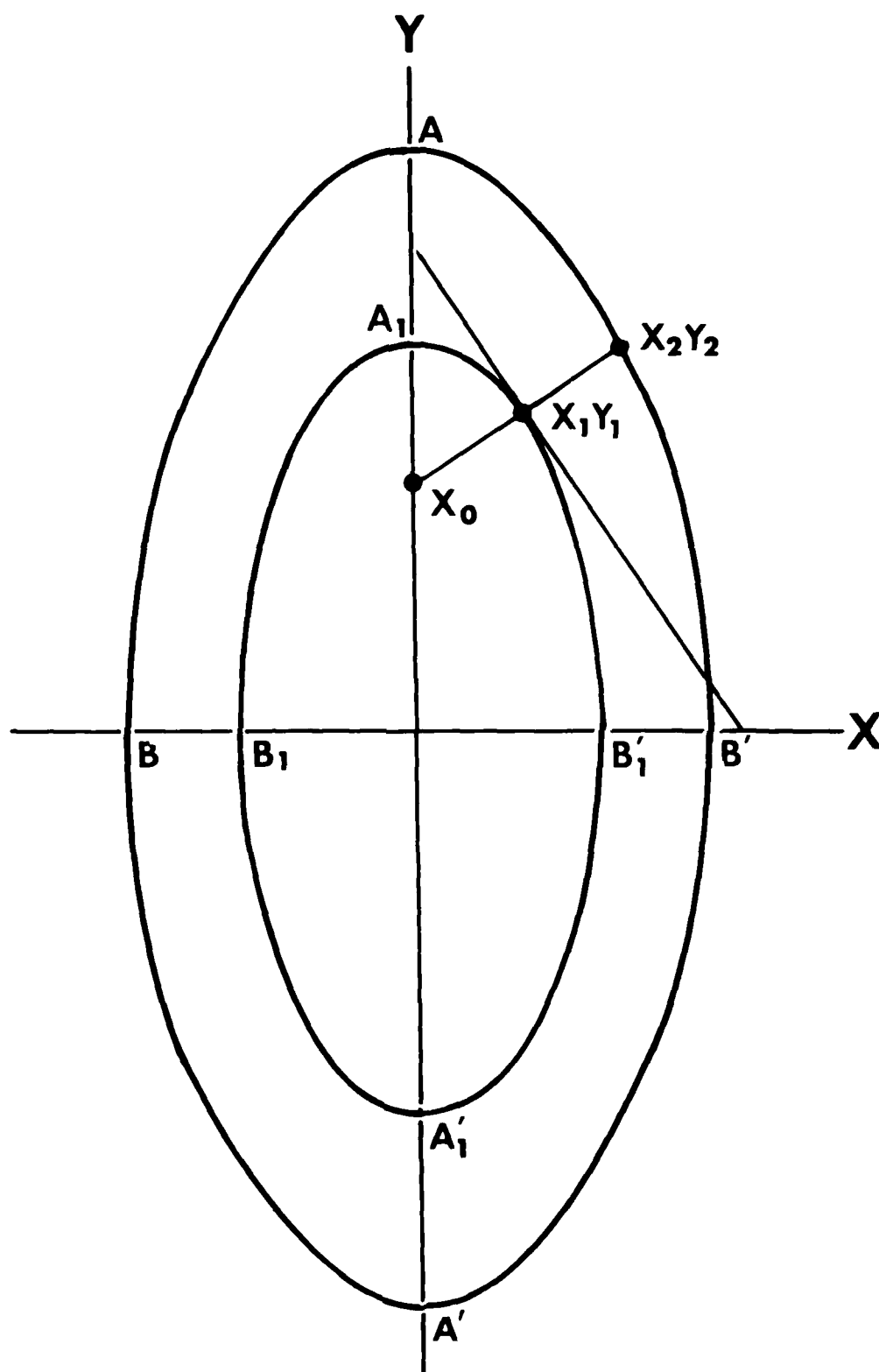


Figure 3. Location of the shore site (X_1, Y_1) within a storm ellipse (AB) and on a minor ellipse (A_1, B_1).

the major axis of the ellipse. P_1 is the barometric pressure at point X_0 along the A axis. The pressure at X_0 is used in determining the pressure gradient normal to the isobar at point X_1, Y_1 . The final pressure gradient calculation is made in subroutine WIND. X_A and Y_A are used to plot the tangent to the ellipse at X_1, Y_1 for determining the wind direction. The wind direction is assumed to be parallel to the tangent to the ellipse at X_1, Y_1 and in a counterclockwise direction around the center of the ellipse.

Subroutine WIND

The geostrophic wind speed and direction for each storm position are computed in subroutine WIND. The equation for geostrophic wind speed V_g is based on latitude and barometric pressure gradient.

$$V_g = \frac{S}{2 \Omega \sin \phi} \frac{\Delta P}{\Delta N} \quad (6)$$

where S is the specific volume, ($779 \text{ cm}^3/\text{gm}$), Ω is the angular velocity, ($7.29 \times 10^{-5} \text{ rad./sec.}$), ϕ is the latitude in degrees, and $\Delta P/\Delta N$ is the barometric pressure gradient normal to the isobar at the shore location (Godske et al, 1957, p. 370). The barometric pressure gradient is computed at right angles to the tangent of the ellipse through the shore site, (point $X1, Y1$). To compute the gradient, a normal curve is constructed perpendicular to the tangent through point $X1, Y1$. The derivative of the normal curve is taken at point $X1, Y1$ to compute the barometric pressure gradient. The geostrophic wind direction is assumed to be parallel to the tangent of the ellipse at point $X1, Y1$ and heading in a counter-clockwise direction around the center of the ellipse. It is assumed that the small ellipses within the storm ellipse are parallel to isobars. Therefore, wind direction can be determined if the geostrophic wind is directed along the isobars with the high pressure to the right and low pressure to the left of the motion in the northern hemisphere. By means of geostrophic wind equations, the wind direction can be estimated with error of less than 10° , and speed with an error of less than 20% (Cole, 1970, p. 185).

An approximate relationship exists between the speed and direction of the surface wind measured at anemometer level and the upper quasi-geostrophic wind. Owing to differences in surface roughness, this relationship varies from one station to another, and also varies at a single station with stability. Thus it is rather difficult to determine the surface wind accurately from the upper quasi-geostrophic wind. Under average conditions, a rough method may be applied which makes use of the horizontal friction force, SR , near the ground (Figure 4). The equation for horizontal motion can be used for computing the friction force at a given station (Godske, 1957, p. 453).

$$sR = \dot{v}_h + s v_h P + 2\omega_z k \times v_h \quad (7)$$

The horizontal component of the wind speed, v_h and the barometric pressure gradient, $s \nabla_h p$, can be measured directly and inserted into the equation. Although it would be possible to determine v_h , the vertical variation in wind speed, it would involve measurements in time and space which would be very laborious and not too reliable. In practice, v_h includes both a convective term and a local term. However, the influence of v_h is small when mean values over relatively large areas are included (Hasselberg and Sverdrup, 1915). Computations of the average of R based on time-series averages of a series of synoptic series of maps was carried out over land (Baur and Phillips, 1938) and over sea (Westwater, 1943). Based on their computations, the frictional force SR is directed backward to the right of the wind v_h , and is proportional to the wind velocity, v_h .

$$sR = bv_h \quad (8)$$

and forms an angle β with $-v_h$ as shown in Figure 4. To make corrections for wind speed and direction over land and sea, the mean values of b and β are: $b = 1.9 \times 10^{-4} \text{sec}^{-1}$, $\beta = 29^\circ$ over land and $b = 0.65 \times 10^{-4} \text{sec}^{-1}$, $\beta = 50^\circ$ over sea (Baur and Phillips, 1938).

Using b and β , a simple diagram has been constructed to show the configuration of forces when $v_h = 0$. The balance of forces in the diagram along v_h and normal to it gives the following equalities with the angle between the geostrophic wind and the surface wind denoted by α .

$$\begin{aligned} s |\nabla p| \sin \alpha &= sR \cos \beta = bv_h \cos \beta \\ s |\nabla p| \cos \alpha &= sR \sin \beta + 2\Omega_z v_h \\ &= bv_h \sin \beta + 2\Omega_z v_h \end{aligned} \quad (9)$$

therefore, by division

$$\cot \alpha = \tan \beta + \frac{2 \Omega \sin \phi}{b \cos^2 \beta} \quad (10)$$

where ϕ is the latitude. Therefore, the angle α between geostrophic wind and the surface wind can be determined directly from the latitude ϕ when b and β are known for a given station.

The ratio between the surface wind v_h and the geostrophic wind v_g can be derived from equations 9 and 10 and are given below according

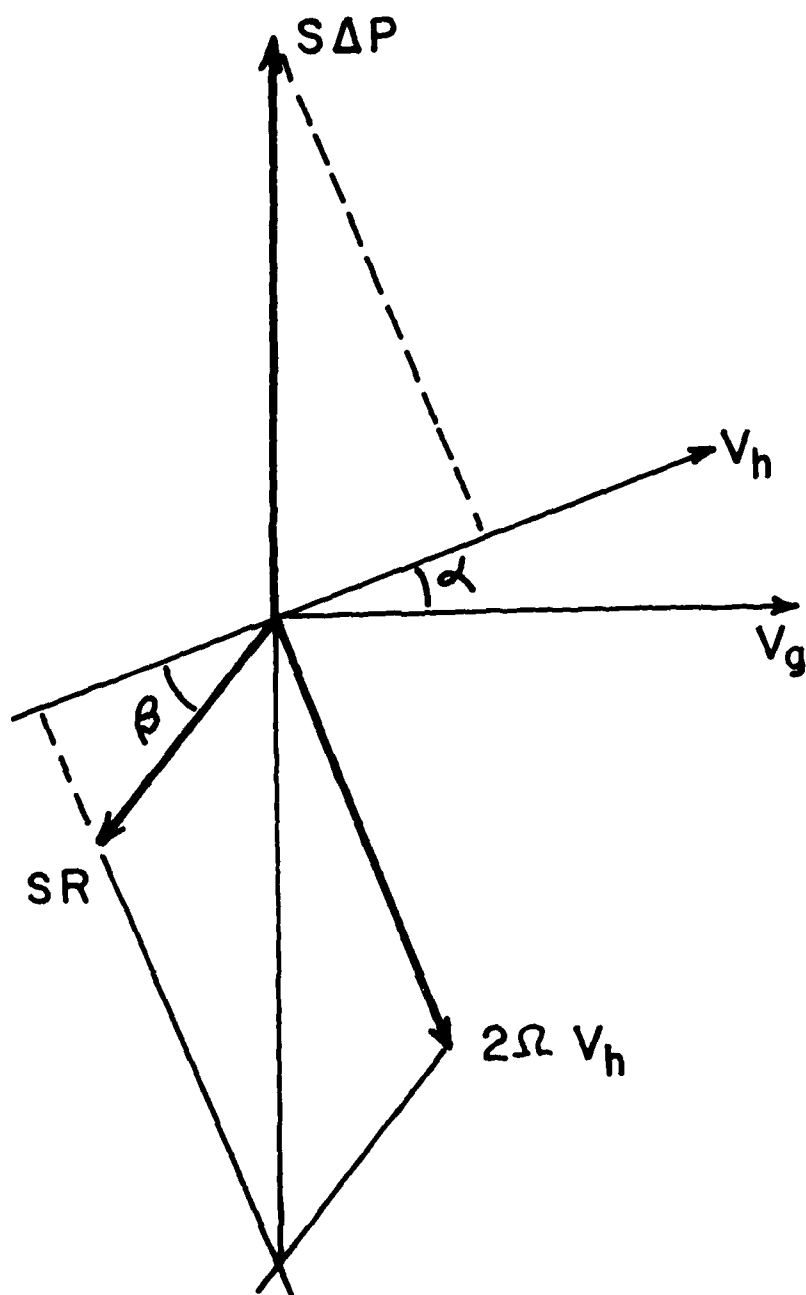


Figure 4. Orientation of the frictional force near the surface of the earth (Godske, et al, 1957, p. 453).

to Godske et al, 1957.

$$\frac{v_h}{v_g} = \frac{v_h}{\frac{s |\nabla p|}{2\Omega \sin \phi}} = \frac{s |\nabla p| \sin \alpha \sin \phi}{b \cos \beta s |\nabla p|}$$

therefore,

$$\frac{v_h}{v_g} = \frac{2 \Omega \sin \phi \sin \alpha}{b \cos \beta} \quad (11)$$

Once the angle α between the surface wind and geostrophic wind has been computed, it can be inserted into equation 11 to compute the ratio between the surface wind and the geostrophic wind over land or sea. Table 1 gives values at different latitudes for α , the angle between surface wind and geostrophic wind, and v_h/v_g , which are plotted in Figure 5. In subroutine WIND, the correction factors for computing surface wind speed and direction are computed following statement 50.

Since the values for b and β are given for wind blowing over land or over sea, intermediate values must be computed for winds blowing along the shore. Winds blowing directly onshore with a wind angle of zero would have values of $b = .000065$ and $\beta = 50$. In this case, the wind is blowing from the sea and the land does not have any frictional effect on the wind. In like manner, if the wind is blowing over the land in an offshore direction, values for the land, $b = .000190$ and $\beta = 20$ are applied. For the transition zones, a cosine transformation is used to compute the intermediate values. Within the transition zone, angle A is computed from 0 to 90° with 0 being land and 90° being sea. The new angle A is used in equations 12 and 13 to compute the transition values for b and β .

$$b = .0001 \cdot (1.275 + .625 (\sin A)) \quad (12)$$

$$\beta = 39.5 - 10.5 \cdot \sin A \quad (13)$$

The computed values for b and β are substituted in equations 10 and 11 to compute the surface wind speed and direction from the geostrophic wind.

The final step in subroutine WIND is to compute the effective wind speed which is carried over into subroutines FETCH and WAVES for determining effective fetch length and wave height. The effec-

tive wind speed is that which will generate waves which will in turn have an effect on the beach. If the wind is blowing directly onshore, the full force of the wind is used in generating waves which will hit the coast. However, if the wind is blowing directly offshore, small waves will be generated in the nearshore area (Resio and Hayden, 1973). Based on empirical observations, onshore winds are about three times as effective in generating local waves as offshore wind (Davis and Fox, 1974 and Owens, 1975). Therefore, a cosine transformation is used in subroutine WIND to compute effective wind speed from the surface wind speed and direction. When the wind is blowing directly onshore, the effective wind is equal to the surface wind. On the other hand, when the wind is blowing along the shore, the effective wind is equal to $2/3$ of the surface wind, and when the surface wind is blowing directly offshore, the effective wind is $1/3$ the surface wind. Although the values for effective wind may be rough in some cases, they seem to give good estimates where comparative wind and wave data are available.

Latitude ϕ	α_L	α_S	$\frac{v_h}{v_g}$ L	$\frac{v_h}{v_g}$ S
0	61	40	----	----
10	55	29	----	----
20	49.5	23	----	----
30	45	19	0.31	0.56
40	42	16	0.38	0.63
50	39	14.5	0.42	0.67
60	37	13	0.46	0.70
70	36	12.5	0.485	0.715
80	35	12	0.495	0.723
90	35	12	----	----

Table 1. The angle between surface wind and geostrophic over land α_L and over sea α_S , and the ratio between surface wind speed and geostrophic wind speed over land and sea for different latitudes ϕ , according to Baur and Phillip (1938, p. 292).

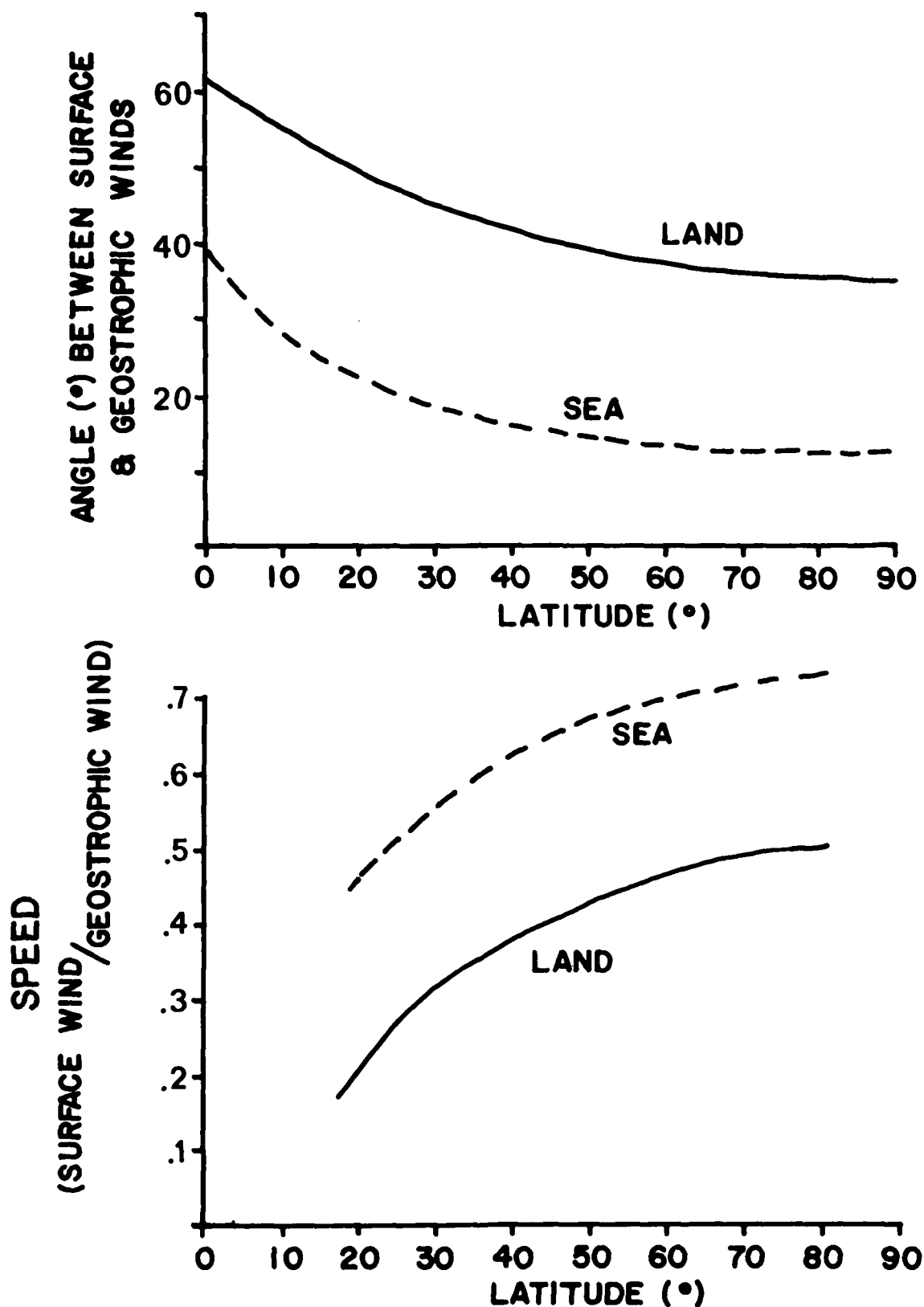


Figure 5. Angles between surface and geostrophic winds and ratio of surface to geostrophic wind speed.

Subroutine DECAY

Subroutine DECAY is used to determine the height of a given wave after it has decayed for a specified length of time. Snodgrass, et al (1966) presented empirical data on the attenuation of selected frequencies which they observed in their study of propagation of ocean swell in the Pacific. In general, they found the attenuation to be large within the limits of the wind area of the storm, and small outside the storm area. The empirical attenuation data were logarithmic coefficients reported in units of decibels per latitude degree of propagation distance. For the range of frequencies 0.06 to 0.08 Hertz, these data fit an attenuation function of the form

$$e^{-2ax} \quad (14)$$

where a is the modulus of amplitude decay in $\text{degree}^{-1} = 0.1151 \beta$, where β is the logarithmic attenuation coefficient in decibels/degree, and where x is the propagation distance in degrees. The logarithmic attenuation coefficient versus frequency was plotted on a graph (Kaufman, 1973), and equation (15) was derived from the line on the graph.

$$\beta = 10 \left(\frac{F-0.06}{0.0324} \right)^{-1} \quad (15)$$

where F is the frequency of the wave being decayed.

The propagation distance x is found by multiplying the wave velocity $1.5606 \cdot T$ (where T is the wave period) times the time interval $TINT$. This distance is then reduced to degrees by multiplying it by the constant value

$$\frac{360^\circ/\text{circle}}{40074\text{km}/\text{circle}}$$

(using the circumference of the earth at the equator). To find the decayed wave height then, the original wave height is multiplied by the attenuation function. This decay factor was tested with several different wave heights, periods, and time intervals, giving very reasonable decay results, but there were no empirical data against which to check the results.

Subroutine ETIME

Subroutine ETIME is used to determine the amount of time (referred to as effective duration) which would be required to produce waves of a certain height by wind blowing at a given wind speed. A wave forecasting procedure developed by Sverdrup and Munk (1947), and revised by Bretschneider (1952, 1958) with additional empirical data is called the Sverdrup-Munk-Bretschneider (SMB) method (C.E.R.C., 1973). The SMB curves for forecasting wave height are based on equation 16 from Bretschneider (1958).

$$\frac{gH}{U^2} = 0.283 \tanh \left[0.0125 \left(\frac{gF}{U^2} \right)^{0.42} \right] \quad (16)$$

where g is the acceleration due to gravity, H is the wave height, F is the effective fetch length, and U is the wind speed. Solving equation 16 for F gives

$$F = \frac{U^2}{g} \times \left[\frac{\text{ARCTANH} \left(\frac{gH}{0.283 \times U^2} \right)}{0.0125} \right]^{2.38} \quad (17)$$

Therefore, F is the effective fetch that it would take to generate waves of height H with a wind speed of U .

In terms of storm duration, the effective fetch equation is

$$F = \frac{S}{10}^{0.72} \times 10^{0.3} \times D^{1.25} \quad (18)$$

Where F is effective fetch, W is wind speed, and D is storm duration. Solving this for D , we have:

$$D = \left(\frac{F}{\frac{S}{10}^{0.72} \times 10^{0.3}} \right)^{0.8} \quad (19)$$

Therefore, D is the effective duration that it would take to build waves of a certain height (used to find the effective fetch) with winds of a given speed. Then, this effective duration is added to the current time increment of the storm to give a duration which takes into account the wave built in previous time increments.

Subroutine ETIME was tested by running the data from subroutine WAVES back through it to arrive at the original data. For example,

the following wave heights and wind speeds were tested using the C.E.R.C. charts and the subroutine (Table 2).

Wave Height	Wind Speed	<u>Effective Duration</u>	
		From SMB Curves	Derived
14 ft	80 kts	1.1 hrs	1.05 hrs
1 ft	12 kts	1.4 hrs	1.38 hrs
45 ft	80 kts	9.9 hrs	10.23 hrs
3 ft	12 kts	21.0 hrs	21.40 hrs
14 ft	30 kts	21.0 hrs	21.76 hrs

Table 2. Test for subroutine ETIME comparing effective duration available from SMB curves with derived duration for selected wave heights and wind speeds.

Subroutine FETCH

Subroutine FETCH is used to determine the maximum wind generating area and the average wind speed within that area for a circular storm on the open ocean. Three cases are considered for determining the actual storm fetch as the storm passes across a shoreline.

For a storm on the open ocean, the wind speed varies with the slope (first derivative) of a normal curve as one crosses the storm. The area of the storm with wind speed greater than one half of the maximum lies within a ring with an outside radius of 1.92 standard deviations and an inner radius of 0.32 standard deviations. This ring between 1.90 and 0.30 was divided into 13 smaller rings. The area of each ring was found and multiplied by the wind speed at the midpoint of the ring. These products were summed and then divided by the total area to give an average wind speed of 0.8847 of the maximum wind speed. The total area was found to be 7.7598 square standard deviations. Since the wind is being generated in a circular pattern, approximately one quarter of the wind is blowing along each axis of a grid with its center at the origin. Since the storm fetch area has a shape resembling an ellipse, the fetch for winds blowing in any one direction can be considered an ellipse with an area equal to one quarter of the maximum wind generating area (1.9400 square standard deviations) and centered on the maximum wind speed circle (1 standard deviations). The short half diameter was taken to be 0.7 standard deviations (1.0-0.3).

$$\text{Area} = \pi \times a \times b$$

$$1.9400 = 3.1415 \times a \times .7$$

$$a = 0.8822 \text{ standard deviations} \quad (20)$$

Therefore, the maximum storm fetch length is twice that, or 1.7644 standard deviations. Converting to storm radii, the fetch is 0.5881 radii.

Where the storm crosses the shoreline three cases must be considered; Case 1, where $1/3 R > x \geq 0$; Case 2, where $0.4444 R > x \geq 1/3 R$ and Case 3, where $x > 0.4444 R$, where R is the storm radius and x is the distance from the center of the storm.

For Case 1, ($1/3 R > x \geq 0$) (Figure 6), it is assumed that the fetch area, centered on the $1/3 R$ circle, swings around so that the long axis of the ellipse is always pointing at the beach. We have maximum storm fetch in this case until Y is small enough that the fetch begins to cross the beach as it continues to swing. This point is $Y1$. From the Case One diagram, $D^2 = X^2 + Y1^2$ and $D^2 =$

$(1/3 R)^2 + (1/2 F)^2$ so we have $X^2 + Y1^2 = (1/3 R)^2 + (1/2 F)^2$ or

$$Y1 = \sqrt{(1/3 R)^2 + (1/2 F)^2 - X^2} \quad (21)$$

As the storm continues to cross the beach and rotate, the fetch decreases. When the $1/3 R$ circle of the storm crosses the beach, the storm has swung so that the beach is in the center of the fetch area. Therefore, the storm fetch is one half of maximum at this point (Y2). As the storm continues inland, the fetch length reaches a minimum as Y goes to zero (Y3). This minimum is determined by the equation 22.

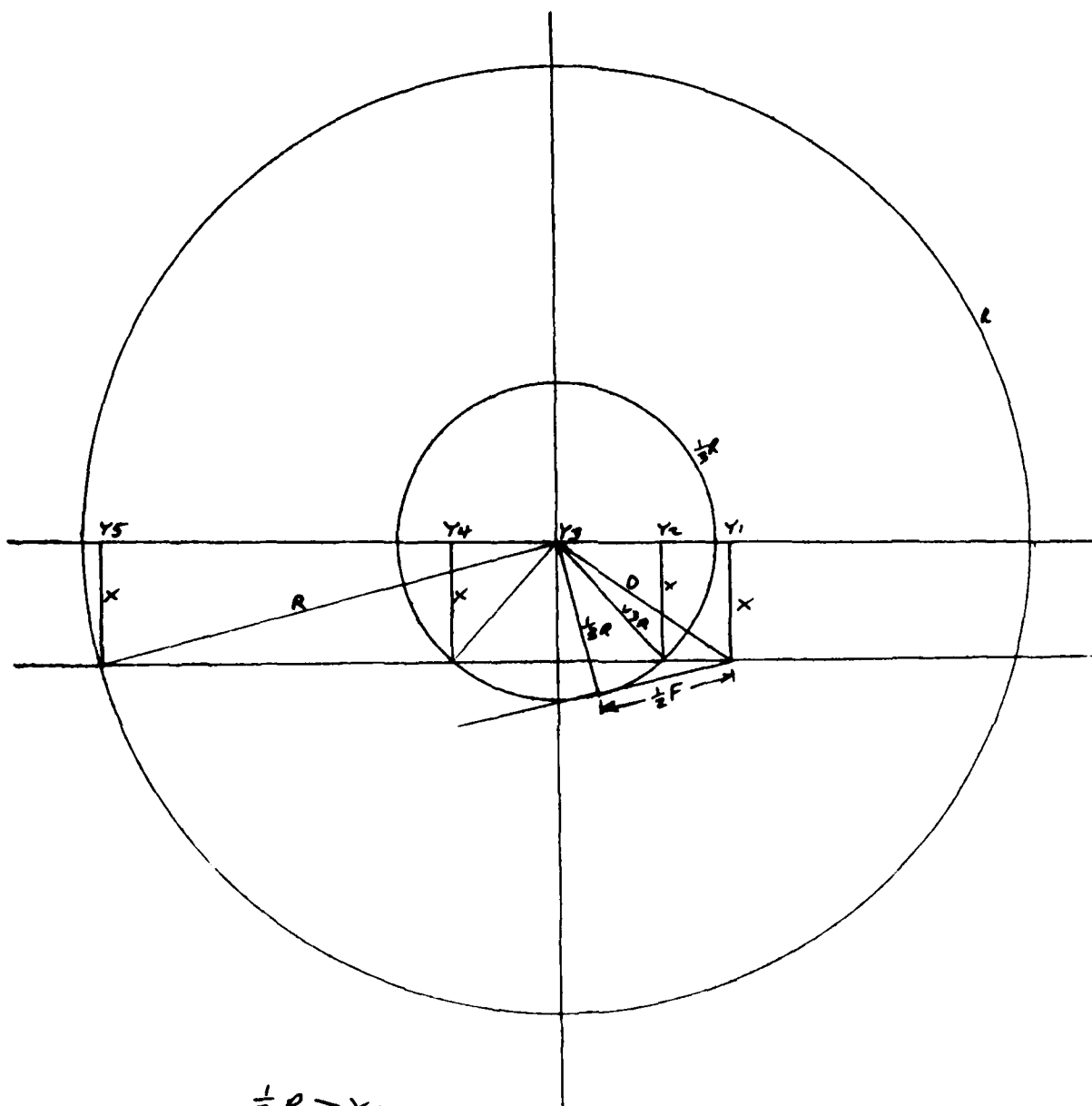
$$FMIN = \frac{|X|}{\sqrt{X^2 + Y2^2}} \cdot FMAX. \quad (22)$$

This gives a diminishing minimum as $|x|$ goes to zero. The fetch then increases to a high equal to $1/2 \cdot FMAX$ as the $1/3 R$ circle again crosses the beach (Y4). The fetch then declines again, finally dropping to zero at Y4, at which point the storm is completely onshore. This gives the "eye of the storm" effect where the winds drop to a minimum when the storm is at its closet point of approach and then increase again as the storm moves on, and finally drop as the storm moves away. Cosine smoothing is used to smooth out the increases and decreases in fetch.

For Case 2 ($0.4444 R > x > 1/3 R$) (Figure 7), again we have full fetch until the fetch area comes into contact with the beach at Y1. The fetch then decreases as the storm moves onshore, hitting zero at Y2. The reason that the fetch doesn't drop and then rise again, as in Case One, is that the eye of the storm (the part inside the $1/3 R$ circle) never passes over the beach.

This case ends at $X = 0.4444 R$ because D in the case two diagram $= \sqrt{(1/2 R)^2 + (1/2 F)^2} = 0.4444 R$. When $X \geq D$, then the geometric relationships that allow us to find Y1 no longer hold, since D, the distance from the origin to the beach, can no longer equal both $\sqrt{X^2 + Y1^2}$ and $\sqrt{(1/3 R)^2 + (1/2 F)^2}$. Again cosine curves are used to smooth out the changes in storm fetch.

For Case 3, ($x > 0.4444 R$) (Figure 8) the storm fetch area never actually crosses the beach, but the fetch decreases as the storm passes over the shore farther along the coast. Thus the storm fetch is at its maximum until the fetch area starts going onshore at Y1. Here the fetch is perpendicular to the storm path. Y1 is at zero since at that point, the whole half of the storm that is generating along-shore waves is still over the water, so we still have full fetch. As the entire storm passes onshore (Y2), the fetch drops to zero. Y2 is $-\sqrt{R^2 - (0.4444 R)^2}$. Y2 is frozen, using an X value of $0.4444 R$.



$$\frac{1}{3}R > X \geq 0$$

$$Y_1 = \sqrt{\left(\frac{1}{3}R\right)^2 + \left(\frac{1}{2}F\right)^2 - X^2}$$

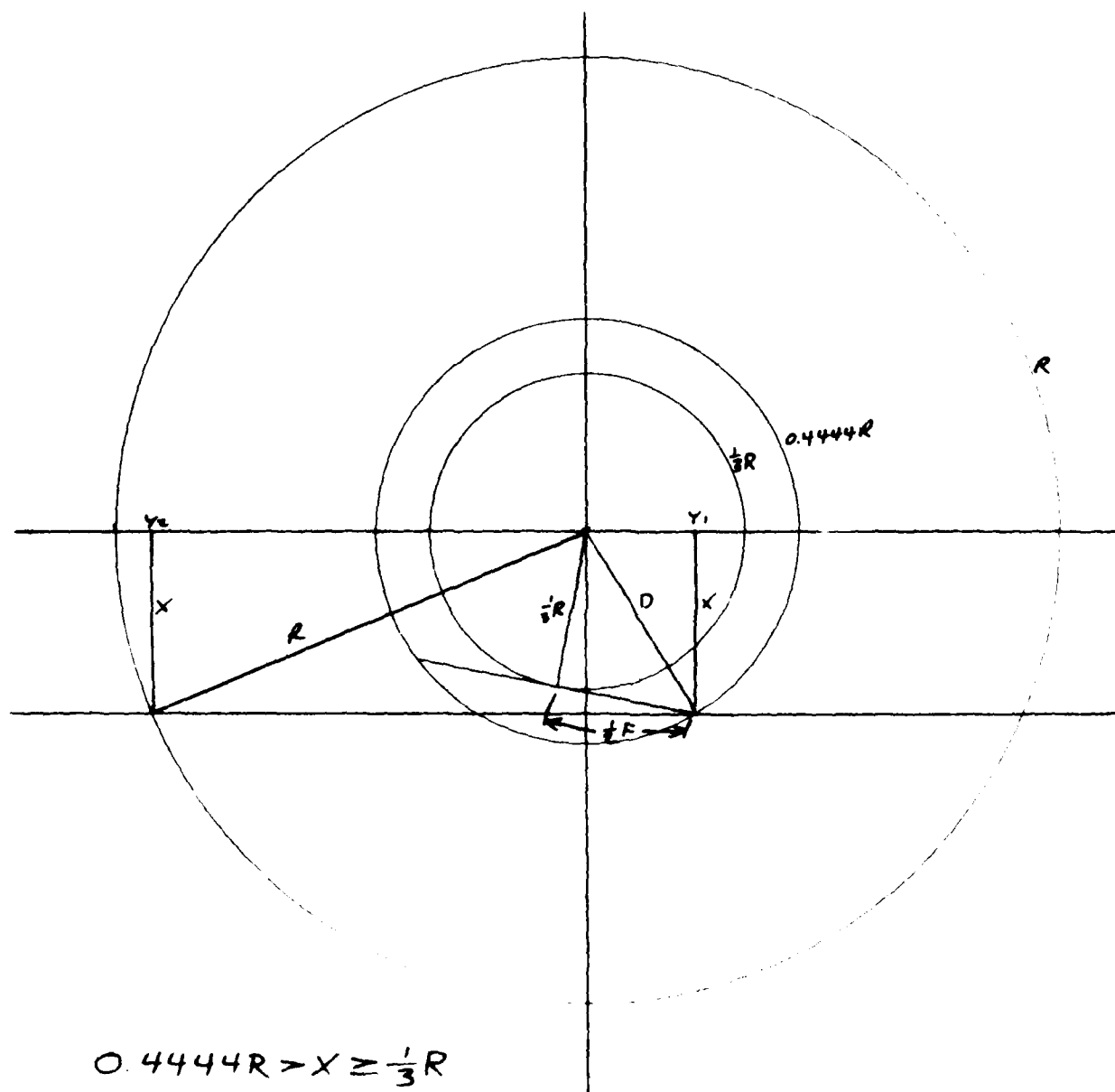
$$Y_2 = \sqrt{\left(\frac{1}{3}R\right)^2 - X^2}$$

$$Y_3 = 0.0$$

$$Y_4 = -\sqrt{\left(\frac{1}{3}R\right)^2 - X^2}$$

$$Y_5 = -\sqrt{R^2 - X^2}$$

Figure 6. Case 1 - storm fetch when the distance from center of storm X is less than $1/3$ storm radius, R .

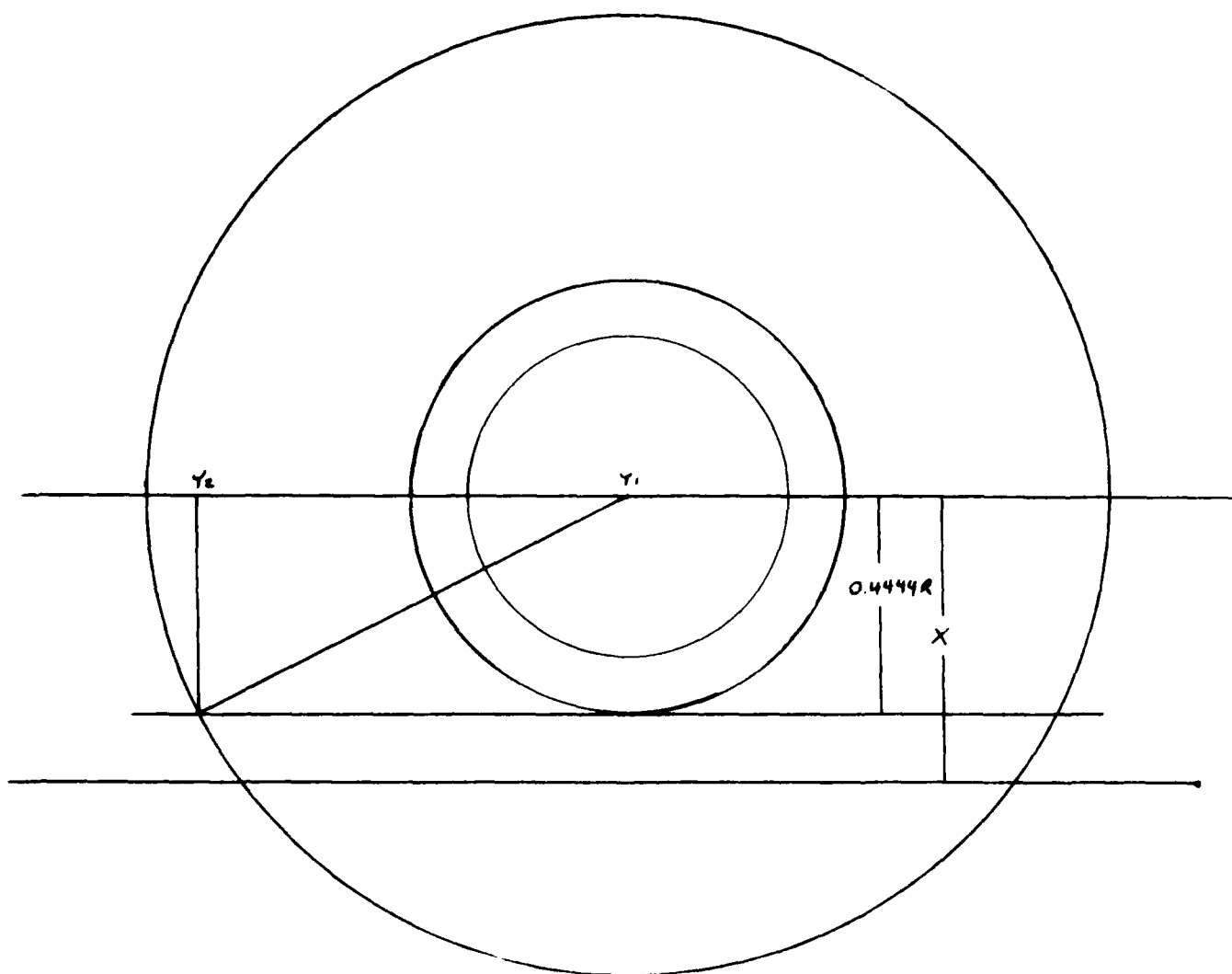


$$0.4444R > X \geq \frac{1}{3}R$$

$$Y_1 = \sqrt{\left(\frac{1}{3}R\right)^2 + \left(\frac{1}{2}F\right)^2 - X^2}$$

$$Y_2 = -\sqrt{R^2 - X^2}$$

Figure 7. Case 2 - storm fetch when the distance from center of storm X is less than 0.4444 and greater than $1/3$ storm radius, R .



$$X \geq 0.4444 R$$

$$Y_1 = 0 \ 0$$

$$Y_2 = -\sqrt{R^2 - (0.4444 R)^2}$$

Figure 8. Case 3 - storm fetch when the distance from center of storm X is greater than 0.4444 storm radius, R .

The reason that this is valid, is that from $X = 0.4444 R$ on out, the fetch area never actually passes over the beach, so that all these cases are essentially the same, as far as the size of their storm fetches goes. Only the distance from the storm fetch to the beach changes.

Subroutine FETCH was tested in two ways. First X and Y were varied independently, running Y from $+R$ to $-R$ for each value of X . This simulated storms with paths perpendicular to the shoreline. Second, X and Y were varied simultaneously by a constant amount, simulating storms crossing the shoreline at an angle. In both cases, the program produced continuous curves of fetch varying with storm location, with smooth transitions between all cases.

Subroutine WAVES

The equations for predicting significant wave height and period in subroutine WAVES are based on the Sverdrup-Munk-Bretschneider (SMB) method revised by Bretschneider (1958) and plotted as a series of curves by C.E.R.C. (1973). The SMB wave forecasting curves for fetches of 1 to 1000 miles are given in Figure 9. The wave prediction curves use the wind speed in knots, storm duration in hours, and storm fetch to calculate the significant wave height and significant wave period.

In order to use the SMB method in the model, the first task was to find equations to approximate the effective fetch from the wave prediction curves. The effective fetch is the limiting fetch which corresponds to a given wind speed and duration. The effective fetch is determined by moving to the left across the chart at the level of the wind speed until you hit the appropriated storm duration line. Then drop straight down to the fetch length axis from the intersection of the wind speed line with the duration line. This value on the fetch length axis is the effective fetch, if it is less than the actual fetch.

To develop an equation for effective fetch, the first problem is to determine the intercept of the proper duration line. To do this, the intercept of each line with the fetch length axis was plotted against the storm duration. Log scales were used on both axes since the original fetch length axis had a log scale and the duration lines themselves were spaced logarithmically. These formed a nearly linear trend and the equation for the line was found, in terms of the log axes, to be:

$$I = 10^{0.3} \times D^{1.25} \quad (23)$$

where I is the intercept and D is the storm duration.

The next step was to determine the slope of the storm duration lines given in the following equation.

$$F = \left(\frac{S}{10}\right)^{0.72} \times I \quad (24)$$

where F is the effective fetch, S is the wind speed, and I is the intercept of the duration line with the fetch length line. Combining equations 23 and 24 we get equation 25 for the effective fetch in terms of wind speed and storm duration:

$$F = \left(\frac{S}{10}\right)^{0.72} \times (10^{0.3} \times D^{1.25}) \quad (25)$$

If this value is less than the actual storm fetch then it decreases the relevant fetch length which is used in the rest of the equations.

The SMB forecasting curves were constructed from equations 26 and 27, which were empirically derived by Bretschneider (1958).

$$\frac{gH}{U^2} = 0.283 \tanh \left(0.0125 \left(\frac{gF}{U^2} \right)^{0.42} \right) \quad (26)$$

$$\frac{gT}{2pU} = 1.20 \tanh \left(0.077 \left(\frac{gF}{U^2} \right)^{0.25} \right) \quad (27)$$

where g is the gravitational constant, p is π (3.1459), H is the significant wave height, U is the wind speed, F is the effective fetch, and T is the significant wave period. Solving these equations for H and T , we get equations 28 and 29.

$$H = \frac{U^2 \times 0.283 \times \tanh \left(0.125 \left(\frac{gF}{U^2} \right)^{0.42} \right)}{g} \quad (28)$$

$$T = \frac{2pU \times 1.20 \times \tanh \left(0.077 \left(\frac{gF}{U^2} \right)^{0.25} \right)}{g} \quad (29)$$

The values for wind speed, storm duration, and effective fetch are then inserted into equations 28 and 29 to yield the wave height and period. For example in the case of a storm with a duration of 10 hours, a wind speed of 35 knots, and an actual fetch of 200 nautical miles, this gives us an effective fetch of 87.44 nautical miles, a wave height of 12.78 feet, and a wave period of 7.85 seconds. But suppose that we have a storm the same as the last one, but with a fetch of only 80 nautical miles. In this case the actual fetch is smaller than the computed fetch, so it remains as the effective fetch. This gives us a wave height of 12.36 feet and a wave period of 7.72 seconds.

The program has an option so that the results can either be metric or, to facilitate checking the results against the SMB curves, the results can be in nautical miles and feet. The subprogram was tested with numerous combinations of wind speeds, durations, and fetch lengths, with the results agreeing very well with the SMB forecasting curves.

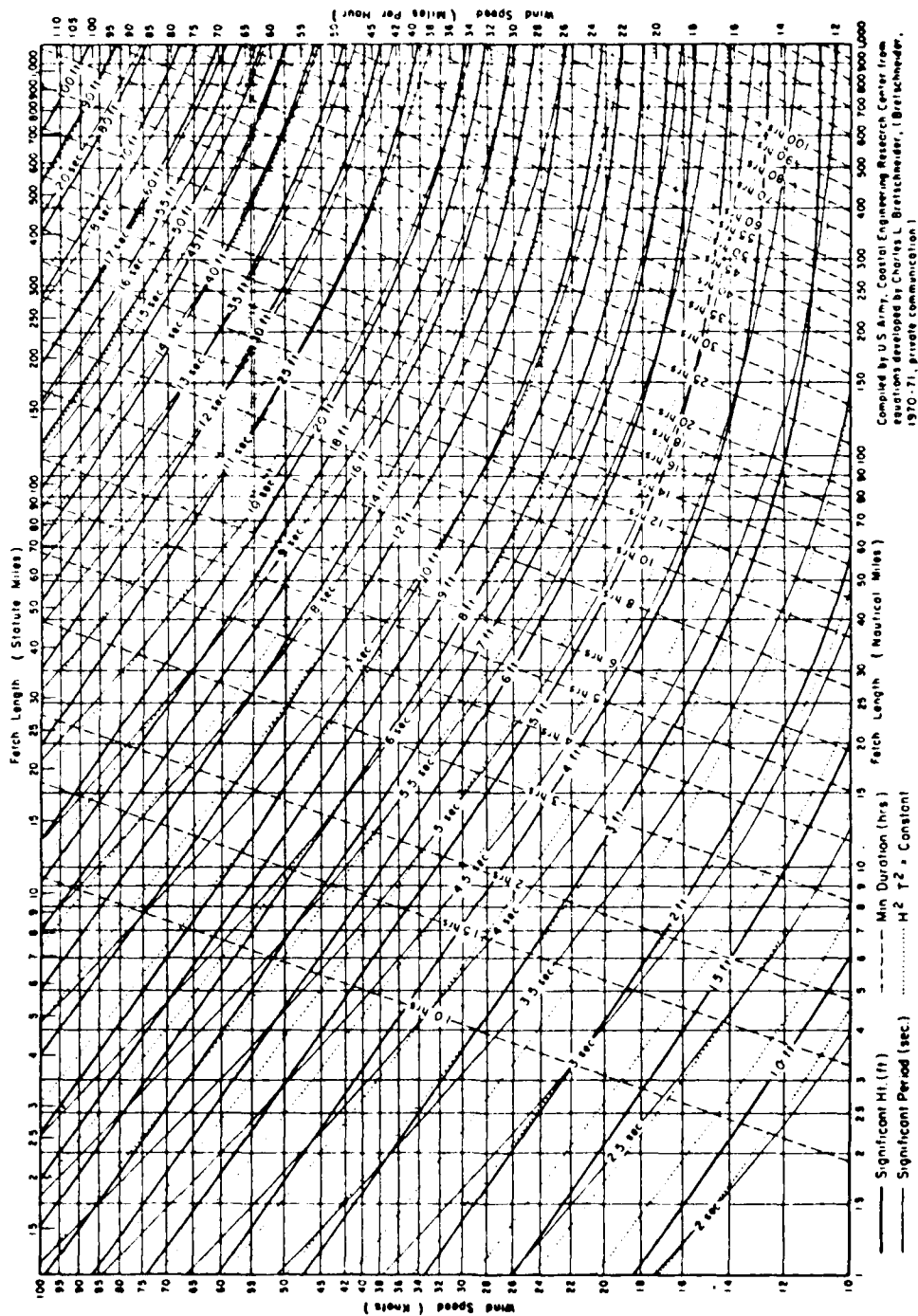


Figure 9. Deepwater wave forecasting curves as a function of wind speed, fetch length and wind duration based on the S.M.B. method.

Subroutine TIDE

Subroutine TIDE is used to determine the tide level at each hour, the spring tide range (ST), the neap tide range (NT), the number of days since the last spring high tide (TDAY), the hour of the last high spring tide (THR), and the tidal form number (FN). Four principal tidal components, M_2 - Principal lunar, S_2 - Principal solar, K_1 - Lunar-solar diurnal, and O_1 - Principal lunar diurnal are used for making a prediction of the hourly tide level. The periods of the semi-diurnal components ($TM_2 = 12.42$ hours and $TS_2 = 12.00$ hours) and the diurnal components ($TK_1 = 23.93$ hours and $TO_1 = 25.82$ hours) are constants in the subroutine. The tidal form number FN is used to classify the tides of a locality according to equation 30 (Defant, 1960, p. 306).

$$FN = \frac{K_1 + O_1}{M_2 + S_2} \quad (30)$$

The following classification based on Dietrich (1944, p. 69) is used to classify tides according to their form number.

FN = 0 - 0.25	Semi-diurnal tide
FN = 0.25 - 1.50	Mixed- mainly semi-diurnal tide
FN = 1.50 - 3.00	Mixed- mainly diurnal tide
FN = greater than 3.0	Diurnal tide

As examples of the different types of tides, Immingham, England has a semi-diurnal tide with a form number of 0.11. San Francisco, California has a mixed, dominately semi-diurnal tide with a form number of 0.90. Manila has a mixed, dominately diurnal tide with a form number of 2.15, and Do San, Viet Nam on the Gulf of Tonkin has a pronounced diurnal tide with a form number of 19.2. The four major components are responsible for the general form of the tides and generally account for about 70 percent of the total variance. If the next three most important tidal components, N_2 , K_2 and P_1 are included, the percentage of the total variance increases to about 83% (Defant, 1960).

If some simplifying assumptions are made concerning the major tidal components, it is possible to make a good approximation of the hourly tide level from the maximum spring tide range, minimum neap tide range, and the tidal form number. First, it is necessary to assume that the diurnal components, K_1 and O_1 are approximately equal. Second, assume that the maximum spring tide range is equal

to the sum of the four major components according to equation 31.

$$ST = M_2 + S_2 - (K_1 + O_1) \quad (31)$$

Next it is assumed that the neap tide range is approximately equal to the lunar components minus the solar components.

$$TN = M_2 + K_1 - (S_2 + O_1) \quad (32)$$

If K_1 and O_1 are approximately equal, it follows that

$$TN = M_2 - S_2 \quad (33)$$

The form number is the diurnal components over the semidiurnal components in equation 30, however, if $K_1 = O_1$, then

$$FN = \frac{2 K_1}{M_2 + S_2} \quad (34)$$

By combining the equations for the form number (Equation 30), the spring tide range, and the neap tide range, it is possible to solve for M_1 and S_2 .

$$M_1 = \frac{ST + TN}{4 (1 + FN)} \quad (35)$$

and

$$S_2 = \frac{ST - TN}{4 (1 - FN)} \quad (36)$$

If it is now assumed the lunar components are proportional, an approximation of the K_1 component can be derived from the M_2 component

$$K_1 = FN \cdot M_2 \quad (37)$$

and the solar components are related in like manner, therefore,

$$O_1 = FN \cdot S_2 \quad (38)$$

The amplitude of the maximum spring tide was taken at the last previous spring tide for each run, therefore, the phases for the four major components are considered 0 at that time. By computing the time differences from the last spring high tide to the hour for the prediction, the contribution for each tidal component can be calculated. The argument (ARG) is equal to 2 pi times the number of hours since the last spring tide. The tide is computed by adding together the contribution for each of the tidal components.

$$\begin{aligned} \text{TIDE} = & M_2 \cdot \cos\left(\frac{\text{ARG}}{T_{M_2}}\right) + S_2 \cdot \cos\left(\frac{\text{ARG}}{T_{S_2}}\right) + \\ & K_1 \cdot \cos\left(\frac{\text{ARG}}{T_{K_1}}\right) + O_1 \cdot \cos\left(\frac{\text{ARG}}{T_{O_1}}\right) \end{aligned} \quad (39)$$

Although some rough approximations were made in deriving the major tidal components from the spring tide range, neap tide range and form number, the resulting tide predictions work out quite closely with the tide tables. The tide tables give the time of high and low tides for each day, and the predicted times of high and low tides fall within 1 hour using subroutine TIDE. The subroutine was tested for Plum Island, Massachusetts, Cedar Island, Virginia, Sapelo Island, Georgia and Mustang Island, Texas, and gave satisfactory predictions for each of the areas.

One of the major reasons for making tidal predictions in the model is to determine the effect that tides have on the nearshore bottom slope. The slope at low tide SLBOT, the slope at high tide SLTOP and the tide level are used to determine the intermediate slope between high and low tide.

$$\text{SLOPE} = \text{SLBOT} + \text{TLOC} * (\text{SLTOP} - \text{SLBOT}) \quad (40)$$

The final tide level which is included with the output is computed by adding the relative tide level TIDX to the mean low tide level TMEAN.

Subroutine SURF

Breaker height, angle and longshore current velocity are computed in Subroutine SURF. The critical value, $H_b/h_b = .78$ where H_b and h_b are breaker height and depth, are used for a breaking criterion (Munk, 1949). Applying any wave theory and assuming conservation of energy flux, Komar and Gaughan (1972) derived the relationship

$$H_b = 0.73 \text{ cm} + .383 g^{1/5} (T H_\infty^2)^{2/5} \quad (41)$$

where H_b is the breaker height, g is gravity, T is wave period and H_∞ is the deep water wave height.

The breaker angle α_b is computed by first finding the shallow water wave length and then taking the ratio of shallow water to deep water wave length using Snell's law to determine the breaker angle.

$$\sin \alpha_b = \sin \alpha_0 \text{TANH} \left(\frac{2\pi H_b}{L_b} \right) \quad (42)$$

where α_c is the deep water wave angle which is assumed to be the same as the wind angle, H_b is the breaker height and L_b is the breaker depth.

The refracted breaker height, H_R , is obtained from the refraction coefficient, KR ,

$$KR = \frac{\cos (\alpha_0)}{\cos (\alpha_b)} \quad (43)$$

which is multiplied times the breaker height, H_b

$$H_R = KR \cdot H_b \quad (44)$$

Four different options are available for computing the longshore current velocity. The longshore current equations by Longuet-Higgins (1970), Komar and Inman (1970), Fox and Davis (1972) and Coastal Engineering Research Center (C.E.R.C., 1973) used basic different assumptions with the same set of variables. The variation

in longshore current velocity across the surf zone and along the shore, as well as differences in nearshore topography brought about by bars and rip channels make any prediction of average longshore current velocity very difficult. However, in making predictions about the surf zone, it is essential to at least have a good estimate of the maximum longshore current velocity.

The radiation stress theory of Longuet-Higgins (1970) has been tested with laboratory data from Galvin and Eagleson (1965), and field data from Putman, Munk and Traylor (1949). The longshore current velocity in the surf zone, V_b , is a function of the bottom slope, m , the breaker height, H_b , and breaker angle, α_b , between the wave crest and the shoreline (Longuet-Higgins, 1970).

$$V_b = M_1 m (gH_b)^{1/2} \sin 2\alpha_b \quad (45)$$

where M_1 , the friction factor is:

$$M_1 = \frac{0.694 \Gamma (2\beta)^{-1/2}}{f_f} \quad (46)$$

The longshore current, V_b is measured at the breaking position and Γ is a mixing coefficient with a range of 0.17 (little mixing) to 0.5 (complete mixing) with a mode at about 0.2. The depth to height ratio in shallow water, β , is taken to be 1.2 and f_f the friction coefficient is set at 0.01. By inserting the above values in equation 46, the value for M_1 becomes 9.0. Therefore, the longshore current equation according to Longuet-Higgins (1970) can be reduced to:

$$V_b = 9.0 m (gH_b)^{1/2} \sin 2\alpha_b \quad (47)$$

When equation 47 was applied to test sets of field and laboratory data by C.E.R.C. (1973), the data yields predictions that average about 0.43 of the measured values. The measured values were taken in the fastest field of flow shoreward of the breaker zone, whereas the predictions were made for longshore current at the line of breakers. Therefore, it has been proposed by C.E.R.C. (1973) that the Longuet-Higgins equation be multiplied by 2.3 to yield the C.E.R.C. equation:

$$V = 20.7 m (gH_b)^{1/2} \sin 2\alpha_b \quad (48)$$

Komar and Inman (1970) derived a longshore current equation based on radiation stress. Where the radiation stress components defined by Longuet-Higgins and Stewart (1964) is the excess flow of momentum due to the presence of waves. The Komar and Inman (1970) equation is:

$$V = C_1 U_m \frac{\tan \beta}{C_f} \sin \alpha_b \cos \alpha_b \quad (49)$$

where V is the longshore current velocity, $\tan \beta$ is the beach slope, C_f is the bottom frictional drag coefficient. U_m is the maximum horizontal component of the orbital velocity of the waves and C_1 is a dimensional coefficient of proportionality. However, Komar (1969) suggested that:

$$(\tan \beta \cos \alpha_b) / C_f = \text{constant} \quad (50)$$

indicating that the variation in beach slope does not produce a change in longshore current velocity. Therefore, the Komar and Inman (1970) longshore current equation becomes:

$$V = C_1 U_m \sin \alpha_b \quad (51)$$

A fourth equation developed by Fox and Davis (1972) uses empirical data subjected to linear regression analysis to predict longshore current velocity. The linear regression analysis is based on 3 sets of data collected at Stevensville, Michigan (Fox and Davis, 1970), Holland, Michigan (Fox and Davis, 1971a) and Sheboygan, Wisconsin (Fox and Davis, 1972). Each set of data consists of 360 observations taken at 2 hour intervals for 30 days of longshore current speed and direction, breaker height, period and breaker angle. Using a stepwise regression analysis, the contribution of each variable was tested separately, and then in various combinations. The ratio, H_b/T is related to the mass flux on volume of water which enters the surf zone and must be removed by the longshore current. The breaker angle, α_b , defines the angle between the breaker crest and the shoreline and is therefore related to the momentum transfer in the longshore direction. Using the regression program, a series of combinations was tested for the sin of the angle including $\sin A$, $\sin 2A$, $\sin 3A$, $\sin 4A$... $\sin 8A$. The closest fit was obtained when $\sin 4A$ was used for the angles. For the 1969 set of data from Stevensville, Michigan, the following equation,

$$V = 5.42 \left(\frac{H_b}{T} \right) \sin 4A \quad (52)$$

gave the best fit and accounted for 83.5 percent of the total sum of squares. For the 1970 data from Holland, Michigan, the coefficient of proportionality was 3.47 and the equation accounted for 78.8 percent of the total sum of squares. For the 1972 data from Sheboygan, Wisconsin, the coefficient was 2.98 and the equation accounted for 77.8 percent of the total sum of squares.

The three areas differed in the nearshore bottom slope and the occurrence of sand bars which influenced the coefficient of proportionality. The coefficient for each case was approximately equal to 100 times the bottom slope. Therefore, the longshore current velocity according to Fox and Davis (1973) is

$$V = 100 m \left(\frac{H_b}{T} \right) \sin 4 \alpha_b \quad (53)$$

When the four longshore current equations were tested in the model, the equation by Longuet-Higgins (1970) and Fox and Davis (1973) gave very similar results for breaker angles up to about 20 degrees. For higher breaker angles, the predicted results from the Fox and Davis (1973a) equation were too low. The values for longshore current predicted by Komar and Inman (1970) and C.E.R.C. (1973) were consistently too high. Although the four equations are available as options, it is recommended that the Longuet-Higgins (1970) equation be used for making predictions. If possible, it is best to test predictions with hindcast data from the same area.

Subroutine ENRGY

Subroutine ENRGY is used to determine the wave energy during each hour of the storm which is summed to give the total wave energy for the storm. The deep water wave energy E_0 (C.E.R.C., 1973) is given by

$$E_0 = \frac{\rho g H^2 L_0}{8} = \frac{5.12 \rho g (HT)^2}{8} \quad (54)$$

where ρ is the mass density of the water which is 1.94 slugs/cubic foot for fresh water and 2.0 slugs/cubic foot for salt water, H is the deep water wave height and T is the wave period. Conversion factors are included to change from foot pounds/foot to Joules/meter. The subroutine was tested using wave energy calculation from previous studies (Fox and Davis, 1971b).

Subroutine ARCTA

Subroutine ARCTA is a customized arctangent subroutine for finding the angle in radians from the arctangent of a function (Louden, 1967, p. 119). The library arctangent function ATAN accepts as an argument the tangent of an angle (sin/cos) and produces as output the angle in radians. Since the tangent of an angle repeats itself every 180 degrees, it is not possible to use the library function ATAN to determine a full range of angles from 0 to 360 degrees. To compute the correct angle for all possible combinations of X and Y , it is necessary to test for positive, near zero and negative X , and positive near zero and negative Y . The IF statements accomplish these test and produce an angle in radians ranging from 0 to 2 pi.

HINDCAST ANALYSIS WITH COASTAL STORM MODEL

Hindcast Tests of Model

The coastal storm simulation model can be used to hindcast wind, wave and current conditions at a shore site during the passage of a coastal storm. Hindcast analysis differs from forecast analysis discussed in the previous section because exact storm positions are known in hindcasting, whereas a constant azimuth and storm velocity are used in forecasting. The results of hindcast analysis at several sites are included in Appendix C. On the Great Lakes, the sites include Holland and Stevensville, Michigan, and Sheboygan, Wisconsin. On the east coast of the United States and Canada, sites include the Magdalen Islands on the Gulf of Saint Lawrence; Plum Island, Massachusetts; Cedar Island, Virginia and Sapelo Island, Georgia. Mustang Island, Texas was studied on the Gulf Coast. On the west coast of the United States, hindcasts were made for Monterey, California and South Beach, Oregon.

Sites were selected for hindcast analysis which had weather and wave data available for several storms. Several of the sites were studied by Davis and Fox using time series analysis from 1969 through 1975. Other sites were chosen in which there was good beach profile data which could be correlated with wave and current conditions during a storm.

Stevensville, Michigan, July 1969

A storm which passed over Lake Michigan in late July 1969 has been chosen as an example of hindcast analysis. When the storm passed over, a 30 day time-series study was being conducted at Stevensville, Michigan by Fox and Davis (1970a and b). Stevensville is located on the southeastern shore of Lake Michigan about 11 kilometers south of Benton Harbor, Michigan. The shoreline is oriented roughly north-south with an average nearshore slope of about 0.033.

The storm which affected the Stevensville area was tracked from 2000 on July 26, 1969 through 0800 on July 30 (Table 3). The size, shape, intensity and path of the storm were interpreted from weather maps for July 26 through 30, 1969. When the storm was closest to the coastal site at Stevensville, the barometric pressure at the center of the low was estimated as 994 millibars. The pressure at the largest encircling isobar was 1012 millibars, and therefore, the maximum pressure included in the storm was 1014.6 millibars. The storm had an elliptical shape with the length of the major half axis equal to 960 kilometers and the minor half axis

1. The following information was obtained from the records of the Department of the Interior, Bureau of Land Management, regarding the land owned by the United States in the State of California, as of January 1, 1940:

2. The total area of land owned by the United States in the State of California, as of January 1, 1940, was 1,111,111 acres.

3. The total area of land owned by the United States in the State of California, as of January 1, 1940, was 1,111,111 acres.

4. The total area of land owned by the United States in the State of California, as of January 1, 1940, was 1,111,111 acres.

5. The total area of land owned by the United States in the State of California, as of January 1, 1940, was 1,111,111 acres.

6. The total area of land owned by the United States in the State of California, as of January 1, 1940, was 1,111,111 acres.

7. The total area of land owned by the United States in the State of California, as of January 1, 1940, was 1,111,111 acres.

8. The total area of land owned by the United States in the State of California, as of January 1, 1940, was 1,111,111 acres.

9. The total area of land owned by the United States in the State of California, as of January 1, 1940, was 1,111,111 acres.

10. The total area of land owned by the United States in the State of California, as of January 1, 1940, was 1,111,111 acres.

No.		Section		Township		Range		County		Acres		Value		Remarks	
1		2		3		4		5		6		7		8	
1		1		1		1		1		1		1		1	
2		2		2		2		2		2		2		2	
3		3		3		3		3		3		3		3	
4		4		4		4		4		4		4		4	
5		5		5		5		5		5		5		5	
6		6		6		6		6		6		6		6	
7		7		7		7		7		7		7		7	
8		8		8		8		8		8		8		8	
9		9		9		9		9		9		9		9	
10		10		10		10		10		10		10		10	
11		11		11		11		11		11		11		11	
12		12		12		12		12		12		12		12	
13		13		13		13		13		13		13		13	
14		14		14		14		14		14		14		14	
15		15		15		15		15		15		15		15	
16		16		16		16		16		16		16		16	
17		17		17		17		17		17		17		17	
18		18		18		18		18		18		18		18	
19		19		19		19		19		19		19		19	
20		20		20		20		20		20		20		20	
21		21		21		21		21		21		21		21	
22		22		22		22		22		22		22		22	
23		23		23		23		23		23		23		23	
24		24		24		24		24		24		24		24	
25		25		25		25		25		25		25		25	
26		26		26		26		26		26		26		26	
27		27		27		27		27		27		27		27	
28		28		28		28		28		28		28		28	
29		29		29		29		29		29		29		29	
30		30		30		30		30		30		30		30	
31		31		31		31		31		31		31		31	
32		32		32		32		32		32		32		32	
33		33		33		33		33		33		33		33	
34		34		34		34		34		34		34		34	
35		35		35		35		35		35		35		35	
36		36		36		36		36		36		36		36	
37		37		37		37		37		37		37		37	
38		38		38		38		38		38		38		38	
39		39		39		39		39		39		39		39	
40		40		40		40		40		40		40		40	
41		41		41		41		41		41		41		41	
42		42		42		42		42		42		42		42	
43		43		43		43		43		43		43		43	
44		44		44		44		44		44		44		44	
45		45		45		45		45		45		45		45	
46		46		46		46		46		46		46		46	
47		47		47		47		47		47		47		47	
48		48		48		48		48		48		48		48	
49		49		49		49		49		49		49		49	
50		50		50		50		50		50		50		50	
51		51		51		51		51		51		51		51	
52		52		52		52		52		52		52		52	
53		53		53		53		53		53		53		53	
54		54		54		54		54		54		54		54	
55		55		55		55		55		55		55		55	
56		56		56		56		56		56		56		56	
57		57		57		57		57		57		57		57	
58		58		58		58		58		58		58		58	
59		59		59		59		59		59		59		59	
60		60		60		60		60		60		60		60	
61		61		61		61		61		61		61		61	
62		62		62		62		62		62		62		62	
63		63		63		63		63		63		63		63	
64		64		64		64		64		64		64		64	
65		65		65		65		65		65		65		65	
66		66		66		66		66		66		66		66	
67		67		67		67		67		67		67		67	
68		68		68		68		68		68		68		68	
69		69		69		69		69		69		69		69	
70		70		70		70		70		70		70		70	
71		71		71		71		71		71		71		71	
72		72		72		72		72		72		72		72	
73		73		73		73		73		73		73		73	
74		74		74		74		74		74		74		74	
75		75		75		75		75		75		75		75	
76		76		76		76		76		76		76		76	
77		77		77		77		77		77		77		77	
78		78		78		78		78		78		78		78	
79		79		79		79		79		79		79		79	
80		80		80		80		80		80		80		80	
81		81		81		81		81		81		81		81	
82		82		82		82		82		82		82		82	
83		83		83		83		83		83		83		83	
84		84		84		84		84		84		84		84	
85		85		85		85		85		85		85		85	
86		86		86		86		86		86		86		86	
87		87		87		87		87		87		87		87	
88		88		88		88		88		88		88		88	
89		89		89		89		89		89		89		89	
90		90		90		90		90		90		90		90	
91		91		91		91		91		91		91		91	
92		92		92		92		92		92		92		92	
93		93		93		93		93		93		93		93	
94		94		94		94		94		94		94		94	
95		95		95		95		95		95		95		95	
96		96		96		96		96		96		96		96	
97		97		97		97		97		97		97		97	
98		98		98		98		98		98		98		98	
99		99		99		99		99		99		99		99	
100		100		100		100		100		100		100		100	

equal to 700 kilometers. The orientation of the major half axis was 30 degrees west of north. For this particular example, the equation by Fox and Davis (1972) was used to compute the long-shore current velocity.

The position of the shoreline at Stevensville is given in the X-Y coordinate system with X equal to 1043 and Y equal to 486 kilometers. The X axis runs east-west and the Y axis north-south with the origin located to the southeast of Stevensville. The latitude at the shore location is 42° north and the onshore azimuth is 90 degrees. The nearshore slope from the shoreline out across the nearshore bars is 0.033. The average fetch distance for the southeastern shore of Lake Michigan is about 200 kilometers.

The storm positions were plotted at 6 hour intervals in kilometers on the X-Y coordinate system (Table 3). The initial position of the storm at 2000 on July 26 was to the northwest of the shore site with X equal to 333 and Y equal to 1229 kilometers. The storm passed over the shoreline about 0230 on July 28. At that time, the storm center was located 178 kilometers north of the shore site ($664 - 486 = 178$ kilometers). When the storm tracking was complete, the final storm position at 0800 on July 30 was X equal to 1907 and Y equal to 1830 kilometers. In general, the storm made a loop swinging down from the northwest, passing eastward across the shore, then moving off to the northeast.

The X_1 , Y_1 coordinate is oriented with the X_1 axis parallel to the shore and the Y_1 axis normal to the coast (Figure 2). The origin of the X_1 , Y_1 coordinate system is at the center of the storm with the positive X_1 direction to the right and the positive Y_1 direction toward the coast. The X_1 , Y_1 coordinate system is used to locate the shore position with reference to the center of the storm. The units of the X_1 , Y_1 coordinate system are in terms of storm radii. The storm radius is 1.5 times the length of the major half axis which is measured from the center of the storm to the largest encircling isobar. Using an inverted normal curve to simulate the storm cross-section the largest encircling isobar is defined as 2 standard deviations from the center of the storm. The full radius would extend out 3 standard deviations from the center of the low. As the storm approaches shoreline, the Y_1 value decreases, and it becomes negative after the storm has passed over the coast. When the storm is to the north of shore site the X_1 values are positive. Therefore, the storm at Stevensville remained to the north of the shore site for the entire run.

In the hindcast analysis, the barometric pressure decreases from 1012.4 millibars on July 26 to a minimum of 995.2 at 2200 on July 27, then increased to 1014.6 on July 30, 1969 (Table 3 and Figure 10). In the actual barometric pressure record at Stevensville, the pressure dropped to 1000.2 millibars (29.54 inches) at

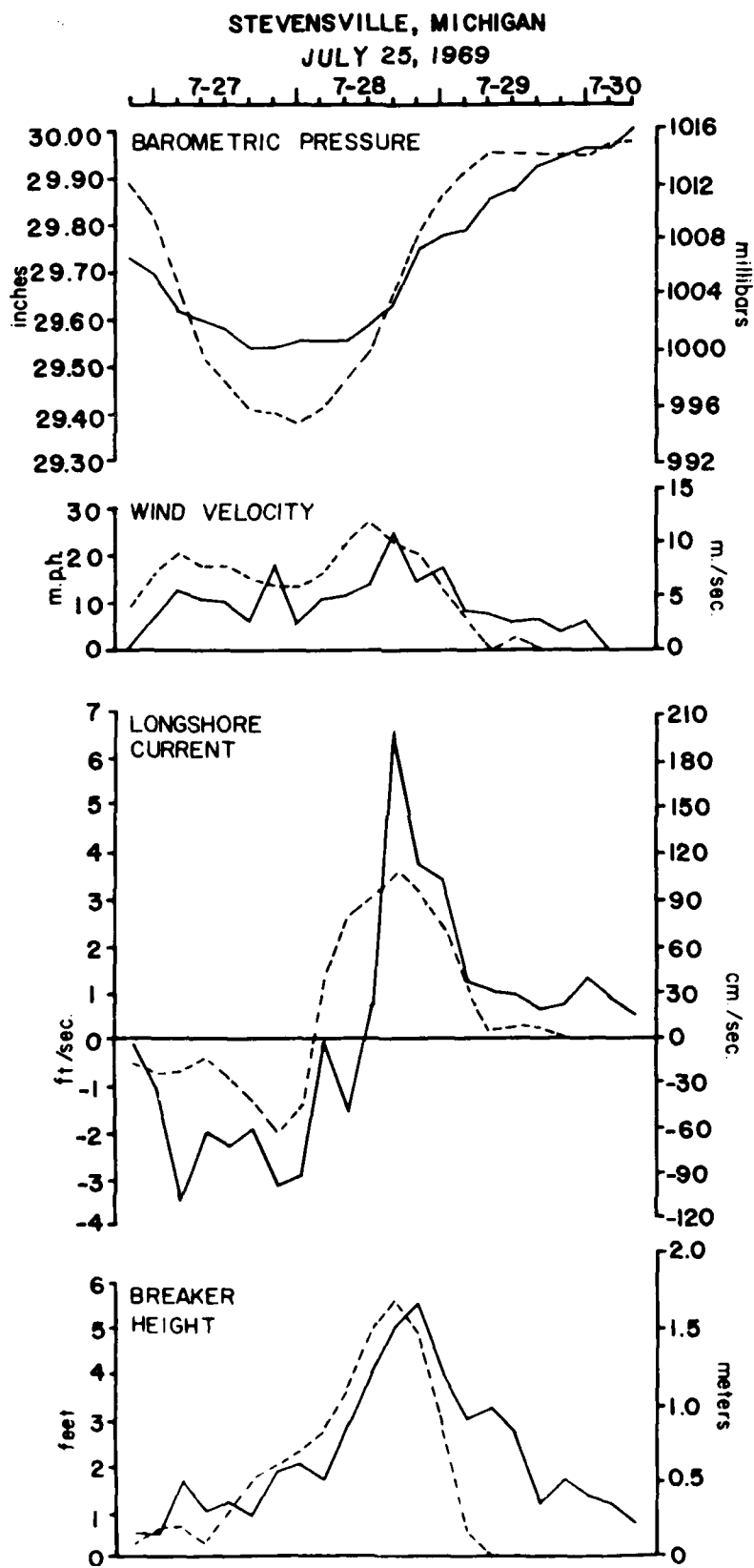


Figure 10. Observed and hindcast curves for barometric pressure, wind velocity, longshore current and breaker height at Stevensville, Michigan, July 26-30, 1969.

2000 on July 27. Since small scale weather maps were used for determining the storm position and pressure values, more accurate results could be obtained by using large scale maps available at 3 hour intervals. The plot for barometric pressure is a function of accurate plotting of the storm positions and a careful estimate of the size and intensity of the storm. Therefore, a correspondence of the observed and hindcast curves for barometric pressure is not a test of the predictive capabilities of the model, but is more a test of the accuracy of the weather maps and of the plotting ability of the operator.

In the wind observations at Stevensville, the maximum wind speed during the storm was 12.4 meters/second (28.4 knots) at 1600 on July 28 (Fox and Davis, 1970a). For the hindcast, the maximum wind speed was 12.0 meters/second at 1400 on July 28. The overall pattern for the observed and hindcast winds are also quite similar (Figure 10).

The observed longshore current velocity at Stevensville reached -116 centimeters/second (northerly) at 2200 on July 27, and 215 centimeters/second (southerly) at 1800 on July 28 (Fox and Davis, 1970a). The maximum hindcast values were -62.9 centimeters/second at 2100 on July 27 and 101.9 centimeters/second at 1700 on July 28 (Figure 10 and Table 3). The instantaneous longshore current values were much higher in the observed than the hindcast values, however, the minimum and maximum values occurred within one hour of the hindcast values. The observed longshore current during the storm was exceptionally high and may be accounted for by the well developed trough between the nearshore bar and the shore which channeled the current along the coast. The value used for nearshore slope could also be too low in the hindcast. When the longshore current curve was smoothed using the 15 term Fourier plot, the hindcast more closely resembles the observed curve for longshore current (Fox and Davis, 1970a and b).

The observed and hindcast curves for breaker height are very close (Figure 10). For the observed curve, the maximum breaker height of 1.82 meters (6 feet) occurred at 1800 on July 28. For the hindcast, the maximum height was 1.83 meters, also at 1800 on July 28. The overall shapes of the observed and hindcast curves for breaker height are also very similar but the hindcast curve drops off more rapidly than the observed curve (Figure 10).

Additional Hindcast Examples

Additional examples of the hindcast tests are presented in Appendix B and Figures 26, 27, 28 and 29. Since the input parameters are given in Appendix B and comparative plots are in Figure 26 through 29, a full discussion will not be included for each of the examples.

The observed data for the Holland, Michigan examples was extracted from a 30-day time series study during July 1970 (Fox and Davis, 1971a). Holland is located on the southeastern shore of Lake Michigan about 96 kilometers north of Stevensville. The hindcast values for longshore current and breaker height were quite close for July 3, 1970 (Figure 11), but were somewhat low for July 18, 1970 (Figure 12).

The observed data for the Sheboygan, Wisconsin examples come from a 30-day time series study conducted at Sheboygan during July 1972 (Fox and Davis, 1973a). Sheboygan is located on the western shore of Lake Michigan about 72 kilometers north of Milwaukee, Wisconsin. At this location, the storms moved in a northeast direction and generally offshore. Therefore, the characteristic reversal of longshore current direction observed on the eastern shore of Lake Michigan was not observed at Sheboygan. The curves for July 16 show generally low observed and hindcast curves for longshore current and breaker height with pronounced peaks on July 17, 1972 (Figure 13). The curves for July 22 show a substantial drop in barometric pressure, but very low values for longshore current and breaker height (Figure 14). There is a reversal in longshore current direction on July 24 for both the observed and hindcast curves. Since the winds were blowing predominately offshore, the waves and longshore currents are quite subdued.

Several additional tables of hindcast results are given in Appendix B. The output for the Atlantic, the Gulf and the Pacific coasts of the United States includes a variety of conditions for storms of varying sizes, shapes and intensities. Tidal predictions are also included for the oceanic sites where the tide tables are available. Some of the hindcast results followed quite closely with the observed data, while at other places, the fit was not as good as expected.

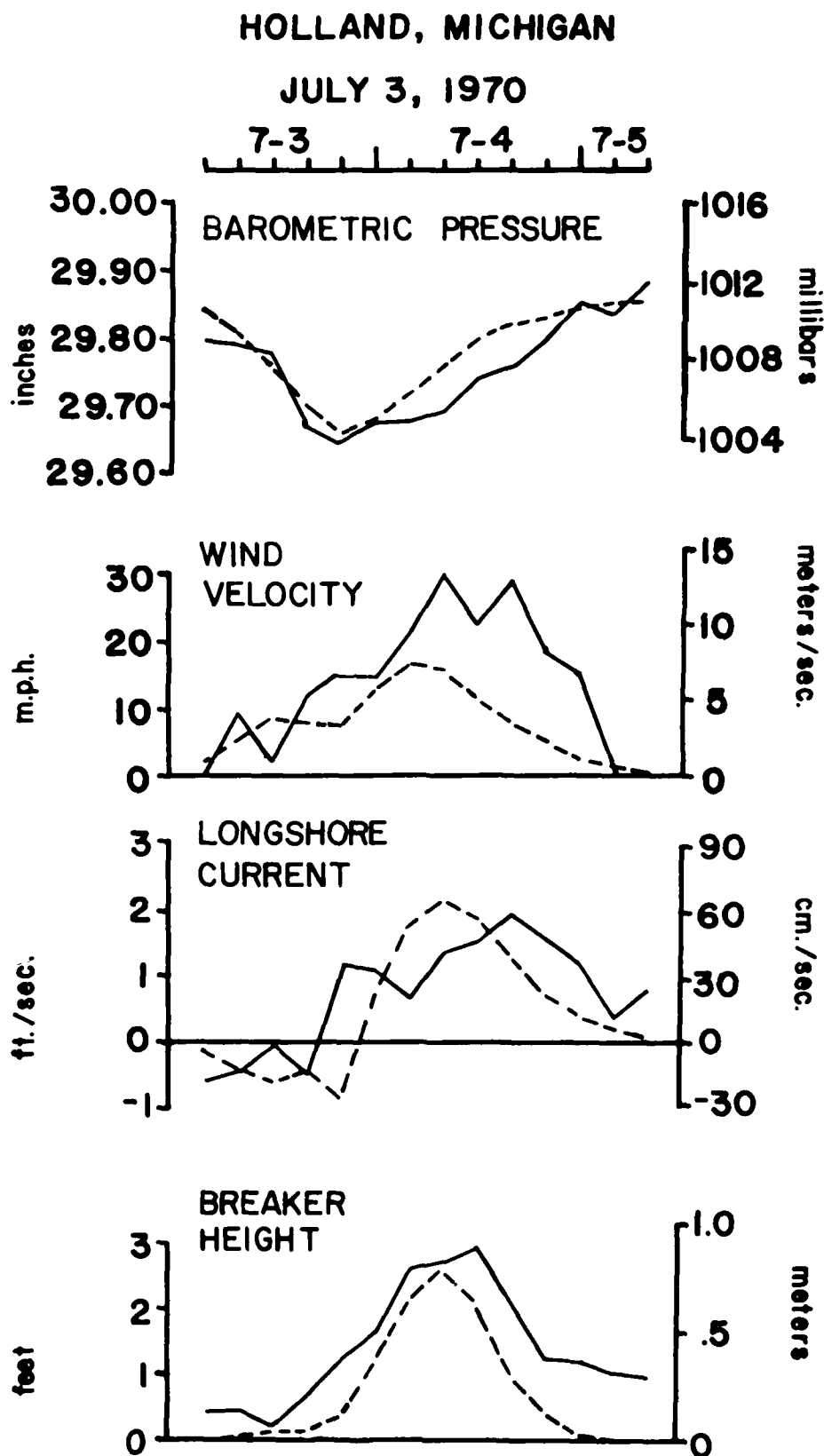


Figure 11. Observed and hindcast curves for Holland, Michigan, July 3-5, 1970.

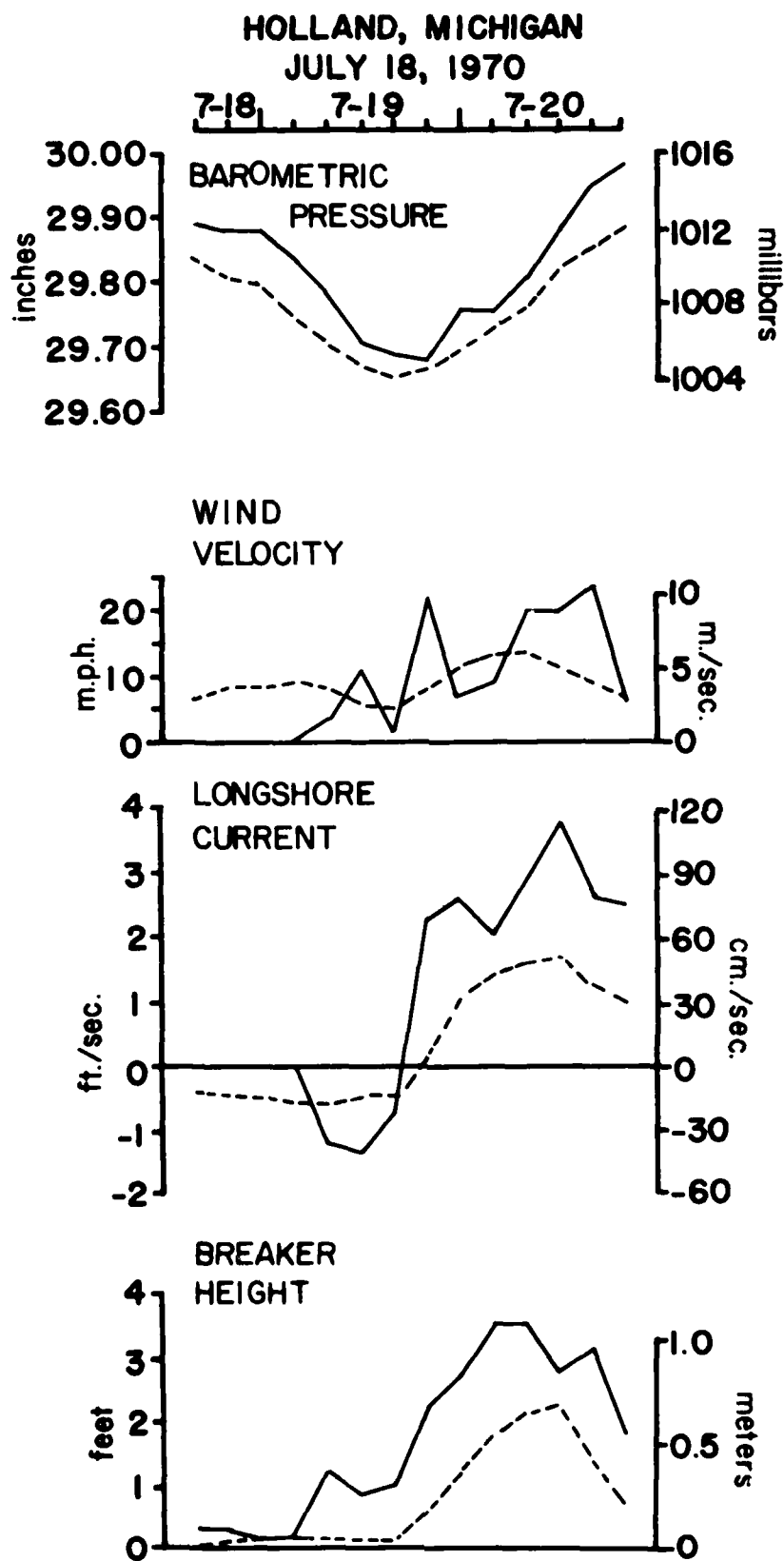


Figure 12. Observed and hindcast curves for Holland, Michigan, July 18-20, 1970.

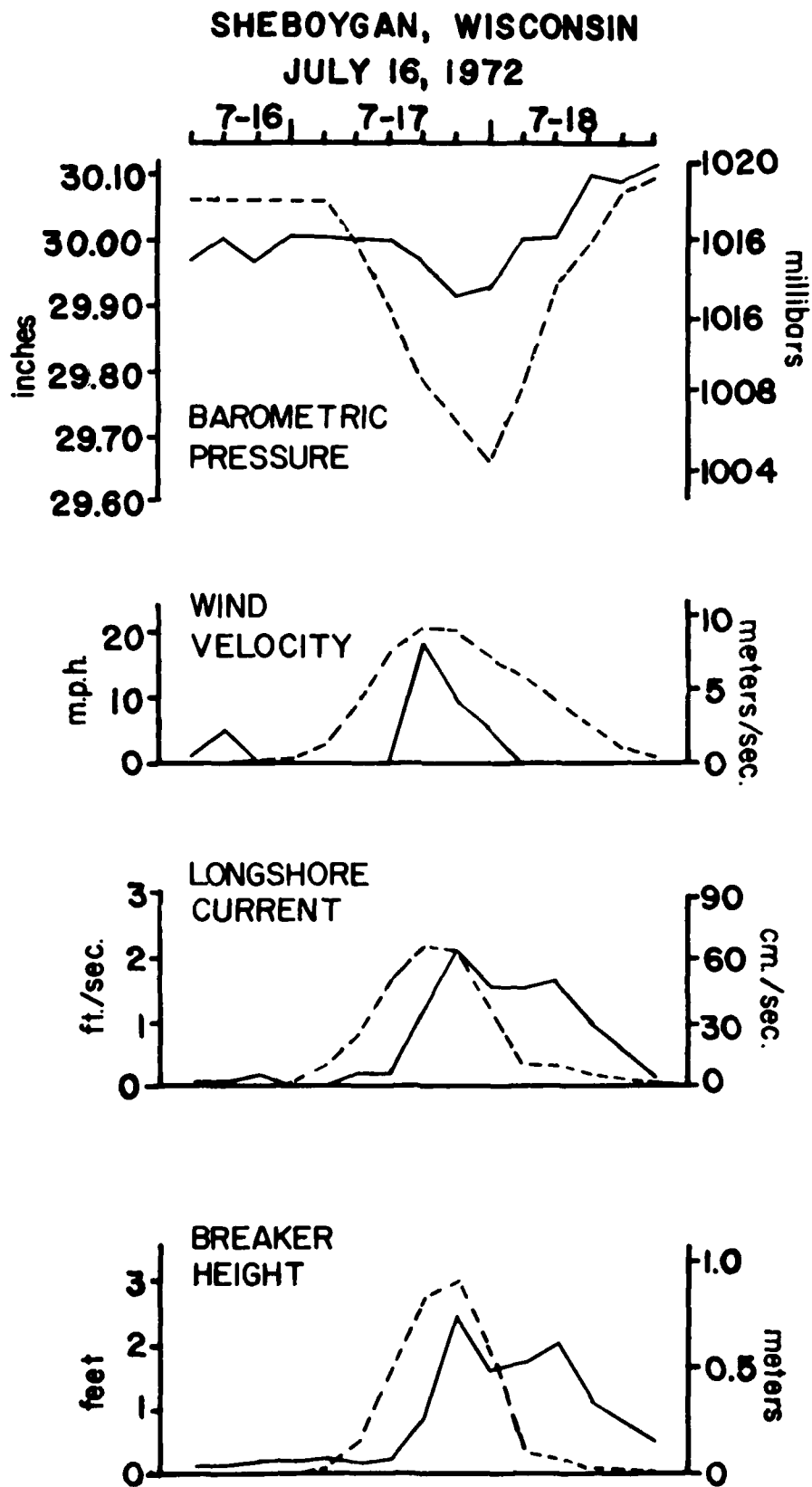


Figure 13. Observed and hindcast curves for Sheboygan, Wisconsin, July 16-18, 1972.

**SHEBOYGAN, WISCONSIN
JULY 22, 1972**

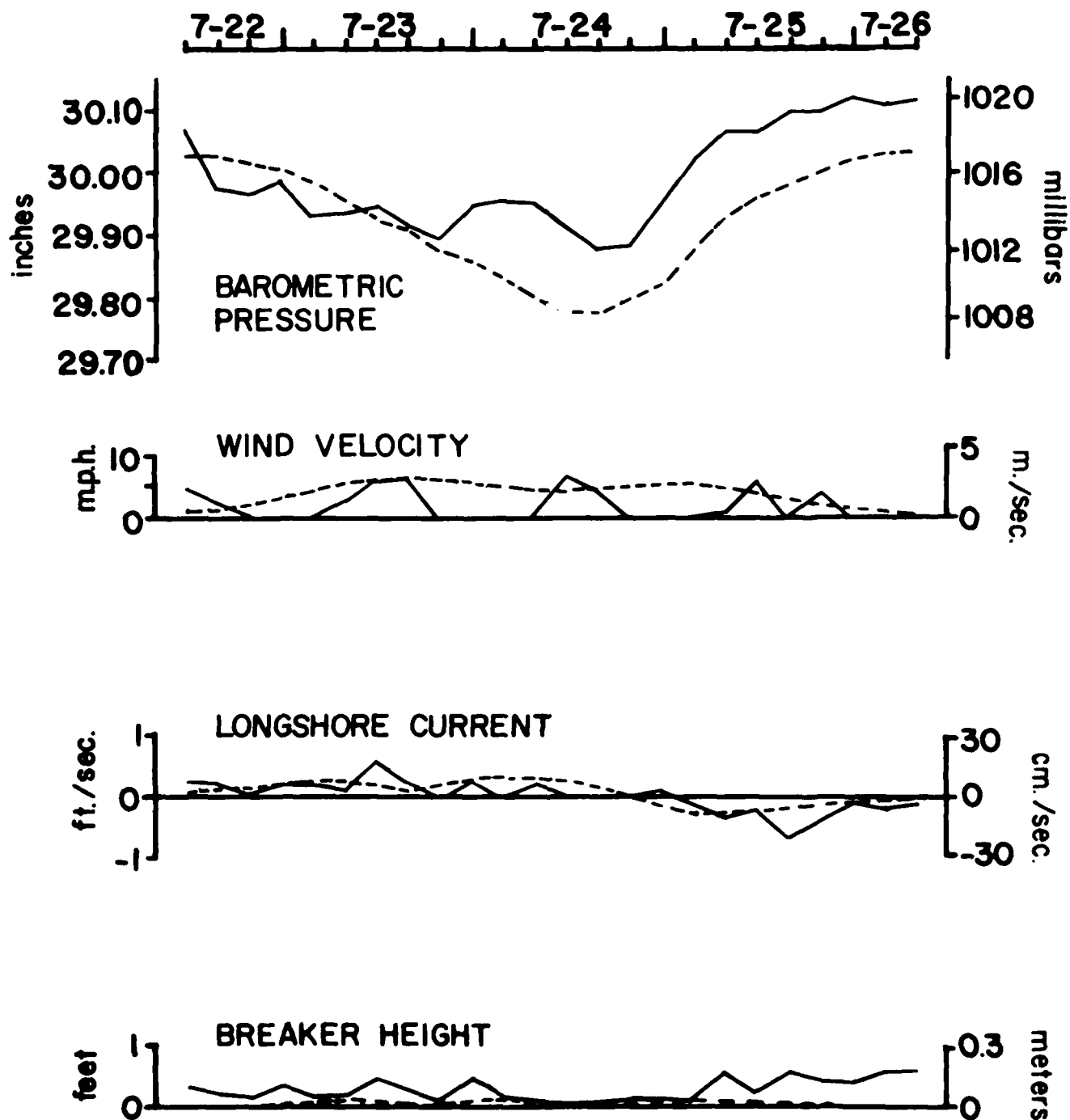


Figure 14. Observed and hindcast curves for Sheboygan, Wisconsin, July 22-26, 1972.

FORECAST ANALYSIS WITH THE COASTAL STORM MODEL

Short-term Forecasts

Short-term predictions of wave height and longshore current velocity can be made using the forecast mode of the coastal storm model. Given the initial coordinates of the storm, its size, shape and intensity, along with the position and orientation of the shoreline, it is possible to predict the wind, waves and currents as the storm passes over the coast. In the forecast mode, the storm azimuth and velocity are used to plot a straight storm path as the storm proceeds toward the shore. In general, the forecast is run for 72 hours which is the usual limit for short-term weather prediction. Examples of output using the forecast mode are given in Appendix C.

In the forecast mode, it is assumed that the size, shape and intensity of the storm remain constant, as well as the direction of the storm path and the speed of the storm along the path. The operators experience with weather prediction plays an important role in estimating the speed and path of the storm. For 12 to 24 hours, the speed and path may remain fairly constant, but for longer periods of time, the storm may veer off on another path or change its speed along the path. Since it is almost impossible to predict the path of a storm for several days, a series of diagrams have been devised for predicting wave and current conditions for a storm with a given size, shape and intensity, but without a fixed storm path.

Circular Storm Test

A circular storm test is used as an example to explain how the forecast mode works with the coastal storm model. The circular storm test is based on a series of intense storms which crossed over the Oregon coast during late fall of 1973 (Fox and Davis, 1974). The size, shape and intensity of the storm, and the orientation of the shoreline are similar to those encountered at South Beach, Oregon in November 1973 (Fox and Davis, 1974). The computer listings for the circular storm are given in Appendix C.

For the circular storm, the barometric pressure at the center of the low was set at 1000 millibars. The pressure at the largest encircling isobar was placed at 1020 millibars to give a range of 20 millibars within the central portion of the storm. The plot of barometric pressure for the circular storm model is generated by rotating an inverted normal curve around its center. Therefore, the barometric pressure surface has a basin shape with the low pressure at the center, the steepest pressure gradient at one standard deviation out from the center, and gradually reaches a

maximum pressure at 3 standard deviations away from the center. Since the outer margin of a storm often interferes with other high or low pressure systems, it is assumed that the largest encircling isobar occurs at 2 standard deviations away from the center, or 2/3 of the total storm radius. Therefore, the total storm radius would be 1.5 times the radius measured at the largest encircling isobar, and the maximum pressure at the margin of the storm would be 1.145 times the pressure range from the center to the largest isobar. In the circular storm test, the pressure at the 2 standard deviations is 1020 and the maximum pressure included in the storm is 1022.9 millibars at 3 standard deviations.

The size of the storm is determined by measuring the lengths of the major and minor half axes of the storm. For an elliptical or wave-shaped storm, the length of the major half axis is measured from the center of the low to the largest isobar, where it is farthest from the storm center. The length of the minor half axis is measured at right angles to the major half axis from the storm center to the largest isobar. A circular storm exists when the major and minor half axes are equal. For the circular storm test, lengths of the major and minor half axes are 300 kilometers. When the major and minor half axes have different lengths, the orientation of the major half axis is plotted in degrees from north. Therefore, for the circular storm test, the orientation of the major half axis is 0 degrees.

For the circular storm model, the storm velocity is set at 40 kilometers/hour with a storm azimuth of 90 degrees. This means that the storm will proceed from its initial position along a path 90 degrees east of north at 40 kilometers/hour. Therefore, if the storm is tracked for 30 hours, it will move a distance of 1200 kilometers.

For the shore position coordinates in the circular storm test, X is set at 1000 and Y is set at 0 kilometers. In the X-Y coordinate system used for plotting storm position and shore location on a weather map, the shore site is located 1000 kilometers east along the X axis and 0 kilometers north along the Y axis. The shore latitude for the test case is 43 degrees north, the approximate latitude of the Oregon coast. The onshore azimuth is 90 degrees which indicates that the coastline runs north-south with land to the east and sea to the west, the same orientation as the Oregon coast. The nearshore slope is at 0.033 which is close to the average nearshore slope in the different areas studied. A value of 1000 kilometers was used for the average fetch which would indicate open ocean. If the average fetch is greater than the storm radius, the fetch distance will not have an effect on the wave and current calculations. However, if the fetch distance is smaller than the storm radius, the waves will be fetch limited when the average fetch is less than the effective fetch.

In compiling the output for the circular storm test, the storm outlined above was tracked along 12 paths normal to the shoreline and parallel to each other (Figure 15). The location of the shore site, orientation of the shoreline, and three storm tracks are given in Figure 15A. The diagram extends 1200 kilometers in a north-south direction, 600 kilometers to the north (positive) and 600 kilometers to the south (negative) of the study site which is located in the center of the diagram. The diagram also extends 1200 kilometers in an east-west direction, 600 kilometers offshore (negative) and 600 kilometers onshore (positive) of the shore site. A time scale is included along the bottom of the diagram to indicate the length of time in hours from the initial tracking of the storm to any position along the storm path. The speed of the storm was set at 40 kilometers/hour, therefore, if the storm started at the left edge of the diagram, its center would pass over the shoreline after 15 hours and would move off the right side of the diagram after 30 hours.

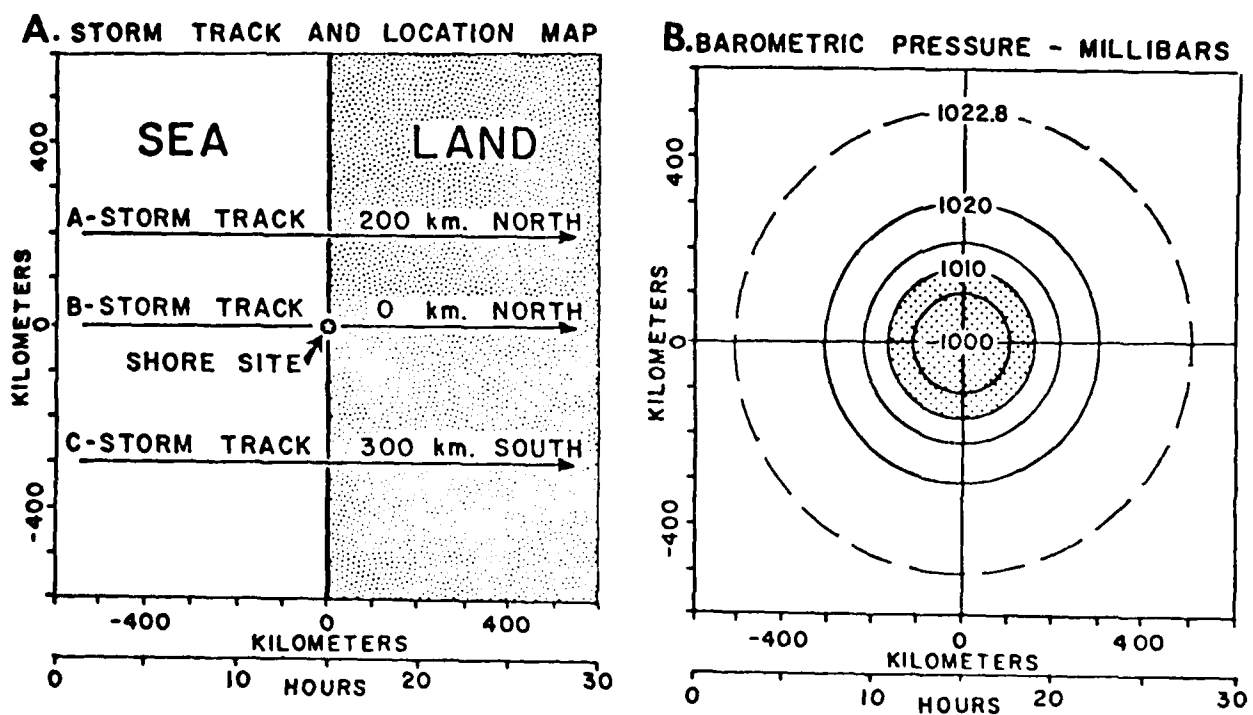


Figure 15. Map of storm tracks and time-distance plot of barometric pressure for a circular storm.

Barometric Pressure

The barometric pressure diagram (Figure 15B) is set up with the same coordinate system as the storm track diagram (Figure 15A). The barometric pressure which would be recorded at the shore site is plotted at the storm location as the storm moves across the diagram. After 12 storms were tracked normal to the shore at 100 kilometer spacings along the shore, the barometric pressure values plotted along the storm tracks were contoured to produce the barometric pressure diagram (Figure 15B).

The use of the barometric pressure diagram can be explained by examining a series of profiles through the diagram (Figure 16). Three storm tracks are plotted on the pressure diagram indicating storms which moved from west to east across the shoreline. Barometric pressure profiles are shown when the storm track is 200 kilometers north, directly over the shore site, and 200 kilometers south of the site (Figure 16). When the storm passes 200 kilometers north of the shore site, the pressure at the shore location drops from 1022.8 millibars to 1013.4, then increases again to 1022.8. When the storm passes directly over the shore location, the pressure at the shore site drops from 1022.8 millibars to 1000.0, then increases to 1022.8. When the storm passes 200 kilometers south of the shore site, the pressure profile is identical to the profile which was made 200 kilometers north of the shore site. For a circular storm, the barometric pressure diagram is symmetrical, so that profiles cut through the storm a given distance north or south of the shore site will result in identical patterns.

It should be emphasized that the values plotted at the storm locations are for observations recorded at the shore site when the storm follows along a given path. Therefore, the pressure profile in Figure 16 are profiles of the pressure at the shore site when the storm passes to the north, over the site, or to the south. Although the diagram for barometric pressure is identical to a weather map with storm center located directly over the shore, it should not be interpreted in that way. The X axis represents time, and distance along the X axis is used to show the storm position at a given time. With the other diagrams, such as wind speed and breaker height, it is impossible to use the time distance diagram as a map with the storm center located at the shore site.

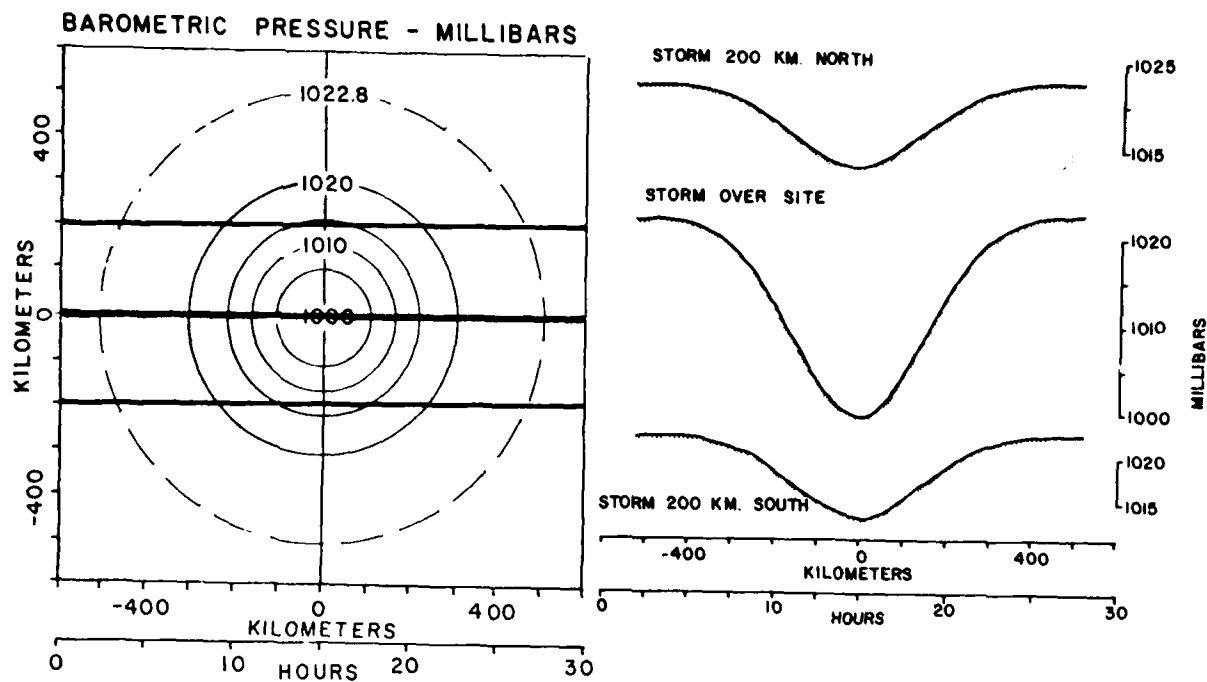


Figure 16. Time-distance plot of barometric pressure and pressure profiles 200 km north, over the site, and 200 km south of the site.

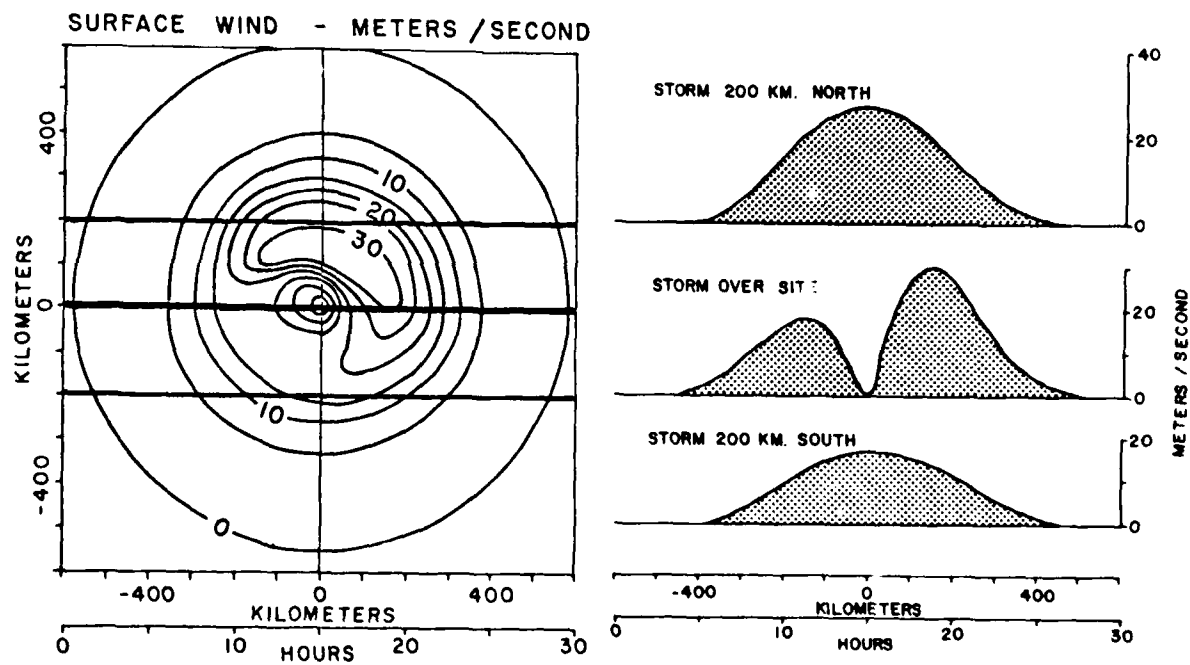


Figure 17. Time-distance plot of surface wind speed and three profiles of wind speed in a circular storm.

Wind Speed and Direction

The time distance diagram for surface wind speed is not symmetrical because the maximum wind speeds occur when the storm track is between 100 and 200 kilometers north of the study site (Figure 17). When the storm passes 200 kilometers north of the study site, the surface wind speed reaches 28 meters/second at the shore site. However, when the storm passes directly over the shore site, the surface wind speed reaches 18.8 meters/second as the storm approaches, drops down to zero as the center of the storm passes over the coast, then increases to 30.8 meters/second. When the storm track is 200 kilometers to the south of the shore site, the surface wind speed reaches 17.0 meters/second. The highest wind velocities are recorded when the storm passes to the north, and after the storm has passed over the coastline.

To understand the wind pattern during a coastal storm, it is necessary to consider both wind speed and direction. Time-distance diagrams are plotted for surface wind speed, wind direction, on-shore component, and alongshore component of the wind in a circular storm (Figures 18A, B, C and D). The surface wind speeds in the storm were computed by the geostrophic wind equation (Equation 6) with corrections applied for speed and direction (Equations 10 and 11) to account for the frictional effects of land or sea (Figure 5). For example, at 40° north latitude, the angle between the surface wind and the geostrophic wind would be 42° if the wind is from the land, and 16° if the wind is from the sea (Figure 5 and Table 1).

When the storm passes to the north of the shore site, the wind blowing around the storm center in a counterclockwise direction is generally onshore at the shore site (Figure 18B). The contour lines indicating wind direction radiate out from the center of the diagram and the arrows along each contour line point in the direction the wind is blowing along that line (Figure 18B). The dark lines on the diagram indicate the major wind directions with onshore winds = 0° , north winds = 90° , offshore winds = 180° and south winds = 270° . When a storm follows a path 200 kilometers north of the study site, the wind direction at the study site starts out from the south (274°), slowly shifts over to onshore (0°), and ends up out of the northwest (52°). When a storm passes 200 kilometers to the south of the shore site, the wind starts off blowing offshore (209°) and then shifts over to the north (71°). Different patterns are used to show area where the winds are blowing generally onshore, from the north, offshore are from the south. These patterns related to similar areas for the onshore and alongshore components of the wind (Figures 18C and D).

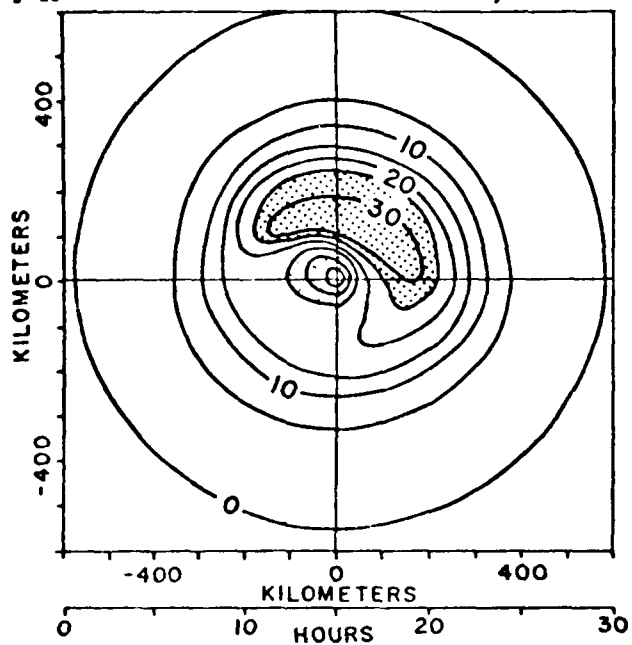
Diagrams for the onshore and alongshore components of the surface wind speed are given in Figures 18C and D. The onshore component of the surface wind is obtained by taking the cosine of the

wind direction times the wind speed, and the alongshore component is produced by taking the sine of the wind direction times the wind speed. Storms which follow a path to the north of the shore site generally have a strong onshore wind component, while those following a path to the south of the shore site are predominately offshore (Figure 18C). The dividing line between the onshore and offshore components of the wind follows north-south wind direction lines (0° to 180°) (Figure 18B). The onshore wind reaches a maximum of 28.2 meters/second along a storm path 100 kilometers north of the shore site. The offshore wind reaches 18.6 meters/second when the storm passes 100 kilometers south of the shore site and before its center moves across the coast. The onshore wind speed is greater than the offshore wind speed because the friction is less when the wind is blowing over the water.

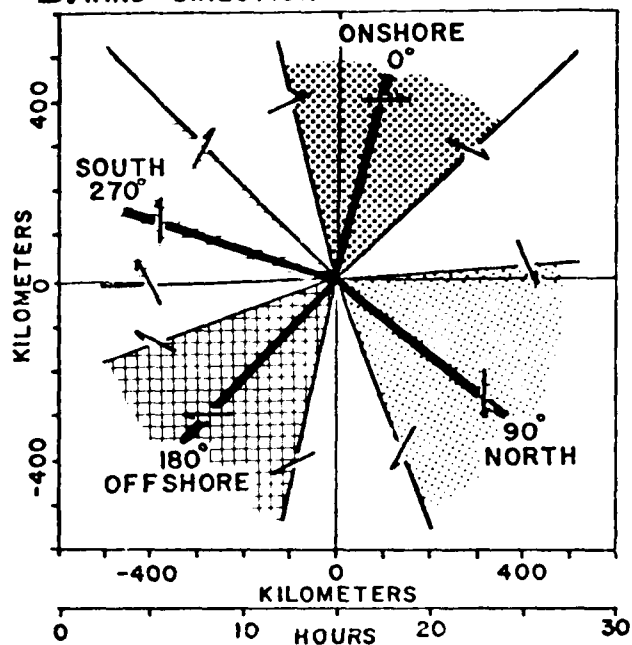
The time distance diagram for alongshore wind component indicates that the winds are from the south as the storm approaches the coast and shift over to the north after the storm passes (Figure 18D). To the north of the shore site, the shift in the alongshore component from south to north takes place after the storm has passed over the coast, but to the south, the shift takes place before the storm reaches the coast. The boundary line between the north and south components of the longshore wind (Figure 18D) follows the onshore-offshore line (90° - 270°) in the wind direction diagram (Figure 18B). The reversal from south to north wind is very abrupt near the center of the storm, and more gradual near its margin. When the storm passes to the north, the low in barometric pressure reaches a minimum when the storm passes over the coast (Figure 17), but the shift in wind direction from south to north does not take place until several hours after the low has passed. This lag in wind direction reversal behind the low in pressure was observed during storms at Holland and Stevensville, which passed to the north of the study areas (Fox and Davis, 1970 and 1971a). Also, the maximum wind speeds were observed after the lows had passed and the wind shifted over to the north.

Figure 18. Time-distance plots of A - surface wind speed, B - wind direction, C - onshore wind, and D - alongshore wind in a circular storm.

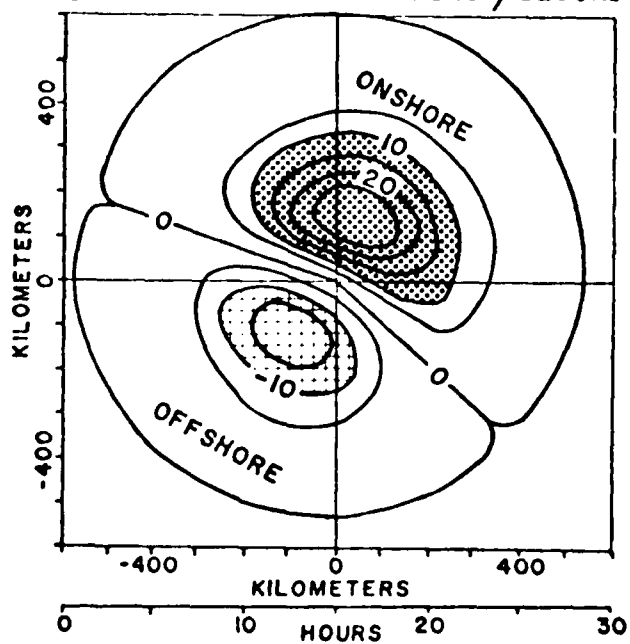
A. SURFACE WIND - METERS / SECOND



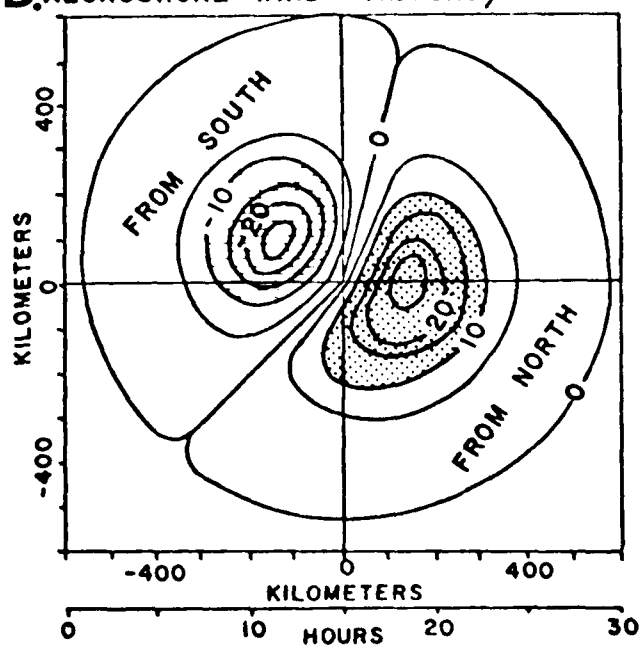
B. WIND DIRECTION - DEGREES



C. ONSHORE WIND - METERS / SECOND



D. ALONGSHORE WIND - METERS / SECOND



Wave Period and Breaker Height

The diagrams for wave period and breaker height are quite similar (Figures 21A and B), and both resemble the plots for surface wind and onshore wind (Figures 18A and C). Three profiles were plotted across the breaker height diagram to show what the height would be at the shore site as the storm moves across (Figure 19). If the storm moves 200 kilometers north of the shore site, the breaker height will reach 5.30 meters 3 hours after the storm crosses the coast. If the storm passes directly over the shore site, the breaker height will reach .86 meters as the storm approaches, drop down as the center of the storm passes, then reaches 3.63 meters 5 hours after the center passes over the coast. The decrease in wave height as the storm center passes directly over the shore site corresponds to the zero wind velocity at the center of the storm. While wind velocity may drop to zero at the storm center, the zero wave height is probably an artifact of the computer model and does not occur in nature. Residual waves would most likely remain in the area and could be built model if so desired.

The surface wind speed is not used directly for determining breaker height and wave period, because strong onshore wind is effective in generating waves which will reach the coast, and a strong offshore wind tends to subdue existing waves. On the Texas coast during studies made at Mustang Island, offshore wind was accompanied by a sharp drop in breaker height (Davis and Fox, 1972c). On Lake Michigan, where a single storm system was studied as it moved offshore at Zion, Illinois and onshore at South Haven, Michigan, breaker height was over 2 times as great where wind was blowing onshore than where it was blowing offshore (Davis and Fox, 1974b). Therefore, the effective wind speed was used in determining wave height and period in place of the surface wind. For an onshore wind, the effective wind is equal to the onshore wind. However, for an offshore wind, the effective wind is about one third of the surface wind speed. For a wind blowing along the shore, the effective wind speed is two thirds of the surface wind speed. A cosine transformation was used to produce a smooth gradient in effective wind from onshore through alongshore to offshore.

The plot for wave period closely resembles the plot for breaker height with the maxima to the north of the shore site and displaced landward of the shoreline (Figure 21A). The maximum wave period of 9.5 seconds occurs at the same time as the maximum breaker height, 3 hours after the storm has passed over the coast. The plot for wave period has a broad relatively flat area surrounding the maximum, while the plot for breaker height is much steeper, reaching a peak and rapidly dropping off after the peak has been passed. The wave height and periods forecast in the model correspond closely to those encountered on the Oregon coast during November 1973 (Fox and Davis, 1974).

Breaker Angle and Longshore Current Velocity

The plots of breaker angle and longshore current velocity (Figures 21C and D) are similar in many respects to the plot for alongshore wind (Figure 18D). The boundary line which separates the north and south components of the wind is the same as the boundary which separates the north and south breaker angles and longshore currents. For field studies conducted at Holland and Stevensville, Michigan, there was also a close correspondence between the longshore component of the wind and longshore current velocity (Fox and Davis, 1970a and b, and 1971a).

The breaker angle is defined as the acute angle between the wave crest and the shoreline as the wave passes over the nearshore bar. In deep water the wave direction is roughly parallel to the wind direction, and the wave crests are about normal to the wind. The dominate wind direction is often used in wave refraction computer programs to determine the deep water wave angle (Dobson, 1967). As a wave enters shallow water, the celerity decreases and the wave crest is refracted so that it becomes closer to parallel to the beach. Snell's Law of geometrical optics is used for computing the refraction coefficient and breaker angle in the surf zone.

In the breaker angle diagram, the area to the left of the zero line has breaker angles open to the north, and to the right of the zero line, the breaker angles are open to the south (Figure 21C). The largest breaker angles are about 32 degrees when the wind is blowing directly out of the north or the south. As the wind direction swings around from alongshore to onshore or offshore, the breaker angles decrease from 30 degrees to zero (Figures 18B and 21C). When the wind is blowing directly onshore or offshore, the breakers are parallel to the beach and breaker angle is zero.

The plot for longshore current velocity is very similar to the plot for the alongshore component of the wind (Figure 18D and 21D). Three profiles are plotted when the storm passes 200 kilometers north, over the shore site and 200 kilometers south (Figure 20). When the storm path is 200 kilometers north, the longshore current velocity reaches 97.4 centimeters/second to the north, reverses direction after the low has passed, and increases to 81.6 centimeters/second to the south. When the storm passes directly over the study site, the current reverses from 63.0 centimeters/second to the north to 129.7 centimeters/second to the south. However, when the storm path is 200 kilometers south of the shore site, the current to the north is only 4.8 centimeters/second and the southward current is 58.1 centimeters/second. When the storm passes to the south, the reversal in current direction takes place before the low in barometric pressure passes the shore. The maximum long-

Figure 19. Time-distance plot of breaker height and three profiles of breaker height in a circular storm.

Figure 20. Time-distance plot of longshore current and three profiles of longshore current in a circular storm.

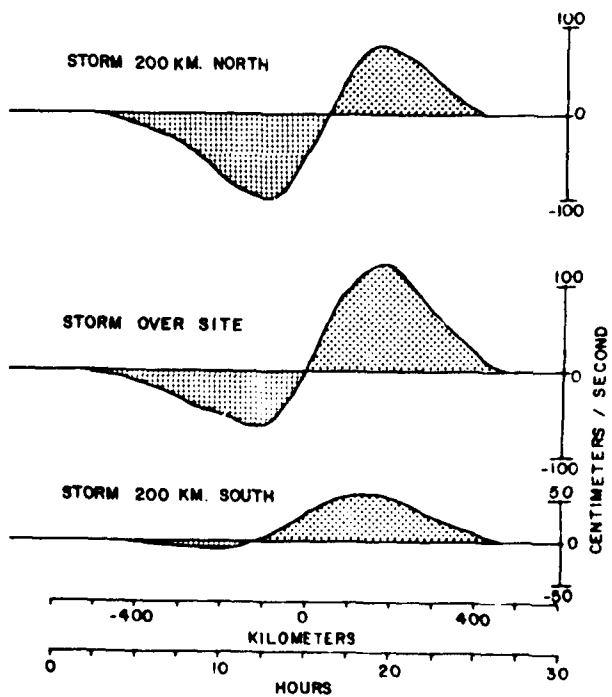
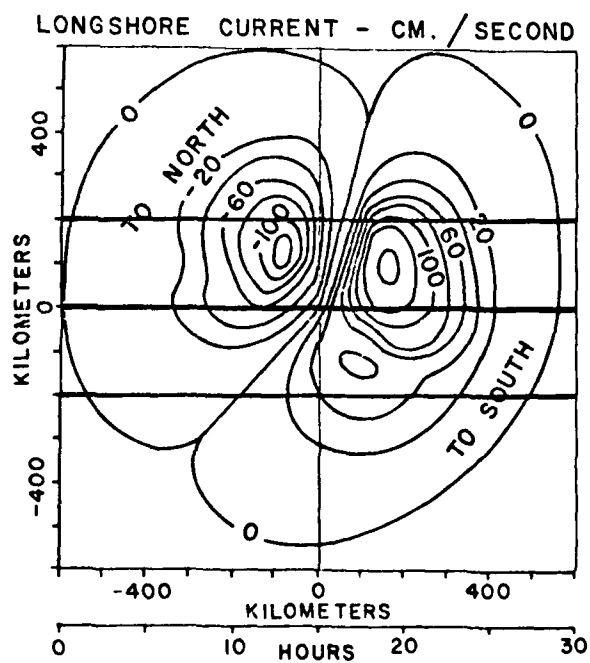
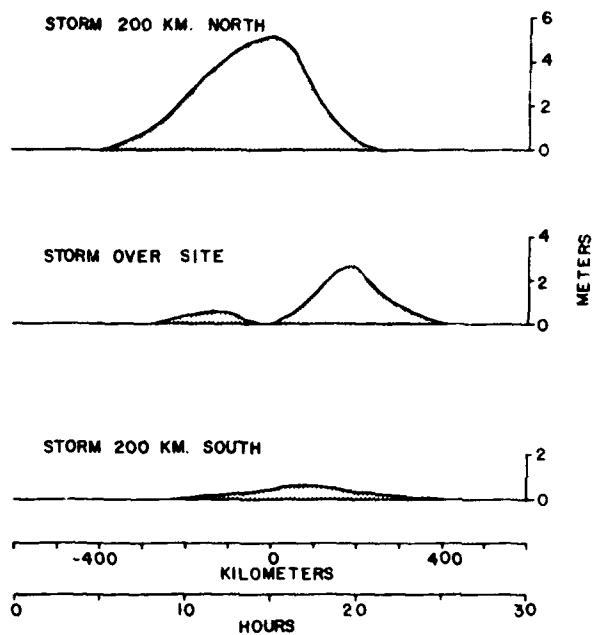
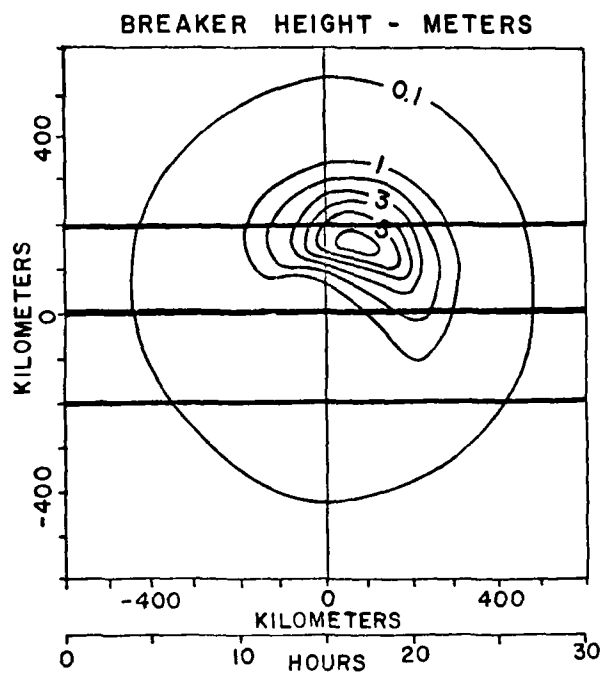
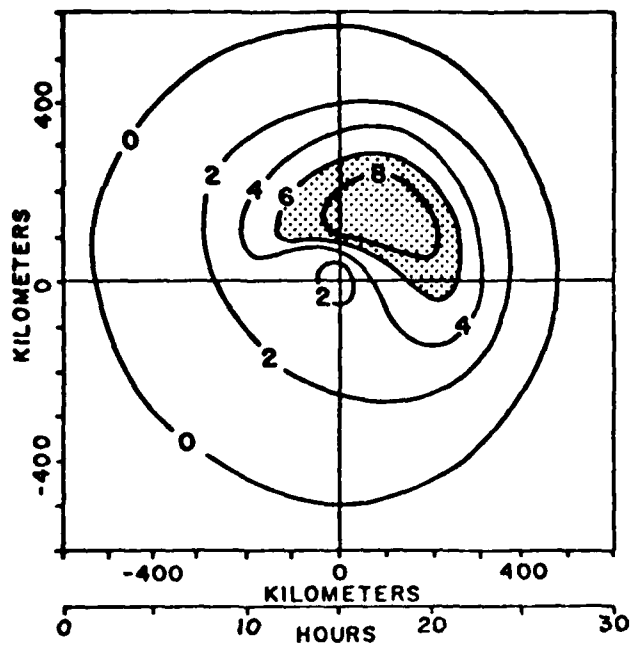
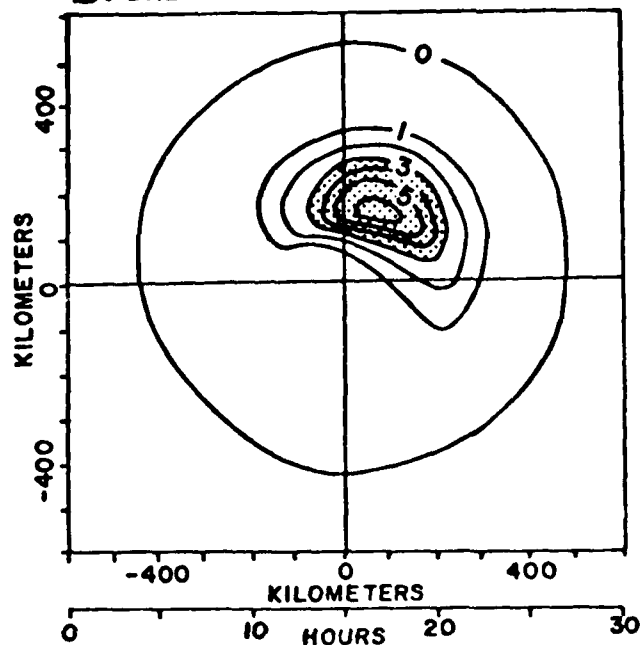


Figure 21. Time-distance plot of A - wave period, B - breaker height, C - breaker angle, and D - longshore current in a circular storm.

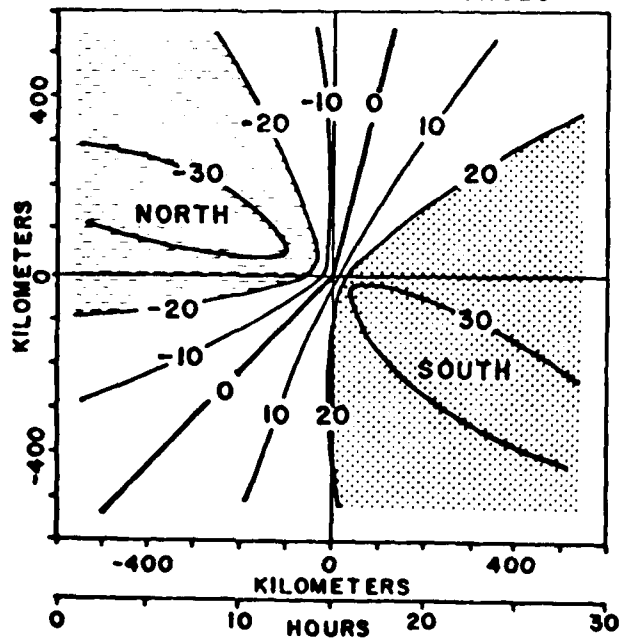
A. WAVE PERIOD - SECONDS



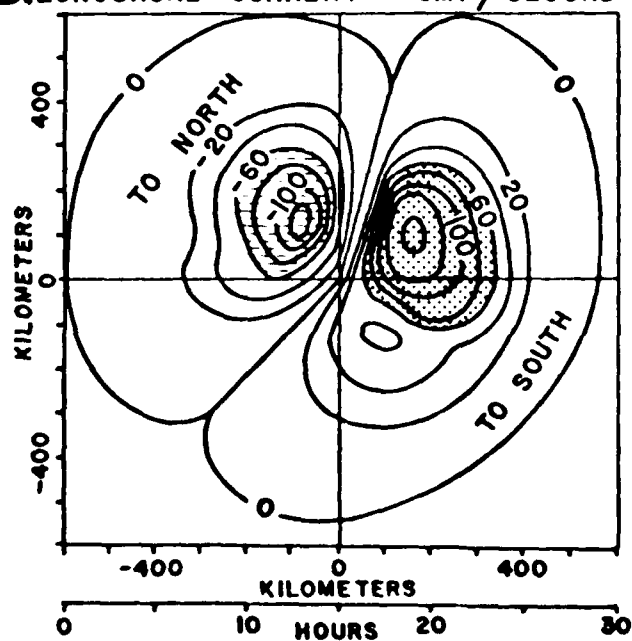
B. BREAKER HEIGHT - METERS



C. BREAKER ANGLE - DEGREES



D. LONGSHORE CURRENT - CM. / SECOND



shore current was 144 centimeters/second to the south 4 hours after the storm passed over the shoreline on a path 100 kilometers north of the shore site (Figure 20).

The longshore current velocity is a function of nearshore slope, breaker height and breaker angle (Longuet-Higgins, 1970). The influence of both breaker angle and breaker height can be seen in the plot for longshore current velocity (Figures 19B, C and D). Other longshore current equations were tested which gave similar patterns, but different absolute velocities.

The circular storm test illustrates the general patterns which emerge in barometric pressure, wind, waves and longshore currents as a storm passes over a coast. If the shape and path of the storm, and the orientation of the shoreline are held constant while the size or intensity of the storm are varied, the same patterns will persist, but the absolute values will change for each of the variables. However, if the shape or path of the storm are changed, the patterns as well as the absolute values will change for each of the variables. In the next section an elliptical storm is used to demonstrate the effect which a change in storm shape would have on the wind, waves and currents.

Elliptical Storm Test

With the coastal storm model, it is possible to vary the size and shape of the storm while holding the intensity constant. The elliptical storm test provides a good example of an oval shaped storm which has its long axis extending to the north-northeast (Figure 22). In both the circular and elliptical tests, the shoreline orientation and nearshore bottom slope are the same.

In the circular and the elliptical storms, the minimum barometric pressure at the center is 1000 millibars, and the pressure at the largest encircling isobar is 1020 millibars (Figures 16 and 22). In the circular storm, the major and minor axes are the same, 300 kilometers. In the elliptical storm, however, the major axis (500 kilometers) is twice the length of the minor axis (250 kilometers). The major axis in the elliptical storm is oriented 30° east of north. Therefore, a low pressure trough extends in a north-northeast direction with the lowest value at the storm center.

The time-distance plot of barometric pressure is identical to a weather map made when the storm center is over the shore site (Figure 22). When the storm track is located to the south of the shore site, the low pressure trough reaches the shore site before the low pressure center passes over the coast. However, when the storm track is to the north of the shore site, the low pressure center reaches the coast before the trough passes over the shore site. Therefore, the long axis of the storm marks the time when the low pressure trough passes over the shoreline.

Although the range in barometric pressure is the same in the circular storm and the elliptical storm, the pressure gradient is steeper in the constricted part of the elliptical storm. The pressure gradient is a function of the size of the storm and the range in barometric pressure. In the circular storm, both the major and minor axis have lengths of 300 kilometers, and therefore the pressure gradient is equal on all side of the storm. In the elliptical storm, the major axis is 500 kilometers and the minor axis is 250 kilometers. Therefore, along the minor axis the pressure gradient is steeper, while it is more gentle along the major axis.

The time-distance plot of surface wind speed has an elliptical shape with the high winds concentrated on the right side of the diagram (Figure 23A). The high wind speeds are a function of the steeper pressure gradient along the minor axis and differences in surface friction over land and sea. With the higher pressure gradient, the wind speed reaches 36.8 meters/second in the elliptical storm, while in the circular storm, it only reaches 30.9 meters/second. The winds greater than 20 meters/second are split into

two areas in the elliptical storm, a major area down the right side of the storm, and a minor area in the northwest quadrant. At the center of the storm along the major axis, the surface wind speed drops down to zero.

The pattern for wind direction in the elliptical storm is significantly different from the pattern in the circular storm (Figures 18B and 23B). In the circular storm, the wind direction contours radiate out from the center and are rotated in a clockwise direction from 14° to 45° . The zero wind direction indicates onshore wind and 180° is an offshore wind. The elliptical storm is constructed along the minor axis and extended along the major axis. Therefore, the wind direction contours are gathered around the major axis which is pointed 30° east of north. Similarly, the contours are spread out from the minor axis. In the elliptical storm the zero contour extends 45° east of north, and the 180° contour extends 67° west of south. The 270° contour indicating south winds points 17° east of north and the 90° contour for north winds extends 25° west of south.

The difference in wind direction pattern results in major changes in the onshore and alongshore wind patterns in the elliptical storm (Figures 23C and D). In the circular storm, the boundary line between onshore and offshore winds runs in a generally east-west direction with onshore winds when the storm track is to the north and offshore winds when the storm track is to the south of the study site. In the elliptical storm, on the other hand, the boundary between onshore and offshore winds has shifted so that it runs generally north-south with onshore winds to the east and offshore winds to the west (Figure 23C). As the storm approaches the coast the winds are offshore, and after the storm has passed over the shoreline the winds shift to onshore. When the storm passes to the south of the shore site, the shift from offshore to onshore winds takes place shortly after the low pressure trough passes over, but when the storm track is to the north, the shift in wind direction shortly precedes the low pressure trough. The maximum offshore wind is 21.4 meters/second as the storm approaches, and the maximum onshore wind is 30.2 meters/second after the storm has passed over the coast.

The boundary for the alongshore wind which separates the north wind from the south wind extends generally in a northwest-southeast direction (Figure 23D). It resembles the alongshore wind diagram for the circular storm, but the axes are rotated about 30° in a clockwise direction (Figures 18D and 23D). The maximum south wind of 21.1 meters/second occurs when the storm track is to the north of the shore site and after the storm has passed over the coast. For the north wind, the maximum of 28.1 meters/second occurs along a storm track 200 kilometers south of the shore site after the storm has passed the coast.

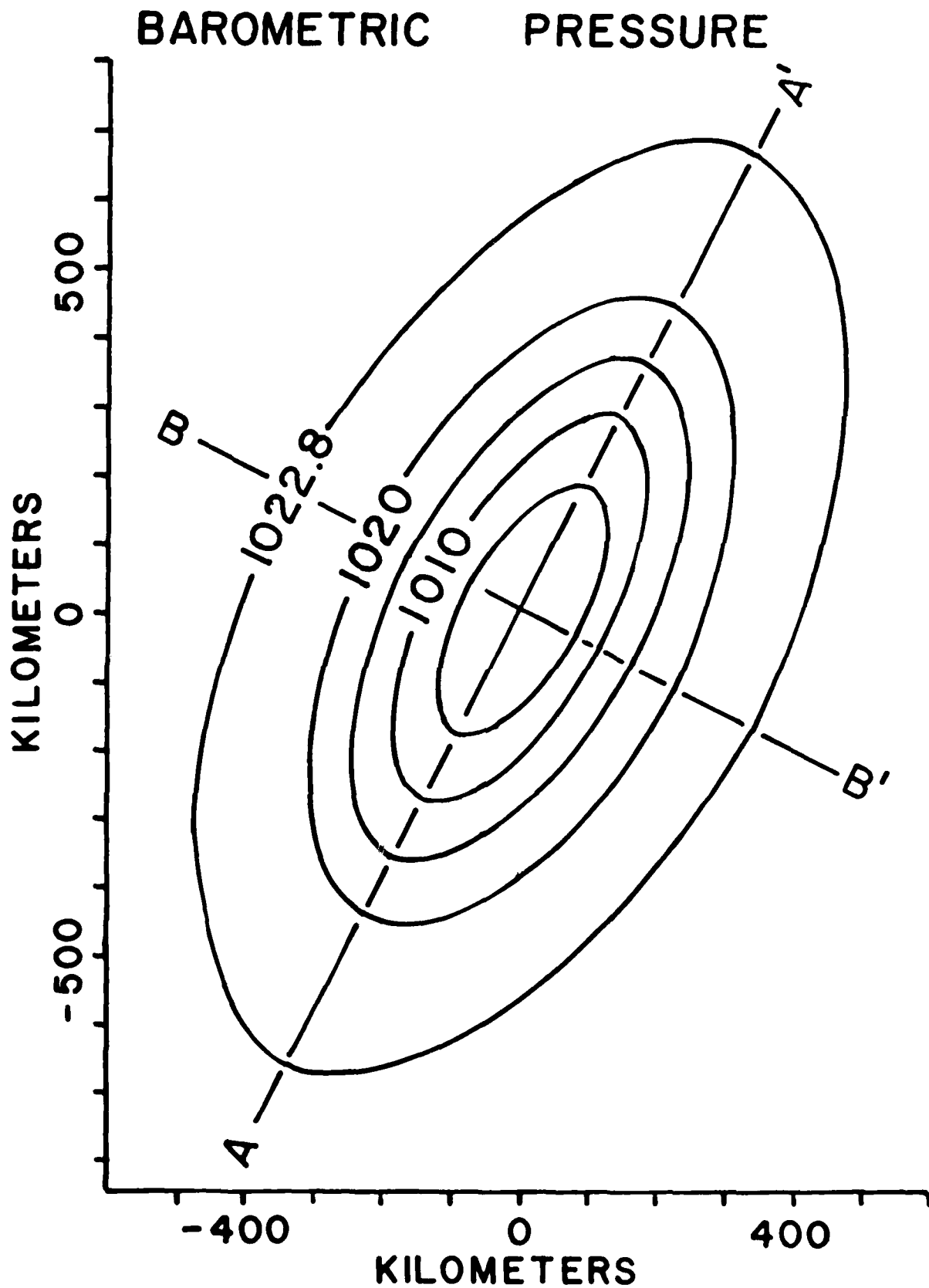
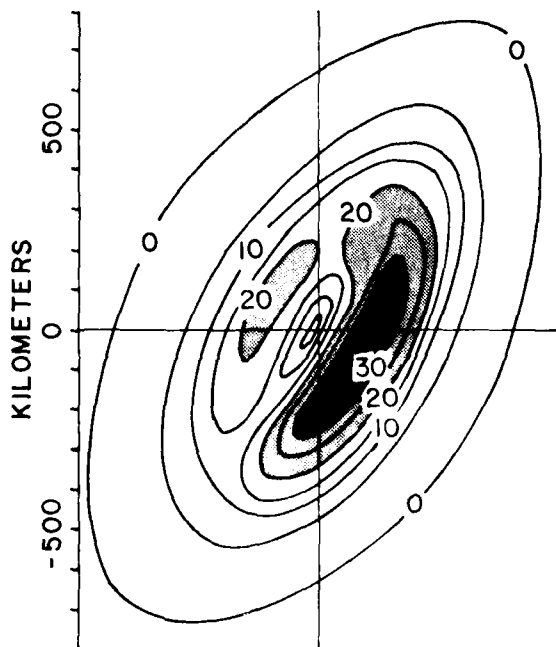


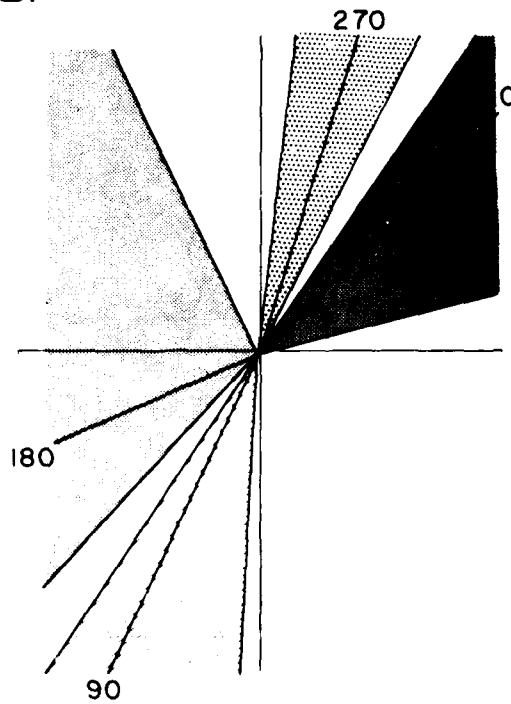
Figure 22. Time-distance plot of barometric pressure in an elliptical storm.

Figure 23. Time-distance plot of A - surface wind speed, B - wind direction, C - onshore wind and D - alongshore wind in an elliptical storm.

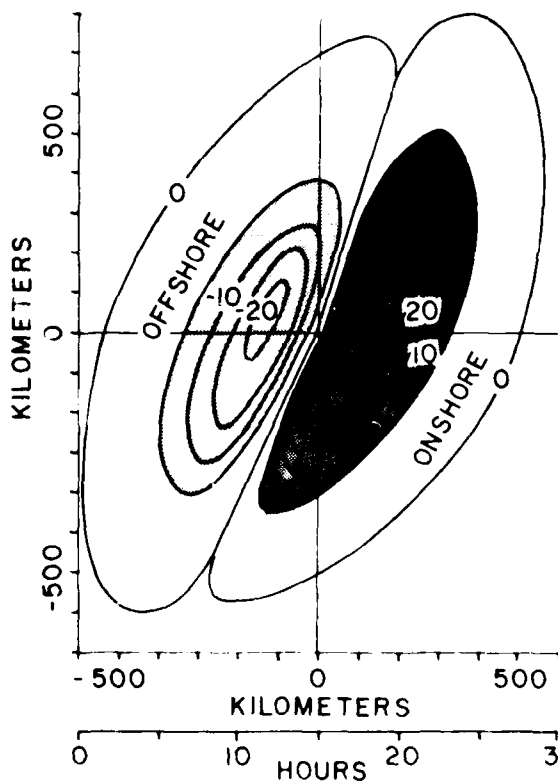
A. SURFACE WIND



B. WIND DIRECTION



C. ONSHORE WIND



D. ALONGSHORE WIND

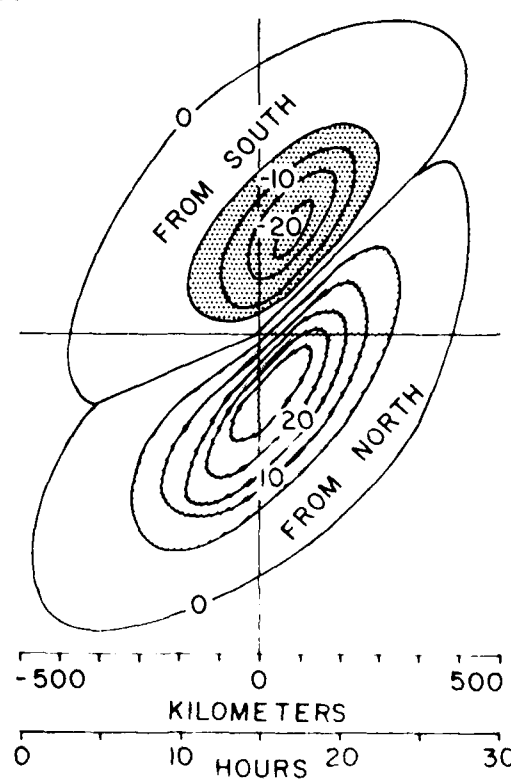
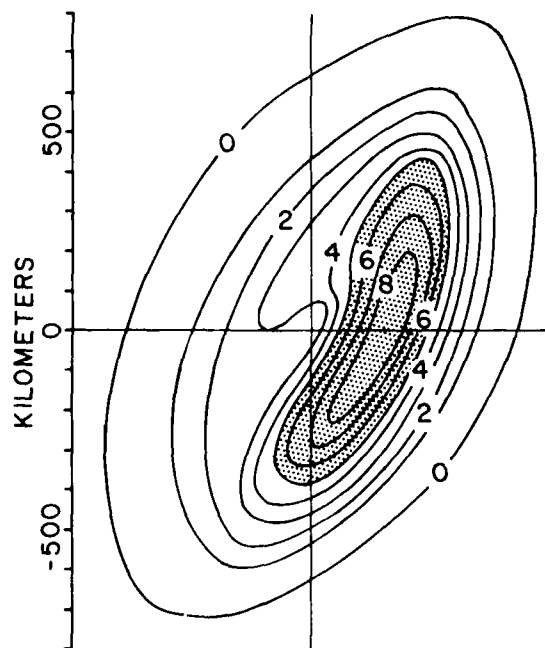
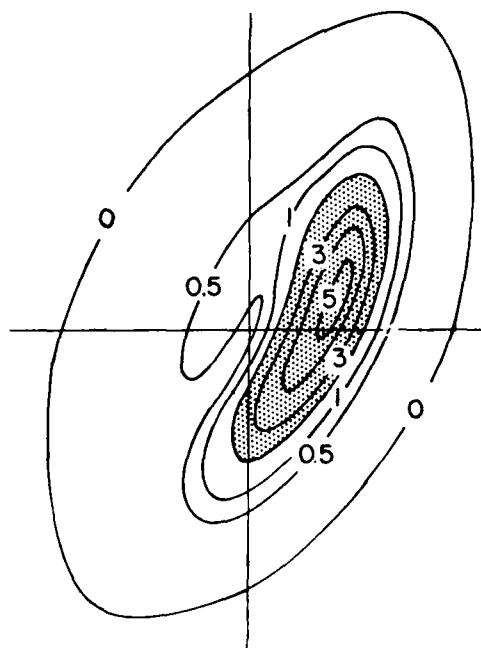


Figure 24. Time-distance plot of A - wave period, B - breaker height, C - breaker angle and D - longshore current in an elliptical storm.

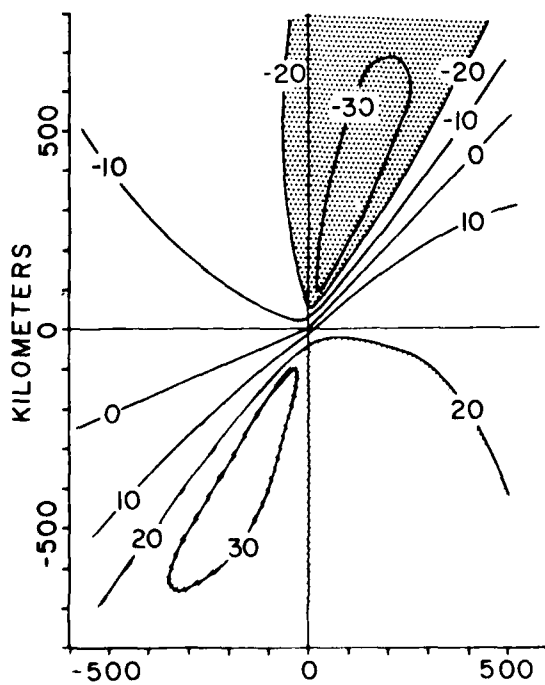
A. WAVE PERIOD



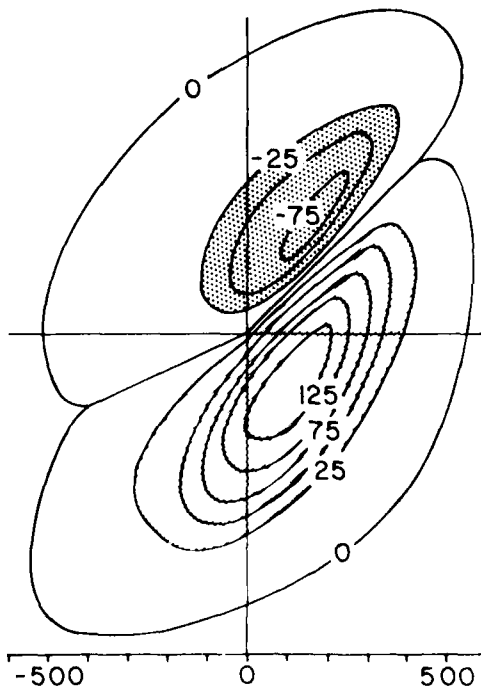
B. BREAKER HEIGHT



C. BREAKER ANGLE



D. LONGSHORE CURRENT



0 10 20 30
KILOMETERS
HOURS

0 10 20 30
KILOMETERS
HOURS

The plots for wave period and wave height in the elliptical storm are very similar and closely resemble the plots for wind speed and onshore wind (Figures 23A and C, and 24A and B). Both wave period and breaker height reach their maxima after the storm trough has passed over the coast and the wind has shifted from offshore to onshore. In the elliptical storm, the maximum wave period is 8.9 seconds and the greatest breaker height is 5.1 meters.

The greatest breaker angles for the elliptical storm occur when the wind is blowing out of the south (270°) or the north (90°) (Figures 22B and 23C). When the storm track is to the north of the shore site, the greatest northerly breaker angles (32.3°) are present just before the low pressure trough passes over the coast. However, when the storm track is to the south of the study site, the largest southerly breaker angles (32.4°) occur just after the storm trough has passed the shore.

The plot for longshore current in an elliptical storm is very similar to the plot for alongshore wind (Figures 23D and 24D). The boundaries between north and south winds and north and south currents follow the same line and the maxima are in the same position. The maximum northward flowing longshore current (44 centimeters/second) occurs when the storm is on a track 300 kilometers north of the shore site, while the maximum southward flowing current (143 centimeters/second) occurs on a storm track 100 kilometers south of the shore site.

In summarizing the comparison between a circular storm and an elliptical storm of the same intensity, the differences in barometric pressure and wind direction influence the other environmental parameters. In the circular storm, the highest surface winds are found when the storm track is to the north of the shore site while in the elliptical storm, the maximum winds occur in a north-northeast trending zone to the right of the low pressure trough. The boundary between offshore and onshore winds lies generally east-west for the circular storm and north-south for the elliptical storm. For alongshore winds, the boundary between north and south winds is rotated about 30° in a clockwise direction in the elliptical storm. In both the circular and elliptical storm, the wind direction contours radiate out from the center and are rotated clockwise due to surface friction, but in the elliptical storm, the contours are gathered around the major axis. Wave period and breaker height in the circular storm resemble wind speed and form pods to the north of the shore site, while in the elliptical storm, period and breaker height form linear trends to the east of the shore site. For both storms, the longshore current follows the same pattern as the alongshore wind.

CONCLUSIONS

A mathematical model has been developed and programmed for a computer to forecast barometric pressure, wind, waves and longshore currents during passage of a storm across a coastal site. The following set of conclusions can be drawn from the coastal storm model.

1. The shape of a coastal storm can be approximated with an elliptical model by specifying the lengths of the major and minor half axes and the orientation of the major axis.
2. The barometric pressure profiles along the major and minor axes of the ellipse are represented by a series of inverted normal curves.
3. Geostrophic wind speed and direction at any point on the earth's surface under a storm are computed from the latitude and barometric pressure gradient.
4. Geostrophic wind speed and direction are used to compute surface wind speed and direction over land or sea.
5. Wave period, height and direction are calculated from the wind speed, fetch and duration as the storm passes over the coast.
6. Longshore current speed and direction are computed from wave height, period and direction, and nearshore bottom slope.
7. Wave and current hindcast data can be used to test the model when the size, shape, intensity and track of the storm are known.
8. If the storm azimuth and velocity are assumed to be constant, forecasts of wind, wave and longshore currents can be made for a coastal storm.

REFERENCES CITED

- Baur, F. and Phillips, H., 1938, Untersuchungen der Reibung bei Luftstromungen über dem Meer. Ann. Hydrogr. u. mar. Meteor., vol. 66, no. 6, pp. 279-296 (cited in Godske et al, 1957).
- Birkemeier, W.A., and Dalrymple, R.A., 1976, Numerical models for the prediction of wave set-up and nearshore circulation: Tech. Rept. no. 1, ONR Contract N00014-76-C-0342, University of Delaware, 127 p.
- Bretschneider, C.L., 1952, Revised wave forecasting relationships, Proc. of 2nd Conf. on Coastal Engineering, A.S.C.E., Council on Wave Research.
- Bretschneider, C.L., 1958, Revisions in wave forecasting, deep and shallow water, Proc. of 6th Conf. on Coastal Engineering, A.S.C.E. Council on Wave Research.
- C.E.R.C., 1973, U. S. Army Coastal Engineering Research Center, Shore Protection Manual, TR 4, vol. 1, pp. 1-496.
- Cole, F.W., 1970, Introduction to Meteorology, John Wiley and Sons, New York, 388 p.
- Collins, J.I., 1971, Longshore currents and wave statistics in the surf zone: Tech. Rept. No. TC-149-2, ONR Contract N00014-64-C-0107, Tetra Tech, 46 p.
- Davis, R.A., Jr., and Fox, W.T., 1971, Beach and nearshore dynamics in eastern Lake Michigan: Tech. Rept. No. 4, ONR Contract N00014-69-C-0151, Williams College, 145 p.
- Davis, R.A. Jr., and Fox W.T., 1972a, Four-dimensional model for beach and inner nearshore sedimentation: Jour. of Geology, vol. 80, pp. 484-493.
- Davis, R.A. Jr., and Fox, W.T., 1972b, Coastal processes and near-shore sand bars: Jour. Sed. Petrology, vol. 42, pp. 401-412.
- Davis, R.A. Jr., and Fox, W.T., 1972c, Coastal dynamics along Mustang Island, Texas: Tech. Rept. no. 9, ONR Contract N00014-69-C-0151, Williams College, 69 p.
- Davis, R.A. Jr., and Fox, W.T., 1974a, Coastal dynamics of Cedar Island, Virginia, Tech. Rept. no. 11, ONR Contract N00014-69-C-0151, 66 p.

- Davis, R.A. Jr., and Fox, W.T., 1974, Simultaneous process-response study on the east and west coasts of Lake Michigan: Tech. Rept. no. 13, Contract N00014-69-C-0151, 61 p.
- Davis, R.A. Jr., and Fox, W.T., 1975, Process-response patterns in beach and nearshore sedimentation: I, Mustang Island, Texas, Jour. Sed. Petrology, vol. 45, pp. 852-865.
- Defant, A., 1961, Physical Oceanography, vol. 2, Pergamon Press, New York, 598 p.
- Detrick, G., 1944, Die Gezeiten des Weltmeeres als geograph. Erscheinung Z d. ges. Erdkunde, p. 69. Berlin.
- Dobson, R.S., 1967, Some applications of a digital computer to hydraulic engineering problems: Tech. Rept. no. 8, Contract NONR 225 (85), Stanford Univ. 163 p.
- Fox, W.T., and Davis, R.A. Jr., 1970a, Fourier analysis of weather and wave data from Lake Michigan, Tech. Rept. no. 1, ONR Contract N00014-69-C-0151, 47 p.
- Fox, W.T., and Davis, R.A. Jr., 1970b, Profile of a storm-wind, waves and erosion on the southeastern shore of Lake Michigan, Proc. 13th Conf. on Great Lakes Research, p. 233-241.
- Fox, W.T., and Davis, R.A. Jr., 1971a, Fourier analysis of weather and wave data from Holland, Michigan, July 1970: Tech. Rept. no 3, Contract N00014-69-C-0151, 79 p.
- Fox, W.T., and Davis, R.A. Jr., 1971b, Computer simulation processes in eastern Lake Michigan: Tech. Rept. no. 5, ONR Contract N00014-69-C-0151, 114 p.
- Fox, W.T., and Davis, R.A. Jr., 1972, Coastal processes and beach dynamics at Sheboygan, Wisconsin, July 1972: Tech. Rept. no. 10, ONR Contract N00014-69-C-0151, 94 p.
- Fox, W.T., and Davis, R.A. Jr., 1973, Simulation model for storm cycles and beach erosion on Lake Michigan: Geol. Soc. Amer. Bull., vol. 84, pp. 1769-1790.
- Fox, W.T., and Davis, R.A. Jr., 1973, Beach processes on the Oregon Coast: Tech. Rept. no. 12, ONR Contract N00014-69-C-0151, 81 p.
- Galvin, C.J. Jr., and Eagleson, P.S., 1965, Experimental study of longshore currents on a plane beach, T M-10, U.S. Army Coastal Engineering Research Center, Washington, D.C., 80 p.

- Godske, C.L., Bergeron, T., Bjerknes, J., and Bundgaard, R.C., 1957, Dynamic Meteorology and Weather Forecasting, Amer. Meteorology Society, Boston, Mass., and Carnegie Inst. of Washington, 800 p.
- Goldsmith, V., Morris, W.D., Byrne, R.J., and Whitlock, C.H., 1974, Wave climate model of mid-Atlantic and shoreline (Virginian Sea), NASA SP-358, V.I.M.S. SRAMSOE no. 38, 146 p.
- Hesselberg, Th., and Sverdrup, H.U., 1915, Die Riebung in der Atmosphere. Veroff. Geophys. Inst. Univ. Leipzig, ser. 2, vol. 1, pp. 241-301, (cited in Godske, et al, 1957).
- Kauffman, C.F., 1973, Swell prediction by a multiple point-source swell generation model, M.S. Thesis, Naval Postgraduate School, Monterey, Calif., 73 p.
- Komar, P.D., 1969, Longshore transport of sand on beaches, Ph. D. Thesis, San Diego, Univ. of California, 143 p.
- Komar, P.D., 1973, Computer models of delta growth due to sediment input from rivers and longshore currents, Geol. Soc. Amer. Bull. vol. 84, pp. 2217-2226.
- Komar, P.D., and Gaughan, M., 1973, Airy wave theory and breaker height prediction, Proc. Thirteenth Conf. Coastal Engr., 1: 405-418.
- Komar, P.D., and Inman, D.L., 1970, Longshore sand transport on beaches, Jour. Geophys. Research, vol. 75, pp. 5915-5927.
- Lewis, W.V., 1931, Effect of wave incidence on the configuration of a shingle beach, Geog. Jour., vol. 78, pp. 131-148.
- Longuet-Higgins, M.S., 1970, Longshore currents generated by obliquely incident sea waves: Jour. Geophys. Research, vol. 75, pp. 6778-6801.
- Longuet-Higgins, M.S., and Stewart, 1964, Radiation stress in water waves: a physical discussion with application, Deep-Sea Research, vol. 11, pp. 529-562.
- Louden, R.K., 1967, Programming the IBM 1130 and 1800, Prentice-Hall, Inc., Englewood Cliffs, N.J., 433 p.
- McCammon, R.B., 1971, Environment pattern reconstruction from sample data. L. Mississippi Delta Region, Tech. Rept. no. 1, ONR Contract N00014-69-A-0090, Univ. of Ill. at Chicago Circle, 82 p.

- McCallagh, M.J., and King, C.A.M., 1970, SPITSYM, a Fortran IV computer program for spit simulation, Kansas Geol. Surv. Computer Contr., 50, 20 p.
- Munk, W.H., 1949, Solitary wave theory and its application to surf problems, Annals of New York Academy of Sciences, vol. 51, pp. 376-424.
- Noda, E.K., Sonu, C.J., Rupert, V.C., and Collins, J.I., 1974, Nearshore circulations under sea breeze conditions and wave-current interactions in the surf zone; Tech. Report TC-149-4, ONR Contract N00014-69-C-0107, Tetra Tech, Inc., Pasadena, Calif., 216 p.
- Owens, E.H., and Frobel, D.H., 1975, Environmental, morphological and sediment size data from two barrier beaches in the Magdalen Islands, Quebec, G.S.C. Project 740009, Bedford Institute, Dartmouth, Nova Scotia, Canada, 447 p.
- Putnam, J.A., Munk, W.H., and Traylor, M.A., 1949, The prediction of longshore currents, Trans. Amer. Geophys. Union, vol. 30, pp. 337-345.
- Resio, D.T., and Hayden, B.P., 1973, An integrated model of storm-generated waves, Tech. Rept. no. 8, Contract N00014-69-A-0060, Univ. of Virginia, 288 p.
- Snodgrass, F.E., and others, 1966, Propagation of ocean swell across the Pacific. Philosophical Trans., Royal Soc. of London, vol. 259, pp. 431-497.
- Sonu, C.J., and van Beek, J.L., 1971, Systematic beach changes on the Outer Banks, North Carolina, Jour. Geol., vol. 79, pp. 416-425.
- Sverdrup, H.U., and Munk, W.H., 1947, Wind, Sea and Swell; Theory of Relations for forecasting, Publication No. 601, U.S. Navy Hydrographic Office, Washington, D. C.
- Westwater, F.L., 1943, Wind structure over the sea, Quart. Jour. R. Metero. Soc., vol. 69, pp. 207-213.

APPENDIX A. COASTAL STORM PROGRAMS

```

// JOB
// FOR
*IOCS(CARD,1132,PRINTK)
*ONE WORD INTEGERS
*LIST SOURCE PROGRAM
COMMON U(130),V(130)
DIMENSION TITLE(20),DAY(5)
DATA A1/' KIL',' NAU','A2/'OMET','TICA','A3/'ERS','L MI','
1 A4/' 'LES','B1/' MET',' FEE','B2/'ERS','T '
2C1/' JOW',' FOO','C2/'LES','T PO','C3/' 'JUNDS'

CARD 1 - TITLE

CARD 2 - STARTING DATE, TIME AND INPUT-OUTPUT OPTIONS

COLS. 1-2 ISTR- STARTING HOUR
COLS. 3-22 DAY - STARTING DATE

COL. 23 INAUT- INPUT OPTION
0 = METRIC UNITS
1 = NAUTICAL MILES AND FEET

COL. 24 NAUT - OUTPUT OPTION
0 = METRIC UNITS
1 = NAUTICAL MILES, FEET AND KNOTS

CARD 3 - STORM PARAMETERS

COL. 1 STORM INPUT OPTIONS - SEE CARD 6
1 = HINDCASTING - STORM POSITION AT 6 HOUR INTL
2 = FORECASTING - INITIAL POSITION, AZIMUTH AND VELOCITY

COL. 2 TIDE PREDICTION OPTION
0 = TIDE PREDICTION NOT INCLUDED - OMIT CARD 4
1 = TIDE PREDICTION INCLUDED - SEE CARD 4

COL. 3 LONGSHORE CURRENT EQUATION OPTION
1 = FOX AND DAVIS, 1972
2 = LONGUET-HIGUINS, 1970
3 = C.E.R.C., 1972
4 = KOMAR AND INMAN, 1970

COLS. 4-6 NX - NUMBER OF STORM POSITIONS
SIX HOUR INTERVALS FOR HINDCASTING
ONE HOUR INTERVALS FOR FORECASTING

COLS. 7-12 BNFC- AVERAGE BASIN FETCH IN KM. (NAUT. MI.)
COLS. 13-17 TINT - TIME INTERVAL BETWEEN STORM POSITIONS
NORMAL SETTING IS 1.0 HOURS

COLS. 18-24 PMIN - MINIMUM BAROMETRIC PRESSURE IN MILLIBARS
COLS. 25-31 PMAAX- PRESSURE AT LARGEST ENCIRCLING ISOBAR
COLS. 32-38 SLAT - LATITUDE AT SHORE SITE

*** STORM SIZE ***

COLS. 39-42 AH - MAJOR HALF-AXIS (EFFECTIVE LONG RADIUS)
COLS. 43-46 BR - MINOR HALF-AXIS (EFFECTIVE SHORT RADIUS)
COLS. 49-54 LAZ - ORIENTATION OF MAJOR HALF AXIS PLUS OR MINUS 90 DEGREES FROM NORTH.

CARD 4 - TIDE PREDICTION - OPTION FROM CARD 3

COLS. 1-5 ST - SPRING TIDE RANGE IN FEET
COLS. 6-10 TN - NEAP TIDE RANGE IN FEET
COLS. 11-17 DAY - NUMBER OF DAYS FROM LAST SPRING TIDE
COLS. 18-24 THH - HOUR OF LAST HIGH SPRING TIDE

COLS. 25-31 FN - TIDAL FURN NUMBER
0.0 TO .25 = SEMIDIURNAL TIDE
.25 TO .50 = MIXED SEMIDIURNAL TIDE
.50 TO .75 = MIXED DIURNAL TIDE
GREATER THAN .75 = DIURNAL TIDE

COLS. 32-34 SCLF - NEARSHORE BOTTOM SLOPE AT LOW TIDE
COLS. 35-37 SCLH - NEARSHORE BOTTOM SLOPE AT HIGH TIDE
COLS. 38-40 TOLN - NEAR TIDE LEVEL IN FEET

CARD 5 - SHORE SITE LOCATION

COLS. 1-5 LON - LONGITUDE IN NAUTICAL MILES
COLS. 6-10 LAT - LATITUDE IN NAUTICAL MILES
COLS. 11-15 SHAZ - SHORE DIRECTION - CLOCKWISE FROM NORTH
COLS. 16-20 SCLF - AVERAGE NEARSHORE BOTTOM SLOPE
COLS. 21-25 ISLN - ISLAND CONTINENTAL, EAST OF BARKER ISLAND
0 = SMALL OFFSHORE ISLAND
COLS. 26-30 BLCH - BAROMETRIC PRESSURE IN
CARD 6 - STORM VELOCITY

FOR OPTION 1 - HINDCASTING - STORM POSITIONS AT 6 HOUR INTERVALS FROM INITIAL HOUR

COLS. 1-5 LON - LONGITUDE IN NAUTICAL MILES
COLS. 6-10 LAT - LATITUDE IN NAUTICAL MILES

FOR OPTION 2 - FORECASTING - VELOCITY, AZIMUTH AND POSITION

COLS. 1-5 VEL - STORM VELOCITY IN KNOTS

```

[illegible]

[illegible]

```

      ESUM=ESUM+E
      UPT=U(1)+A*CK+*.5
      VPT=V(1)+A*CK+*.5
      WSRF=W*SRF*CKTS
      UN=ONSH*CKTS
      AL=ALSH*CKTS
      EF=EFWD*CKTS
      HTI=HEIGT*CMF
      HBI=HB*CMF
      TID1=TIDX*CMF
      VI=VLS*CCMF
      PP=P/CPQ
      WRITE(3,530) 1HOUR,UPT,VPT,X,Y,PP,SHANG+W*SRF,ON+AL,EF,HTI,PEKJU,
530 1 HBI,BRANG,VI
      FORMAT(3X,'2F7.0,2F7.2,F7.1,F7.1,F7.1,F7.1,F7.2,F7.1,F7.2')
      IF(IFTD.GT.O) WRITE(3,531) TID1
531 FORMAT(1H+'114X',F5.2)
      1HOUR=1HOUR+IFIX(TINT)
      IF(1HOUR.GT.=24) 1HOUR=1HOUR-24
50 CONTINUE
      ELCT=E+EP
      ESUM=ESUM+CJOUJL
      ELCT=ELCT+CJOUJL
      EP=E*CJOUJL
      EN=E*CJOUJL
      WRITE(3,540) ESUM,C1(NN),C2(NN),C3(NN),ELCT,C1(NN),C2(NN),C3(NN)
540 FORMAT(1X,'/',1X,T5,WAVE ENERGY IN THE BREAKER ZONE ='E10.3+3A4//
      11X,T5,'TOTAL LONG-SHORE CURRENT ENERGY ='E10.3+3A4//)
      WRITE(3,542) EP,C1(NN),C2(NN),C3(NN),EN,C1(NN),C2(NN),C3(NN)
542 FORMAT(1X,T5,'TOTAL POSITIVE LONG-SHORE CURRENT ENERGY ='E10.3+
      3A4//1X,T5,'TOTAL NEGATIVE LONG-SHORE CURRENT ENERGY ='E10.3+3A4//)
      GO TO 80BQ
1000 CALL EXIT
END

// JOB
*DELETE STMX
*STORE AS UA STMX

// JOB FORE 3-B6-001
// FOR
*IOCS(CARD+1132,PRINTEN)
*ONE WORD INTEGERS
*LIST SOURCE PROGRAM
SUBROUTINE FCR(XA,A,NAUT)
COMMON U(130),V(130)

FCRCASTING = COMPUTE STORM POSITIONS FROM INITIAL POSITION,
VELOCITY AND AZIMUTH

TINT=1.0
RAD=.572958
READ(2,903) SVFL,AZI,U(1),V(
903 FORMAT(4F7.0)
IF(NAUT) 1,1,2
1 WRITE(3,910) SVFL,AZI
910 FORMAT(9X,'STORM VELOCITY ='F4.0,' KILOMETERS/HOUR'/
1 9X,'STORM AZIMUTH ='F4.0/)
GO TO 5
2 WRITE(3,911) SVFL,AZI
911 FORMAT(9X,'STORM VELOCITY ='F4.0,' KNOTS'/
1 9X,'STORM AZIMUTH ='F4.0/)
5 CONTINUE
U(1)=U(1)/A
V(1)=V(1)/A
DIST=SVFL*TINT/A
AZM=90.-AZI
IF(AZM) 31,32,33
31 AZM=Azm+360.
32 DO 35 I=2,NX
U(I)=(U(1)-1)*DIST*COS(AZM/RAD)
V(I)=(V(1)-1)*DIST*SIN(AZM/RAD)
35 CONTINUE
RETURN
END

// DUP
*DELETE FORE
*STORE AS UA FORE

// JOB HIND 3-B6-001
// FOR
*IOCS(CARD+1132,PRINTEN)
*ONE WORD INTEGERS
*LIST SOURCE PROGRAM
SUBROUTINE HIND(XA,A)
COMMON U(130),V(130)
DIMENSION X(30),Y(30)

HINDCASTING = COMPUTE STORM POSITIONS AT 1 HOUR INTERVALS FROM
6 HOUR POSITIONS ON WEATHER MAPS

DO 15 I=1,NX
XA(I)=X(902) *X(1),Y(I)=
902 FORMAT(2F7.0)
X(1)=X(1)/A
Y(1)=Y(1)/A
15 CONTINUE
NX=NX-1
DO 20 I=1,NXI
I(1)=I*6-5
U(1)=U(1)

```

```

      V(I1)=Y(I1)
      DIFU=(X(I1+1)-X(I1))/6.
      DIFV=(Y(I1+1)-Y(I1))/6.
      DO 20 J=1+5
      M=I1+J
      U(M)=U(M-1)+DIFU
      V(M)=V(M-1)+DIFV
20  CONTINUE
      I1=NX*6-5
      U(I1)=X(NX)
      V(I1)=Y(NX)
      NX=I1
      RETURN
      END

// DUP
*DELETE
*STORE      WS  UA  HIND

// JOB
// FOR
*IOCS(CARD,1132,PRINTER)
*ONE WORD INTEGERS
*LIST SOURCE PROGRAM
      SUBROUTINE LOCAT(IUST,VST,ULOC,VLOC,SHAZ,X,Y,EAZ,P,J)
C
C      U AND V COORDINATES ARE READ INTO THE PROGRAM IN KILOMETERS AND
C      CONVERTED TO UNITS PROPORTIONAL TO THE MAJOR AXIS. THE U AND V
C      COORDINATE SYSTEM IS A RECTANGULAR GRID WITH U POINTING EAST,
C      V POINTING NORTH, AND THE ORIGIN LOCATED TO THE SOUTHWEST OF THE
C      SHORE LOCATION.
C
C      SUBROUTINE LOCAT IS USED TO ESTABLISH THE X AND Y COORDINATE
C      SYSTEM WITH THE ORIGIN AT THE CENTER OF THE STORM AND POSITIVE
C      Y POINTING INSHORE, NEGATIVE Y POINTING OFFSHORE, POSITIVE X
C      TO THE RIGHT FACING INSHORE, AND NEGATIVE X TO THE LEFT FACING
C      INSHORE.
C
      RAD=57.2958
      U=UST-ULOC
      V=VST-VLOC
      Z=SQRT(U**2+V**2)
      CALL ARCTAN(U,V)
      A=ATN(SHAZ/RAD)
      X=Z*COS(A)
      Y=Z*SIN(A)
      DIF=EAZ+90.-SHAZ
      IF(DIF.GT.360.) DIF=DIF-360.
      AZ=A-DIF/RAD
      P=2*CCS(AZ)
      Q=2*SIN(AZ)
      RETURN
      END

// DUP
*DELETE
*STORE      WS  UA  LOCAT

// JOB T
// XEC CSTRM 2
*LOCALCSTRM,LOCAT,WIND,DECAY,ETIME,FETCH,WAVES,SUMF,ENRGY,TIDE,HIND,
*LOCALFOREC
HOLLAND, MICHIGAN
1 JULY 7, 1970      11
101 24 150. 1.0      42.
1000. 0.      90.      .033

// JOB
// FOR
*IOCS(CARD,1132,PRINTER)
*ONE WORD INTEGERS
*LIST SOURCE PROGRAM
      SUBROUTINE ELIPS(A,B,X1,Y1,PMIN,PMAX,P1,ERAD,XA,YA,DZA)
C
C      SUBROUTINE ELIPS IS USED TO DETERMINE THE WIND ANGLE AND PRESSURE
C      GRADIENT AT ANY POINT WITHIN AN ELLIPTICAL STORM.
C
      RAD=57.2958
      R=B/A
      AA=A/A
      BA=B/A
C
C      A AND B ARE THE MAJOR AND MINOR AXES OF THE STORM ELLIPSE
C      POINT X1,Y1 LIES ON A SECOND ELLIPSE WITH AXES A1 AND B1.
C
      A1=SQRT(X1**2+Y1**2/R**2)
      B1=AA*A1
      C1=A1-B1**2/A1**2*X1
C
C      X2 IS THE INTERSECTION OF THE A AXIS WITH A LINE NORMAL TO THE
C      TANGENT OF THE SECOND ELLIPSE AT X1,Y1.
C
      X2=C1/(1.-BA**2/AA**2)
      Y2=SQRT(BA**2*(1.-X2**2/AA**2))
C
C      X2 AND Y2 ARE AT THE INTERSECTION OF THE LINE NORMAL TO THE
C      TANGENT OF THE SECOND ELLIPSE AND THE STORM ELLIPSE.
C
      IF(Y2.LT.1E-2)
      1 Y2=-Y2
      2 CONTINUE

```



```

D2=SQR(1+(X0)**2 + Y1**2)
D2=SQR(1+(X2-A0)**2 + Y2**2)
D2A=D2/A
IF(D2A.GT.A) D2A=A
ENAD=D1/D2
Z1=3.*A*D
PDIF=PMAX-PMIN
PINC=PCIF*(P1-Z1**2/Z1)
H2=PMAX-PINC

C      P1 IS THE BAROMETRIC PRESSURE AT X0 COMPUTED ON A NORMAL CURVE
C      ALONG THE MAJOR AXIS. THIS PRESSURE VALUE IS USED IN DETERMINING
C      THE PRESSURE GRADIENT NORMAL TO THE ISOBAR AT POINT A(X,Y).
C
      IF(Y1.EQ.0.D) Y1=Y1+.71
      IF(X1.EQ.0.D) X1=X1-.61
      XA=X1**2/Y1
      YA=Y1**2/X1

C      COMPUTE THE TANGENT TO THE ELLIPSE AT X1 AND Y1 TO DETERMINE
C      THE WIND DIRECTION.
C
      IF(X1.GT.0.D.AND.Y1.GT.0.D) GO TO 11
      IF(X1.GT.0.D.AND.Y1.LT.0.D) GO TO 12
      IF(X1.LT.0.D.AND.Y1.GT.0.D) GO TO 12
      IF(X1.LT.0.D.AND.Y1.LT.0.D) GO TO 11
11  XA=-YA
   12  YA=-XA
13  CONTINUE
   14  TURN
   END

// SUBR
*DELETE          ELIPS
*STORE           WS UA ELIPS

// SUBB
// FOR
*IGS(CARD,1132 PRINT)
*ONE WORD INTEGERS
*LIST SOURCE PROGRAM
SUBROUTINE WIND(X,Y,P,PMIN,PMAX,SLAT,R,SURF,ALSH,UNSH,SHANG,EHAL,
1PI,XA,XA,YA,SHAZ,EAZ,D2A,ISLAND,FIND)

C      SUBROUTINE WIND IS USED TO DETERMINE THE GEOSTROPHIC WIND SPEED
C      AND DIRECTION FROM THE BAROMETRIC PRESSURE GRADIENT. THE SURFACE
C      WIND SPEED AND DIRECTION ARE DETERMINED OVER LAND AND SEA FROM
C      CORRECTIONS APPLIED TO THE GEOSTROPHIC WIND. THE ONSHORE AZIMUTH
C      IS USED TO FIND THE ONSHORE AND ALONGSHORE COMPONENTS OF THE WIND.
C      THE EFFECTIVE WIND SPEED IS USED TO FIND THE WAVE HEIGHT, PERIOD,
C      AND ONSHORE CURRENT VELOCITY.

      HAU=SLAT*H
      U1=U194
      UFEA=MOD(U194,24)

C      THE BAROMETRIC PRESSURE GRADIENT ALONG A NORMAL CURVE IS USED TO
C      CALCULATE THE GEOSTROPHIC WIND SPEED.

      COR=2.*POMEGA*SIN(SLAT)*RAD
      Z1=3.*A*D
      PDIF=PMAX-P1
      PINC=PCIF*(P1-Z1**2/Z1)
      H2=PMAX-PINC
      D2A=D1/D2
      WHET=HSI*TCUR*(DPDN/5000.)
      CALL ANGTAN(XA,XA,YA)
      DIF=HAZ+90.-SHAZ
      IF(DIF.GT.90.D) DIF=DIF-360.
      WANG=-PAO+WANG-DIF
      IF(WANG.LT.0.D) WANG=WANG+360.
      IF(WANG.GT.360.D) WANG=WANG-360.

C      H AND BETA ARE CORRECTION FACTORS USED TO DETERMINE SURFACE WIND
C      SPEED AND DIRECTION FROM GEOSTROPHIC WIND OVER LAND AND SEA

      F = LAND = H * .48 / (.70 AND BETA * 24
        - SEA = B * .42 / (.65 AND BETA * 50

      IF F > 0.0 THEN F = POSITIVE Y
      IF F < 0.0 THEN F = POSITIVE X
      IF F > 0.0 THEN F = NEGATIVE Y
      IF F < 0.0 THEN F = NEGATIVE X

      WANG=WANG
      WANG=
      WANG=

C      IF ISLAND OPTION, H AND BETA VALUES FOR THE SEA ARE USED
      IF ISLAND THEN
        H=.42/.65
        BETA=.50
      ELSE
        H=.48/.70
        BETA=.24
      END IF

C      A COSINE TRANSFORMATION IS USED IN A 30 DEGREE TRANSITION ZONE
C      IN EACH SIDE OF THE SHORTLINE. FULL LAND AND SEA CORRECTIONS ARE
C      USED OUTSIDE THE TRANSITION ZONE. PROPORTIONATE VALUES ARE USED
C      INSIDE LAND AND SEA CORRECTIONS WITHIN THE TRANSITION ZONE.

```

AD-A087 858

WILLIAMS COLL WILLIAMSTOWN MASS
COASTAL STORM MODEL.(U)

F/8 4/2

APR 76 W T FOX, R A DAVIS

N00014-69-C-0151

NI

UNCLASSIFIED

TR-14

2 (P) 2

AD
- 300785H



END
DATE
FILMED
9-80
DTIC

```

C
29 SINS=SIN(SANG/RAD)
   IF(SINS+.5) 35,30,30
30 B=.00019
   BETA=29.
   GO TO 50
35 IF(SINS+.5) 36,40,40
36 B=.000065
   BETA=50.
   GO TO 80
40 IF(SANG-90.) 41,41,42
41 SANA=SANG*3.
   GO TO 48
42 IF(SANG-180.) 43,43,44
43 SANA=180.-3.*(180.-SANG)
   GO TO 48
44 IF(SANG-270.) 45,45,46
45 SANA=180.+3.*(SANG-180.)
   GO TO 48
46 SANA=360.-3.*(360.-SANG)
48 B=.0001*(1.275+0.625*SIN(SANA/RAD))
   BETA=39.5-10.5*SIN(SANA/RAD)
50 BETR=BETA/RAD
   COTA=SIN(BETR)/COS(BETR)+COR/(B*COS(BETR))
   ALPHA=ATAN(1./COTA)*RAD
   IF(NX) 51,52,52
51 SHANG=SANG+90.-ALPHA
   SANG=SANG-ALPHA
   NX=1
   GO TO 27
52 CONTINUE
   VMCOR=COR*SIN(ALPHA/RAD)/(B*COS(BETR))
   WSURF=VMCOR*WSGEO

C
C      ONSHORE AND LONGSHORE COMPONENTS OF THE SURFACE WIND
C
   ONSH=WSURF*COS(SHANG/RAD)
   ALSH=WSURF*SIN(SHANG/RAD)

C
C      EFWND IS THE EFFECTIVE WIND SPEED USED IN DETERMINING WAVES
C      AN OFFSHORE WIND IS ASSUMED TO BE .333 TIMES AS EFFECTIVE IN
C      GENERATING WAVES AS AN ONSHORE WIND.
C
   EFWND=WSURF*(.6667+.3333*COS(SHANG/RAD))
   IF(SHANG) 55,60,60
55 SHANG=SHANG+360.
60 CONTINUE
   IF(SHANG-360.) 70,70,65
65 SHANG=SHANG-360.
70 CONTINUE
   RETURN
   END

// DUP
*DELETE          WIND
*STORE          WS UA WIND
// *

// JOB                      DECAY          3-86-001
// FOR
*IOCS(CARD,1132 PRINTER)
*ONE WORD INTEGERS
*LIST SOURCE PROGRAM
   SUBROUTINE DECAY(TINT,PEROD,HEIGHT)
C
C      SUBROUTINE DECAY IS USED TO FIND THE DECAY IN WAVE HEIGHT AS
C      THE WAVES MOVE AWAY FROM THE STORM CENTER.
C
C
C... FIND LOGARITHMIC ATTENUATION COEFFICIENT
C
   FREQ=1./PEROD
   ATCOF=10.*((FREQ-0.06)/(0.0324))-1.
   IF(ATCOF.GT.1.0) ATCOF=1.0
   IF(ATCOF.LT.0.1) ATCOF=0.1
C
C... FIND PROPAGATION DISTANCE IN DEGREES
C
   DIST=1.5607*PEROD*TINT*360./40074.
C
C... FIND DECAYED WAVE HEIGHT
C
   HEIGHT=HEIGHT*(2.7183)**(-2.*(0.1191*ATCOF)*DIST)
   RETURN
   END

// DUP
*DELETE          DECAY
*STORE          WS UA DECAY

// JOB                      ETIME          3-86-001
// FOR
*IOCS(CARD,1132 PRINTER)
*ONE WORD INTEGERS
*LIST SOURCE PROGRAM
   SUBROUTINE ETIME(WSNEW,OLDH,HOURS,DRATN)
C
C      SUBROUTINE ETIME IS USED TO DETERMINE THE EFFECTIVE FETCH AND
C      DURATION FOR THE NEW WIND SPEED FROM THE LAST PREVIOUS WIND SPEED.
C
C... CONVERT M TO FT AND M/SEC TO FT/SEC

```

```

C
H=OLDH/0.3048
WS=WSNEW/0.3048
C
C... FIND EFFECTIVE FETCH USING NEW WIND SPEED AND OLD WAVE HEIGHT
C
U=((32.1*H)/(0.283*WS**2.))
SUM=U
DO 10 K=1,51,2
I=K+2
SUM=SUM+U**1/I
10 CONTINUE
F=(WS**2./32.1)*(SUM/0.0129)**2.38
C
C... CONVERT FROM FT TO NM AND FT/SEC TO KTS
C
F=F/6076.
WSKTS=WS*3600./6076.
C
C... FIND EFFECTIVE DURATION USING DERIVED EFFECTIVE FETCH
C
EFDUR=(F/(WSKTS/10.)*0.72*10.**0.3)**0.8
DRATN=HOURS+EFDUR
RETURN
END
// DUP
*DELETE ETIME
*STORE WS UA ETIME
// JOB
// FOR
*IOCS(CARD=1132,PRINTER)
*ONE WORD INTEGERS
*LIST SOURCE PROGRAM
SUBROUTINE FETCH(A,B,XA,YA,F)
C
C SUBROUTINE FETCH IS USED TO FIND THE EFFECTIVE FETCH AS A STORM
C MOVES ONSHORE OR OFFSHORE. THE FETCH LENGTH IS DETERMINED FROM
C THE FETCH AREA WHERE THE WIND IS BLOWING TOWARD THE SHORE SITE.
C THE EFFECTIVE FETCH AREA IS AN ELLIPSE WITHIN WHICH THE WIND IS
C BLOWING AT GREATER THAN HALF THE MAXIMUM WIND SPEED. THE MAXIMUM
C EFFECTIVE FETCH IS THE MAJOR AXIS OF THE ELLIPSE.
C
R=(A+B)/2.
FMAX=0.5881*R
PI=3.14159
RAD=57.2958
X=XA*A
Y=YA*A
IF (ABS(X).GE.(0.) .AND. ABS(X).LT.(1./3.*R)) GO TO 100
IF (ABS(X).GE.(1./3.*R) .AND. ABS(X).LT.(0.444444*R)) GO TO 200
IF (ABS(X).GE.(0.444444*R)) GO TO 300
GO TO 400
C
C... X GREATER THAN OR EQUAL TO ZERO AND LESS THAN 1/3 R
C
100 Y1=SURT((1./3.*R)**2.+(1./2.*FMAX)**2.-X**2.)
Y2=SURT((1./3.*R)**2.-X**2.)
Y3=0.0
Y4=-Y2
Y5=-SURT(R**2.-X**2.)
IF (Y.GE.Y1) GO TO 110
IF (Y.LT.Y1 .AND. Y.GE.Y2) GO TO 120
IF (Y.LT.Y2 .AND. Y.GE.Y3) GO TO 130
IF (Y.LT.Y3 .AND. Y.GE.Y4) GO TO 140
IF (Y.LT.Y4 .AND. Y.GE.Y5) GO TO 150
IF (Y.LT.Y5) GO TO 160
GO TO 400
110 F=FMAX
GO TO 500
120 RATIO=(Y-Y2)/(Y1-Y2)
CURVE=1.-(1.-COS(PI*RATIO))/2.
F=1./2.*FMAX*CURVE+1./2.*FMAX
GO TO 500
130 RATIO=ABS(X)/SURT(X**2.+Y2**2.)
FMIN=RATIO*1./2.*FMAX
RANGE=1./2.*FMAX-FMIN
CURVE=1.-COS((1.-(Y2-Y)/(Y2-Y3))*PI/2.)
F=CURVE*RANGE+FMIN
GO TO 500
140 RATIO=ABS(X)/SURT(X**2.+Y4**2.)
C
C... NOTE... THIS IS THE SAME RATIO AS 130 SINCE Y2 = Y4
C
FMIN=RATIO*1./2.*FMAX
RANGE=1./2.*FMAX-FMIN
CURVE=1.-COS((Y-Y4)/(Y3-Y4)*PI)/2.
F=CURVE*RANGE+FMIN
GO TO 500
150 RATIO=(Y-Y5)/(Y4-Y5)
CURVE=1.-COS((1.-RATIO)*PI)/2.
F=CURVE*1./2.*FMAX
GO TO 500
160 F=0.0
GO TO 500
C
C... X GREATER THAN OR EQUAL TO 1/3 R AND LESS THAN 0.444444 R
C
200 Y1=SURT((1./2.*FMAX)**2.+(1./3.*R)**2.-X**2.)
Y2=-SURT(R**2.-X**2.)

```

```

      IF(Y.GT.Y1) GO TO 210
      IF(Y.LE.Y1.AND.Y.GT.Y2) GO TO 220
      IF(Y.LE.Y2) GO TO 230
      GO TO 400
210   F=FMAX
      GO TO 300
220   RATIO=(Y1-Y)/(Y1-Y2)
      CURVE=(1.+COS(RATIO*PI))/2.
      F=FMAX*CURVE
      GO TO 300
230   F=0.0
      GO TO 300
C
C... X GREATER THAN OR EQUAL TO 0.444444 R
C
300   Y1=0.0
      Y2=-SQRT(R**2.-(0.444444*R)**2.)
      IF(Y.GT.Y1) GO TO 310
      IF(Y.LE.Y1.AND.Y.GT.Y2) GO TO 320
      IF(Y.LE.Y2) GO TO 330
      GO TO 400
310   F=FMAX
      GO TO 300
320   RATIO=(Y1-Y)/(Y1-Y2)
      CURVE=(1.+COS(RATIO*PI))/2.
      F=FMAX*CURVE
      GO TO 300
330   F=0.0
      GO TO 300
C
C... ERROR CONDITION
C
400   WRITE(3,410)
410   FORMAT(1X,'LOGIC ERROR ENCOUNTERED IN SUBROUTINE FETCH...')
      F=0.0
      RETURN
500   IF(X.LT.(0.)) F=0.5*F
      RETURN
      END
// DUP
*DELETE          WS      UA      FETCH
*STORE           WS      UA      FETCH
WAVES           3-86-001
// JOB
// FOR
*IOCS(CARD,1132 PRINTER)
*ONE WORD INTEGERS
*LIST SOURCE PROGRAM
SUBROUTINE WAVES(SPEED,TIME,FETCH,EFETC,HEIGT,PEROD,IOUT)
C
C   SUBROUTINE WAVES IS USED TO DETERMINE WAVE PERIOD AND HEIGHT FROM
C   WIND SPEED, DURATION AND FETCH.
C
C... UNIT CONVERSION PACKAGE...KM TO NM...M/SEC TO KNOTS
C
      FCHNM=0.5400*FETCH
      SPDKT=1.9439*SPEED
C
C... EFFECTIVE FETCH PACKAGE
C
      EFETC=(SPDKT/10.)**0.72*10.**0.3*TIME**1.25
      IF(FCHNM.LT.EFETC) EFETC=FCHNM
C
C... UNIT CONVERSION PACKAGE...NM TO METERS...KNOTS TO M/SEC
C
      EFETC=EFETC/0.5400*1000.
      SPDMS=SPDKT/1.9439
C
C... WAVE PARAMETER PACKAGE
C
      CONST=(9.8062*EFETC)/SPDMS**2.
      HEIGT=(SPDMS**2.*0.283*TANH(0.0125*CONST**0.4211/9.8062
      PEROD=(2.*3.14159*SPDMS*1.20*TANH(0.077*CONST**0.2511/9.8062
      EFETC=EFETC/1000.
      IF(IOUT.EQ.1) RETURN
      IF(IOUT.EQ.2) GO TO 200
C
C... ERROR CONDITION
C
      WRITE(3,100)
100   FORMAT(1X,'ILLEGAL OUTPUT OPTION IN SUBROUTINE WAVES')
      RETURN
C
C... NON-METRIC OUTPUT OPTION
C
200   EFETC=EFETC*0.9400
      HEIGT=HEIGT*9.2808
      RETURN
      END
// DUP
*DELETE          WS      UA      WAVES
*STORE           WS      UA      WAVES
WAVES
// JOB
// FOR
*IOCS(CARD,1132 PRINTER)
*ONE WORD INTEGERS
*LIST SOURCE PROGRAM

```

```

SUBROUTINE TIDE (ST,TN,FN,ISTRT,THR,TDAY,TIDX,SLTOP,SLBOT,SLOPE,1,
1 TMEAN)
C
C PERIODS FOR THE MAJOR DIURNAL AND SEMIDIURNAL TIDAL COMPONENTS
C
TM2=12.42
TS2=12.00
TK1=23.93
TO1=25.82
HR=24.0*TDAY+FLOAT(ISTRT)+FLOAT(1-1)-THR
ARG=6.2832*HR
C
C COMPUTE THE AMPLITUDE OF THE TIDAL COMPONENTS FROM THE SPRING
C AND NEAP TIDE RANGES AND THE TIDAL FORM NUMBER.
C
FM2=(ST+TN)/(4.0*(1.0+FN))
S2=(ST-TN)/(4.0*(1.0+FN))
FK1=FN*FM2
O1=FN*S2
C
C TIDE LEVEL IS THE SUM OF THE FOUR MAJOR TIDAL COMPONENTS
C AT EACH HOUR.
C
TIDX = FM2*COS(ARG/TM2) + S2*COS(ARG/TS2) + FK1*COS(ARG/TK1) +
1 O1*COS(ARG/TO1)
C
C BOTTOM SLOPE IS COMPUTED FROM THE TIDE LEVEL, AND THE SLOPE
C AT HIGH AND LOW TIDES.
C
TLOC = (TIDX+ST/2.0) / ST
SLOPE = SLBOT + TLOC * (SLTOP-SLBOT)
TIDX=TIDX+TMEAN
RETURN
END
// DUP
*DELETE TIDE
*STORE WS UA TIDE
// JOB SURF 3-86-001
// FOR
*IOCS(CARD,1132 PRINTER)
*ONE WORD INTEGERS
*LIST SOURCE PROGRAM
SUBROUTINE SURF(SHANG,PEROD,HEIGT,SLOPE,HB,BRANG,VLS,DEPTH,LSCOP)
C
C COMPUTE BREAKER HEIGHT, ANGLE AND LONGSHORE CURRENT VELOCITY
C
PI=3.14159
RAD=57.2958
G=980.62
HTCM=100.0*HEIGT
HBCM=.383*G**0.2*(PEROD*HTCM**2)**0.4
DEPTH=1.2*HBCM
WLO=G/(2.0*PI)*PEROD**2
WL1=WLO
C
C DISPERSION EQUATION USED TO DETERMINE SHALLOW WATER WAVE LENGTH
C
DO 10 I=1,20
WL1=WLO*TANH(2.0*PI*DEPTH/WL1)
10 CONTINUE
C
C SNELL'S LAW USED TO DETERMINE BREAKER ANGLE AND HEIGHT
C DUE TO WAVE REFRACTION.
C
SINA=SIN(SHANG/RAD)*TANH(2.0*PI*DEPTH/WL1)
COSA=SQRT(1.0-SINA**2)
CALL ARCTA(BANG,COSA,SINA)
BRANG=RAD*BANG
REFRC=SQRT(COS(SHANG/RAD)/COS(BANG))
HB=REFRC*HBCM
C
C OPTION OF FOUR DIFFERENT LONGSHORE CURRENT EQUATIONS.
C
GO TO (1,2,3,4),LSCOP
C
C LONGSHORE CURRENT - FOX AND DAVIS, 1972
C
1 VLS=100.0*SLOPE*HB/PEROD*SIN(4.0*BRANG/RAD)
GO TO 5
C
C LONGSHORE CURRENT - LONGUET-HIGGINS, 1970
C
2 VLS = 9.0*SLOPE*SQRT(G*HB) *SIN(2.0*BRANG/RAD)
GO TO 5
C
C LONGSHORE CURRENT - C.E.R.C., 1973
C
3 VLS =20.7*SLOPE*SQRT(G*HB) *SIN(2.0*BRANG/RAD)
GO TO 5
C
C LONGSHORE CURRENT - KOMAR AND INMAN, 1970
C
4 G1=G/100.
VLS=100.0*G1*HEIGT **2/8.0*G1*PEROD/(4.0*PI)*SIN(2.0*BRANG/RAD)*
1 COS(2.0*BRANG/RAD)
5 HB=HB/100.
RETURN
END
// DUP

```

```

*DELETE
*STORE      WS UA SURF

```

```

// JOB
// FOR
// IOCS(CARD,1132 PRINTER)
// ONE WORD INTEGERS
// LIST SOURCE PROGRAM
SUBROUTINE ENRGY(H,T,TIME,ISALT,E,IUNIT)
C
C SUBROUTINE ENRGY IS USED TO DETERMINE WAV2 ENERGY DURING EACH
C HOUR. THIS ENERGY IS DERIVED FROM THE ENERGY WITHIN A SINGLE WAVE
C AND SUMED TO FIND THE TOTAL ENERGY IN THE STORM.
C
C... FIND NUMBER OF WAVES IN GIVEN TIME PERIOD
C
C WAVES=TIME*3600./T
C
C... FIND PROPER MASS DENSITY OF WATER (0=FRESH,1=SALT)
C
C IF(ISALT.EQ.0) DENSE=1.94
C IF(ISALT.EQ.1) DENSE=2.0
C IF(ISALT.GT.1) GO TO 500
C
C... CONVERT WAVE HEIGHT FROM METERS TO FEET
C
C HT=M/0.3048
C
C... FIND ENERGY FOR A SINGLE WAVE
C
C E=5.12*DENSE*32.1*(HT*T)**2./8.
C
C... FIND TOTAL ENERGY
C
C E=E*WAVES
C
C... IF OUTPUT IS DESIRED IN FT-LBS/FT,RETURN
C
C IF(IUNIT.EQ.0) RETURN
C IF(IUNIT.NE.1) GO TO 500
C
C... CONVERT FT-LBS/FT TO JOULES/METER
C
C E=E*1.35582/0.3048
C
C RETURN
C
C... ERROR CONDITION
C
C 500 WRITE(3,600)
C 600 FORMAT(1X,'ILLEGAL OPTION IN SUBROUTINE ENRGY')
C
C RETURN
C
C END

```

```

// DUP
*DELETE
*STORE      WS UA ENRGY

```

ARCTA 3-86-001

```

// JOB
// FOR
// IOCS(CARD,1132 PRINTER)
// ONE WORD INTEGERS
// LIST SOURCE PROGRAM
SUBROUTINE ARCTA(ANGLE,X,Y)
C
C ARCTANGENT ROUTINE IS USED TO DETERMINE THE ANGLE FROM X AND Y
C COORDINATES, OR SIN AND COSIN.
C
C
C ANGLE = 0.0
C IF(ABS(X)-.001)2,9,9
C 9 IF(X) 1,3,3
C 3 IF(Y) 4,5,5
C 4 ANGLE = 6.2831825
C GO TO 5
C 1 ANGLE = 3.1415926
C 5 ANGLE = ANGLE+ATAN(Y/X)
C RETURN
C 2 IF (ABS(Y)-.001) 8,10,10
C 10 IF(Y)6,7,7
C 6 ANGLE=4.7123889
C RETURN
C 7 ANGLE = 1.5707963
C 8 RETURN
C
C END

```

```

// DUP
*DELETE
*STORE      WS UA ARCTA

```

```

// JOB
// FOR
*IOCS(CARD,1132,PRINTER,TYPEWRITER,KEYBOARD)
*ONE WORD INTEGERS
COMMON U(130),V(130)
DIMENSION TITLE(20),DAY(5)
DIMENSION A1(2),A2(2),A3(2),A4(2),B1(2),B2(2),C1(2),C2(2),C3(2)
DATA A1/' KIL',' NAU'/,A2/'OMET','TICA'/,A3/'ERS','L MI'/,
1 A4/' ','LES '/,B1/' MET',' FEE'/,B2/'ERS','T '/,
2 C1/' JOU',' FOO'/,C2/'LES','T PO'/,C3/' ','UNDS'/

C
C STORM PROGRAM LIMITED TO FORECAST MODE
C TYPEWRITER INPUT FOR THE STORM PARAMETERS
C
C CARD 1 - TITLE
C
C CARD 2 - STARTING DATE, TIME AND INPUT-OUTPUT OPTIONS
C
C COLS. 1-2 ISTR- STARTING HOUR
C COLS. 3-22 DAY - STARTING DATE
C
C COL. 23 INAUT- INPUT OPTION
C 0 = METRIC UNITS
C 1 = NAUTICAL MILES AND FEET
C
C COL. 24 NAUT - OUTPUT OPTION
C 1 = NAUTICAL MILES, FEET AND KNOTS
C 0 = METRIC UNITS
C
C CARD 3 - STORM PARAMETERS
C
C COL. 2 TIDE PREDICTION OPTION
C 0 = TIDE PREDICTION NOT INCLUDED - OMIT CARD 4
C 1 = TIDE PREDICTION INCLUDED - SEE CARD 4
C
C COL. 3 LONGSHORE CURRENT EQUATION OPTION
C 1 = FOX AND DAVIS, 1972
C 2 = LONGUET-HIGGINS, 1970
C 3 = C.E.R.C., 1973
C 4 = KOMAR AND INMAN, 1970
C
C COLS. 4-6 NX - NUMBER OF STORM POSITIONS
C SIX HOUR INTERVALS FOR HINDCASTING
C ONE HOUR INTERVALS FOR FORECASTING
C
C COLS. 7-12 BNFC- AVERAGE BASIN FETCH IN KM. (NAUT. MI.)
C COLS. 13-17 TINT - TIME INTERVAL BETWEEN STORM POSITIONS
C NORMAL SETTING IS 1.0 HOURS
C
C COLS. 32-36 SLAT - LATITUDE AT SHORE SITE
C
C CARD 4 - TIDE PREDICTION - OPTION FROM CARD 3
C
C COLS. 0-5 ST - SPRING TIDE RANGE IN FEET
C COLS. 6-10 TN - NEAP TIDE RANGE IN FEET
C COLS. 11-15 TDAY - NUMBER OF DAYS FROM LAST SPKING TIDE
C COLS. 16-20 THR - HOUR OF LAST HIGH SPRING TIDE
C
C COLS. 21-25 FN - TIDAL FORM NUMBER
C 0.0 TO .25 - SEMIDIURNAL TIDE
C .25 TO 1.5 - MIXED SEMIDIURNAL TIDE
C 1.5 TO 3.0 - MIXED DIURNAL TIDE
C GREATER THAN 3.0 - DIURNAL TIDE
C
C COLS. 26-32 SLPLO- NEARSHORE BOTTOM SLOPE AT LOW TIDE
C COLS. 33-39 SLPHI- NEARSHORE BOTTOM SLOPE AT HIGH TIDE
C COLS. 40-46 TMEAN- MEAN TIDE LEVEL IN FEET
C
C CARD 5 - SHORE SITE LOCATION
C
C COLS. 1-7 ULOC - X-COORDINATE IN NAUTICAL MILES
C COLS. 8-14 VLOC - Y-COORDINATE IN NAUTICAL MILES
C COLS. 15-21 SHAZ - ONSHORE DIRECTION - CLOCKWISE FROM NORTH
C COLS. 22-28 SLOPE- AVERAGE NEARSHORE BOTTOM SLOPE
C COL. 30 ISLND- 0 - CONTINENTAL COAST OR BARRIER ISLAND
C
C THE FOLLOWING INFORMATION IS TYPED IN FROM THE CONSOLE FOR EACH
C STORM SIMULATION RUN:
C
C TYPE PHIN - MINIMUM BAROMETRIC PRESSURE IN MILLIBARS
C PMAXR- PRESSURE AT LARGEST ENCIRCLING ISOBAR
C IN AR - MAJOR HALF-AXIS (EFFECTIVE LONG RADIUS)
C BR - MINOR HALF-AXIS (EFFECTIVE SHORT RADIUS)
C EAZ - ORIENTATION OF MAJOR HALF AXIS PLUS OR
C MINUS 90 DEGREES FROM NORTH.
C SVEL - STORM VELOCITY IN KNOTS
C AZI - STORM AZIMUTH - CLOCKWISE FROM NORTH
C X(1) - INITIAL X-COORDINATE FOR THE STORM.
C Y(1) - INITIAL Y-COORDINATE FOR THE STORM.
C
C CNK=1.85319
C CKN=.53961
C CFM=.3048
C CMF=.2808
C CKTS=1.9425
C CCMF=.032808
C CJOUL = .797961

```



```

C      RAD=37.2958
8080 READ (2,915) TITLE
915  FORMAT(20A4)
    READ(2,917) ISTRT,DAY,INAUT,NAUT
917  FORMAT(12,5A4,2I1)
    NN=NAUT+1
    IF(INAUT) 1,1,2
      1 CNK=1.0
        CFM=1.0
      2 IF(NAUT) 11,11,12
    11 CNK=1.0
      CMF=1.0
      CKTS=1.0
      CCMF=1.0
      CJOUL=1.0
    12 IF (ISTRT.EQ.0.0) GO TO 1000
    READ(2,901) INOPT,IFTID,LSCOP,NX,BNFC1,TINT,SLAT
901  FORMAT(3I1,13,F6.0,F5.1,14X,F5.1)
    BNFC1=BNFC1*CNK
    IF(IFTID) 5,5,6
      4 READ(2,923) S1,T1,TDAY,THR,FN,SLPLO,SLPHI,TMEA1
920  FORMAT(5F5.2,3F7.2)
    ST=S1*CFM
    TH=T1*CFM
    TMEA1=TMEA1*CFM
      5 READ(2,907) ULC1,VLC1,SHAZ,SLOPE,ISLND
907  FORMAT(4F7.0,12)
    ULC1=ULC1*CNK
    VLC1=VLC1*CNK
945 WRITE(1,947)
947 FORMAT(' TYPE IN THE MINIMUM AND MAXIMUM BAROMETRIC PRESSURE IN MI
    1LLIBARS - FORMAT AAAA.BBBB.')
    READ(6,948) PMIN,PMAXR
948 FORMAT(2F5.0)
    WRITE(1,955)
955 FORMAT(' TYPE IN THE LENGTH OF THE MAJOR AND MINOR HALF AXES OF TH
    1E STORM - FORMAT XXXX.YYYY.')
    READ(6,956) AR1,BR1
956 FORMAT(2F5.0)
    WRITE(1,960)
960 FORMAT(' TYPE IN THE ORIENTATION OF THE MAJOR HALF AXIS IN DEGREES
    1 FROM NORTH - FORMAT XXX.')
    READ(6,961) EAZ
961 FORMAT(F5.0)

C
C      BAROMETRIC PRESSURE AT LARGEST ENCIRCLING ISOBAR IS ASSUMED TO BE
C      AT TWO STANDARD DEVIATIONS FROM THE CENTER OF THE STORM. TO
C      FIND THE ACTUAL STORM SIZE, THE MAJOR AND MINOR AXES ARE
C      MULTIPLIED BY 1.5 AND THE MAXIMUM PRESSURE IS MULTIPLIED BY
C      1.145 TO DETERMINE THE PRESSURE AT THE MARGIN OF THE STORM.
C
    AR=AR1*CNK
    BR=BR1*CNK
    RANGP=PMAXR-PMIN
    PMAX=RANGP*1.145+PMIN

C
C      AR AND BR ARE RADII OF THE STORM OUT TO TWO STANDARD DEVIATIONS...
C      MULTIPLY BY 1.5 TO YIELD THE FULL LENGTHS.
C
    A=1.5*AR
    B=1.5*BR
    CALL FOREC(INX,A,SVEL,AZ1)
    DO 42 I=1,NX
      U(I)=U(I)*CNK
    42 V(I)=V(I)*CNK
    ULOC=ULC1/A
    VLOC=VLC1/A
    U1=U(I)*A+.005
    V1=V(I)*A+.005
    UL=ULOC*A
    VL=VLOC*A

C
C      WRITE SHORE AND TIDE DATA
C
    UL1=UL*CKN+.05
    VL1=VL*CKN+.05
    BNFC1=BNFC1*CKN
    WRITE(3,916) TITLE
916  FORMAT(1M1//,1X,20A4/)
    WRITE(3,918) ISTRT,DAY
918  FORMAT(1X,'RUN BEGINS AT HOUR ',12,' ON ',5A4)
    WRITE(3,905) PMIN,PMAXR,PMAX
905  FORMAT(1M0,'STORM - BAROMETRIC PRESSURE AT CENTER OF LOW =',F7.1,
    1' MILLIBARS',/9X,'PRESSURE AT LARGEST ENCIRCLING ISOBAR =',F7.1,
    2' MILLIBARS',/9X,'MAXIMUM PRESSURE INCLUDED IN STORM =',F7.1,
    3' MILLIBARS',/1)
    AR1=AR*CKN+.05
    BR1=BR*CKN+.05
    WRITE(3,926) AR1,A1(INN),A2(INN),A3(INN),A4(INN),BR1,A1(INN),A2(INN),
    1 A3(INN),A4(INN),EAZ
926  FORMAT(9X,'LENGTH OF MAJOR HALF AXIS =',F7.1,4A4/
    19X,'LENGTH OF MINOR HALF AXIS =',F7.1,4A4/
    29X,'ORIENTATION OF MAJOR AXIS =',F7.1,' DEGREES FROM NORTH',/1)
    IF(INAUT)601,601,602
601  WRITE(3,910) SVEL,AZ1
910  FORMAT(9X,'STORM VELOCITY =',F4.0,' KILOMETERS/HOUR',
    1 9X,'STORM AZIMUTH =',F4.0,/)
    GO TO 605
602  WRITE(3,911) SVEL,AZ1
911  FORMAT(9X,'STORM VELOCITY =',F4.0,' KNOTS',
    1 9X,'STORM AZIMUTH =',F4.0,/)
605  CONTINUE

```

```

WRITE(3,970)IUL1,VL1,A1(NN),A2(NN),A3(NN),A4(NN),SLAT,SHAZ,SLOPE,
1 BNFC1,A1(NN),A2(NN),A3(NN),A4(NN)
970 FORMAT(' SHORE - POSITION COORDINATES - X =',F7.1,' Y =',F7.1,
1 4A4 //9X'SHORE LATITUDE =',F6.0,' ONSHORE AZIMUTH
2 =',F6.0,' DEGREES',/9X,'NEARSHORE SLOPE =',F6.3,' AVERAGE FETCH
3 =',F6.0,4A4/)
IF(IFTID) 59,59,58
58 S1=ST*CMF
T1=TN*CMF
WRITE(3,927) S1,T1,B1(NN),B2(NN),SLPLO,SLPHI
927 FORMAT(' TIDES - SPRING TIDE RANGE =',F6.2,' NEAP TIDE RANGE =',
1 F6.2,2A4 //9X,'SLOPE AT LOW TIDE =',F6.3,' SLOPE AT HIGH TIDE
1 =',F6.3/)
IF(FN.LE.25) WRITE(3,941) FN
941 FORMAT(9X,'SEMI DIURNAL TIDE - FORM NUMBER IS',F6.2/)
IF(FN.GT.25.AND.FN.LE.1.5) WRITE(3,942) FN
942 FORMAT(9X,'MIXED SEMI DIURNAL TIDE - FORM NUMBER IS',F6.2/)
IF(FN.GT.1.5.AND.FN.LE.3.0) WRITE(3,943) FN
943 FORMAT(9X,'MIXED DIURNAL TIDE - FORM NUMBER IS',F6.2/)
IF(FN.GT.3.0) WRITE(3,944) FN
944 FORMAT(9X,'DIURNAL TIDE - FORM NUMBER IS',F6.2/)
59 WRITE(1,830)
830 FORMAT(' PLEASE CHECK TO SEE THAT THE INFORMATION ON THE PRINTER I
15 CORRECT' / ' IF THE PROGRAM IS ALL SET TO GO, PRESS THE 1 KEY, 0
2 OTHERWISE, PRESS THE 2 KEY')
READ(6,831) NNN
831 FORMAT(I1)
IF(NNN=1) 590,590,945
590 WRITE(3,500)
500 FORMAT(1H0,' HOUR' ,T11,'X',T18,'Y',T24,'X1',T31,'Y1',T37,'BARO.',
1 T45,'WIND',T52,'SURF',T59,'ONSH',T66,'ALSH',T72,'EFFLCT',T81,
2 'WAVE',T88,'WAVE',T98,'BREAKER',T109,'LSC',/1X,T36,'PRESS',T44,
3 'ANGLE',T52,'WIND',T59,'WIND',T66,'WIND',T73,'WIND',T83,'H',T90,
4 'T',T97,'H',T101,'ANGLE',T108,'VELOC.')
```

```

IF(IFTID.GT.0) WRITE(3,951)
951 FORMAT(1H,T11,'TIDE')
IF(NAUT) 800,800,809
800 WRITE(3,801)
801 FORMAT(1H0,T10,'KM',T17,'KM',T24,'RAD',T31,'RAD',T38,'MB',T45,
1 'DEG',T53,'M/S',T60,'M/S',T67,'M/S',T74,'M/S',T83,'M',T89,'SEC'
2 ,T97,'M',T102,'DEG',T108,'CM/SEC')
IF(IFTID.GT.0) WRITE(3,802)
802 FORMAT(1H,T118,'M')
GO TO 815
809 WRITE(3,820)
820 FORMAT(1H0,T10,'NM',T17,'NM',T24,'RAD',T31,'RAD',T38,'MB',T45,
1 'DEG',T53,'KTS',T60,'KTS',T67,'KTS',T74,'KTS',T82,'FT',T89,'SEL'
2 ,T96,'FT',T102,'DEG',T108,'FT/SEC')
IF(IFTID.GT.0) WRITE(3,822)
822 FORMAT(1H,T118,'FT')
815 WRITE(3,952)
952 FORMAT(10X)
C
C CALL SUBROUTINES TO DETERMINE LOCATION AND COMPUTE WIND, WAVES,
C AND TIDES AT EACH LOCATION
C
DO 50 I=1,NX
CALL LOCAT(U(I),V(I),ULOC,VLOC,SHAZ,X,Y,EAZ,P,Q)
CALL ELIPS(A,B,P,Q,PMIN,PMAX,P1,ERAD,XA,YA,D2A)
CALL WIND(X,Y,P,PMIN,PMAX,SLAT,WSURF,ALSH,ONSH,SHANG,ERAD,P1,A,XA,
1 YA,SHAZ,EAZ,D2A,ISLND,EFWIND)
IF(I.EQ.1) GO TO 510
CALL DECAY(TINT,PEROD,HEIGHT)
HDECY=HEIGHT
CALL ETIME(EFWIND,HEIGHT,TINT,DRTN)
GO TO 520
510 DRTN=TINT
ESUM=0.0
EN=0.0
EP=0.0
IMOUR=ISTRT
520 CALL FETCH(A,B,X,Y,STFCH)
TLFCH=STFCH
IF(BNFC=LT,STFCH)TLFCH=BNFC
CALL WAVES(EFWIND,DRTN,TLFCH,EFETC,HEIGHT,PEROD,1)
IF(IFTID) 56,56,55
55 CALL TIDE(ST,TH,FN,ISTRT,THR,TDAY,TIDX,SLPHI,SLPLO,SLOPE,1,TMEAN)
56 CALL SURF(SHANG,PEROD,HEIGHT,SLOPE,HB,BRANG,VLS,DEPTH,LSLSCOP)
IF(BRANG=180./49.49,48
48 BRANG=BRANG+360.
49 CONTINUE
C
C COMPUTE WAVE AND LONGSHORE CURRENT ENERGY
C
ELS=.0257*(0.6*VLS)**2.*DEPTH**2./SLOPE
IF(VLS) 45,46,47
45 EN=EN+ELS
GO TO 46
47 EP=EP+ELS
CONTINUE
CALL ENRGY(HB,PEROD,TINT,1,E,1)
ESUM=ESUM+E
UPT=U(I)*A*CKN+.5
VPT=V(I)*A*CKN+.5
WSRF=WSURF*CKTS
ON=ONSH*CKTS
AL=ALSH*CKTS
EF=EFWIND*CKTS
HT1=HEIGHT*CMF
HB1=HB*CMF
V1=VLS*CMF

```

```

      WRITE(3,530) (HOUR,UPT,VPT,X,Y,P,SHANG,WSRF,ON,AL,EF,HT1,PEROD,
1 HB1,BRANG,V)
530 FORMAT(1X,12,2F7.0,2F7.2,F8.1,4F7.1,F7.1,F8.2,F7.1,F7.2,2F7.1)
      IF(IIFTID.GT.0) WRITE(3,531) TIDX
531 FORMAT(1H,114X,F5.2)
      HOUR=IHOUR+IFIX(TINT)
      IF(IHOUR.GT.24) HOUR=IHOUR-24
50 CONTINUE
      ELSC=EN*EP
      ESUM=ESUM+CJOUL
      ELSC=ELSC+CJOUL
      EP=EP*CJOUL
      EN=EN*CJOUL
      WRITE(3,540) ESUM,C1(NN),C2(NN),C3(NN),ELSC,C1(NN),C2(NN),C3(NN)
540 FORMAT(1X,/,1X,T5,'WAVE ENERGY IN THE BREAKER ZONE =',E10.3,3A4,/,
1,11X,T5,'TOTAL LONG-SHORE CURRENT ENERGY =',E10.3,3A4,/)
      WRITE(3,542) EP,C1(NN),C2(NN),C3(NN),EN,C1(NN),C2(NN),C3(NN)
542 FORMAT(1X,T5,'TOTAL POSITIVE LONG-SHORE CURRENT ENERGY =',E10.3,
13A4,/,1X,T5,'TOTAL NEGATIVE LONGSHORE CURRENT ENERGY =',E10.3,
23A4)
      WRITE(3,992)
992 FORMAT(1M1)
      WRITE(1,990)
990 FORMAT(' IF YOU WANT TO TRY ANOTHER SIMULATION RUN, TYPE IN A 1,
1 OTHERWISE TYPE IN A ZERO')
      READ(6,991) NEND
991 FORMAT(I1)
      IF(NEND.EQ.1) GO TO 945
      GO TO 8080
1000 CALL EXIT
      END
// DUP
*DELETE CSTRM
*STORE WS UA CSTRM

// JCB
// FOR
*IOCS(CARD,1132 PRINTER,TYPEWRITER,KEYBOARD)
*ONE WORD INTEGERS
*LIST SOURCE PROGRAM
*LIST SOURCE PROGRAM
SUBROUTINE FOREC(NX,A,SVEL,AZI)
COMMON U(130),V(130)
C
C FORECASTING - COMPUTE STORM POSITIONS FROM INITIAL POSITION,
C VELOCITY AND AZIMUTH
C
      TINT=1.0
      RAD=57.2958
      WRITE(1,975)
975 FORMAT(' TYPE IN THE STORM VELOCITY AND AZIMUTH - FORMAT VVV,AAA, '
1)
      READ(6,976) SVEL,AZI
976 FORMAT(2F4.0)
      WRITE(1,970)
970 FORMAT(' TYPE IN THE INITIAL X AND Y COORDINATES OF THE STORM -
1 FORMAT XXXX.YYYY. ')
      READ(6,971) U(1),V(1)
971 FORMAT(2F5.0)
      U(1)=U(1)/A
      V(1)=V(1)/A
      DIST=SVEL*TINT/A
      AZM=90.-AZI
      IF(AZM) 31,32,32
31 AZM=AZM+360.
32 DO 35 I=2,NX
      U(I)=U(1)+DIST*COS(AZM/RAD)
      V(I)=V(1)+DIST*SIN(AZM/RAD)
35 CONTINUE
      RETURN
      END
// DUP
*DELETE FOREC
*STORE WS UA FOREC

```

APPENDIX B. HINDCAST STORM DATA AND OUTPUT

DATA LIST FOR HINDCAST EXAMPLES

STEVENSVILLE, MICHIGAN
20 JULY 26, 1969 00
101 15200. 1.0 994. 1012. 42. 960. 700. 30.
1043. 486. 90. .033

333 1229
474 960
723 717
824 685
928 646
1024 606
1178 678
1280 749
1408 915
1510 1050
1687 1190
1694 1325
1773 1498
1843 1651
1907 1830

HOLLAND, MICHIGAN
1 JULY 3, 1970 10
101 10 150. 1.0 1003. 1010. 42. 550. 200. 30.
1015 560 90 .033
968 1030
1044 949
1098 845
1102 741
1163 709
1214 682
1271 686
1313 683
1362 686
1401 692

HOLLAND, MICHIGAN
1 JULY 7, 1970 10
101 13 150. 1.0 1002. 1010. 42. 455. 244. 35.
1015 560 90 .033
452 949
588 948
751 913
884 845
1027 790
1102 699
1131 657
1151 624
1190 605
1245 601
1297 627
1339 647
1384 666

HOLLAND, MICHIGAN
13 JULY 18, 1970 10
101 12 150. 1.0 1004. 1012. 42. 550. 300. 28.
1015 560 90 .033
796 705
852 699
871 689
954 686
1014 666
1095 650
1160 643
1196 663
1300 686
1371 735
1443 816
1547 952

SHEBOYGAN, WISCONSIN
7 JULY 13, 1972 00
101 9 200. 1.0 990. 1008. 42. 1750. 875. 25.
1892 1112 270. .030
585 1794
800 1788
1053 1788
1242 1800
1469 1839
1684 1876
1794 2087
1898 2210
2028 2334

SHEBOYGAN, WISCONSIN
7 JULY 16, 1972 00
101 11 200. 1.0 1002. 1016. 42. 1050. 700. 20.
1892 1112 270. .030
176 286
390 345
598 410
793 494
1079 637
1387 947
1593 1196
1825 1417
2028 1837
2080 2243
2191 2515

SHEBOYGAN, WISCONSIN
7 AUGUST 1, 1972 00
101 8 200. 1.0 1002. 1012. 42. 1400. 450. 12.
1892 1112 270. .030
598 1911
845 1203
1027 1625
1196 1566
1345 1560
1651 1644
1930 1800
2161 1983
2424 2203

MAGDALEN ISLANDS - WEST SIDE
2 NOVEMBER 26, 1974 00
111 10 200. 1.0 976. 1008. 48. 860. 860. 0.0
86 .37 10. 21.1 5.0 0.026 0.030 .64
1665. 1110. 270. .026 1

1154 466
1310 588
1499 966
1554 1154
1587 1221
1643 1188
1743 1274
1854 1354
1943 1543
2242 1920

MAGDALEN ISLANDS - EAST SIDE
2 NOVEMBER 26, 1974 00
111 10 200. 1.0 976. 1008. 48. 860. 860. 0.0
86 .37 10. 21.1 5.0 0.026 0.030 .64
1665. 1110. 270. .026 1

1154 466
1310 588
1499 966
1554 1154
1587 1221
1643 1188
1743 1274
1854 1354
1943 1543
2242 1920

PLUM ISLAND, MASSACHUSETTS
1 APRIL 4, 1975
111 154000. 1.0 982. 1012. 42. 1200. 600. 15.
3.50 2.10 7. 0. .11 .016 .032 1.25
1980 834 258 .030
111 139
610 555
1091 610
1258 906
1720 777
1850 925
1961 925
2072 888
2090 906
2202 925
2350 777
2479 666
2720 592
3100 550
3500 500

CEDAR ISLAND, VIRGINIA
7 JULY 14, 1973 00
113 134500. 1.0 1010. 1016. 38. 748. 224. 45.
1.72 .90 14. 16. .40 .035 .039 .55
2287 1537 285 .037
195 948
542 844
932 1115
1323 1323
1758 1512
1922 1474
2085 1436
2243 1386
2419 1399
2552 1613
2621 1814
2684 2048
2715 2249

SAPELO ISLAND, GEORGIA
1 FEBRUARY 14, 1969 00
113 12 3000. 1.0 990. 1012. 33. 925. 925. 0.
2.44 1.63 11. 9. .12 .013 .018 1.12
1575. 525. 290. .0155
819 408
934 385
1005 373
1207 373
1386 402
1485 420
1611 472
1727 529
1824 581
1890 633
1942 679
2000 702

MUSTANG ISLAND, TEXAS
7 JANUARY 12, 1972 00
111 10 1000. 1.0 990. 1018. 28. 2500. 400. 25.
485 .30 14. 16.6 2.5 .016 .020 .24
2.35 0.0 280. .018
2381 1593
2714 1535
2984 1535
3216 1555
3501 1608
3785 1627
4037 1666
4023 1762
4530 1801
4830 1835

MUSTANG ISLAND, TEXAS
7 JANUARY 23, 1972 00
111 9 1000. 1.0 998. 1016. 28. 1800. 500. 33.
485 .30 25. 16.6 2.5 .016 .020 .24
2425. 0. 280. .018
1777 831
2038 811
2256 806
2613 797
2954 879
3096 884
3284 903
3402 947
3521 996

MONTEREY, CALIFORNIA
4 FEBRUARY 13, 1967 00
112 4 4000. 1.0 998. 1012. 37. 700. 390. 50.
2.07 0.49 8. 14. 1.00 .056 .058 1.49
81. 413. 170. .057
445 1235
112 1129
1168 1002
1294 924
1480 817
1734 710
2132 613
2334 487
2476 389

HOLLAND, MICHIGAN

RUN BEGINS AT HOUR 1 ON JULY 3, 1970

STORM - BAROMETRIC PRESSURE AT CENTER OF LOW = 1003.0 MILLIBARS
 PRESSURE AT LARGEST ENCIRCLING ISOBAR = 1010.0 MILLIBARS
 MAXIMUM PRESSURE INCLUDED IN STORM = 1011.0 MILLIBARS

LENGTH OF MAJOR HALF AXIS = 550.0 KILOMETERS
 LENGTH OF MINOR HALF AXIS = 200.0 KILOMETERS
 ORIENTATION OF MAJOR AXIS = 30.0 DEGREES FROM NORTH

LONGSHORE CURRENT EQUATION FROM FOX AND DAVIS, 1972

SHORE - POSITION COORDINATES - X = 1015.0 Y = 560.0 KILOMETERS

SHORE LATITUDE = 42.0 OASHORE AZIMUTH = 90.0 DEGREES
 NEARSHORE SLOPE = 0.033 AVERAGE FETCH = 150.0 KILOMETERS

HOUR	X	Y	X1	Y1	BARO. PRESS.	WIND ANGLE	SURF. WIND	ONSH. WIND	ALSH. WIND	EFFECT. WIND	WAVE M	WAVE T	BREAKER M	BREAKER ANGLE	LSC VELOC.
	KM	KM	RAD	RAD	MB	DEG	M/S	M/S	M/S	M/S	M	SEC	M	DEG	CM/SEC
1	968.	1030.	0.56	0.05	1010.98	210.9	0.2	-0.1	-0.1	0.0	0.00	0.0	0.00	-14.9	-0.94
2	984.	1016.	0.55	0.03	1010.95	211.9	0.4	-0.3	-0.2	0.1	0.00	0.1	0.00	-15.7	-1.03
3	1001.	1003.	0.53	0.01	1010.89	213.1	0.7	-0.6	-0.3	0.2	0.00	0.1	0.00	-16.5	-1.24
4	1017.	989.	0.52	-0.00	1010.79	214.5	1.2	-0.9	-0.6	0.4	0.00	0.2	0.00	-17.3	-1.52
5	1033.	976.	0.50	-0.02	1010.63	216.3	1.8	-1.4	-1.1	0.7	0.01	0.4	0.01	-18.2	-1.85
6	1050.	962.	0.48	-0.04	1010.40	218.5	2.6	-2.1	-1.6	1.0	0.02	0.5	0.01	-19.2	-2.10
7	1066.	949.	0.47	-0.06	1010.08	221.3	3.6	-2.7	-2.4	1.5	0.03	0.7	0.02	-20.5	-2.45
8	1071.	932.	0.45	-0.06	1009.75	222.8	4.4	-3.2	-3.0	1.8	0.05	0.9	0.05	-21.1	-2.77
9	1077.	914.	0.42	-0.07	1009.36	224.6	5.2	-3.7	-3.6	2.2	0.07	1.0	0.06	-21.9	-3.08
10	1082.	897.	0.40	-0.08	1008.91	226.9	5.9	-4.0	-4.3	2.6	0.09	1.2	0.08	-22.8	-3.53
11	1087.	880.	0.38	-0.08	1008.41	229.7	6.4	-4.1	-4.9	2.9	0.12	1.4	0.11	-23.9	-4.08
12	1093.	862.	0.36	-0.09	1007.87	233.4	6.7	-4.0	-5.4	3.1	0.15	1.5	0.12	-25.2	-4.68
13	1098.	845.	0.34	-0.10	1007.31	238.4	6.8	-3.5	-5.8	3.3	0.17	1.6	0.14	-26.9	-5.31
14	1099.	828.	0.32	-0.10	1006.84	242.0	6.7	-3.1	-5.9	3.4	0.19	1.7	0.15	-27.9	-5.92
15	1099.	810.	0.30	-0.10	1006.37	246.6	6.5	-2.6	-6.0	3.5	0.21	1.8	0.15	-29.1	-6.53
16	1100.	793.	0.28	-0.10	1005.92	252.6	6.3	-1.8	-6.0	3.6	0.23	1.9	0.14	-30.3	-7.14
17	1101.	776.	0.26	-0.10	1005.49	260.7	6.1	-0.9	-6.0	3.7	0.25	2.0	0.11	-31.5	-7.75
18	1101.	758.	0.24	-0.10	1005.10	271.4	6.1	0.1	-6.1	4.1	0.27	2.1	0.05	-32.0	-8.27
19	1102.	741.	0.21	-0.10	1004.76	284.3	6.1	1.5	-5.9	4.6	0.31	2.2	0.17	-30.9	-8.74
20	1112.	736.	0.21	-0.11	1004.70	306.2	6.0	3.5	-4.8	5.2	0.36	2.4	0.30	-25.4	-9.15
21	1122.	730.	0.20	-0.13	1004.72	330.4	6.2	5.4	-3.0	5.9	0.42	2.6	0.42	-15.2	-9.24
22	1132.	725.	0.20	-0.14	1004.83	350.0	7.2	7.1	-1.2	7.2	0.52	2.8	0.55	-5.3	-9.92
23	1143.	720.	0.19	-0.15	1005.02	3.1	8.7	8.7	0.4	8.7	0.67	3.2	0.70	1.6	-8.45
24	1153.	714.	0.18	-0.16	1005.28	11.7	10.2	10.0	2.0	10.1	0.85	3.6	0.88	6.2	-3.13
1	1163.	709.	0.18	-0.17	1005.61	17.5	11.5	11.0	3.5	11.4	1.05	4.0	1.08	9.3	-3.71
2	1172.	706.	0.17	-0.19	1005.93	20.8	12.4	11.6	4.4	12.1	1.25	4.4	1.27	10.9	-4.33
3	1181.	703.	0.17	-0.20	1006.27	23.3	13.0	11.9	5.1	12.7	1.43	4.7	1.45	12.2	-4.87
4	1189.	700.	0.17	-0.21	1006.63	25.3	13.4	12.1	5.7	13.0	1.60	5.0	1.62	13.2	-5.37
5	1198.	698.	0.16	-0.22	1007.00	26.9	13.5	12.1	6.1	13.0	1.74	5.2	1.75	14.0	-5.80
6	1207.	695.	0.16	-0.23	1007.36	28.2	13.5	11.8	6.4	12.9	1.86	5.4	1.87	14.6	-6.20
7	1216.	692.	0.16	-0.24	1007.73	29.4	13.2	11.5	6.4	12.6	1.96	5.5	1.95	15.1	-6.57
8	1225.	691.	0.15	-0.25	1008.08	30.2	12.7	10.9	6.4	12.1	2.02	5.6	2.01	15.5	-6.92
9	1234.	690.	0.15	-0.26	1008.41	30.9	12.0	10.3	6.2	11.5	2.06	5.7	2.04	15.8	-7.25
10	1243.	689.	0.15	-0.27	1008.72	31.5	11.3	9.6	5.9	10.7	1.92	5.5	1.90	16.1	-7.58
11	1251.	688.	0.15	-0.28	1009.01	32.0	10.5	8.9	5.7	9.9	1.71	5.2	1.70	16.3	-7.88
12	1262.	687.	0.15	-0.29	1009.28	32.5	9.6	8.1	5.1	9.1	1.50	4.9	1.48	16.5	-8.16
13	1271.	686.	0.15	-0.31	1009.53	32.9	8.7	7.3	4.7	8.2	1.29	4.5	1.28	16.7	-8.40
14	1278.	686.	0.15	-0.31	1009.70	33.2	8.0	6.7	4.6	7.6	1.14	4.3	1.12	16.8	-8.60
15	1285.	685.	0.15	-0.32	1009.86	33.5	7.3	6.1	4.0	6.9	0.99	4.0	0.98	16.9	-8.76
16	1292.	685.	0.15	-0.33	1010.00	33.7	6.7	5.5	3.7	6.3	0.85	3.7	0.84	17.0	-8.89
17	1299.	684.	0.15	-0.34	1010.13	34.0	6.0	5.0	3.3	5.7	0.72	3.4	0.71	17.1	-8.98
18	1306.	684.	0.14	-0.35	1010.24	34.2	5.4	4.5	3.0	5.1	0.61	3.1	0.60	17.1	-9.03
19	1313.	683.	0.14	-0.36	1010.35	34.4	4.8	4.0	2.7	4.5	0.50	2.9	0.49	17.2	-9.08
20	1321.	684.	0.14	-0.37	1010.45	34.5	4.2	3.5	2.4	4.0	0.40	2.6	0.39	17.2	-9.12
21	1329.	684.	0.15	-0.38	1010.54	34.7	3.7	3.0	2.1	3.4	0.31	2.3	0.31	17.1	-9.15
22	1337.	685.	0.15	-0.39	1010.62	34.8	3.1	2.6	1.8	3.0	0.24	2.0	0.23	17.1	-9.18
23	1346.	685.	0.15	-0.40	1010.69	34.9	2.7	2.2	1.5	2.6	0.18	1.7	0.17	17.0	-9.20
24	1354.	686.	0.15	-0.41	1010.75	35.1	2.3	1.8	1.3	2.1	0.13	1.5	0.13	17.0	-9.21
1	1362.	686.	0.15	-0.42	1010.79	35.2	1.9	1.5	1.1	1.8	0.09	1.3	0.09	16.9	-9.22
2	1369.	687.	0.15	-0.42	1010.83	35.2	1.7	1.3	0.9	1.6	0.07	1.1	0.07	16.9	-9.23
3	1375.	688.	0.15	-0.43	1010.85	35.3	1.4	1.2	0.8	1.3	0.05	1.0	0.05	16.7	-9.24
4	1382.	689.	0.15	-0.44	1010.88	35.4	1.2	1.0	0.7	1.1	0.04	0.8	0.04	16.6	-9.24
5	1388.	690.	0.15	-0.45	1010.90	35.4	1.0	0.8	0.6	1.0	0.03	0.7	0.03	16.6	-9.25
6	1395.	691.	0.15	-0.45	1010.92	35.5	0.9	0.7	0.5	0.8	0.02	0.6	0.02	16.5	-9.25
7	1401.	692.	0.16	-0.46	1010.93	35.5	0.7	0.6	0.4	0.7	0.01	0.5	0.01	16.4	-9.25

WAVE ENERGY IN THE BREAKER ZONE = 0.153E 10 JOULES

TOTAL LONG-SHORE CURRENT ENERGY = 0.157E 10 JOULES

TOTAL POSITIVE LONG-SHORE CURRENT ENERGY = 0.156E 10 JOULES

TOTAL NEGATIVE LONG-SHORE CURRENT ENERGY = 0.438E 07 JOULES

HOLLAND, MICHIGAN

RUN BEGINS AT HOUR 1 ON JULY 7, 1970

STORM - BAROMETRIC PRESSURE AT CENTER OF LOW = 1002.0 MILLIBARS
PRESSURE AT LARGEST ENCIRCLING ISOBAR = 1010.0 MILLIBARS
MAXIMUM PRESSURE INCLUDED IN STORM = 1011.1 MILLIBARS

LENGTH OF MAJOR HALF AXIS = 455.0 KILOMETERS
LENGTH OF MINOR HALF AXIS = 244.0 KILOMETERS
ORIENTATION OF MAJOR AXIS = 35.0 DEGREES FROM NORTH

LONGSHORE CURRENT EQUATION FROM FOX AND DAVIS, 1972

SHORE - POSITION COORDINATES - X = 1015.0 Y = 560.0 KILOMETERS

SHORE LATITUDE = 42. ONSHORE AZIMUTH = 90. DEGREES
NEARSHORE SLOPE = 0.033 AVERAGE FETCH = 150. KILOMETERS

HOUR	X	Y	X1	Y1	BARO. PRESS.	WIND ANGLE	SURF. WIND	ONSH WIND	ALSH WIND	EFFECT. WIND	WAVE H	WAVE T	BREAKER H	ANGLE	LSC VELOC.
	KM	KM	RAD	RAD	MB	DEG	M/S	M/S	M/S	M/S	M	SEC	M	DEG	CM/SEC
1	452.	949.	0.56	0.82	1011.15	193.6	0.0	-0.0	-0.0	0.0	0.00	0.0	0.00	-6.5	-0.00
2	475.	949.	0.56	0.79	1011.15	193.9	0.0	-0.0	-0.0	0.0	0.00	0.0	0.00	-6.6	-0.00
3	497.	949.	0.56	0.75	1011.15	194.3	0.0	-0.0	-0.0	0.0	0.00	0.0	0.00	-6.8	-0.00
4	520.	948.	0.56	0.72	1011.15	194.6	0.0	-0.0	-0.0	0.0	0.00	0.0	0.00	-7.0	-0.00
5	543.	948.	0.56	0.69	1011.15	195.0	0.0	-0.0	-0.0	0.0	0.00	0.0	0.00	-7.1	-0.00
6	565.	948.	0.56	0.65	1011.15	195.4	0.0	-0.0	-0.0	0.0	0.00	0.0	0.00	-7.3	-0.00
7	588.	948.	0.56	0.62	1011.15	195.8	0.0	-0.0	-0.0	0.0	0.00	0.0	0.00	-7.5	-0.00
8	615.	942.	0.55	0.58	1011.15	196.2	0.0	-0.0	-0.0	0.0	0.00	0.0	0.00	-7.7	-0.00
9	642.	936.	0.55	0.54	1011.15	196.7	0.0	-0.0	-0.0	0.0	0.00	0.0	0.00	-7.9	-0.00
10	669.	930.	0.54	0.50	1011.15	197.2	0.0	-0.0	-0.0	0.0	0.00	0.0	0.00	-8.2	-0.00
11	697.	925.	0.53	0.46	1011.15	197.8	0.0	-0.0	-0.0	0.0	0.00	0.0	0.00	-8.5	-0.00
12	724.	919.	0.52	0.42	1011.15	198.4	0.0	-0.0	-0.0	0.0	0.00	0.0	0.00	-8.8	-0.00
13	751.	913.	0.51	0.38	1011.14	199.1	0.1	-0.1	-0.0	0.0	0.00	0.0	0.00	-9.2	-0.00
14	773.	902.	0.50	0.35	1011.12	199.6	0.2	-0.1	-0.0	0.0	0.00	0.0	0.00	-9.6	-0.00
15	795.	890.	0.48	0.32	1011.09	200.2	0.3	-0.3	-0.1	0.1	0.00	0.1	0.00	-10.1	-1.14
16	817.	879.	0.46	0.28	1011.03	200.8	0.4	-0.4	-0.2	0.2	0.00	0.1	0.00	-10.6	-1.98
17	840.	868.	0.45	0.25	1010.94	201.6	1.0	-0.9	-0.3	0.3	0.00	0.2	0.00	-11.1	-3.23
18	862.	856.	0.43	0.22	1010.79	202.5	1.5	-1.4	-0.5	0.5	0.00	0.3	0.00	-11.6	-4.95
19	884.	845.	0.41	0.19	1010.57	203.6	2.2	-2.1	-0.9	0.8	0.01	0.4	0.01	-12.2	-7.22
20	908.	836.	0.40	0.15	1010.27	205.2	3.2	-2.9	-1.3	1.1	0.02	0.6	0.02	-13.0	-10.12
21	932.	827.	0.39	0.12	1009.85	207.2	4.2	-3.8	-1.9	1.5	0.03	0.7	0.03	-14.0	-13.60
22	955.	817.	0.37	0.08	1009.32	209.7	5.4	-4.7	-2.6	2.0	0.06	0.9	0.06	-15.3	-17.77
23	979.	808.	0.36	0.05	1008.67	213.1	6.5	-5.4	-3.5	2.5	0.08	1.1	0.08	-16.9	-22.26
24	1003.	799.	0.35	0.01	1007.94	217.8	7.3	-5.8	-4.5	2.9	0.11	1.3	0.11	-19.0	-26.65
1	1027.	790.	0.33	-0.01	1007.17	224.4	7.8	-5.6	-5.5	3.3	0.15	1.5	0.14	-21.8	-29.87
2	1039.	775.	0.31	-0.03	1006.43	229.5	8.0	-5.2	-6.1	3.6	0.18	1.7	0.16	-23.8	-31.50
3	1052.	760.	0.29	-0.05	1005.70	236.6	7.9	-4.5	-6.6	3.8	0.21	1.8	0.17	-26.3	-30.61
4	1064.	744.	0.27	-0.07	1005.03	246.6	7.5	-2.9	-6.8	4.0	0.24	1.9	0.17	-29.2	-25.92
5	1077.	729.	0.24	-0.09	1004.46	261.0	7.4	-1.1	-7.3	4.5	0.28	2.1	0.12	-31.6	-15.95
6	1089.	714.	0.22	-0.10	1004.02	279.3	8.0	1.3	-7.9	5.8	0.36	2.3	0.16	-31.7	-18.39
7	1102.	699.	0.20	-0.12	1003.74	298.9	8.4	4.0	-7.3	6.9	0.47	2.7	0.36	-27.9	-41.26
8	1107.	692.	0.19	-0.13	1003.67	308.5	8.2	5.1	-6.4	7.1	0.56	2.9	0.48	-24.6	-33.43
9	1112.	685.	0.18	-0.14	1003.63	318.5	8.2	6.1	-5.4	7.5	0.64	3.1	0.60	-20.6	-62.10
10	1117.	678.	0.17	-0.14	1003.62	328.3	8.4	7.1	-4.4	7.9	0.73	3.4	0.72	-16.2	-83.62
11	1121.	671.	0.16	-0.15	1003.65	337.3	8.7	8.1	-3.3	8.8	0.82	3.6	0.84	-11.8	-56.58
12	1126.	664.	0.15	-0.16	1003.71	345.4	9.3	9.0	-2.3	9.2	0.93	3.8	0.96	-7.7	-42.66
13	1131.	657.	0.14	-0.16	1003.80	352.3	9.9	9.8	-1.3	9.9	1.04	4.0	1.09	-4.0	-25.01
14	1134.	652.	0.13	-0.17	1003.88	356.8	10.4	10.4	-0.5	10.4	1.16	4.2	1.22	-1.6	-11.07
15	1138.	646.	0.12	-0.17	1003.98	0.8	10.9	10.9	0.1	10.9	1.28	4.5	1.35	0.4	2.47
16	1141.	640.	0.11	-0.18	1004.10	4.2	11.5	11.4	0.8	11.5	1.41	4.7	1.48	2.4	16.51
17	1144.	635.	0.10	-0.18	1004.23	7.3	12.0	11.9	1.5	11.9	1.53	4.9	1.61	3.9	29.23
18	1148.	629.	0.10	-0.19	1004.37	10.0	12.4	12.3	2.1	12.4	1.66	5.1	1.73	5.3	40.98
19	1151.	624.	0.09	-0.19	1004.53	12.5	12.9	12.6	2.8	12.8	1.79	5.3	1.86	6.6	51.72
20	1157.	621.	0.08	-0.20	1004.80	14.3	13.4	12.9	3.3	13.2	1.91	5.5	1.99	7.6	60.46
21	1164.	618.	0.08	-0.21	1005.08	15.9	13.7	13.2	3.7	13.6	2.04	5.6	2.11	8.4	66.23
22	1170.	614.	0.07	-0.22	1005.36	17.3	14.0	13.4	4.1	13.8	2.16	5.8	2.23	9.1	75.11
23	1177.	611.	0.07	-0.23	1005.65	18.5	14.2	13.4	4.5	13.9	2.26	5.9	2.33	9.7	81.17
24	1183.	608.	0.07	-0.24	1005.95	19.6	14.2	13.4	4.8	14.0	2.36	6.1	2.43	10.3	86.48
1	1190.	605.	0.06	-0.25	1006.25	20.6	14.2	13.3	5.0	13.9	2.45	6.2	2.51	10.8	91.09
2	1199.	604.	0.06	-0.26	1006.61	21.1	14.0	13.1	5.0	13.7	2.51	6.3	2.58	11.0	93.93
3	1208.	604.	0.06	-0.28	1006.98	21.6	13.7	12.7	5.0	13.4	2.56	6.4	2.63	11.2	96.22
4	1217.	603.	0.06	-0.29	1007.33	22.0	13.3	12.3	5.0	13.0	2.50	6.3	2.55	11.5	98.15
5	1227.	602.	0.06	-0.31	1007.67	22.4	12.8	11.8	4.9	12.5	2.36	6.1	2.44	11.6	99.62
6	1236.	602.	0.06	-0.32	1007.99	22.7	12.2	11.3	4.7	11.9	2.21	5.9	2.26	11.8	94.35
7	1245.	601.	0.06	-0.33	1008.30	23.0	11.6	10.7	4.5	11.3	2.04	5.7	2.08	12.0	89.51
8	1254.	600.	0.06	-0.34	1008.53	22.7	11.0	10.2	4.2	10.8	1.90	5.5	1.94	11.8	85.46
9	1262.	610.	0.07	-0.36	1008.74	22.3	10.5	9.7	4.0	10.2	1.75	5.3	1.80	11.6	81.30
10	1271.	614.	0.07	-0.37	1008.95	22.0	9.9	9.2	3.7	9.7	1.61	5.0	1.65	11.4	77.08
11	1280.	618.	0.08	-0.38	1009.14	21.7	9.3	8.7	3.4	9.1	1.46	4.8	1.50	11.3	72.84
12	1288.	623.	0.09	-0.40	1009.33	21.5	8.7	8.1	3.2	8.5	1.32	4.6	1.36	11.2	68.54
13	1297.	627.	0.09	-0.41	1009.50	21.2	8.2	7.6	2.9	8.0	1.18	4.3	1.22	11.0	64.24
14	1304.	630.	0.10	-0.42	1009.64	21.0	7.7	7.2	2.7	7.5	1.07	4.1	1.10	10.9	60.78
15	1311.	634.	0.10	-0.43	1009.76	20.8	7.2	6.7	2.5	7.1	0.97	3.9	1.00	10.8	57.36
16	1318.	637.	0.11	-0.44	1009.88	20.7	6.8	6.3	2.4	6.6	0.87	3.7	0.90	10.7	53.98
17	1325.	640.	0.11	-0.45	1010.00	20.5	6.3	5.9	2.2	6.2	0.78	3.5	0.80	10.6	50.65
18	1332.	644.	0.12	-0.46	1010.10	20.3	5.9	5.5	2.0	5.7	0.69	3.3	0.71	10.5	47.37
19	1339.	647.	0.12	-0.47	1010.20	20.2	5.4	5.1	1.9	5.3	0.61	3.1	0.64	10.3	44.15
20	1347.	650.	0.13	-0.48	1010.30	20.1	5.0	4.7	1.7	4.9	0.54	2.9	0.54	10.4	40.84
21	1354.	653.	0.13	-0.49	1010.40	20.0	4.6	4.3	1.5	4.5	0.45	2.7	0.46	10.3	37.58
22	1361.	656.	0.14	-0.50	1010.48	19.8	4.2	3.9	1.4	4.1	0.38	2.5	0.34	10.3	34.44
23	1369.	660.	0.14	-0.51	1010.56	19.7	3.8	3.5	1.2	3.7	0.32	2.3	0.31	10.2	31.44
24	1376.	663.	0.15	-0.52	1010.63	19.6	3.4	3.2	1.1	3.3	0.27	2.1	0.28	10.1	28.53
1	1384.	666.	0.15	-0.54	1010.69	19.6	3.1	2.9	1.0	3.0	0.22	1.9	0.23	10.0	25.76

WAVE ENERGY IN THE BREAKER ZONE = 0.417E 10 JOULES

TOTAL LONG-SHORE CURRENT ENERGY = 0.271E 10 JOULES

TOTAL POSITIVE LONG-SHORE CURRENT ENERGY = 0.265E 10 JOULES

TOTAL NEGATIVE LONG-SHORE CURRENT ENERGY = 0.439E 08 JOULES

HOLLAND: MICHIGAN

RUN BEGINS AT HOUR 13 ON JULY 18, 1970

STORM - BAROMETRIC PRESSURE AT CENTER OF LOW = 1004.0 MILLIBARS
PRESSURE AT LARGEST ENCIRCLING ISOBAR = 1012.0 MILLIBARS
MAXIMUM PRESSURE INCLUDED IN STORM = 1013.1 MILLIBARS

LENGTH OF MAJOR HALF AXIS = 550.0 KILOMETERS
LENGTH OF MINOR HALF AXIS = 300.0 KILOMETERS
ORIENTATION OF MAJOR AXIS = 28.0 DEGREES FROM NORTH

LONGSHORE CURRENT EQUATION FROM FOX AND DAVIS, 1972

SHORE - POSITION COORDINATES - X = 1015.0 Y = 560.0 KILOMETERS

SHORE LATITUDE = 42. ONSHORE AZIMUTH = 90. DEGREES
NEARSHORE SLOPE = 0.033 AVERAGE FETCH = 190. KILOMETERS

HOUR	X	Y	X1	Y1	BARO. PRESS.	WIND ANGLE	SURF. WIND	ONSH WIND	ALSH WIND	EFFECT. WIND	WAVE H	WAVE T	BREAKER H	ANGLE	LSC VELOC.
	KM	KM	RAD	RAD	MB	DEG	M/S	M/S	M/S	M/S	M	SEC	M	DEG	CM/SEC
13	796.	705.	0.17	0.26	1011.16	202.6	4.7	-4.4	-1.8	1.7	0.03	0.7	0.03	-11.8	-11.90
14	805.	704.	0.17	0.25	1010.95	202.9	5.1	-4.6	-1.9	1.8	0.05	0.9	0.05	-11.9	-14.40
15	815.	703.	0.17	0.24	1010.73	203.3	5.4	-4.9	-2.1	1.9	0.06	1.0	0.06	-12.1	-16.10
16	824.	702.	0.17	0.23	1010.50	203.7	5.7	-5.2	-2.3	2.0	0.07	1.1	0.07	-12.3	-17.72
17	833.	701.	0.17	0.22	1010.26	204.1	6.0	-5.5	-2.4	2.1	0.08	1.1	0.09	-12.5	-19.18
18	843.	700.	0.16	0.20	1010.00	204.5	6.3	-5.7	-2.6	2.2	0.09	1.4	0.10	-12.7	-20.50
19	852.	699.	0.16	0.19	1009.74	205.0	6.5	-5.9	-2.7	2.3	0.11	1.3	0.11	-12.9	-21.83
20	855.	697.	0.16	0.19	1009.42	205.1	6.6	-6.0	-2.8	2.4	0.11	1.3	0.12	-12.9	-22.71
21	858.	696.	0.16	0.18	1009.51	205.2	6.7	-6.1	-2.8	2.4	0.12	1.4	0.12	-13.0	-23.46
22	861.	694.	0.16	0.18	1009.39	205.3	6.8	-6.2	-2.9	2.5	0.13	1.4	0.13	-13.0	-24.12
23	865.	692.	0.16	0.18	1009.27	205.4	6.9	-6.2	-2.9	2.5	0.14	1.5	0.14	-13.0	-24.71
24	868.	691.	0.15	0.17	1009.15	205.5	7.0	-6.3	-3.0	2.5	0.14	1.5	0.15	-13.1	-25.25
1	871.	689.	0.15	0.17	1009.02	205.6	7.1	-6.4	-3.0	2.6	0.15	1.5	0.15	-13.1	-25.76
2	885.	688.	0.15	0.15	1008.59	206.7	7.3	-6.5	-3.3	2.7	0.15	1.6	0.16	-13.7	-27.04
3	899.	688.	0.15	0.14	1008.15	208.0	7.4	-6.6	-3.5	2.7	0.16	1.6	0.16	-14.3	-28.38
4	913.	688.	0.15	0.12	1007.71	209.5	7.5	-6.5	-3.7	2.8	0.17	1.6	0.17	-15.0	-29.73
5	928.	687.	0.15	0.10	1007.28	211.4	7.4	-6.3	-3.9	2.8	0.18	1.7	0.18	-15.9	-31.00
6	942.	687.	0.15	0.08	1006.86	213.8	7.3	-6.0	-4.0	2.8	0.18	1.7	0.18	-17.0	-32.08
7	956.	686.	0.15	0.07	1006.46	216.7	7.0	-5.6	-4.2	2.8	0.18	1.7	0.18	-16.2	-32.88
8	968.	683.	0.14	0.05	1006.14	218.9	6.5	-5.2	-4.2	2.7	0.19	1.7	0.18	-19.0	-32.92
9	975.	679.	0.14	0.04	1005.84	221.5	6.3	-4.7	-4.2	2.6	0.19	1.8	0.18	-19.9	-32.44
10	985.	676.	0.14	0.03	1005.56	224.9	5.9	-4.2	-4.2	2.5	0.18	1.7	0.17	-21.1	-31.13
11	995.	673.	0.13	0.02	1005.31	229.1	5.4	-3.5	-4.1	2.4	0.16	1.7	0.15	-22.6	-28.97
12	1004.	669.	0.13	0.01	1005.08	234.7	4.9	-2.8	-4.0	2.3	0.15	1.6	0.13	-24.5	-25.45
13	1014.	666.	0.12	0.00	1004.89	242.2	4.4	-2.0	-3.9	2.2	0.14	1.5	0.11	-26.7	-21.81
14	1028.	663.	0.12	-0.01	1004.71	256.9	3.9	-0.8	-3.8	2.1	0.14	1.5	0.07	-30.3	-14.07
15	1041.	661.	0.12	-0.03	1004.59	276.3	4.1	0.4	-4.0	2.8	0.15	1.5	0.05	-31.7	-9.86
16	1055.	658.	0.11	-0.04	1004.54	296.5	4.3	1.9	-3.8	3.5	0.18	1.7	0.18	-28.3	-24.46
17	1068.	655.	0.11	-0.06	1004.55	319.7	4.2	3.2	-2.7	3.9	0.21	1.8	0.20	-20.0	-36.22
18	1081.	653.	0.11	-0.08	1004.63	340.5	4.8	4.5	-1.6	4.7	0.27	2.0	0.28	-10.4	-29.15
19	1093.	650.	0.10	-0.09	1004.78	355.3	5.7	5.7	-0.6	5.7	0.35	2.3	0.36	-2.4	-6.88
20	1106.	649.	0.10	-0.11	1004.95	370.0	6.6	6.6	0.3	6.6	0.44	2.6	0.46	1.6	6.66
21	1117.	648.	0.10	-0.12	1005.16	387.7	7.5	7.4	1.1	7.4	0.55	2.9	0.57	4.6	20.62
22	1127.	646.	0.10	-0.13	1005.39	412.9	8.3	8.1	1.8	8.2	0.67	3.2	0.69	6.8	32.79
23	1138.	645.	0.10	-0.14	1005.66	446.2	9.1	8.7	2.5	9.0	0.79	3.5	0.82	8.5	43.37
24	1149.	644.	0.10	-0.16	1005.95	486.8	9.8	9.3	3.1	9.6	0.92	3.8	0.95	9.9	52.59
1	1160.	643.	0.10	-0.17	1006.27	530.8	10.4	9.7	3.7	10.2	1.05	4.0	1.07	10.9	60.66
2	1166.	646.	0.10	-0.18	1006.44	570.9	10.6	9.9	3.7	10.3	1.16	4.2	1.19	10.9	63.74
3	1172.	650.	0.10	-0.19	1006.61	610.9	10.7	10.0	3.8	10.5	1.27	4.4	1.30	10.9	66.53
4	1178.	653.	0.11	-0.19	1006.78	650.9	10.9	10.2	3.9	10.6	1.36	4.6	1.40	10.9	68.92
5	1184.	656.	0.11	-0.20	1006.95	690.9	11.0	10.3	3.9	10.8	1.45	4.8	1.48	10.9	71.05
6	1190.	660.	0.12	-0.21	1007.13	730.9	11.1	10.3	3.9	10.8	1.53	4.9	1.56	10.9	72.91
7	1196.	663.	0.12	-0.21	1007.31	770.9	11.2	10.4	4.0	10.9	1.60	5.0	1.64	11.0	74.57
8	1213.	667.	0.12	-0.24	1007.85	821.1	11.3	10.5	4.2	11.0	1.66	5.1	1.70	11.5	76.86
9	1231.	671.	0.13	-0.26	1008.39	871.0	11.2	10.3	4.1	10.9	1.72	5.2	1.75	12.0	78.26
10	1248.	674.	0.13	-0.28	1008.93	920.7	10.9	10.0	4.4	10.6	1.76	5.3	1.79	12.3	80.82
11	1265.	678.	0.14	-0.30	1009.45	970.4	10.4	9.5	4.3	10.1	1.78	5.3	1.81	12.6	83.55
12	1283.	682.	0.14	-0.32	1009.94	1020.9	9.8	8.9	4.1	9.5	1.64	5.1	1.67	12.9	86.11
13	1300.	686.	0.15	-0.34	1010.40	1071.4	9.1	8.2	3.9	8.8	1.47	4.8	1.49	13.1	88.30
14	1312.	694.	0.16	-0.35	1010.67	1121.9	8.5	7.7	3.6	8.3	1.35	4.6	1.37	12.9	90.26
15	1324.	702.	0.17	-0.37	1010.92	1172.4	8.0	7.2	3.3	7.7	1.21	4.4	1.23	12.8	91.60
16	1335.	710.	0.18	-0.38	1011.16	1222.9	7.4	6.7	3.1	7.2	1.06	4.1	1.08	12.6	92.73
17	1347.	719.	0.19	-0.40	1011.39	1273.4	6.9	6.2	2.8	6.6	0.93	3.8	0.94	12.5	93.79
18	1359.	727.	0.20	-0.41	1011.60	1323.9	6.3	5.7	2.5	6.1	0.79	3.6	0.81	12.3	94.84
19	1371.	735.	0.21	-0.43	1011.79	1374.4	5.7	5.2	2.3	5.6	0.67	3.3	0.69	12.2	95.92
20	1383.	749.	0.22	-0.44	1011.97	1424.9	5.2	4.8	2.0	5.0	0.56	3.0	0.57	11.9	96.37
21	1395.	762.	0.24	-0.46	1012.13	1475.4	4.6	4.3	1.7	4.5	0.45	2.7	0.46	11.5	96.94
22	1407.	776.	0.26	-0.47	1012.27	1525.9	4.1	3.8	1.5	4.0	0.37	2.4	0.38	11.2	97.18
23	1419.	789.	0.27	-0.48	1012.40	1576.4	3.7	3.4	1.3	3.6	0.30	2.2	0.31	10.8	97.75
24	1431.	803.	0.29	-0.50	1012.52	1626.9	3.2	3.0	1.1	3.1	0.23	1.9	0.24	10.5	97.57
1	1443.	816.	0.31	-0.51	1012.63	1677.4	2.8	2.6	0.9	2.7	0.18	1.7	0.19	10.2	97.68
2	1460.	839.	0.33	-0.53	1012.76	1727.9	2.2	2.1	0.7	2.2	0.12	1.4	0.12	9.6	98.42
3	1478.	861.	0.36	-0.56	1012.87	1778.4	1.7	1.6	0.5	1.7	0.07	1.1	0.08	9.0	13.83
4	1495.	884.	0.39	-0.58	1012.95	1828.9	1.3	1.2	0.3	1.2	0.04	0.8	0.04	8.5	9.96
5	1512.	907.	0.42	-0.60	1013.02	1879.4	0.9	0.9	0.2	0.9	0.02	0.6	0.02	8.0	6.91
6	1530.	929.	0.44	-0.62	1013.07	1929.9	0.6	0.6	0.1	0.6	0.01	0.4	0.01	7.6	4.57
7	1547.	952.	0.47	-0.64	1013.10	1980.4	0.4	0.4	0.1	0.4	0.00	0.3	0.00	7.1	2.87

WAVE ENERGY IN THE BREAKER ZONE = 0.138E 10 JOULES

TOTAL LONG-SHORE CURRENT ENERGY = 0.965E 09 JOULES

TOTAL POSITIVE LONG-SHORE CURRENT ENERGY = 0.962E 09 JOULES

TOTAL NEGATIVE LONG-SHORE CURRENT ENERGY = 0.263E 07 JOULES

SHEBOYGAN, WISCONSIN

RUN BEGINS AT HOUR 7 ON JULY 13, 1972

STORM - BAROMETRIC PRESSURE AT CENTER OF LOW = 990.0 MILLIBARS
PRESSURE AT LARGEST ENCIRCLING ISOBAR = 1008.0 MILLIBARS
MAXIMUM PRESSURE INCLUDED IN STORM = 1010.6 MILLIBARS

LENGTH OF MAJOR HALF AXIS = 1750.0 KILOMETERS
LENGTH OF MINOR HALF AXIS = 875.0 KILOMETERS
ORIENTATION OF MAJOR AXIS = 25.0 DEGREES FROM NORTH

LONGSHORE CURRENT EQUATION FROM FOX AND DAVIS, 1972

SHORE - POSITION COORDINATES - X = 1892.0 Y = 1112.0 KILOMETERS

SHORE LATITUDE = 42. ONSHORE AZIMUTH = 270. DEGREES
NEARSHORE SLOPE = 0.030 AVERAGE FETCH = 200. KILOMETERS

HOUR	X	Y	X1	Y1	BARO.	WIND	SURF.	ONSH.	ALSH.	EFFECT.	WAVE	WAVE	BREAKER	LSC
	KM	KM	RAD	RAD	PRESS.	ANGLE	WIND	WIND	WIND	WIND	H	T	ANGLE	VELOC.
					MB	DEG	M/S	M/S	M/S	M/S	M	SEC	DEG	CM/SEC
7	585.	1794.	-0.25	-0.49	1010.53	49.2	0.1	0.1	0.1	0.1	0.00	0.1	0.00	1.74
8	621.	1793.	-0.25	-0.48	1010.51	49.3	0.2	0.1	0.1	0.2	0.00	0.1	0.00	2.17
9	657.	1792.	-0.25	-0.47	1010.49	49.4	0.2	0.1	0.2	0.2	0.00	0.1	0.00	2.68
10	692.	1791.	-0.25	-0.45	1010.46	49.6	0.3	0.2	0.2	0.3	0.00	0.2	0.00	3.27
11	728.	1790.	-0.25	-0.44	1010.42	49.7	0.4	0.2	0.3	0.3	0.00	0.2	0.00	3.96
12	764.	1789.	-0.25	-0.42	1010.37	49.8	0.5	0.3	0.4	0.4	0.00	0.2	0.00	4.75
13	800.	1788.	-0.25	-0.41	1010.32	50.0	0.6	0.4	0.4	0.5	0.00	0.3	0.00	5.65
14	842.	1788.	-0.25	-0.39	1010.24	50.2	0.8	0.5	0.6	0.7	0.01	0.4	0.00	6.80
15	884.	1788.	-0.25	-0.38	1010.14	50.4	0.9	0.6	0.7	0.8	0.01	0.5	0.01	8.13
16	926.	1788.	-0.25	-0.36	1010.02	50.6	1.2	0.7	0.9	1.0	0.02	0.5	0.01	9.64
17	969.	1788.	-0.25	-0.35	1009.87	50.8	1.4	0.9	1.1	1.2	0.03	0.6	0.02	11.32
18	1011.	1788.	-0.25	-0.33	1009.70	51.1	1.7	1.1	1.3	1.5	0.04	0.8	0.03	13.18
19	1053.	1788.	-0.25	-0.31	1009.49	51.3	2.0	1.3	1.6	1.8	0.05	0.9	0.04	15.22
20	1085.	1790.	-0.25	-0.30	1009.31	51.5	2.3	1.4	1.8	2.0	0.07	1.0	0.06	17.10
21	1116.	1792.	-0.25	-0.29	1009.12	51.8	2.6	1.6	2.0	2.2	0.08	1.1	0.07	18.96
22	1147.	1794.	-0.25	-0.28	1008.91	52.0	2.9	1.8	2.3	2.5	0.10	1.3	0.09	20.85
23	1179.	1796.	-0.26	-0.27	1008.67	52.2	3.2	1.9	2.5	2.8	0.12	1.4	0.10	22.79
24	1210.	1798.	-0.26	-0.25	1008.41	52.5	3.5	2.1	2.8	3.1	0.15	1.5	0.13	24.77
1	1242.	1800.	-0.26	-0.24	1008.12	52.7	3.9	2.3	3.1	3.4	0.17	1.6	0.15	26.80
2	1280.	1806.	-0.26	-0.23	1007.76	53.1	4.3	2.6	3.4	3.7	0.20	1.8	0.17	28.91
3	1318.	1813.	-0.26	-0.21	1007.38	53.5	4.7	2.8	3.8	4.1	0.24	1.9	0.20	31.08
4	1355.	1819.	-0.26	-0.20	1006.96	53.8	5.2	3.0	4.2	4.4	0.28	2.1	0.24	33.27
5	1393.	1826.	-0.27	-0.18	1006.51	54.3	5.6	3.2	4.5	4.8	0.32	2.2	0.27	35.44
6	1431.	1832.	-0.27	-0.17	1006.04	54.7	6.0	3.4	4.9	5.2	0.37	2.4	0.31	37.57
7	1469.	1839.	-0.27	-0.16	1005.53	55.1	6.4	3.6	5.3	5.5	0.41	2.5	0.35	39.63
8	1505.	1862.	-0.28	-0.14	1005.22	55.7	6.6	3.7	5.5	5.7	0.46	2.7	0.38	41.30
9	1541.	1885.	-0.29	-0.13	1004.92	56.2	6.8	3.8	5.7	5.8	0.50	2.8	0.41	42.70
10	1576.	1907.	-0.30	-0.12	1004.62	56.8	7.0	3.9	5.8	5.9	0.54	2.9	0.44	43.87
11	1612.	1930.	-0.31	-0.10	1004.33	57.3	7.1	3.8	6.0	6.0	0.58	3.0	0.47	44.84
12	1648.	1953.	-0.32	-0.09	1004.05	57.9	7.3	3.8	6.1	6.1	0.61	3.1	0.49	45.62
13	1684.	1976.	-0.32	-0.07	1003.79	58.4	7.3	3.8	6.3	6.2	0.64	3.2	0.51	46.22
14	1702.	1994.	-0.33	-0.07	1003.76	58.6	7.3	3.8	6.3	6.1	0.67	3.2	0.53	46.82
15	1721.	2013.	-0.36	-0.06	1003.73	59.1	7.3	3.7	6.3	6.1	0.69	3.3	0.55	47.25
16	1739.	2031.	-0.35	-0.05	1003.72	59.4	7.3	3.7	6.3	6.1	0.70	3.3	0.56	47.54
17	1757.	2050.	-0.35	-0.05	1003.71	59.7	7.2	3.6	6.2	6.0	0.72	3.4	0.57	47.70
18	1776.	2068.	-0.36	-0.04	1003.71	60.0	7.2	3.6	6.2	6.0	0.73	3.4	0.58	47.75
19	1794.	2087.	-0.37	-0.03	1003.72	60.4	7.1	3.5	6.2	5.9	0.74	3.4	0.58	47.70
20	1811.	2108.	-0.37	-0.03	1003.78	60.7	7.1	3.4	6.1	5.8	0.75	3.5	0.58	47.57
21	1829.	2128.	-0.38	-0.02	1003.84	61.0	7.0	3.4	6.1	5.8	0.75	3.5	0.58	47.34
22	1846.	2149.	-0.39	-0.01	1003.92	61.3	6.9	3.3	6.0	5.7	0.75	3.5	0.58	47.04
23	1863.	2169.	-0.40	-0.01	1003.99	61.7	6.8	3.2	6.0	5.6	0.75	3.5	0.58	46.67
24	1881.	2190.	-0.41	-0.00	1004.08	62.0	6.7	3.1	5.9	5.5	0.75	3.5	0.58	46.22
1	1898.	2210.	-0.41	0.00	1004.17	62.3	6.6	3.0	5.8	5.4	0.74	3.5	0.57	45.66
2	1920.	2231.	-0.42	0.01	1004.22	62.8	6.5	2.9	5.8	5.3	0.72	3.4	0.55	44.97
3	1941.	2251.	-0.43	0.01	1004.28	63.3	6.4	2.9	5.7	5.2	0.70	3.4	0.53	44.41
4	1963.	2272.	-0.44	0.02	1004.34	63.8	6.3	2.8	5.7	5.1	0.68	3.3	0.51	43.19
5	1985.	2293.	-0.44	0.03	1004.42	64.3	6.2	2.7	5.6	5.0	0.65	3.3	0.49	41.91
6	2006.	2313.	-0.45	0.04	1004.50	64.9	6.1	2.5	5.5	4.9	0.63	3.2	0.46	39.55
7	2028.	2334.	-0.46	0.05	1004.60	65.6	6.0	2.4	5.4	4.8	0.60	3.2	0.44	38.13

WAVE ENERGY IN THE BREAKER ZONE = 0.168E 09 JOULES

TOTAL LONG-SHORE CURRENT ENERGY = 0.117E 09 JOULES

TOTAL POSITIVE LONG-SHORE CURRENT ENERGY = 0.117E 09 JOULES

TOTAL NEGATIVE LONG-SHORE CURRENT ENERGY = 0.000E 00 JOULES

SHEBOYGAN, WISCONSIN

RUN BEGINS AT HOUR 7 ON JULY 16, 1972

STORM - BAROMETRIC PRESSURE AT CENTER OF LOW = 1002.0 MILLIBARS
 PRESSURE AT LARGEST ENCIRCLING ISOBAR = 1016.0 MILLIBARS
 MAXIMUM PRESSURE INCLUDED IN STORM = 1018.0 MILLIBARS

LENGTH OF MAJOR HALF AXIS = 1050.0 KILOMETERS
 LENGTH OF MINOR HALF AXIS = 700.0 KILOMETERS
 ORIENTATION OF MAJOR AXIS = 20.0 DEGREES FROM NORTH

LONGSHORE CURRENT EQUATION FROM FOX AND DAVIS, 1972

SHORE - POSITION COORDINATES - X = 1892.0 Y = 1112.0 KILOMETERS

SHORE LATITUDE = 42. ONSHORE AZIMUTH = 270. DEGREES
 NEARSHORE SLOPE = 0.030 AVERAGE FETCH = 200. KILOMETERS

HOUR	X	Y	X1	Y1	BARO. PRESS.	WIND ANGLE	SURF. WIND	ONSH WIND	ALSH WIND	EFFECT. WIND	WAVE H	WAVE T	BREAKER H	BREAKER ANGLE	LSC VELOC.
	KM	KM	RAD	RAD	MB	DEG	M/S	M/S	M/S	M/S	M	SEC	M	DEG	CM/SEC
7	176.	286.	0.52	-1.08	1018.02	29.6	0.0	0.0	0.0	0.0	0.00	0.0	0.00	0.0	0.00
8	212.	296.	0.51	-1.06	1018.02	29.5	0.0	0.0	0.0	0.0	0.00	0.0	0.00	0.0	0.00
9	247.	306.	0.51	-1.04	1018.02	29.3	0.0	0.0	0.0	0.0	0.00	0.0	0.00	0.0	0.00
10	283.	315.	0.50	-1.02	1018.02	29.1	0.0	0.0	0.0	0.0	0.00	0.0	0.00	0.0	0.00
11	319.	325.	0.49	-0.99	1018.02	29.0	0.0	0.0	0.0	0.0	0.00	0.0	0.00	0.0	0.00
12	354.	335.	0.49	-0.97	1018.02	28.8	0.0	0.0	0.0	0.0	0.00	0.0	0.00	0.0	0.00
13	390.	345.	0.48	-0.95	1018.02	28.6	0.0	0.0	0.0	0.0	0.00	0.0	0.00	0.0	0.00
14	425.	356.	0.48	-0.93	1018.02	28.4	0.0	0.0	0.0	0.0	0.00	0.0	0.00	0.0	0.00
15	459.	367.	0.47	-0.90	1018.02	28.3	0.0	0.0	0.0	0.0	0.00	0.0	0.00	0.0	0.00
16	494.	377.	0.46	-0.88	1018.02	28.1	0.0	0.0	0.0	0.0	0.00	0.0	0.00	0.0	0.00
17	529.	388.	0.45	-0.86	1018.02	27.9	0.0	0.0	0.0	0.0	0.00	0.0	0.00	0.0	0.00
18	563.	399.	0.45	-0.84	1018.02	27.7	0.0	0.0	0.0	0.0	0.00	0.0	0.00	0.0	0.00
19	598.	410.	0.44	-0.82	1018.01	27.5	0.0	0.0	0.0	0.0	0.00	0.0	0.00	0.0	0.00
20	630.	424.	0.43	-0.80	1018.01	27.4	0.0	0.0	0.0	0.0	0.00	0.0	0.00	0.0	0.00
21	663.	438.	0.42	-0.78	1018.00	27.3	0.0	0.0	0.0	0.0	0.00	0.0	0.00	0.0	0.00
22	695.	452.	0.41	-0.75	1017.99	27.1	0.1	0.1	0.0	0.1	0.00	0.0	0.00	0.0	0.00
23	728.	466.	0.41	-0.73	1017.97	27.0	0.2	0.1	0.0	0.1	0.00	0.1	0.00	13.7	1.82
24	760.	480.	0.40	-0.71	1017.94	26.9	0.2	0.2	0.1	0.2	0.00	0.1	0.00	13.6	4.59
1	793.	494.	0.39	-0.69	1017.91	26.8	0.3	0.1	0.1	0.3	0.00	0.2	0.00	13.6	3.49
2	841.	518.	0.37	-0.66	1017.83	26.7	0.5	0.5	0.2	0.5	0.00	0.3	0.00	13.7	5.09
3	888.	542.	0.36	-0.63	1017.72	26.5	0.8	0.7	0.3	0.8	0.01	0.4	0.01	13.7	7.13
4	936.	565.	0.34	-0.60	1017.55	26.4	1.2	1.1	0.5	1.2	0.02	0.6	0.02	13.6	9.62
5	984.	589.	0.33	-0.57	1017.33	26.3	1.7	1.5	0.7	1.6	0.04	0.8	0.04	13.6	12.58
6	1031.	613.	0.31	-0.54	1017.03	26.1	2.2	2.0	1.0	2.2	0.06	1.0	0.06	13.5	15.97
7	1079.	637.	0.30	-0.51	1016.64	26.0	2.9	2.6	1.3	2.8	0.10	1.2	0.10	13.5	19.78
8	1130.	689.	0.26	-0.48	1016.07	27.0	3.8	3.4	1.7	3.7	0.15	1.5	0.15	14.0	24.85
9	1182.	740.	0.23	-0.45	1015.37	28.2	4.8	4.2	2.2	4.6	0.22	1.8	0.22	14.6	30.55
10	1233.	792.	0.20	-0.41	1014.53	29.5	5.7	5.0	2.8	5.5	0.30	2.2	0.30	15.2	36.64
11	1284.	844.	0.17	-0.38	1013.58	31.0	6.7	5.7	3.4	6.4	0.40	2.5	0.40	16.0	42.93
12	1336.	895.	0.13	-0.35	1012.51	32.8	7.6	6.3	4.1	7.2	0.51	2.8	0.50	16.8	49.12
13	1387.	945.	0.10	-0.32	1011.38	34.9	8.3	6.8	4.7	7.8	0.61	3.1	0.60	17.8	56.92
14	1421.	989.	0.07	-0.29	1010.61	37.0	8.7	6.9	5.2	8.1	0.71	3.3	0.69	18.7	59.59
15	1456.	1030.	0.05	-0.27	1009.85	39.4	9.0	6.9	5.7	8.3	0.80	3.5	0.76	19.7	63.31
16	1490.	1072.	0.02	-0.25	1009.11	42.0	9.2	6.8	6.1	8.4	0.88	3.7	0.82	20.9	65.93
17	1524.	1113.	-0.00	-0.23	1008.41	45.0	9.3	6.6	6.0	8.4	0.94	3.8	0.87	22.1	67.26
18	1559.	1155.	-0.02	-0.21	1007.77	48.0	9.3	6.2	6.9	8.3	1.01	3.9	0.89	23.3	67.34
19	1593.	1196.	-0.05	-0.18	1007.20	51.0	9.2	5.8	7.2	8.1	1.04	4.0	0.91	24.5	66.36
20	1636.	1233.	-0.07	-0.16	1006.44	53.8	9.0	5.3	7.2	7.8	1.06	4.1	0.89	25.3	64.55
21	1680.	1270.	-0.10	-0.13	1005.79	56.4	8.6	4.7	7.2	7.3	1.07	4.1	0.87	26.1	62.01
22	1723.	1307.	-0.12	-0.10	1005.28	59.0	8.2	4.2	7.0	6.8	0.98	3.9	0.78	26.9	58.33
23	1766.	1343.	-0.14	-0.07	1004.92	61.6	7.7	3.6	6.8	6.3	0.86	3.7	0.67	27.6	50.14
24	1810.	1380.	-0.17	-0.05	1004.73	65.1	7.2	3.0	6.5	5.8	0.75	3.5	0.55	28.5	43.14
1	1853.	1417.	-0.19	-0.02	1004.71	70.9	6.8	2.1	6.2	5.1	0.63	3.2	0.40	29.6	35.94
2	1882.	1504.	-0.24	-0.00	1005.80	77.3	6.6	1.4	6.5	4.9	0.61	3.2	0.32	30.5	26.02
3	1911.	1590.	-0.30	0.01	1007.09	83.1	6.5	0.7	6.4	4.6	0.55	3.0	0.22	30.8	17.92
4	1940.	1677.	-0.35	0.03	1008.52	87.5	6.2	0.2	6.2	4.2	0.48	2.8	0.11	30.9	9.95
5	1970.	1764.	-0.41	0.04	1010.00	90.9	5.8	-0.0	5.8	3.8	0.40	2.6	0.06	30.9	5.65
6	1999.	1850.	-0.46	0.06	1011.47	93.6	5.3	-0.3	5.2	3.4	0.32	2.4	0.04	30.9	10.03
7	2028.	1937.	-0.52	0.08	1012.87	95.8	4.6	-0.4	4.6	2.9	0.24	2.1	0.09	30.1	11.13
8	2057.	1988.	-0.55	0.09	1013.65	95.8	4.2	-0.4	4.2	2.7	0.20	1.9	0.07	29.9	10.33
9	2045.	2039.	-0.58	0.09	1014.37	95.9	3.8	-0.4	3.8	2.4	0.17	1.8	0.06	29.8	9.43
10	2054.	2090.	-0.62	0.10	1015.03	95.9	3.4	-0.3	3.4	2.1	0.13	1.6	0.05	29.6	8.44
11	2063.	2141.	-0.65	0.10	1015.61	95.9	3.0	-0.3	3.0	1.9	0.10	1.4	0.03	29.3	7.41
12	2071.	2192.	-0.68	0.11	1016.12	95.9	2.5	-0.2	2.5	1.6	0.07	1.2	0.02	29.1	6.33
13	2080.	2243.	-0.71	0.11	1016.56	96.0	2.1	-0.2	2.1	1.3	0.05	1.0	0.01	28.9	5.30
14	2099.	2288.	-0.74	0.13	1016.89	97.0	1.7	-0.2	1.7	1.1	0.03	0.8	0.01	28.7	4.70
15	2117.	2334.	-0.77	0.14	1017.16	98.0	1.4	-0.1	1.4	0.8	0.02	0.6	0.00	28.6	4.01
16	2135.	2379.	-0.80	0.15	1017.39	98.9	1.1	-0.1	1.1	0.6	0.01	0.5	0.00	28.4	3.30
17	2154.	2424.	-0.83	0.16	1017.58	99.7	0.8	-0.1	0.8	0.5	0.00	0.4	0.00	28.3	2.61
18	2172.	2470.	-0.86	0.17	1017.72	100.5	0.6	-0.1	0.6	0.3	0.00	0.2	0.00	28.2	1.98
19	2191.	2515.	-0.89	0.18	1017.83	101.2	0.4	-0.0	0.4	0.2	0.00	0.2	0.00	28.2	1.42

WAVE ENERGY IN THE BREAKER ZONE = 0.2246 09 JOULES

TOTAL LONG-SHORE CURRENT ENERGY = 0.1956 09 JOULES

TOTAL POSITIVE LONG-SHORE CURRENT ENERGY = 0.1956 09 JOULES

TOTAL NEGATIVE LONG-SHORE CURRENT ENERGY = 0.0000 00 JOULES

SHEBOYGAN, WISCONSIN

RUN BEGINS AT HOUR 7 ON AUGUST 14, 1972

STORM - BAROMETRIC PRESSURE AT CENTER OF LOW = 1002.0 MILLIBARS
 PRESSURE AT LARGEST ENCIRCLING ISOBAR = 1012.0 MILLIBARS
 MAXIMUM PRESSURE INCLUDED IN STORM = 1013.4 MILLIBARS

LENGTH OF MAJOR HALF AXIS = 1400.0 KILOMETERS
 LENGTH OF MINOR HALF AXIS = 450.0 KILOMETERS
 ORIENTATION OF MAJOR AXIS = 12.0 DEGREES FROM NORTH

LONGSHORE CURRENT EQUATION FROM FOX AND DAVIS, 1972

SHORT - POSITION COORDINATES - X = 1892.0 Y = 1112.0 KILOMETERS

SHORE LATITUDE = 42. ONSHORE AZIMUTH = 270. DEGREES
 NEARSHORE SLOPE = 0.030 AVERAGE FETCH = 200. KILOMETERS

HOUR	X	Y	X1	Y1	BARO. PRESS.	WIND ANGLE	SURF. WIND	ONSH. WIND	ALSH. WIND	EFFECT. WIND	WAVE H	WAVE T	BREAKER H	BREAKER ANGLE	LSC VELOC.
	KM	KM	RAD	RAD	MB	DEG	M/S	M/S	M/S	M/S	M	SEC	M	DEG	CM/SEC
7	598.	1911.	-0.38	-0.61	1013.45	57.5	0.0	0.0	0.0	0.0	0.00	0.0	0.00	0.0	0.00
8	639.	1793.	-0.32	-0.59	1013.45	57.4	0.0	0.0	0.0	0.0	0.00	0.0	0.00	0.0	0.00
9	680.	1675.	-0.26	-0.57	1013.45	57.2	0.0	0.0	0.0	0.0	0.00	0.0	0.00	23.9	0.00
10	721.	1557.	-0.21	-0.55	1013.44	57.0	0.0	0.0	0.0	0.0	0.00	0.0	0.00	23.8	0.00
11	763.	1439.	-0.15	-0.53	1013.44	56.8	0.0	0.0	0.0	0.0	0.00	0.0	0.00	23.7	0.00
12	804.	1321.	-0.09	-0.51	1013.44	56.6	0.0	0.0	0.0	0.0	0.00	0.0	0.00	23.6	0.01
13	845.	1203.	-0.04	-0.49	1013.44	56.5	0.0	0.0	0.0	0.0	0.00	0.0	0.00	23.6	0.01
14	875.	1273.	-0.07	-0.48	1013.44	56.5	0.0	0.0	0.0	0.0	0.00	0.0	0.00	23.7	0.01
15	906.	1344.	-0.11	-0.46	1013.44	56.7	0.0	0.0	0.0	0.0	0.00	0.0	0.00	23.7	0.02
16	936.	1414.	-0.14	-0.45	1013.44	56.9	0.0	0.0	0.0	0.0	0.00	0.0	0.00	23.8	0.03
17	966.	1484.	-0.17	-0.44	1013.44	57.1	0.0	0.0	0.0	0.0	0.00	0.0	0.00	23.8	0.04
18	997.	1555.	-0.21	-0.42	1013.44	57.3	0.0	0.0	0.0	0.0	0.00	0.0	0.00	23.9	0.04
19	1027.	1625.	-0.24	-0.41	1013.44	57.5	0.0	0.0	0.0	0.0	0.00	0.0	0.00	24.0	0.05
20	1055.	1615.	-0.23	-0.39	1013.44	57.5	0.0	0.0	0.0	0.0	0.00	0.0	0.00	24.0	0.09
21	1093.	1605.	-0.23	-0.38	1013.44	57.5	0.0	0.0	0.0	0.0	0.00	0.0	0.00	24.1	0.16
22	1111.	1596.	-0.23	-0.37	1013.44	57.5	0.0	0.0	0.0	0.0	0.00	0.0	0.00	24.2	0.27
23	1140.	1586.	-0.22	-0.35	1013.44	57.6	0.0	0.0	0.0	0.0	0.00	0.0	0.00	24.3	0.43
24	1168.	1576.	-0.22	-0.34	1013.44	57.6	0.0	0.0	0.0	0.0	0.00	0.0	0.00	24.4	0.69
1	1196.	1566.	-0.21	-0.33	1013.42	57.6	0.1	0.0	0.1	0.1	0.00	0.0	0.00	24.5	1.07
2	1221.	1565.	-0.21	-0.31	1013.41	57.6	0.1	0.0	0.1	0.1	0.00	0.1	0.00	25.3	1.49
3	1246.	1564.	-0.21	-0.30	1013.39	57.7	0.2	0.1	0.2	0.2	0.00	0.1	0.00	25.9	2.03
4	1270.	1563.	-0.21	-0.29	1013.37	57.7	0.3	0.1	0.2	0.2	0.00	0.1	0.00	26.1	2.72
5	1295.	1562.	-0.21	-0.28	1013.34	57.8	0.4	0.2	0.4	0.4	0.00	0.2	0.00	26.3	3.58
6	1320.	1561.	-0.21	-0.27	1013.30	57.9	0.6	0.3	0.5	0.5	0.00	0.3	0.00	26.4	4.62
7	1345.	1560.	-0.21	-0.26	1013.25	57.9	0.8	0.4	0.7	0.7	0.01	0.4	0.00	26.5	5.88
8	1396.	1574.	-0.22	-0.23	1013.11	58.1	1.3	0.7	1.1	1.1	0.02	0.5	0.01	26.7	8.44
9	1447.	1588.	-0.22	-0.21	1012.89	58.3	2.0	1.0	1.7	1.7	0.04	0.8	0.03	26.9	11.82
10	1498.	1602.	-0.23	-0.18	1012.57	58.6	2.9	1.9	2.5	2.4	0.07	1.1	0.06	27.0	15.91
11	1549.	1616.	-0.24	-0.16	1012.11	58.9	4.0	2.1	3.4	3.4	0.12	1.4	0.10	27.2	20.56
12	1600.	1630.	-0.24	-0.15	1011.51	59.3	5.3	2.7	4.6	4.4	0.20	1.7	0.16	27.3	25.53
13	1651.	1644.	-0.25	-0.11	1010.75	59.7	6.6	3.3	5.7	5.5	0.29	2.1	0.23	27.5	30.43
14	1697.	1670.	-0.26	-0.09	1010.05	60.3	7.4	3.6	6.4	6.1	0.38	2.4	0.30	27.6	34.44
15	1744.	1696.	-0.27	-0.07	1009.30	61.1	8.0	3.8	7.0	6.6	0.47	2.7	0.36	27.8	37.47
16	1790.	1722.	-0.29	-0.04	1008.55	62.1	8.1	3.8	7.2	6.7	0.54	2.9	0.41	28.1	39.29
17	1837.	1748.	-0.30	-0.02	1007.86	63.5	7.9	3.5	7.0	6.4	0.59	3.1	0.44	28.4	39.56
18	1883.	1774.	-0.31	-0.00	1007.29	66.1	7.1	2.8	6.5	5.7	0.61	3.1	0.43	28.9	37.66
19	1930.	1800.	-0.32	0.01	1006.88	71.5	5.8	1.8	5.5	4.4	0.53	3.0	0.34	29.3	30.18
20	1969.	1831.	-0.34	0.03	1006.81	81.6	4.3	0.6	4.3	3.1	0.27	2.2	0.12	30.0	14.08
21	2007.	1861.	-0.35	0.05	1006.90	97.8	3.0	-0.4	3.0	1.8	0.10	1.4	0.04	29.2	8.40
22	2046.	1891.	-0.37	0.07	1007.13	118.5	2.4	-1.1	2.1	1.2	0.04	0.9	0.03	25.3	11.08
23	2084.	1922.	-0.38	0.09	1007.51	139.4	2.4	-1.8	1.6	1.0	0.03	0.7	0.02	18.3	10.97
24	2123.	1952.	-0.40	0.10	1008.01	156.2	2.6	-2.4	1.0	0.9	0.02	0.7	0.02	11.2	8.33
1	2161.	1983.	-0.41	0.12	1008.60	167.9	2.9	-2.8	0.6	1.0	0.02	0.8	0.02	6.1	5.24
2	2205.	2020.	-0.43	0.14	1009.35	176.7	3.1	-3.1	0.1	1.0	0.02	0.8	0.03	1.6	1.52
3	2249.	2056.	-0.44	0.16	1010.12	182.7	3.1	-3.1	-0.1	1.0	0.02	0.7	0.03	-1.4	-1.28
4	2292.	2093.	-0.46	0.19	1010.86	184.9	2.5	-2.9	-0.3	0.9	0.02	0.7	0.03	-3.3	-2.86
5	2336.	2130.	-0.48	0.21	1011.52	190.0	2.5	-2.5	-0.4	0.8	0.02	0.6	0.02	-4.8	-3.58
6	2380.	2166.	-0.50	0.23	1012.08	192.4	2.1	-2.0	-0.4	0.7	0.01	0.5	0.01	-5.9	-3.62
7	2424.	2203.	-0.51	0.25	1012.53	194.2	1.6	-1.5	-0.4	0.5	0.00	0.4	0.01	-6.8	-3.19

WAVE ENERGY IN THE BREAKER ZONE = 0.204E 08 JOULES

TOTAL LONG-SHORE CURRENT ENERGY = 0.118E 08 JOULES

TOTAL POSITIVE LONG-SHORE CURRENT ENERGY = 0.118E 08 JOULES

TOTAL NEGATIVE LONG-SHORE CURRENT ENERGY = 0.963E 02 JOULES

MAGDALEN ISLANDS - EAST SIDE

RUN BEGINS AT HOUR 2 ON NOVEMBER 26, 1974

STORM - BAROMETRIC PRESSURE AT CENTER OF LOW = 976.0 MILLIBARS
PRESSURE AT LARGEST ENCIRCLING ISOBAR = 1008.0 MILLIBARS
MAXIMUM PRESSURE INCLUDED IN STORM = 1012.6 MILLIBARS

LENGTH OF MAJOR HALF AXIS = 860.0 KILOMETERS
LENGTH OF MINOR HALF AXIS = 860.0 KILOMETERS
ORIENTATION OF MAJOR AXIS = 0.0 DEGREES FROM NORTH

LONGSHORE CURRENT EQUATION FROM FOX AND DAVIS, 1972

SHORE - POSITION COORDINATES - X = 1665.0 Y = 1110.0 KILOMETERS

SHORE LATITUDE = 48° ONSHORE AZIMUTH = 270° DEGREES
NEARSHORE SLOPE = 0.026 AVERAGE FETCH = 200.0 KILOMETERS

TIDES - SPRING TIDE RANGE = 0.86 NEAP TIDE RANGE = 0.37 METERS
SLOPE AT LOW TIDE = 0.026 SLOPE AT HIGH TIDE = 0.030

DIURNAL TIDE - FORM NUMBER IS 5.00

HOUR	X	Y	X1	Y1	BARO. PRESS.	WIND ANGLE	SURF. WIND	ONSH. WIND	ALSH. WIND	EFFECT. WIND	WAVE H	WAVE T	BREAKER H	BREAKER ANGLE	LSC VELOCITY	TIDE
	KM	KM	RAD	RAD	MB	DEG	M/S	M/S	M/S	M/S	M	SEC	M	DEG	CM/SEC	M
2	1154.	466.	0.449	-0.439	1006.74	23.6	8.3	7.6	3.3	8.0	0.37	2.3	1.1	12.5	31.99	0.01
3	1180.	486.	0.448	-0.437	1005.86	23.0	9.1	8.4	3.6	8.9	0.58	2.9	0.78	12.1	40.73	0.03
4	1206.	507.	0.446	-0.435	1004.89	22.4	10.0	9.3	3.8	9.8	0.76	3.4	0.78	11.8	45.56	0.05
5	1232.	527.	0.445	-0.433	1003.83	21.8	10.9	10.1	4.0	10.7	0.95	3.8	0.97	11.5	49.40	0.07
6	1258.	547.	0.443	-0.431	1002.69	21.0	11.8	11.0	4.2	11.5	1.14	4.2	1.16	11.1	52.53	0.09
7	1284.	568.	0.442	-0.429	1001.46	20.2	12.7	11.9	4.4	12.4	1.33	4.5	1.36	10.7	55.05	0.11
8	1310.	588.	0.440	-0.427	1000.16	19.4	13.5	12.7	4.4	13.2	1.53	4.8	1.57	10.2	56.97	0.13
9	1341.	611.	0.435	-0.425	997.02	20.3	15.0	14.1	5.2	14.7	1.76	5.2	1.80	10.7	53.06	0.14
10	1373.	714.	0.430	-0.422	993.60	21.6	16.0	14.9	5.9	15.7	2.01	5.5	2.05	11.4	71.05	0.14
11	1404.	777.	0.425	-0.420	990.04	23.2	16.4	15.0	6.4	15.9	2.22	5.8	2.26	12.1	76.84	0.16
12	1436.	840.	0.420	-0.417	986.53	25.5	15.6	14.3	6.8	15.3	2.38	6.1	2.41	13.3	86.82	0.16
13	1467.	903.	0.416	-0.415	983.27	28.8	14.4	12.6	6.9	13.8	2.46	6.2	2.46	14.8	94.71	0.17
14	1499.	966.	0.411	-0.412	980.28	34.2	12.1	10.0	6.8	11.4	2.30	6.0	2.25	17.3	98.19	0.17
15	1508.	997.	0.408	-0.411	978.51	39.5	10.9	8.4	6.9	10.1	1.90	5.5	1.85	19.1	94.28	0.17
16	1517.	1029.	0.405	-0.411	976.71	46.3	9.8	6.7	7.1	8.8	1.48	4.8	1.39	20.5	80.00	0.16
17	1526.	1060.	0.403	-0.410	976.08	55.3	8.7	4.9	7.1	7.4	1.09	4.2	0.92	20.7	60.17	0.15
18	1536.	1091.	0.401	-0.410	977.65	66.9	7.8	3.0	7.2	6.2	0.77	3.5	0.75	20.1	40.70	0.13
19	1545.	1123.	0.400	-0.409	977.41	81.2	7.3	1.1	7.2	5.2	0.47	2.8	0.51	21.6	21.0	0.11
20	1554.	1154.	0.403	-0.408	977.38	96.8	7.2	-0.8	7.1	4.5	0.40	2.5	0.45	21.8	1.43	0.09
21	1559.	1165.	0.404	-0.408	977.37	102.8	7.2	-1.5	7.0	4.2	0.37	2.4	0.42	20.7	12.00	0.08
22	1565.	1176.	0.405	-0.407	977.39	108.7	7.2	-2.3	6.8	4.0	0.35	2.3	0.42	19.9	1.3	0.07
23	1570.	1187.	0.406	-0.407	977.45	114.5	7.3	-3.0	6.7	3.9	0.33	2.3	0.42	18.6	1.66	0.07
24	1576.	1199.	0.406	-0.406	977.53	120.0	7.5	-3.7	6.5	3.7	0.32	2.3	0.42	17.5	1.97	0.06
1	1581.	1210.	0.407	-0.406	977.64	125.2	7.8	-4.5	6.3	3.7	0.31	2.2	0.42	16.3	2.28	0.05
2	1587.	1221.	0.408	-0.406	977.77	130.1	8.1	-5.2	6.2	3.6	0.31	2.2	0.42	15.1	2.58	0.04
3	1594.	1231.	0.408	-0.407	977.83	132.1	7.5	-5.0	5.8	3.3	0.28	2.1	0.42	13.9	3.14	0.03
4	1606.	1240.	0.407	-0.406	977.91	134.5	7.0	-4.9	5.9	3.0	0.22	1.9	0.42	11.9	4.17	0.02
5	1615.	1204.	0.407	-0.403	977.11	137.3	6.5	-4.7	6.4	2.7	0.18	1.7	0.47	10.7	4.61	0.02
6	1624.	1199.	0.406	-0.403	976.93	140.6	5.9	-4.6	3.8	2.4	0.15	1.6	0.47	19.2	4.00	0.01
7	1634.	1193.	0.406	-0.402	976.77	144.6	5.4	-4.4	3.1	2.1	0.12	1.4	0.41	17.4	3.60	0.01
8	1643.	1188.	0.406	-0.401	976.64	149.4	5.0	-4.3	2.5	1.9	0.09	1.3	0.40	15.2	2.70	0.00
9	1650.	1202.	0.407	-0.400	976.83	151.8	5.6	-5.4	1.7	1.9	0.09	1.2	0.40	9.3	1.69	0.00
10	1676.	1217.	0.406	0.400	977.12	171.2	6.5	-6.4	0.9	2.2	0.10	1.3	0.40	4.5	7.19	0.00
11	1673.	1231.	0.409	0.402	977.49	178.2	7.4	-7.4	0.2	2.4	0.11	1.3	0.42	3.9	1.79	0.00
12	1710.	1245.	0.410	0.403	977.95	183.4	8.4	-8.4	0.5	2.5	0.1	1.4	0.44	1.4	3.37	0.00
13	1726.	1260.	0.411	0.404	978.50	187.4	9.4	-9.4	-1.1	3.1	0.15	1.5	0.46	0.7	4.71	0.00
14	1743.	1274.	0.412	0.406	979.12	190.6	10.4	-10.2	-1.4	3.5	0.18	1.7	0.49	0.6	1.00	0.00
15	1761.	1287.	0.413	0.407	979.62	193.7	11.3	-11.0	-2.7	3.9	0.22	1.8	0.52	0.7	1.29	0.00
16	1780.	1301.	0.414	0.408	980.59	196.2	12.4	-11.7	-3.4	4.2	0.25	1.9	0.56	0.8	1.58	0.00
17	1798.	1314.	0.415	0.410	981.44	198.4	13.0	-12.3	-4.1	4.5	0.29	2.0	0.60	0.9	1.87	0.00
18	1817.	1327.	0.416	0.411	982.34	200.1	13.7	-12.9	-4.8	0.33	2.1	0.64	1.0	2.16	1.98	0.00
19	1835.	1341.	0.417	0.413	983.33	201.6	14.4	-13.4	-5.5	4.1	0.37	2.2	0.68	1.1	2.45	0.00
20	1854.	1354.	0.418	0.414	984.32	202.9	15.0	-13.8	-5.8	5.4	0.41	2.3	0.72	1.2	2.74	0.00
21	1864.	1366.	0.421	0.415	985.96	201.6	15.6	-14.1	-6.1	5.6	0.46	2.4	0.77	1.3	3.03	0.00
22	1894.	1417.	0.423	0.416	987.08	199.6	16.1	-14.1	-6.7	5.7	0.49	2.5	0.81	1.4	3.32	0.00
23	1918.	1449.	0.426	0.418	989.44	199.7	16.3	-15.4	-6.5	6.7	0.53	2.6	0.86	1.5	3.61	0.00
24	1933.	1480.	0.427	0.421	992.21	199.6	16.3	-15.4	-6.3	5.7	0.56	2.6	0.91	1.6	3.90	0.00
1	1928.	1512.	0.431	0.427	992.99	198.4	16.1	-15.0	-6.1	4.6	0.58	2.6	0.96	1.7	4.19	0.00
2	1943.	1543.	0.433	0.429	994.75	197.9	15.8	-15.0	-6.8	5.5	0.59	2.6	0.97	1.8	4.48	0.00
3	1993.	1606.	0.438	0.425	998.54	198.6	14.3	-14.6	-7.4	4.9	0.59	2.6	0.97	1.8	4.77	0.00
4	2043.	1659.	0.443	0.424	1001.72	199.2	12.4	-11.7	-6.0	4.3	0.50	2.5	0.87	1.7	4.06	0.00
5	2093.	1731.	0.448	0.433	1004.77	199.7	10.1	-7.1	-3.4	3.6	0.35	2.0	0.67	1.5	2.75	0.00
6	2142.	1794.	0.453	0.437	1007.06	200.0	7.9	-7.5	-2.7	2.8	0.24	1.6	0.49	1.2	1.44	0.00
7	2192.	1857.	0.457	0.440	1008.51	200.4	5.9	-7.8	-2.0	2.1	0.12	1.0	0.23	0.9	0.60	0.00
8	2242.	1920.	0.462	0.444	1010.11	200.6	4.3	-8.0	-1.5	1.5	0.06	1.1	0.07	0.9	0.71	0.00

WAVE ENERGY IN THE BREAKER LINE = 0.178E 10 JOULES

TOTAL LONGSHORE CURRENT ENERGY = 0.152E 10 JOULES

TOTAL POSITIVE LONGSHORE CURRENT ENERGY = 0.150E 10 JOULES

TOTAL NEGATIVE LONGSHORE CURRENT ENERGY = 0.143E 10 JOULES

MAGDALEN ISLANDS - WEST SIDE

RUN BEGINS AT HOUR 2 ON NOVEMBER 26, 1974

STORM - BAROMETRIC PRESSURE AT CENTER OF LOW = 976.0 MILLIBARS
 PRESSURE AT LARGEST ENCIRCLING ISOBAR = 1008.0 MILLIBARS
 MAXIMUM PRESSURE INCLUDED IN STORM = 1012.0 MILLIBARS

LENGTH OF MAJOR HALF AXIS = 860.0 KILOMETERS
 LENGTH OF MINOR HALF AXIS = 860.0 KILOMETERS
 ORIENTATION OF MAJOR AXIS = 0.0 DEGREES FROM NORTH

LONGSHORE CURRENT EQUATION FROM FOX AND DAVIS, 1972

SHORE - POSITION COORDINATES - X = 1665.0 Y = 1110.0 KILOMETERS

SHORE LATITUDE = 48. ONSHORE AZIMUTH = 90. DEGREES
 NEARSHORE SLOPE = 0.026 AVERAGE FETCH = 200. KILOMETERS

TIDES - SPRING TIDE RANGE = 0.86 NEAP TIDE RANGE = 0.37 METERS
 SLOPE AT LOW TIDE = 0.026 SLOPE AT HIGH TIDE = 0.040

DIURNAL TIDE - FORM NUMBER IS 5.00

HOUR	X	Y	X1	Y1	BARO. PRESS.	WIND ANGLE	SURF. WIND	ONSH WIND	ALSH WIND	EFFECT. WIND	WAVE H	WAVE T	BREAKER H	ANGLE	LSC VELOC.	TIDE
	KM	KM	KM	KM	MB	DEG	M/S	M/S	M/S	M/S	M	SEC	M	DEG	CM/SEC	M
2	1154.	488.	-0.49	0.39	1008.74	203.6	8.3	-7.6	-3.3	3.0	0.08	1.1	0.08	-12.3	-15.90	0.56
3	1180.	488.	-0.48	0.37	1005.86	203.0	9.1	-8.4	-3.6	3.3	0.13	1.4	0.13	-14.0	-18.97	0.53
4	1206.	507.	-0.46	0.35	1004.89	202.4	10.0	-9.3	-3.8	3.6	0.16	1.6	0.17	-11.7	-21.09	0.50
5	1232.	527.	-0.45	0.33	1003.83	201.8	10.9	-10.1	-4.0	3.9	0.20	1.8	0.21	-11.3	-22.73	0.47
6	1258.	547.	-0.43	0.31	1002.69	201.0	11.8	-11.0	-4.2	4.2	0.24	1.9	0.25	-11.0	-24.05	0.44
7	1284.	568.	-0.42	0.29	1001.46	200.2	12.7	-11.9	-4.4	4.5	0.28	2.1	0.29	-10.6	-25.08	0.42
8	1310.	588.	-0.40	0.27	1000.16	199.4	13.5	-12.7	-4.6	4.7	0.32	2.2	0.33	-10.1	-25.83	0.42
9	1341.	611.	-0.35	0.25	997.02	200.3	15.0	-14.1	-5.2	5.3	0.37	2.4	0.38	-10.6	-28.85	0.42
10	1373.	714.	-0.30	0.22	993.60	201.6	16.0	-14.9	-5.9	5.7	0.42	2.6	0.43	-11.3	-32.31	0.44
11	1404.	777.	-0.25	0.20	990.04	203.2	16.4	-15.0	-6.4	5.9	0.47	2.7	0.48	-12.1	-36.06	0.48
12	1435.	840.	-0.20	0.17	986.53	205.5	15.8	-14.3	-6.8	5.8	0.51	2.8	0.52	-13.2	-39.98	0.54
13	1467.	903.	-0.16	0.15	983.27	208.8	14.4	-12.6	-6.9	5.4	0.53	2.9	0.53	-14.8	-43.86	0.61
14	1499.	966.	-0.11	0.12	980.48	214.2	12.1	-10.0	-6.8	4.7	0.50	2.8	0.50	-17.2	-45.71	0.69
15	1508.	997.	-0.08	0.12	979.51	219.5	10.9	-8.4	-6.9	4.4	0.44	2.7	0.44	-19.5	-48.47	0.77
16	1517.	1029.	-0.06	0.11	978.71	226.3	9.8	-6.7	-7.1	4.2	0.39	2.5	0.39	-20.9	-51.24	0.85
17	1526.	1060.	-0.03	0.11	978.08	235.3	8.7	-4.9	-7.1	4.1	0.35	2.3	0.29	-25.7	-55.20	0.90
18	1538.	1091.	-0.01	0.10	977.65	246.9	7.8	-3.0	-7.2	4.2	0.31	2.2	0.22	-29.1	-59.94	0.93
19	1545.	1123.	0.00	0.09	977.41	261.2	7.3	-1.1	-7.2	4.5	0.34	2.3	0.19	-31.6	-65.36	0.94
20	1554.	1154.	0.03	0.08	977.38	276.8	7.2	3.8	-7.1	5.1	0.37	2.4	0.14	-31.8	-74.11	0.91
21	1559.	1165.	0.04	0.08	977.37	282.8	7.2	1.5	-7.0	5.3	0.41	2.5	0.22	-31.2	-80.69	0.86
22	1565.	1176.	0.05	0.07	977.39	288.7	7.2	2.3	-6.8	5.6	0.46	2.7	0.29	-30.2	-86.91	0.80
23	1570.	1187.	0.06	0.07	977.45	294.5	7.3	3.0	-6.7	5.9	0.50	2.8	0.36	-28.9	-93.06	0.72
24	1576.	1199.	0.06	0.06	977.53	300.0	7.5	3.7	-6.5	6.3	0.55	2.9	0.43	-27.3	-99.05	0.65
1	1581.	1210.	0.07	0.06	977.64	305.2	7.8	4.5	-6.3	6.7	0.61	3.1	0.51	-25.7	-104.67	0.59
2	1587.	1221.	0.08	0.06	977.77	310.1	8.1	5.2	-6.2	7.1	0.67	3.2	0.59	-24.0	-109.69	0.53
3	1596.	1218.	0.08	0.05	977.53	312.1	7.5	5.0	-5.6	6.7	0.71	3.3	0.64	-23.1	-111.74	0.49
4	1606.	1210.	0.07	0.04	977.31	314.5	7.0	4.9	-5.0	6.3	0.73	3.4	0.67	-22.1	-113.14	0.45
5	1615.	1204.	0.07	0.03	977.11	317.3	6.8	4.7	-4.6	5.9	0.71	3.4	0.67	-20.9	-114.94	0.43
6	1624.	1199.	0.06	0.03	976.93	320.6	5.9	4.6	-3.8	5.5	0.63	3.2	0.60	-19.5	-116.85	0.41
7	1634.	1193.	0.06	0.02	976.77	324.6	5.4	4.4	-3.1	5.1	0.55	3.0	0.54	-17.7	-118.02	0.40
8	1643.	1188.	0.06	0.01	976.64	329.4	5.0	4.3	-2.5	4.7	0.48	2.8	0.48	-15.5	-121.03	0.39
9	1650.	1202.	0.07	0.00	976.83	341.8	5.6	5.4	-1.7	5.3	0.51	2.8	0.53	-9.4	-130.70	0.40
10	1676.	1217.	0.08	-0.00	977.12	351.2	6.5	6.4	-0.9	6.5	0.57	3.0	0.59	-4.6	-17.02	0.42
11	1693.	1231.	0.09	-0.02	977.49	358.2	7.4	7.4	-0.2	7.4	0.65	3.2	0.68	-0.9	-3.81	0.45
12	1710.	1245.	0.10	-0.03	977.95	364	8.4	8.4	0.5	8.4	0.75	3.4	0.79	1.8	8.14	0.51
13	1726.	1260.	0.11	-0.04	978.50	369	9.4	9.4	1.2	9.4	0.88	3.7	0.92	3.9	18.96	0.58
14	1743.	1274.	0.12	-0.06	979.12	376	10.4	10.4	1.9	10.2	1.02	4.0	1.07	5.6	28.99	0.67
15	1761.	1287.	0.13	-0.07	979.82	383	11.3	11.3	2.7	11.2	1.18	4.3	1.23	7.3	39.91	0.76
16	1780.	1301.	0.14	-0.08	980.59	389	12.2	11.7	3.4	12.0	1.35	4.6	1.39	8.6	50.00	0.85
17	1798.	1314.	0.15	-0.10	981.44	394	13.0	12.3	4.1	12.8	1.52	4.8	1.57	9.7	60.26	0.93
18	1817.	1327.	0.16	-0.11	982.36	399	13.7	12.9	4.7	13.5	1.70	5.1	1.74	10.6	67.60	0.98
19	1835.	1341.	0.17	-0.13	983.30	404	14.4	13.4	5.3	14.1	1.87	5.4	1.91	11.4	74.92	0.99
20	1854.	1354.	0.18	-0.14	984.32	409	15.0	13.8	5.8	14.8	2.05	5.6	2.08	12.0	81.15	0.98
21	1869.	1368.	0.21	-0.15	985.96	414	15.6	14.5	5.8	15.3	2.23	5.9	2.27	11.4	86.87	0.93
22	1884.	1407.	0.23	-0.16	987.68	420	16.1	15.1	5.8	15.8	2.40	6.1	2.46	11.8	90.17	0.85
23	1898.	1444.	0.26	-0.18	989.44	427	16.3	15.4	5.5	16.0	2.57	6.3	2.64	10.4	79.10	0.77
24	1913.	1480.	0.28	-0.19	991.22	430	16.3	15.4	5.3	16.0	2.71	6.5	2.79	10.0	77.73	0.68
1	1928.	1512.	0.31	-0.20	992.99	434	16.1	15.3	5.1	15.9	2.83	6.6	2.94	9.7	76.18	0.59
2	1943.	1543.	0.33	-0.21	994.73	437	15.8	15.0	4.8	15.5	2.93	6.8	3.02	9.4	74.56	0.52
3	1959.	1608.	0.38	-0.25	998.54	446	14.3	13.6	4.6	14.1	2.96	6.8	3.05	9.7	76.40	0.46
4	2043.	1669.	0.43	-0.29	1001.92	452	12.4	11.7	4.0	12.1	2.51	6.3	2.58	10.0	71.24	0.41
5	2093.	1731.	0.48	-0.33	1004.77	457	10.1	9.5	3.4	9.9	1.90	5.5	1.96	10.4	61.67	0.40
6	2142.	1794.	0.53	-0.37	1007.36	460	7.9	7.5	2.7	7.8	1.32	4.6	1.37	10.4	52.57	0.38
7	2192.	1857.	0.57	-0.40	1008.62	464	5.9	5.6	2.0	5.8	0.84	3.7	0.87	10.4	41.69	0.37
8	2242.	1920.	0.62	-0.44	1010.11	468	4.3	4.0	1.5	4.2	0.47	2.8	0.49	10.4	30.94	0.37

WAVE ENERGY IN THE BREAKER ZONE = 0.0136 10 JOULES

TOTAL LONGSHORE CURRENT ENERGY = 0.0216 10 JOULES

TOTAL POSITIVE LONGSHORE CURRENT ENERGY = 0.0224 10 JOULES

TOTAL NEGATIVE LONGSHORE CURRENT ENERGY = 0.0016 10 JOULES

0-5446-1-5 A9 m. 100 1-76 A91.2 no. 14/5

LENGTH OF MAJOR HALF AXIS = 1200.0 KILOMETERS
LENGTH OF MINOR HALF AXIS = 600.0 KILOMETERS
DISTANCE OF CENTER OF GRAVITY FROM NORTH

U.S. DEPARTMENT OF COMMERCE OFFICE OF FOREIGN TRADE April 1971

SMITHSONIAN INSTITUTION, WASHINGTON, D.C. 20560-0001

SHORE LA TITUDE = 42. ONSHORE AZIMUTH = 255. DEGREES
SEASONAL WINDS = 3-230. AVERAGE FETCH = 4000. KILOMETERS

TIDES - SPRING TIDE RANGE = 3.50 NEAP TIDE RANGE = 2.10 METERS

EMILIO MORALES, *Ph.D., is a senior research advisor at the Center for Strategic Studies, RAND Corporation, and a senior advisor at the U.S. State Department. He is also a senior advisor at the U.S. Defense Intelligence Agency. He has been a senior advisor at the U.S. State Department since 1995. He has been a senior advisor at the U.S. Defense Intelligence Agency since 1995. He has been a senior advisor at the U.S. State Department since 1995. He has been a senior advisor at the U.S. Defense Intelligence Agency since 1995.*

[illegible]

MAJOR CONTRIBUTORS TO THE PUBLICATION OF THIS JOURNAL

1998, 1999, 2000, 2001, 2002, 2003, 2004, 2005, 2006, 2007, 2008, 2009, 2010, 2011, 2012, 2013, 2014, 2015, 2016, 2017, 2018, 2019, 2020, 2021, 2022, 2023, 2024, 2025, 2026, 2027, 2028, 2029, 2030, 2031, 2032, 2033, 2034, 2035, 2036, 2037, 2038, 2039, 2040, 2041, 2042, 2043, 2044, 2045, 2046, 2047, 2048, 2049, 2050, 2051, 2052, 2053, 2054, 2055, 2056, 2057, 2058, 2059, 2060, 2061, 2062, 2063, 2064, 2065, 2066, 2067, 2068, 2069, 2070, 2071, 2072, 2073, 2074, 2075, 2076, 2077, 2078, 2079, 2080, 2081, 2082, 2083, 2084, 2085, 2086, 2087, 2088, 2089, 2090, 2091, 2092, 2093, 2094, 2095, 2096, 2097, 2098, 2099, 2100, 2101, 2102, 2103, 2104, 2105, 2106, 2107, 2108, 2109, 2110, 2111, 2112, 2113, 2114, 2115, 2116, 2117, 2118, 2119, 2120, 2121, 2122, 2123, 2124, 2125, 2126, 2127, 2128, 2129, 2130, 2131, 2132, 2133, 2134, 2135, 2136, 2137, 2138, 2139, 2140, 2141, 2142, 2143, 2144, 2145, 2146, 2147, 2148, 2149, 2150, 2151, 2152, 2153, 2154, 2155, 2156, 2157, 2158, 2159, 2160, 2161, 2162, 2163, 2164, 2165, 2166, 2167, 2168, 2169, 2170, 2171, 2172, 2173, 2174, 2175, 2176, 2177, 2178, 2179, 2180, 2181, 2182, 2183, 2184, 2185, 2186, 2187, 2188, 2189, 2190, 2191, 2192, 2193, 2194, 2195, 2196, 2197, 2198, 2199, 2200, 2201, 2202, 2203, 2204, 2205, 2206, 2207, 2208, 2209, 2210, 2211, 2212, 2213, 2214, 2215, 2216, 2217, 2218, 2219, 2220, 2221, 2222, 2223, 2224, 2225, 2226, 2227, 2228, 2229, 2230, 2231, 2232, 2233, 2234, 2235, 2236, 2237, 2238, 2239, 2240, 2241, 2242, 2243, 2244, 2245, 2246, 2247, 2248, 2249, 2250, 2251, 2252, 2253, 2254, 2255, 2256, 2257, 2258, 2259, 2260, 2261, 2262, 2263, 2264, 2265, 2266, 2267, 2268, 2269, 2270, 2271, 2272, 2273, 2274, 2275, 2276, 2277, 2278, 2279, 2280, 2281, 2282, 2283, 2284, 2285, 2286, 2287, 2288, 2289, 2290, 2291, 2292, 2293, 2294, 2295, 2296, 2297, 2298, 2299, 2300, 2301, 2302, 2303, 2304, 2305, 2306, 2307, 2308, 2309, 2310, 2311, 2312, 2313, 2314, 2315, 2316, 2317, 2318, 2319, 2320, 2321, 2322, 2323, 2324, 2325, 2326, 2327, 2328, 2329, 2330, 2331, 2332, 2333, 2334, 2335, 2336, 2337, 2338, 2339, 2340, 2341, 2342, 2343, 2344, 2345, 2346, 2347, 2348, 2349, 2350, 2351, 2352, 2353, 2354, 2355, 2356, 2357, 2358, 2359, 2360, 2361, 2362, 2363, 2364, 2365, 2366, 2367, 2368, 2369, 2370, 2371, 2372, 2373, 2374, 2375, 2376, 2377, 2378, 2379, 2380, 2381, 2382, 2383, 2384, 2385, 2386, 2387, 2388, 2389, 2390, 2391, 2392, 2393, 2394, 2395, 2396, 2397, 2398, 2399, 2400, 2401, 2402, 2403, 2404, 2405, 2406, 2407, 2408, 2409, 2410, 2411, 2412, 2413, 2414, 2415, 2416, 2417, 2418, 2419, 2420, 2421, 2422, 2423, 2424, 2425, 2426, 2427, 2428, 2429, 2430, 2431, 2432, 2433, 2434, 2435, 2436, 2437, 2438, 2439, 2440, 2441, 2442, 2443, 2444, 2445, 2446, 2447, 2448, 2449, 2450, 2451, 2452, 2453, 2454, 2455, 2456, 2457, 2458, 2459, 2460, 2461, 2462, 2463, 2464, 2465, 2466, 2467, 2468, 2469, 2470, 2471, 2472, 2473, 2474, 2475, 2476, 2477, 2478, 2479, 2480, 2481, 2482, 2483, 2484, 2485, 2486, 2487, 2488, 2489, 2490, 2491, 2492, 2493, 2494, 2495, 2496, 2497, 2498, 2499, 2500, 2501, 2502, 2503, 2504, 2505, 2506, 2507, 2508, 2509, 2510, 2511, 2512, 2513, 2514, 2515, 2516, 2517, 2518, 2519, 2520, 2521, 2522, 2523, 2524, 2525, 2526, 2527, 2528, 2529, 2530, 2531, 2532, 2533, 2534, 2535, 2536, 2537, 2538, 2539, 2540, 2541, 2542, 2543, 2544, 2545, 2546, 2547, 2548, 2549, 2550, 2551, 2552, 2553, 2554, 2555, 2556, 2557, 2558, 2559, 2560, 2561, 2562, 2563, 2564, 2565, 2566, 2567, 2568, 2569, 2570, 2571, 2572, 2573, 2574, 2575, 2576, 2577, 2578, 2579, 2580, 2581, 2582, 2583, 2584, 2585, 2586, 2587, 2588, 2589, 2590, 2591, 2592, 2593, 2594, 2595, 2596, 2597, 2598, 2599, 2600, 2601, 2602, 2603, 2604, 2605, 2606, 2607, 2608, 2609, 2610, 2611, 2612, 2613, 2614, 2615, 2616, 2617, 2618, 2619, 2620, 2621, 2622, 2623, 2624, 2625, 2626, 2627, 2628, 2629, 2630, 2631, 2632, 2633, 2634, 2635, 2636, 2637, 2638, 2639, 2640, 2641, 2642, 2643, 2644, 2645, 2646, 2647, 2648, 2649, 2650, 2651, 2652, 2653, 2654, 2655, 2656, 2657, 2658, 2659, 2660, 2661, 2662, 2663, 2664, 2665, 2666, 2667, 2668, 2669, 2670, 2671, 2672, 2673, 2674, 2675, 2676, 2677, 2678, 2679, 26

© 1994 Blackwell Science Ltd, *Journal of Internal Medicine* 235: 201-208

1998, 1999, 2000, 2001, 2002, 2003, 2004, 2005, 2006, 2007, 2008, 2009, 2010, 2011, 2012, 2013, 2014, 2015, 2016, 2017, 2018, 2019, 2020, 2021, 2022, 2023, 2024, 2025, 2026, 2027, 2028, 2029, 2030, 2031, 2032, 2033, 2034, 2035, 2036, 2037, 2038, 2039, 2040, 2041, 2042, 2043, 2044, 2045, 2046, 2047, 2048, 2049, 2050, 2051, 2052, 2053, 2054, 2055, 2056, 2057, 2058, 2059, 2060, 2061, 2062, 2063, 2064, 2065, 2066, 2067, 2068, 2069, 2070, 2071, 2072, 2073, 2074, 2075, 2076, 2077, 2078, 2079, 2080, 2081, 2082, 2083, 2084, 2085, 2086, 2087, 2088, 2089, 2090, 2091, 2092, 2093, 2094, 2095, 2096, 2097, 2098, 2099, 2100, 2101, 2102, 2103, 2104, 2105, 2106, 2107, 2108, 2109, 2110, 2111, 2112, 2113, 2114, 2115, 2116, 2117, 2118, 2119, 2120, 2121, 2122, 2123, 2124, 2125, 2126, 2127, 2128, 2129, 2130, 2131, 2132, 2133, 2134, 2135, 2136, 2137, 2138, 2139, 2140, 2141, 2142, 2143, 2144, 2145, 2146, 2147, 2148, 2149, 2150, 2151, 2152, 2153, 2154, 2155, 2156, 2157, 2158, 2159, 2160, 2161, 2162, 2163, 2164, 2165, 2166, 2167, 2168, 2169, 2170, 2171, 2172, 2173, 2174, 2175, 2176, 2177, 2178, 2179, 2180, 2181, 2182, 2183, 2184, 2185, 2186, 2187, 2188, 2189, 2190, 2191, 2192, 2193, 2194, 2195, 2196, 2197, 2198, 2199, 2200, 2201, 2202, 2203, 2204, 2205, 2206, 2207, 2208, 2209, 2210, 2211, 2212, 2213, 2214, 2215, 2216, 2217, 2218, 2219, 2220, 2221, 2222, 2223, 2224, 2225, 2226, 2227, 2228, 2229, 2230, 2231, 2232, 2233, 2234, 2235, 2236, 2237, 2238, 2239, 2240, 2241, 2242, 2243, 2244, 2245, 2246, 2247, 2248, 2249, 2250, 2251, 2252, 2253, 2254, 2255, 2256, 2257, 2258, 2259, 2260, 2261, 2262, 2263, 2264, 2265, 2266, 2267, 2268, 2269, 2270, 2271, 2272, 2273, 2274, 2275, 2276, 2277, 2278, 2279, 2280, 2281, 2282, 2283, 2284, 2285, 2286, 2287, 2288, 2289, 2290, 2291, 2292, 2293, 2294, 2295, 2296, 2297, 2298, 2299, 2300, 2301, 2302, 2303, 2304, 2305, 2306, 2307, 2308, 2309, 2310, 2311, 2312, 2313, 2314, 2315, 2316, 2317, 2318, 2319, 2320, 2321, 2322, 2323, 2324, 2325, 2326, 2327, 2328, 2329, 2330, 2331, 2332, 2333, 2334, 2335, 2336, 2337, 2338, 2339, 2340, 2341, 2342, 2343, 2344, 2345, 2346, 2347, 2348, 2349, 2350, 2351, 2352, 2353, 2354, 2355, 2356, 2357, 2358, 2359, 2360, 2361, 2362, 2363, 2364, 2365, 2366, 2367, 2368, 2369, 2370, 2371, 2372, 2373, 2374, 2375, 2376, 2377, 2378, 2379, 2380, 2381, 2382, 2383, 2384, 2385, 2386, 2387, 2388, 2389, 2390, 2391, 2392, 2393, 2394, 2395, 2396, 2397, 2398, 2399, 2400, 2401, 2402, 2403, 2404, 2405, 2406, 2407, 2408, 2409, 2410, 2411, 2412, 2413, 2414, 2415, 2416, 2417, 2418, 2419, 2420, 2421, 2422, 2423, 2424, 2425, 2426, 2427, 2428, 2429, 2430, 2431, 2432, 2433, 2434, 2435, 2436, 2437, 2438, 2439, 2440, 2441, 2442, 2443, 2444, 2445, 2446, 2447, 2448, 2449, 2450, 2451, 2452, 2453, 2454, 2455, 2456, 2457, 2458, 2459, 2460, 2461, 2462, 2463, 2464, 2465, 2466, 2467, 2468, 2469, 2470, 2471, 2472, 2473, 2474, 2475, 2476, 2477, 2478, 2479, 2480, 2481, 2482, 2483, 2484, 2485, 2486, 2487, 2488, 2489, 2490, 2491, 2492, 2493, 2494, 2495, 2496, 2497, 2498, 2499, 2500, 2501, 2502, 2503, 2504, 2505, 2506, 2507, 2508, 2509, 2510, 2511, 2512, 2513, 2514, 2515, 2516, 2517, 2518, 2519, 2520, 2521, 2522, 2523, 2524, 2525, 2526, 2527, 2528, 2529, 2530, 2531, 2532, 2533, 2534, 2535, 2536, 2537, 2538, 2539, 2540, 2541, 2542, 2543, 2544, 2545, 2546, 2547, 2548, 2549, 2550, 2551, 2552, 2553, 2554, 2555, 2556, 2557, 2558, 2559, 2560, 2561, 2562, 2563, 2564, 2565, 2566, 2567, 2568, 2569, 2570, 2571, 2572, 2573, 2574, 2575, 2576, 2577, 2578, 2579, 2580, 2581, 2582, 2583, 2584, 2585, 2586, 2587, 2588, 2589, 2590, 2591, 2592, 2593, 2594, 2595, 2596, 2597, 2598, 2599, 2600, 2601, 2602, 2603, 2604, 2605, 2606, 2607, 2608, 2609, 2610, 2611, 2612, 2613, 2614, 2615, 2616, 2617, 2618, 2619, 2620, 2621, 2622, 2623, 2624, 2625, 2626, 2627, 2628, 2629, 2630, 2631, 2632, 2633, 2634, 2635, 2636, 2637, 2638, 2639, 2640, 2641, 2642, 2643, 2644, 2645, 2646, 2647, 2648, 2649, 2650, 2651, 2652, 2653, 2654, 2655, 2656, 2657, 2658, 2659, 2660, 2661, 2662, 2663, 2664, 2665, 2666, 2667, 2668, 2669, 2670, 2671, 2672, 2673, 2674, 2675, 2676, 2677, 2678, 2679, 26

CELANA ISLAND, VIRGINIA

NOV BEIGIN AT NOON T ON JULY 14, 1973

STORM - BAROMETRIC PRESSURE AT CENTER OF LOW = 1013.0 MILLIBARS
PRESSURE AT LOWEST CYCLONIC ISOBAR = 1010.0 MILLIBARS
MAXIMUM PRESSURE INCLUDED IN STORM = 1016.0 MILLIBARS

LENGTH OF MAJOR HALF AXIS = 749.0 KILOMETERS
LENGTH OF MINOR HALF AXIS = 224.0 KILOMETERS
ORIENTATION OF MAJOR AXIS = 49.0 DEGREES FROM NORTH

LONGSHORE CURRENT EQUATION FROM CEA-4-6-73

SHORE - POSITION COORDINATES - X = 2287.0 Y = 1537.0 KILOMETERS

SHORE LATITUDE = 36° ONSHORE AZIMUTH = 285.0 DEGREES
NEARSHORE SLOPE = 0.037 AVERAGE FETCH = 4500.0 KILOMETERS

TIDES - SPRING TIDE RANGE = 1.672 NEAR TIDE RANGE = 0.490 METERS
SLOPE AT LOW TIDE = 0.035 SLOPE AT HIGH TIDE = 0.039

MIXED SEMIDIURNAL TIDE - FORM NUMBER IS 0490

MOON	X	Y	AL	YI	HARG.	WIND	SURF.	ONSH.	ALSH.	EFFECT.	WAVE	WAVE	BREAKER	OSC.	TIDE
	KM	KM	HAD	HAD	MM	DEG	M/S	M/S	M/S	M/S	M	SEC	M	DEG	CM/SEC
7	195.	548.	1.33	-1.57	1016.87	29.2	0.0	0.0	0.0	0.0	0.0	0.0	0.0	0.0	0.0
8	293.	597.	1.27	-1.53	1016.87	29.6	0.0	0.0	0.0	0.0	0.0	0.0	0.0	0.0	0.0
9	311.	647.	1.22	-1.49	1016.87	30.0	0.0	0.0	0.0	0.0	0.0	0.0	0.0	0.0	0.0
10	368.	676.	1.18	-1.45	1016.87	30.3	0.0	0.0	0.0	0.0	0.0	0.0	0.0	0.0	0.0
11	426.	745.	1.11	-1.41	1016.87	30.7	0.0	0.0	0.0	0.0	0.0	0.0	0.0	0.0	0.0
12	484.	775.	1.05	-1.38	1016.87	31.1	0.0	0.0	0.0	0.0	0.0	0.0	0.0	0.0	0.0
13	542.	844.	0.99	-1.34	1016.87	31.5	0.0	0.0	0.0	0.0	0.0	0.0	0.0	0.0	0.0
14	607.	889.	0.94	-1.29	1016.87	31.8	0.0	0.0	0.0	0.0	0.0	0.0	0.0	0.0	0.0
15	672.	934.	0.89	-1.25	1016.87	32.2	0.0	0.0	0.0	0.0	0.0	0.0	0.0	0.0	0.0
16	737.	974.	0.83	-1.21	1016.87	32.5	0.0	0.0	0.0	0.0	0.0	0.0	0.0	0.0	0.0
17	802.	1025.	0.78	-1.16	1016.87	32.8	0.0	0.0	0.0	0.0	0.0	0.0	0.0	0.0	0.0
18	867.	1070.	0.72	-1.11	1016.87	33.2	0.0	0.0	0.0	0.0	0.0	0.0	0.0	0.0	0.0
19	932.	1115.	0.67	-1.06	1016.87	33.6	0.0	0.0	0.0	0.0	0.0	0.0	0.0	0.0	0.0
20	997.	1150.	0.63	-1.02	1016.87	33.9	0.0	0.0	0.0	0.0	0.0	0.0	0.0	0.0	0.0
21	1062.	1184.	0.58	-0.97	1016.87	34.3	0.0	0.0	0.0	0.0	0.0	0.0	0.0	0.0	0.0
22	1128.	1219.	0.54	-0.92	1016.87	34.7	0.0	0.0	0.0	0.0	0.0	0.0	0.0	0.0	0.0
23	1193.	1254.	0.49	-0.87	1016.87	35.0	0.0	0.0	0.0	0.0	0.0	0.0	0.0	0.0	0.0
24	1258.	1288.	0.45	-0.82	1016.87	35.4	0.0	0.0	0.0	0.0	0.0	0.0	0.0	0.0	0.0
1	1323.	1323.	0.40	-0.78	1016.87	35.8	0.0	0.0	0.0	0.0	0.0	0.0	0.0	0.0	0.0
2	1388.	1355.	0.36	-0.72	1016.87	35.5	0.0	0.0	0.0	0.0	0.0	0.0	0.0	0.0	0.0
3	1468.	1386.	0.31	-0.67	1016.86	35.9	0.0	0.0	0.0	0.0	0.0	0.0	0.0	0.0	0.0
4	1540.	1417.	0.27	-0.61	1016.86	36.2	0.0	0.0	0.0	0.0	0.0	0.0	0.0	0.0	0.0
5	1611.	1448.	0.23	-0.55	1016.86	36.6	0.0	0.0	0.0	0.0	0.0	0.0	0.0	0.0	0.0
6	1685.	1480.	0.18	-0.50	1016.86	37.1	0.0	0.0	0.0	0.0	0.0	0.0	0.0	0.0	0.0
7	1758.	1512.	0.14	-0.44	1016.85	37.7	0.0	0.0	0.0	0.0	0.0	0.0	0.0	0.0	0.0
8	1795.	1546.	0.10	-0.38	1016.83	37.5	0.0	0.0	0.0	0.0	0.0	0.0	0.0	0.0	0.0
9	1813.	1609.	0.06	-0.32	1016.80	37.3	0.0	0.0	0.0	0.0	0.0	0.0	0.0	0.0	0.0
10	1810.	1640.	0.02	-0.26	1016.73	37.5	0.0	0.0	0.0	0.0	0.0	0.0	0.0	0.0	0.0
11	1807.	1687.	0.01	-0.20	1016.73	38.0	0.0	0.0	0.0	0.0	0.0	0.0	0.0	0.0	0.0
12	1805.	1740.	0.01	-0.14	1016.63	38.4	0.0	0.0	0.0	0.0	0.0	0.0	0.0	0.0	0.0
13	1822.	1784.	0.01	-0.09	1016.43	38.8	0.0	0.0	0.0	0.0	0.0	0.0	0.0	0.0	0.0
14	1840.	1848.	0.00	-0.02	1015.73	39.5	0.0	0.0	0.0	0.0	0.0	0.0	0.0	0.0	0.0
15	1976.	1861.	0.01	0.02	1015.19	40.5	0.0	0.0	0.0	0.0	0.0	0.0	0.0	0.0	0.0
16	2111.	1843.	0.01	0.06	1014.51	40.0	0.0	0.0	0.0	0.0	0.0	0.0	0.0	0.0	0.0
17	2031.	1844.	0.01	0.02	1013.77	39.9	0.0	0.0	0.0	0.0	0.0	0.0	0.0	0.0	0.0
18	2058.	1842.	0.01	0.02	1012.89	39.1	0.0	0.0	0.0	0.0	0.0	0.0	0.0	0.0	0.0
19	2055.	1836.	0.01	0.01	1012.08	38.2	0.0	0.0	0.0	0.0	0.0	0.0	0.0	0.0	0.0
20	2111.	1828.	0.01	0.02	1011.47	37.2	0.0	0.0	0.0	0.0	0.0	0.0	0.0	0.0	0.0
21	2115.	1814.	0.01	0.01	1010.88	36.2	0.0	0.0	0.0	0.0	0.0	0.0	0.0	0.0	0.0
22	2144.	1811.	0.01	0.00	1010.35	35.2	0.0	0.0	0.0	0.0	0.0	0.0	0.0	0.0	0.0
23	2190.	1803.	0.01	0.00	1010.75	34.0	0.0	0.0	0.0	0.0	0.0	0.0	0.0	0.0	0.0
24	2217.	1794.	0.01	0.00	1011.13	32.5	0.0	0.0	0.0	0.0	0.0	0.0	0.0	0.0	0.0
1	2243.	1786.	0.01	0.00	1011.74	30.2	0.0	0.0	0.0	0.0	0.0	0.0	0.0	0.0	0.0
2	2272.	1788.	0.01	0.00	1012.29	27.4	0.0	0.0	0.0	0.0	0.0	0.0	0.0	0.0	0.0
3	2314.	1790.	0.01	0.00	1012.94	24.5	0.0	0.0	0.0	0.0	0.0	0.0	0.0	0.0	0.0
4	2351.	1792.	0.01	0.00	1013.55	20.4	0.0	0.0	0.0	0.0	0.0	0.0	0.0	0.0	0.0
5	2360.	1795.	0.01	0.00	1014.17	19.2	0.0	0.0	0.0	0.0	0.0	0.0	0.0	0.0	0.0
6	2390.	1797.	0.00	0.01	1014.75	17.0	0.0	0.0	0.0	0.0	0.0	0.0	0.0	0.0	0.0
7	2419.	1799.	0.00	0.01	1015.26	14.7	0.0	0.0	0.0	0.0	0.0	0.0	0.0	0.0	0.0
8	2453.	1803.	0.00	0.01	1015.67	12.5	0.0	0.0	0.0	0.0	0.0	0.0	0.0	0.0	0.0
9	2483.	1805.	0.00	0.01	1016.00	10.2	0.0	0.0	0.0	0.0	0.0	0.0	0.0	0.0	0.0
10	2485.	1806.	0.00	0.01	1016.59	7.8	0.0	0.0	0.0	0.0	0.0	0.0	0.0	0.0	0.0
11	2508.	1804.	0.00	0.01	1016.41	5.2	0.0	0.0	0.0	0.0	0.0	0.0	0.0	0.0	0.0
12	2530.	1807.	0.00	0.01	1016.27	2.4	0.0	0.0	0.0	0.0	0.0	0.0	0.0	0.0	0.0
13	2552.	1813.	0.00	0.01	1016.17	0.0	0.0	0.0	0.0	0.0	0.0	0.0	0.0	0.0	0.0
14	2574.	1821.	0.00	0.01	1016.09	0.0	0.0	0.0	0.0	0.0	0.0	0.0	0.0	0.0	0.0
15	2575.	1824.	0.00	0.01	1016.04	0.0	0.0	0.0	0.0	0.0	0.0	0.0	0.0	0.0	0.0
16	2587.	1814.	0.00	0.01	1015.97	0.0	0.0	0.0	0.0	0.0	0.0	0.0	0.0	0.0	0.0
17	2598.	1804.	0.00	0.00	1015.87	0.0	0.0	0.0	0.0	0.0	0.0	0.0	0.0	0.0	0.0
18	2604.	1788.	0.00	0.00	1015.76	0.0	0.0	0.0	0.0	0.0	0.0	0.0	0.0	0.0	0.0
19	2611.	1808.	0.00	0.00	1015.62	0.0	0.0	0.0	0.0	0.0	0.0	0.0	0.0	0.0	0.0
20	2632.	1803.	0.00	0.00	1015.46	0.0	0.0	0.0	0.0	0.0	0.0	0.0	0.0	0.0	0.0
21	2662.	1802.	0.00	0.00	1015.26	0.0	0.0	0.0	0.0	0.0	0.0	0.0	0.0	0.0	0.0
22	2674.	1801.	0.00	0.00	1015.03	0.0	0.0	0.0	0.0	0.0	0.0	0.0	0.0	0.0	0.0
23	2673.	1801.	0.00	0.00	1014.78	0.0	0.0	0.0	0.0	0.0	0.0	0.0	0.0	0.0	0.0
24	2678.	1801.	0.00	0.00	1014.51	0.0	0.0	0.0	0.0	0.0	0.0	0.0	0.0	0.0	0.0
1	2684.	1801.	0.00	0.00	1014.14	0.0	0.0	0.0	0.0	0.0	0.0	0.0	0.0	0.0	0.0
2	2686.	1801.	0.00	0.00	1013.67	0.0	0.0	0.0	0.0	0.0	0.0	0.0	0.0	0.0	0.0
3	2689.	1802.	0.00	0.00	1013.25	0.0	0.0	0.0	0.0	0.0	0.0	0.0	0.0	0.0	0.0
4	2694.	1803.	0.00	0.00	1012.83	0.0	0.0	0.0	0.0	0.0	0.0	0.0	0.0	0.0	0.0
5	2702.	1804.	0.00	0.00	1012.40	0.0	0.0	0.0	0.0	0.0	0.0	0.0	0.0	0.0	0.0
6	2713.	1805.	0.00	0.00	1011.98	0.0	0.0	0.0	0.0	0.0	0.0	0.0	0.0	0.0	0.0
7	2726.	1806.	0.00	0.00	1011.56	0.0	0.0	0.0	0.0	0.0	0.0	0.0	0.0	0.0	0.0
8	2739.	1807.	0.00	0.00	1011.13	0.0	0.0	0.0	0.0	0.0	0.0	0.0	0.0	0.0	0.0
9	2753.	1808.	0.00	0.00	1010.69	0.0	0.0	0.0	0.0	0.0	0.0	0.0	0.0	0.0	0.0
10	2769.	1809.	0.00	0.00	1010.23	0.0	0.0	0.0	0.0	0.0	0.0	0.0	0.0	0.0	0.0

SAFETY ISLAND, ERMEDIA

NOV BEINGS AT HIGH 12 FEBRUARY 1969

STORM - BAROMETRIC PRESSURE AT CENTER OF LOW = 990.0 MILLIBARS
PRESSURE AT LARGEST ENCLOSURE ISOBAR = 1012.0 MILLIBARS
MAXIMUM PRESSURE INCLUDED IN STORM = 1019.4 MILLIBARS

LENGTH OF MAJOR HALF AXIS = 920.0 KILOMETERS
LENGTH OF MINOR HALF AXIS = 920.0 KILOMETERS
DIRECTION OF MAJOR AXIS = 200 DEGREES FROM NORTH

ONSHORE CURRENT EQUATION FROM 1966-1973

SHORE - POSITION COORDINATES - X = 1575.0 Y = 525.0 KILOMETERS

SHORE LATITUDE = 33° ONSHORE AZIMUTH = 290° DEGREES
NEARSHORE SLOPE = 0.15 AVERAGE FETCH = 3000 KILOMETERS

TIDES - SPRING TIDE RANGE = 2.44 NEAP TIDE RANGE = 1.83 METERS
SLOPE AT LOW TIDE = 0.013 SLOPE AT HIGH TIDE = 0.018

SEMI-DIURNAL TIDE - FURN NUMBER IS 1012

NOON	X	Y	A	B	PHASE	WIND	SURF	ONSH	ALSH	EFFECT	WAVE	WAVE	BREAKER	LSC	TIDE	
	KM	KM	MAD	MAD	MB	DEG	WIND	M/S	M/S	M/S	M	SEC	M	CM/SEC	M	
1	81.9	40.8	0.26	-0.48	1008.77	02.0	8.7	4.0	7.7	7.1	0.31	2.1	0.43	28.7	38.45	1.35
2	83.8	41.4	0.26	-0.46	1008.34	02.4	9.4	4.2	8.0	7.4	0.46	2.0	0.35	28.4	40.80	0.67
3	85.7	42.0	0.26	-0.44	1007.90	02.8	9.4	4.4	8.3	7.7	0.57	2.0	0.44	28.4	50.00	1.05
4	87.6	42.6	0.25	-0.44	1007.44	03.9	9.8	4.6	8.6	8.0	0.66	2.0	0.54	28.1	64.65	1.64
5	89.6	43.2	0.25	-0.42	1006.96	05.7	10.4	4.8	8.9	8.3	0.77	2.0	0.65	28.0	72.14	2.01
6	91.6	43.8	0.25	-0.41	1006.48	08.4	10.4	5.0	9.4	8.6	0.86	2.0	0.67	27.9	77.64	2.17
7	93.6	44.4	0.25	-0.39	1005.98	11.1	10.7	5.2	9.4	8.9	0.95	2.0	0.74	27.8	80.59	2.09
8	95.6	45.0	0.24	-0.38	1005.48	13.8	11.1	5.4	9.7	9.2	1.03	2.0	0.80	27.7	81.03	1.78
9	97.6	45.6	0.24	-0.36	1004.96	16.5	11.4	5.6	9.9	9.4	1.11	2.0	0.87	27.6	79.54	1.23
10	99.6	46.2	0.24	-0.35	1004.43	19.2	11.7	5.7	10.2	9.7	1.19	2.0	0.94	27.5	77.11	0.64
11	101.6	46.8	0.23	-0.33	1003.89	21.9	11.9	5.9	10.4	9.9	1.27	2.0	1.00	27.4	73.14	0.06
12	103.6	47.4	0.23	-0.32	1003.34	24.6	12.1	6.1	10.6	10.1	1.35	2.0	1.06	27.4	74.78	0.22
13	105.6	48.0	0.23	-0.31	1002.79	27.3	12.4	6.3	10.7	10.4	1.42	2.0	1.12	27.3	78.85	0.23
14	107.6	48.6	0.23	-0.30	1002.24	29.9	12.6	6.5	10.8	10.6	1.49	2.0	1.18	27.2	81.45	0.47
15	109.6	49.2	0.23	-0.29	1001.69	32.6	12.8	6.7	10.9	10.8	1.55	2.0	1.23	27.1	87.93	0.67
16	111.6	49.8	0.23	-0.28	1001.14	35.3	13.0	6.9	11.0	11.0	1.60	2.0	1.28	27.0	95.00	1.33
17	113.6	50.4	0.23	-0.27	999.94	38.0	13.2	7.1	11.1	11.1	1.65	2.0	1.33	26.9	101.37	1.73
18	115.6	51.0	0.23	-0.26	999.29	40.7	13.4	7.3	11.2	11.2	1.70	2.0	1.38	26.8	105.44	1.97
19	117.6	51.6	0.23	-0.25	998.64	43.4	13.6	7.5	11.3	11.3	1.75	2.0	1.43	26.7	106.34	1.95
20	119.6	52.2	0.23	-0.24	997.99	46.1	13.8	7.7	11.4	11.4	1.79	2.0	1.48	26.6	103.47	1.41
21	121.6	52.8	0.23	-0.23	997.34	48.8	14.0	7.9	11.5	11.5	1.84	2.0	1.53	26.5	98.47	0.81
22	123.6	53.4	0.23	-0.22	996.69	51.5	14.2	8.1	11.6	11.6	1.89	2.0	1.58	26.4	92.45	0.21
23	125.6	54.0	0.23	-0.21	996.04	54.2	14.4	8.3	11.7	11.7	1.94	2.0	1.63	26.3	84.47	0.04
24	127.6	54.6	0.23	-0.20	995.39	56.9	14.6	8.5	11.8	11.8	1.99	2.0	1.68	26.2	74.45	0.06
25	129.6	55.2	0.23	-0.19	994.74	59.6	14.8	8.7	11.9	11.9	2.04	2.0	1.73	26.1	62.45	0.09
26	131.6	55.8	0.23	-0.18	994.09	62.3	15.0	8.9	12.0	12.0	2.09	2.0	1.78	26.0	49.45	0.12
27	133.6	56.4	0.23	-0.17	993.44	65.0	15.2	9.1	12.1	12.1	2.14	2.0	1.83	25.9	35.45	0.15
28	135.6	57.0	0.23	-0.16	992.79	67.7	15.4	9.3	12.2	12.2	2.19	2.0	1.88	25.8	20.45	0.18
29	137.6	57.6	0.23	-0.15	992.14	70.4	15.6	9.5	12.3	12.3	2.24	2.0	1.93	25.7	5.45	0.21
30	139.6	58.2	0.23	-0.14	991.49	73.1	15.8	9.7	12.4	12.4	2.29	2.0	1.98	25.6	-9.45	0.24
31	141.6	58.8	0.23	-0.13	990.84	75.8	16.0	9.9	12.5	12.5	2.34	2.0	2.03	25.5	-24.45	0.27
32	143.6	59.4	0.23	-0.12	990.19	78.5	16.2	10.1	12.6	12.6	2.39	2.0	2.08	25.4	-39.45	0.30
33	145.6	60.0	0.23	-0.11	989.54	81.2	16.4	10.3	12.7	12.7	2.44	2.0	2.13	25.3	-54.45	0.33
34	147.6	60.6	0.23	-0.10	988.89	83.9	16.6	10.5	12.8	12.8	2.49	2.0	2.18	25.2	-69.45	0.36
35	149.6	61.2	0.23	-0.09	988.24	86.6	16.8	10.7	12.9	12.9	2.54	2.0	2.23	25.1	-84.45	0.39
36	151.6	61.8	0.23	-0.08	987.59	89.3	17.0	10.9	13.0	13.0	2.59	2.0	2.28	25.0	-99.45	0.42
37	153.6	62.4	0.23	-0.07	986.94	92.0	17.2	11.1	13.1	13.1	2.64	2.0	2.33	24.9	-114.45	0.45
38	155.6	63.0	0.23	-0.06	986.29	94.7	17.4	11.3	13.2	13.2	2.69	2.0	2.38	24.8	-129.45	0.48
39	157.6	63.6	0.23	-0.05	985.64	97.4	17.6	11.5	13.3	13.3	2.74	2.0	2.43	24.7	-144.45	0.51
40	159.6	64.2	0.23	-0.04	984.99	100.1	17.8	11.7	13.4	13.4	2.79	2.0	2.48	24.6	-159.45	0.54
41	161.6	64.8	0.23	-0.03	984.34	102.8	18.0	11.9	13.5	13.5	2.84	2.0	2.53	24.5	-174.45	0.57
42	163.6	65.4	0.23	-0.02	983.69	105.5	18.2	12.1	13.6	13.6	2.89	2.0	2.58	24.4	-189.45	0.60
43	165.6	66.0	0.23	-0.01	983.04	108.2	18.4	12.3	13.7	13.7	2.94	2.0	2.63	24.3	-204.45	0.63
44	167.6	66.6	0.23	0.00	982.39	110.9	18.6	12.5	13.8	13.8	2.99	2.0	2.68	24.2	-219.45	0.66
45	169.6	67.2	0.23	0.01	981.74	113.6	18.8	12.7	13.9	13.9	3.04	2.0	2.73	24.1	-234.45	0.69
46	171.6	67.8	0.23	0.02	981.09	116.3	19.0	12.9	14.0	14.0	3.09	2.0	2.78	24.0	-249.45	0.72
47	173.6	68.4	0.23	0.03	980.44	119.0	19.2	13.1	14.1	14.1	3.14	2.0	2.83	23.9	-264.45	0.75
48	175.6	69.0	0.23	0.04	979.79	121.7	19.4	13.3	14.2	14.2	3.19	2.0	2.88	23.8	-279.45	0.78
49	177.6	69.6	0.23	0.05	979.14	124.4	19.6	13.5	14.3	14.3	3.24	2.0	2.93	23.7	-294.45	0.81
50	179.6	70.2	0.23	0.06	978.49	127.1	19.8	13.7	14.4	14.4	3.29	2.0	2.98	23.6	-309.45	0.84
51	181.6	70.8	0.23	0.07	977.84	129.8	20.0	13.9	14.5	14.5	3.34	2.0	3.03	23.5	-324.45	0.87
52	183.6	71.4	0.23	0.08	977.19	132.5	20.2	14.1	14.6	14.6	3.39	2.0	3.08	23.4	-339.45	0.90
53	185.6															

MUSTANG ISLAND, TEXAS

NOON BEGINS AT HOUR 12 ON JANUARY 23, 1972

STORM - BAROMETRIC PRESSURE AT CENTER OF LOW = 998.0 MILLIBARS
PRESSURE AT LARGEST ENCIRCLING ISOBAR = 1016.0 MILLIBARS
MAXIMUM PRESSURE INCLUDED IN STORM = 1018.6 MILLIBARS

LENGTH OF MAJOR HALF AXIS = 1800.0 KILOMETERS
LENGTH OF MINOR HALF AXIS = 500.0 KILOMETERS
ORIENTATION OF MAJOR AXIS = 33.0 DEGREES FROM NORTH

LONGSHORE CURRENT EQUATION FROM FOX AND DAVIS, 1972

SHORE - POSITION COORDINATES - X = 2415.0 Y = 0.0 KILOMETERS

SHORE LATITUDE = 28.0 ONSHORE AZIMUTH = 280.0 DEGREES
NEARSHORE SLOPE = 0.018 AVERAGE FETCH = 1000.0 KILOMETERS

TIDES - SPRING TIDE RANGE = 0.85 NEAP TIDE RANGE = 0.30 METERS
SLOPE AT LOW TIDE = 0.016 SLOPE AT HIGH TIDE = 0.020

MIXED DIURNAL TIDE - FURN NUMBER IS 2.50

HOUR	X	Y	A ₁	Y ₁	HANDS PRESS.	WIND ANGLE	SURF. WIND	ONSH WIND	ALSH WIND	EFFECT. WIND	WAVE H	WAVE T	BREAKER ANGLE	OSC. VELOC.	TIDE	
	KM	KM	RAD	RAD	MB	DEG	M/S	M/S	M/S	M/S	M	SEC	M	CM/SEC	M	
7	1777.	831.	-0.26	-0.28	1018.60	47.6	0.0	0.0	0.0	0.00	0.0	0.00	27.2	0.25	0.24	
8	1820.	828.	-0.26	-0.27	1018.59	47.7	0.0	0.0	0.0	0.00	0.0	0.00	21.6	0.45	0.23	
9	1864.	824.	-0.26	-0.25	1018.58	47.8	0.1	0.0	0.0	0.1	0.00	0.0	0.00	22.1	0.78	0.28
10	1907.	821.	-0.26	-0.23	1018.57	47.9	0.2	0.1	0.1	0.1	0.00	0.1	0.00	22.5	1.28	0.37
11	1951.	818.	-0.26	-0.22	1018.56	48.1	0.3	0.2	0.2	0.3	0.00	0.1	0.00	22.8	2.04	0.45
12	1994.	814.	-0.26	-0.20	1018.50	48.2	0.5	0.3	0.4	0.4	0.00	0.2	0.00	23.1	3.08	0.52
13	2038.	811.	-0.27	-0.18	1018.45	48.4	0.8	0.5	0.6	0.7	0.01	0.4	0.00	23.2	4.47	0.57
14	2074.	810.	-0.27	-0.17	1018.38	48.5	1.1	0.7	0.8	1.0	0.01	0.5	0.01	23.3	5.92	0.57
15	2111.	809.	-0.27	-0.16	1018.28	48.7	1.5	1.0	1.1	1.3	0.03	0.7	0.02	23.4	7.57	0.55
16	2147.	808.	-0.27	-0.15	1018.18	48.8	2.0	1.3	1.5	1.8	0.04	0.8	0.04	23.5	9.43	0.48
17	2183.	808.	-0.27	-0.13	1018.00	49.0	2.6	1.7	2.0	2.3	0.07	1.0	0.06	23.6	11.49	0.40
18	2220.	807.	-0.28	-0.12	1017.78	49.2	3.4	2.2	2.5	3.0	0.11	1.3	0.10	23.7	13.74	0.31
19	2256.	806.	-0.28	-0.10	1017.52	49.4	4.3	2.8	3.2	3.8	0.16	1.6	0.14	23.9	16.18	0.21
20	2316.	804.	-0.28	-0.08	1017.23	49.6	5.1	3.9	4.6	5.3	0.26	2.0	0.23	24.1	19.97	0.13
21	2375.	803.	-0.29	-0.06	1016.83	50.3	6.2	5.2	6.3	7.2	0.41	2.5	0.36	24.4	24.53	0.07
22	2435.	801.	-0.29	-0.04	1016.39	50.8	7.6	6.6	8.1	9.1	0.61	3.0	0.53	24.6	29.47	0.04
23	2494.	800.	-0.29	-0.02	1015.82	51.4	9.2	8.8	9.8	11.0	0.86	3.6	0.74	24.9	34.39	0.03
24	2554.	798.	-0.30	-0.00	1015.16	52.2	10.4	9.8	11.3	12.5	1.12	4.1	0.96	25.2	38.81	0.02
1	2613.	797.	-0.30	0.02	1014.79	53.1	11.5	9.2	12.3	13.3	1.36	4.5	1.16	25.5	42.22	0.03
2	2653.	811.	-0.31	0.03	1014.13	53.8	12.2	9.0	12.3	13.1	1.55	4.9	1.31	25.6	44.57	0.04
3	2693.	824.	-0.31	0.04	1013.52	54.6	12.8	8.6	12.1	12.7	1.69	5.1	1.42	25.8	45.90	0.04
4	2733.	835.	-0.32	0.06	1012.98	55.6	13.1	8.0	11.7	12.1	1.79	5.3	1.49	26.0	46.44	0.05
5	2774.	852.	-0.33	0.07	1012.54	56.7	13.2	7.2	11.0	11.2	1.84	5.4	1.51	26.3	46.16	0.05
6	2814.	865.	-0.34	0.08	1012.20	58.3	13.0	6.3	10.2	10.1	1.85	5.4	1.49	26.8	45.11	0.07
7	2854.	879.	-0.34	0.10	1011.99	60.8	12.6	5.2	9.3	8.8	1.83	5.3	1.43	27.2	42.92	0.10
8	2894.	880.	-0.35	0.11	1011.67	67.0	8.7	3.4	8.0	7.0	1.30	4.7	0.92	28.3	31.56	0.16
9	2935.	881.	-0.35	0.13	1011.56	81.9	6.0	0.8	6.0	4.3	0.53	3.1	0.23	28.8	11.57	0.23
10	2975.	881.	-0.35	0.14	1011.88	103.6	4.0	-0.9	3.4	2.3	0.16	1.7	0.09	28.3	8.65	0.32
11	3015.	882.	-0.36	0.16	1012.02	126.5	3.7	-2.4	3.0	1.7	0.09	1.3	0.08	22.9	11.26	0.42
12	3056.	883.	-0.36	0.17	1012.58	144.8	4.2	-3.5	2.4	1.0	0.08	1.2	0.08	16.2	11.38	0.51
13	3096.	884.	-0.36	0.19	1013.31	157.2	4.9	-4.5	1.9	1.7	0.08	1.2	0.08	11.4	10.15	0.58
14	3127.	884.	-0.36	0.20	1013.98	163.6	5.3	-5.1	1.5	1.8	0.08	1.1	0.08	8.4	8.21	0.61
15	3159.	884.	-0.37	0.21	1014.70	168.3	5.6	-5.5	1.1	1.9	0.08	1.2	0.09	6.0	6.20	0.61
16	3190.	894.	-0.37	0.22	1015.46	172.0	5.8	-5.7	0.8	1.9	0.09	1.2	0.09	4.1	4.36	0.56
17	3221.	897.	-0.37	0.23	1016.22	174.9	5.8	-5.8	0.5	1.9	0.09	1.2	0.09	2.6	2.78	0.47
18	3253.	900.	-0.38	0.24	1016.99	177.2	5.7	-5.7	0.2	1.9	0.09	1.2	0.10	1.4	1.45	0.37
19	3284.	903.	-0.38	0.25	1017.73	174.1	5.5	-5.5	0.0	1.8	0.09	1.3	0.10	0.4	0.41	0.26
20	3315.	907.	-0.38	0.27	1018.54	180.9	5.1	-5.1	-0.0	1.7	0.08	1.3	0.09	-0.4	-0.44	0.16
21	3347.	911.	-0.39	0.28	1019.28	182.4	4.6	-4.6	-0.2	1.5	0.07	1.1	0.07	-1.1	-1.49	0.08
22	3379.	915.	-0.39	0.29	1019.94	183.7	4.1	-4.1	-0.2	1.3	0.05	1.0	0.06	-1.7	-1.21	0.03
23	3412.	919.	-0.40	0.31	1021.51	184.7	3.5	-3.5	-0.2	1.1	0.04	0.9	0.04	-2.4	-1.32	0.00
24	3445.	923.	-0.40	0.32	1017.00	185.6	2.9	-2.9	-0.2	0.9	0.02	0.7	0.03	-2.7	-1.30	0.00
1	3478.	927.	-0.40	0.33	1017.40	186.4	2.3	-2.3	-0.2	0.8	0.01	0.6	0.02	-3.1	-1.21	0.01
2	3509.	938.	-0.41	0.33	1017.40	186.2	2.3	-2.3	-0.2	0.8	0.01	0.5	0.01	-3.0	-1.23	0.03
3	3508.	950.	-0.41	0.33	1017.34	185.4	2.3	-2.3	-0.2	0.8	0.01	0.5	0.01	-2.9	-1.19	0.04
4	3511.	961.	-0.42	0.33	1017.34	185.7	2.3	-2.3	-0.2	0.8	0.01	0.5	0.01	-2.8	-1.15	0.05
5	3515.	973.	-0.42	0.33	1017.34	185.4	2.3	-2.3	-0.2	0.7	0.01	0.5	0.01	-2.7	-1.10	0.05
6	3518.	984.	-0.43	0.33	1017.34	185.4	2.3	-2.3	-0.2	0.7	0.01	0.5	0.01	-2.6	-1.05	0.06
7	3521.	996.	-0.43	0.33	1017.38	185.9	2.3	-2.3	-0.2	0.7	0.01	0.5	0.01	-2.4	-1.00	0.08

WAVE ENERGY IN THE BREAKER ZONE = 0.6016 09 JOULES

TOTAL LONGSHORE CURRENT ENERGY = 0.1996 09 JOULES

TOTAL POSITIVE LONGSHORE CURRENT ENERGY = 0.3996 09 JOULES

TOTAL NEGATIVE LONGSHORE CURRENT ENERGY = 0.1616 09 JOULES

MUSTANG ISLAND, TEXAS

RUN BEGINS AT HOUR 7 ON JANUARY 12, 1972

STORM - BAROMETRIC PRESSURE AT CENTER OF LOW = 990.0 MILLIBARS
PRESSURE AT LARGEST ENCIRCLING ISOBAR = 1018.0 MILLIBARS
MAXIMUM PRESSURE INCLUDED IN STORM = 1022.0 MILLIBARS

LENGTH OF MAJOR HALF AXIS = 2500.0 KILOMETERS
LENGTH OF MINOR HALF AXIS = 400.0 KILOMETERS
ORIENTATION OF MAJOR AXIS = 25.0 DEGREES FROM NORTH

LONGSHORE CURRENT EQUATION FROM FOX AND DAVIS, 1972

SHORE - POSITION COORDINATES - X = 2415.0 Y = 0.0 KILOMETERS

SHORE LATITUDE = 28.0 ONSHORE AZIMUTH = 280.0 DEGREES
NEARSHORE SLOPE = 0.018 AVERAGE FETCH = 1000.0 KILOMETERS

TIDES - SPRING TIDE RANGE = 0.85 NEAP TIDE RANGE = 0.30 METERS
SLOPE AT LOW TIDE = 0.016 SLOPE AT HIGH TIDE = 0.020

MIXED DIURNAL TIDE - FORM NUMBER IS 2.50

HOUR	X	Y	X1	Y1	BARO. PRESS.	WIND ANGLE	SURF. WIND	ONSH WIND	ALSH WIND	EFFECT. WIND	WAVE H	WAVE T	BREAKER H	LSC VELOC.	TIDE
	KM	KM	RAD	RAD	MB	DEG	M/S	M/S	M/S	M/S	M	SEC	M	DEG	CM/SEC
7	2381.	1593.	-0.41	-0.08	1022.04	52.5	0.1	0.0	0.0	0.0	0.00	0.0	0.00	23.5	0.53
8	2436.	1583.	-0.41	-0.06	1022.02	52.6	0.2	0.1	0.2	0.2	0.00	0.1	0.00	24.4	1.36
9	2492.	1574.	-0.41	-0.05	1021.96	52.8	0.6	0.3	0.5	0.5	0.00	0.3	0.00	24.8	2.96
10	2547.	1564.	-0.41	-0.03	1021.84	52.9	1.4	0.8	1.1	1.2	0.02	0.6	0.02	25.0	5.70
11	2603.	1554.	-0.41	-0.02	1021.57	53.1	2.9	1.7	2.3	2.5	0.07	1.0	0.06	25.2	10.06
12	2658.	1545.	-0.41	-0.00	1021.06	53.3	5.2	3.1	4.2	4.5	0.17	1.6	0.15	25.5	16.44
13	2714.	1535.	-0.41	0.00	1020.19	53.6	8.7	5.1	7.0	7.5	0.38	2.4	0.32	25.7	24.95
14	2759.	1525.	-0.41	0.00	1019.25	53.9	11.7	6.9	9.5	10.1	0.65	3.1	0.55	25.9	33.27
15	2804.	1515.	-0.42	0.03	1018.04	54.3	14.9	8.7	12.1	12.8	1.00	3.8	0.84	26.1	41.55
16	2849.	1505.	-0.42	0.04	1016.55	54.7	17.7	10.2	14.5	15.2	1.39	4.5	1.16	26.2	48.96
17	2894.	1495.	-0.42	0.05	1014.87	55.3	19.7	11.2	16.2	16.8	1.78	5.2	1.48	26.4	54.48
18	2939.	1485.	-0.42	0.06	1013.11	56.1	20.1	11.2	16.7	17.1	2.11	5.6	1.74	26.6	57.29
19	2984.	1475.	-0.42	0.07	1011.46	57.4	18.7	10.0	15.8	15.8	2.30	6.0	1.87	26.8	58.61
20	3023.	1465.	-0.43	0.08	1010.35	59.4	16.1	8.2	13.8	13.4	2.38	6.1	1.89	27.4	53.67
21	3061.	1452.	-0.43	0.09	1009.57	64.4	12.4	5.3	11.2	10.0	2.34	6.2	1.74	28.4	40.09
22	3100.	1435.	-0.43	0.10	1009.19	82.4	7.0	0.9	7.0	5.0	0.71	3.6	0.30	29.7	12.61
23	3139.	1418.	-0.44	0.11	1009.25	120.9	3.9	-2.0	3.3	1.9	0.11	1.4	0.09	24.5	10.37
24	3177.	1402.	-0.44	0.12	1009.76	157.4	4.9	-4.5	1.8	1.7	0.09	1.3	0.09	10.6	8.20
1	3216.	1386.	-0.44	0.13	1010.67	175.9	6.6	-6.6	0.4	2.2	0.09	1.2	0.10	2.1	7.36
2	3264.	1364.	-0.44	0.15	1012.19	186.2	8.3	-8.2	-0.8	2.7	0.12	1.3	0.12	-3.2	-3.52
3	3311.	1343.	-0.45	0.16	1013.94	191.6	9.0	-8.9	-1.8	3.0	0.14	1.3	0.15	-6.1	-7.07
4	3358.	1321.	-0.45	0.17	1015.73	194.9	8.9	-8.6	-2.2	3.0	0.16	1.6	0.17	-7.8	-9.37
5	3406.	1299.	-0.46	0.18	1017.40	197.2	7.9	-7.5	-2.3	2.7	0.16	1.6	0.17	-8.9	-10.69
6	3453.	1277.	-0.46	0.19	1018.81	199.0	6.5	-6.1	-2.1	2.2	0.15	1.7	0.16	-9.1	-10.61
7	3501.	1255.	-0.47	0.21	1019.93	200.4	4.9	-4.6	-1.7	1.7	0.08	1.3	0.09	-9.7	-7.67
8	3548.	1233.	-0.47	0.22	1020.76	201.6	3.4	-3.1	-1.2	1.2	0.04	0.9	0.04	-10.2	-5.55
9	3596.	1211.	-0.47	0.23	1021.32	202.6	2.1	-2.0	-0.8	0.7	0.01	0.6	0.01	-10.6	-3.69
10	3643.	1189.	-0.48	0.24	1021.67	203.4	1.2	-1.1	-0.5	0.4	0.00	0.3	0.00	-11.0	-2.26
11	3691.	1167.	-0.48	0.26	1021.86	204.0	0.7	-0.6	-0.2	0.2	0.00	0.1	0.00	-11.3	-1.28
12	3738.	1145.	-0.48	0.27	1021.97	204.6	0.3	-0.3	-0.1	0.1	0.00	0.0	0.00	-11.5	-0.67
13	3786.	1123.	-0.49	0.28	1022.02	205.1	0.1	-0.1	-0.0	0.0	0.00	0.0	0.00	-11.8	-0.32
14	3827.	1101.	-0.49	0.29	1022.04	205.4	0.0	-0.0	-0.0	0.0	0.00	0.0	0.00	-11.9	-0.16
15	3868.	1079.	-0.49	0.30	1022.05	205.7	0.0	-0.0	-0.0	0.0	0.00	0.0	0.00	-12.0	-0.07
16	3909.	1057.	-0.50	0.31	1022.05	206.0	0.0	-0.0	-0.0	0.0	0.00	0.0	0.00	-12.2	-0.03
17	3951.	1035.	-0.50	0.32	1022.05	206.2	0.0	-0.0	-0.0	0.0	0.00	0.0	0.00	-12.3	-0.01
18	3992.	1013.	-0.50	0.33	1022.05	206.5	0.0	-0.0	-0.0	0.0	0.00	0.0	0.00	-12.4	-0.00
19	4033.	991.	-0.51	0.34	1022.05	206.7	0.0	-0.0	-0.0	0.0	0.00	0.0	0.00	-12.5	-0.00
20	4031.	969.	-0.51	0.34	1022.05	206.6	0.0	-0.0	-0.0	0.0	0.00	0.0	0.00	-12.4	-0.00
21	4030.	947.	-0.52	0.34	1022.05	206.5	0.0	-0.0	-0.0	0.0	0.00	0.0	0.00	-12.4	-0.00
22	4028.	925.	-0.52	0.34	1022.05	206.4	0.0	-0.0	-0.0	0.0	0.00	0.0	0.00	-12.3	-0.00
23	4026.	903.	-0.52	0.34	1022.05	206.3	0.0	-0.0	-0.0	0.0	0.00	0.0	0.00	-12.3	-0.00
24	4025.	881.	-0.53	0.34	1022.05	206.2	0.0	-0.0	-0.0	0.0	0.00	0.0	0.00	-12.2	-0.00
1	4023.	859.	-0.53	0.34	1022.05	206.1	0.0	-0.0	-0.0	0.0	0.00	0.0	0.00	-12.1	-0.00
2	4111.	837.	-0.54	0.36	1022.05	206.6	0.0	-0.0	-0.0	0.0	0.00	0.0	0.00	-12.4	-0.00
3	4199.	815.	-0.54	0.38	1022.05	207.0	0.0	-0.0	-0.0	0.0	0.00	0.0	0.00	-12.6	-0.00
4	4286.	793.	-0.55	0.40	1022.06	207.3	0.0	-0.0	-0.0	0.0	0.00	0.0	0.00	-12.8	-0.00
5	4374.	771.	-0.56	0.43	1022.06	207.6	0.0	-0.0	-0.0	0.0	0.00	0.0	0.00	-13.0	-0.00
6	4462.	749.	-0.56	0.45	1022.06	207.9	0.0	-0.0	-0.0	0.0	0.00	0.0	0.00	-13.0	-0.00
7	4550.	727.	-0.57	0.47	1022.06	208.1	0.0	-0.0	-0.0	0.0	0.00	0.0	0.00	-13.0	-0.00
8	4597.	705.	-0.57	0.48	1022.06	208.2	0.0	-0.0	-0.0	0.0	0.00	0.0	0.00	-13.0	-0.00
9	4643.	683.	-0.57	0.50	1022.06	208.3	0.0	-0.0	-0.0	0.0	0.00	0.0	0.00	-13.0	-0.00
10	4690.	661.	-0.58	0.51	1022.06	208.4	0.0	-0.0	-0.0	0.0	0.00	0.0	0.00	-13.0	-0.00
11	4737.	639.	-0.58	0.52	1022.06	208.5	0.0	-0.0	-0.0	0.0	0.00	0.0	0.00	-13.0	-0.00
12	4783.	617.	-0.59	0.53	1022.06	208.6	0.0	-0.0	-0.0	0.0	0.00	0.0	0.00	-13.0	-0.00
13	4830.	595.	-0.59	0.54	1022.06	208.6	0.0	-0.0	-0.0	0.0	0.00	0.0	0.00	-13.0	-0.00

WAVE ENERGY IN THE BREAKER ZONE = 0.7218 09 JOULES

TOTAL LONG-SHORE CURRENT ENERGY = 0.5936 04 JOULES

TOTAL POSITIVE LONG-SHORE CURRENT ENERGY = 0.5406 09 JOULES

TOTAL NEGATIVE LONG-SHORE CURRENT ENERGY = 0.0496 05 JOULES

MONTEREY, CALIFORNIA

RUN BEGINS AT HOUR 4 ON FEBRUARY 13 1967

STORM - BAROMETRIC PRESSURE AT CENTER OF LOW = 998.0 MILLIBARS
PRESSURE AT LARGEST ENCINCLING ISOBAR = 1012.0 MILLIBARS
MAXIMUM PRESSURE INCLUDED IN STORM = 1014.0 MILLIBARS

LENGTH OF MAJOR HALF AXIS = 700.0 KILOMETERS
LENGTH OF MINOR HALF AXIS = 390.0 KILOMETERS
ORIENTATION OF MAJOR AXIS = 50.0 DEGREES FROM NORTH

LONGSHORE CURRENT EQUATION FROM LONGUET-HIGGINS, 1973

SHORE - POSITION COORDINATES - X = 817.0 Y = 813.0 KILOMETERS

SHORE LATITUDE = 37. ONSHORE AZIMUTH = 120. DEGREES
NEARSHORE SLOPE = 0.057 AVERAGE FETCH = 50000. KILOMETERS

TIDES - SPRING TIDE RANGE = 2.07 NEAP TIDE RANGE = 0.91 METERS
SLOPE AT LOW TIDE = 0.056 SLOPE AT HIGH TIDE = 0.058

MIXED SEMIDIURNAL TIDE - FORM NUMBER IS 1.00

HOUR	X	Y	X1	Y1	BARO. PRESS.	WIND ANGLE	SURF. WIND	ONSH WIND	ALSH WIND	EFFECT. WIND	WAVE H	WAVE T	BREAKER ANGLE	OSC. CM/SEC	TIDE
	KM	KM	RAD	RAD	MB	DEG	M/S	M/S	M/S	M/S	M	SEC	M	DEG	M
4	885.	1235.	0.38	0.14	1010.24	239.3	6.7	-3.4	-5.7	3.3	0.10	1.2	0.08	-27.4	-31.00
5	906.	1217.	0.37	0.11	1009.45	243.0	7.4	-3.3	-6.6	3.8	0.16	1.5	0.12	-28.4	-46.36
6	927.	1200.	0.37	0.09	1008.60	247.5	8.1	-3.1	-7.5	4.4	0.21	1.8	0.15	-29.5	-53.42
7	948.	1182.	0.36	0.06	1007.72	252.6	8.8	-2.6	-8.4	5.0	0.28	2.1	0.17	-30.6	-58.55
8	970.	1164.	0.36	0.04	1006.85	259.2	9.5	-1.7	-9.4	5.8	0.36	2.3	0.17	-31.6	-60.43
9	991.	1147.	0.35	0.01	1006.02	266.8	10.4	-0.5	-10.4	6.7	0.46	2.6	0.12	-32.2	-50.87
10	1012.	1129.	0.35	-0.01	1005.28	275.3	11.4	1.0	-11.3	7.9	0.58	3.0	0.10	-32.2	-65.53
11	1038.	1108.	0.34	-0.04	1004.57	286.1	12.4	3.4	-11.9	9.4	0.75	3.4	0.44	-31.0	-95.45
12	1064.	1087.	0.34	-0.07	1003.91	298.9	12.7	6.1	-11.1	10.5	0.93	3.8	0.72	-28.0	-113.99
13	1090.	1066.	0.33	-0.10	1003.24	314.2	12.2	8.5	-8.7	11.0	1.09	4.1	0.99	-22.5	-134.56
14	1116.	1044.	0.33	-0.13	1002.59	330.3	12.2	10.6	-6.0	11.7	1.26	4.4	1.25	-15.3	-154.77
15	1142.	1023.	0.32	-0.16	1001.95	344.9	12.7	12.3	-3.3	12.6	1.44	4.7	1.49	-7.9	-174.18
16	1168.	1002.	0.32	-0.19	1001.26	356.8	13.4	13.3	-0.7	13.3	1.62	5.0	1.70	-1.7	-193.54
17	1189.	989.	0.32	-0.22	1000.58	3.2	13.7	13.7	0.7	13.7	1.79	5.3	1.88	1.7	-193.54
18	1210.	976.	0.32	-0.24	1000.76	8.5	13.8	13.6	2.0	13.7	1.94	5.5	2.03	4.5	-186.07
19	1231.	963.	0.32	-0.27	1000.58	12.7	13.5	13.2	3.0	13.4	2.05	5.7	2.14	6.7	-154.34
20	1252.	950.	0.32	-0.29	1000.41	16.2	13.0	12.5	3.6	12.9	2.13	5.8	2.21	8.5	-120.53
21	1273.	937.	0.31	-0.31	1000.22	19.1	12.3	11.6	4.0	12.0	2.18	5.9	2.25	10.0	-84.86
22	1294.	924.	0.31	-0.34	1000.98	21.6	11.3	10.5	4.1	11.0	2.17	5.9	2.23	11.2	-42.07
23	1322.	906.	0.31	-0.37	1010.91	24.3	9.7	8.8	4.0	9.4	1.67	5.1	1.70	12.6	89.55
24	1349.	888.	0.31	-0.40	1011.70	26.8	8.0	7.2	3.6	7.7	1.20	4.4	1.21	13.7	51.50
1	1377.	870.	0.31	-0.43	1012.35	28.5	6.4	5.6	3.0	6.1	0.80	3.6	0.80	14.5	7.45
2	1405.	853.	0.31	-0.46	1012.86	30.0	4.8	4.2	2.4	4.6	0.49	2.8	0.49	15.2	57.56
3	1432.	835.	0.31	-0.49	1013.24	31.4	3.5	3.0	1.8	3.3	0.28	2.1	0.28	15.7	44.57
4	1460.	817.	0.30	-0.52	1013.52	32.5	2.4	2.0	1.3	2.3	0.14	1.5	0.14	16.1	32.64
5	1505.	799.	0.31	-0.57	1013.78	33.5	1.3	1.1	0.7	1.2	0.04	0.9	0.04	16.3	18.39
6	1551.	781.	0.32	-0.62	1013.92	34.3	0.6	0.5	0.3	0.6	0.01	0.4	0.01	16.3	9.21
7	1596.	763.	0.33	-0.66	1013.98	35.0	0.2	0.2	0.1	0.2	0.00	0.2	0.00	16.6	4.15
8	1641.	746.	0.33	-0.71	1014.01	35.6	0.1	0.0	0.0	0.1	0.00	0.0	0.00	0.0	0.00
9	1687.	728.	0.34	-0.75	1014.02	36.1	0.0	0.0	0.0	0.0	0.00	0.0	0.00	0.0	0.00
10	1732.	710.	0.35	-0.80	1014.02	36.6	0.0	0.0	0.0	0.0	0.00	0.0	0.00	0.0	0.00
11	1789.	694.	0.36	-0.85	1014.02	36.9	0.0	0.0	0.0	0.0	0.00	0.0	0.00	0.0	0.00
12	1845.	678.	0.37	-0.91	1014.02	37.2	0.0	0.0	0.0	0.0	0.00	0.0	0.00	0.0	0.00
13	1902.	661.	0.39	-0.96	1014.02	37.4	0.0	0.0	0.0	0.0	0.00	0.0	0.00	0.0	0.00
14	1959.	645.	0.40	-1.02	1014.03	37.6	0.0	0.0	0.0	0.0	0.00	0.0	0.00	0.0	0.00
15	2015.	629.	0.41	-1.07	1014.03	37.8	0.0	0.0	0.0	0.0	0.00	0.0	0.00	0.0	0.00
16	2072.	613.	0.43	-1.13	1014.03	38.0	0.0	0.0	0.0	0.0	0.00	0.0	0.00	0.0	0.00
17	2116.	592.	0.43	-1.17	1014.03	38.3	0.0	0.0	0.0	0.0	0.00	0.0	0.00	0.0	0.00
18	2160.	571.	0.44	-1.22	1014.03	38.6	0.0	0.0	0.0	0.0	0.00	0.0	0.00	0.0	0.00
19	2203.	550.	0.44	-1.26	1014.03	38.8	0.0	0.0	0.0	0.0	0.00	0.0	0.00	0.0	0.00
20	2247.	529.	0.44	-1.31	1014.03	39.1	0.0	0.0	0.0	0.0	0.00	0.0	0.00	0.0	0.00
21	2291.	508.	0.45	-1.36	1014.03	39.3	0.0	0.0	0.0	0.0	0.00	0.0	0.00	0.0	0.00
22	2335.	487.	0.45	-1.40	1014.03	39.5	0.0	0.0	0.0	0.0	0.00	0.0	0.00	0.0	0.00
23	2392.	471.	0.46	-1.46	1014.03	39.5	0.0	0.0	0.0	0.0	0.00	0.0	0.00	0.0	0.00
24	2449.	454.	0.48	-1.51	1014.03	39.6	0.0	0.0	0.0	0.0	0.00	0.0	0.00	0.0	0.00
1	2505.	438.	0.49	-1.57	1014.03	39.7	0.0	0.0	0.0	0.0	0.00	0.0	0.00	0.0	0.00
2	2562.	422.	0.50	-1.62	1014.03	39.7	0.0	0.0	0.0	0.0	0.00	0.0	0.00	0.0	0.00
3	2619.	405.	0.52	-1.68	1014.03	39.8	0.0	0.0	0.0	0.0	0.00	0.0	0.00	0.0	0.00
4	2676.	389.	0.53	-1.73	1014.03	39.8	0.0	0.0	0.0	0.0	0.00	0.0	0.00	0.0	0.00

WAVE ENERGY IN THE BREAKER ZONE = 0.155E 10 JOULES

TOTAL LONG-SHORE CURRENT ENERGY = 0.430E 09 JOULES

TOTAL POSITIVE LONG-SHORE CURRENT ENERGY = 0.389E 09 JOULES

TOTAL NEGATIVE LONG-SHORE CURRENT ENERGY = 0.141E 09 JOULES

SOUTH BEACH, OREGON

RUN BEGINS AT HOUR 4 ON DECEMBER 16, 1973

STORM - BAROMETRIC PRESSURE AT CENTER OF LOW = 990.0 MILLIBARS
PRESSURE AT LARGEST ENCIRCLING ISOBAR = 1024.0 MILLIBARS
MAXIMUM PRESSURE INCLUDED IN STORM = 1028.9 MILLIBARS

LENGTH OF MAJOR HALF AXIS = 500.0 KILOMETERS
LENGTH OF MINOR HALF AXIS = 500.0 KILOMETERS
ORIENTATION OF MAJOR AXIS = 0.0 DEGREES FROM NORTH

LONGSHORE CURRENT EQUATION FROM FOX AND DAVIS, 1972

SHORE - POSITION COORDINATES - X = 4400.0 Y = 1520.0 KILOMETERS

SHORE LATITUDE = 43. ONSHORE AZIMUTH = 90. DEGREES
NEARSHORE SLOPE = 0.020 AVERAGE FETCH = 5000. KILOMETERS

TIDES - SPRING TIDE RANGE = 3.81 NEAP TIDE RANGE = 1.85 METERS
SLOPE AT LOW TIDE = 0.017 SLOPE AT HIGH TIDE = 0.023

MIXED SEMIDIURNAL TIDE - FORM NUMBER IS 0.90

HOUR	X	Y	X1	Y1	BARO.	WIND	SURF.	ONSH.	ALSH.	EFFECT.	WAVE	WAVE	BREAKER	LSC	TIDE
	KM	KM	RAD	RAD	MB	DEG	M/S	M/S	M/S	M/S	M	SEC	M	DEG	CM/SEC
4	3173.	1085.	-0.58	1.63	1028.92	211.3	0.0	-0.0	-0.0	0.0	0.00	0.0	0.00	-14.5	-0.00
5	3243.	1062.	-0.61	1.54	1028.92	208.6	0.0	-0.0	-0.0	0.0	0.00	0.0	0.00	-13.5	-0.00
6	3313.	1040.	-0.64	1.44	1028.92	205.8	0.0	-0.0	-0.0	0.0	0.00	0.0	0.00	-12.5	-0.00
7	3383.	1017.	-0.67	1.35	1028.92	202.9	0.0	-0.0	-0.0	0.0	0.00	0.0	0.00	-11.5	-0.00
8	3453.	994.	-0.70	1.26	1028.92	200.0	0.0	-0.0	-0.0	0.0	0.00	0.0	0.00	-10.5	-0.00
9	3523.	972.	-0.73	1.16	1028.92	197.0	0.0	-0.0	-0.0	0.0	0.00	0.0	0.00	-9.5	-0.00
10	3593.	949.	-0.76	1.07	1028.91	193.7	0.0	-0.0	-0.0	0.0	0.00	0.0	0.00	-8.5	-0.00
11	3663.	926.	-0.79	0.98	1028.88	190.4	0.1	-0.1	-0.0	0.0	0.00	0.0	0.00	-7.5	-0.00
12	3733.	903.	-0.82	0.89	1028.82	187.1	0.3	-0.2	-0.0	0.1	0.00	0.0	0.00	-6.5	-0.00
13	3803.	880.	-0.85	0.80	1028.67	182.6	0.6	-0.6	-0.1	0.2	0.00	0.1	0.00	-5.5	-0.00
14	3873.	857.	-0.88	0.71	1028.35	172.1	1.3	-1.3	-0.2	0.4	0.00	0.2	0.00	-4.5	-0.00
15	3943.	834.	-0.91	0.62	1027.74	161.6	2.5	-2.5	-0.5	0.8	0.01	0.4	0.01	-3.5	-0.00
16	4013.	811.	-0.94	0.53	1026.64	150.8	4.4	-4.4	-0.8	1.5	0.03	0.7	0.03	-2.5	-0.00
17	4083.	788.	-0.97	0.44	1024.90	139.8	7.0	-6.9	-1.3	2.3	0.06	1.0	0.07	-1.5	-0.00
18	4153.	765.	-1.00	0.35	1022.26	129.7	10.2	-10.0	-1.9	3.4	0.12	1.4	0.13	-0.5	-0.00
19	4223.	742.	-1.03	0.26	1018.57	119.6	13.8	-13.5	-2.5	4.6	0.21	1.8	0.21	0.5	-0.00
20	4293.	719.	-1.06	0.17	1013.82	109.5	17.0	-16.7	-3.1	5.7	0.31	2.2	0.32	1.5	-0.00
21	4363.	696.	-1.09	0.08	1008.24	99.4	19.0	-18.7	-3.9	6.4	0.40	2.5	0.41	2.5	-0.00
22	4433.	673.	-1.12	0.00	1002.34	89.1	19.0	-18.7	-4.3	6.4	0.48	2.7	0.49	3.5	-0.00
23	4503.	650.	-1.15	0.17	997.45	79.2	16.8	-16.3	-3.7	5.7	0.51	2.8	0.52	4.5	-0.00
24	4573.	627.	-1.18	0.12	993.49	69.1	12.5	-11.9	-3.9	4.4	0.37	2.4	0.38	5.5	-0.00
1	4643.	604.	-1.21	0.07	990.98	59.0	7.0	-5.6	-4.2	2.8	0.14	1.5	0.13	6.5	-0.00
2	4713.	581.	-1.24	0.02	989.28	51.4	6.2	-4.2	-4.6	5.5	0.26	2.0	0.25	7.5	-0.00
3	4783.	558.	-1.27	0.03	991.49	44.0	14.0	0.7	14.0	0.89	3.6	0.92	1.6	8.14	-0.00
4	4853.	535.	-1.30	0.08	994.44	36.6	22.7	22.0	5.5	22.5	1.94	5.2	1.98	7.7	0.00
5	4923.	512.	-1.33	0.16	1000.62	29.6	30.4	27.7	12.1	29.4	3.21	6.7	3.21	12.8	0.00
6	4993.	489.	-1.36	0.25	1007.99	22.9	31.2	27.6	14.6	30.0	4.13	7.7	4.09	14.8	0.00
7	5063.	466.	-1.39	0.34	1014.48	16.3	26.7	23.1	13.5	25.5	4.54	8.3	4.49	15.8	0.00
8	5133.	443.	-1.42	0.43	1021.26	10.8	19.6	16.7	10.3	18.6	4.20	8.1	4.16	16.8	0.00
9	5203.	420.	-1.45	0.51	1024.40	5.8	12.5	10.5	6.8	11.9	2.29	6.0	2.26	16.7	0.00
10	5273.	397.	-1.48	0.52	1026.72	3.6	7.0	5.8	3.9	6.6	0.89	3.7	0.87	17.0	0.00
11	5343.	374.	-1.51	0.60	1028.10	3.1	3.0	2.5	1.6	2.9	0.21	1.8	0.21	16.0	0.00
12	5413.	351.	-1.54	0.72	1028.66	3.0	1.1	0.9	0.5	1.0	0.03	0.7	0.03	14.9	0.00
13	5483.	328.	-1.57	0.82	1028.85	2.9	0.3	0.3	0.1	0.3	0.00	0.2	0.00	14.3	0.00
14	5553.	305.	-1.60	0.93	1028.91	2.8	0.0	0.0	0.0	0.0	0.00	0.0	0.00	13.7	0.00
15	5623.	282.	-1.63	1.03	1028.92	2.6	0.0	0.0	0.0	0.0	0.00	0.0	0.00	13.1	0.00
16	5693.	259.	-1.66	1.13	1028.92	2.4	0.0	0.0	0.0	0.0	0.00	0.0	0.00	12.5	0.00
17	5763.	236.	-1.69	1.23	1028.92	2.3	0.0	0.0	0.0	0.0	0.00	0.0	0.00	11.9	0.00
18	5833.	213.	-1.72	1.33	1028.92	2.2	0.0	0.0	0.0	0.0	0.00	0.0	0.00	11.3	0.00
19	5903.	190.	-1.75	1.43	1028.92	2.1	0.0	0.0	0.0	0.0	0.00	0.0	0.00	10.7	0.00
20	5973.	167.	-1.78	1.53	1028.92	2.0	0.0	0.0	0.0	0.0	0.00	0.0	0.00	10.1	0.00
21	6043.	144.	-1.81	1.63	1028.92	1.9	0.0	0.0	0.0	0.0	0.00	0.0	0.00	9.5	0.00
22	6113.	121.	-1.84	1.73	1028.92	1.8	0.0	0.0	0.0	0.0	0.00	0.0	0.00	8.9	0.00
23	6183.	98.	-1.87	1.83	1028.92	1.7	0.0	0.0	0.0	0.0	0.00	0.0	0.00	8.3	0.00
24	6253.	75.	-1.90	1.93	1028.92	1.6	0.0	0.0	0.0	0.0	0.00	0.0	0.00	7.7	0.00
1	6323.	52.	-1.93	2.03	1028.92	1.5	0.0	0.0	0.0	0.0	0.00	0.0	0.00	7.1	0.00
2	6393.	29.	-1.96	2.13	1028.92	1.4	0.0	0.0	0.0	0.0	0.00	0.0	0.00	6.5	0.00
3	6463.	6.	-1.99	2.23	1028.92	1.3	0.0	0.0	0.0	0.0	0.00	0.0	0.00	5.9	0.00
4	6533.	-17.	-2.02	2.33	1028.92	1.2	0.0	0.0	0.0	0.0	0.00	0.0	0.00	5.3	0.00
5	6603.	-40.	-2.05	2.43	1028.92	1.1	0.0	0.0	0.0	0.0	0.00	0.0	0.00	4.7	0.00
6	6673.	-63.	-2.08	2.53	1028.92	1.0	0.0	0.0	0.0	0.0	0.00	0.0	0.00	4.1	0.00
7	6743.	-86.	-2.11	2.63	1028.92	0.9	0.0	0.0	0.0	0.0	0.00	0.0	0.00	3.5	0.00
8	6813.	-109.	-2.14	2.73	1028.92	0.8	0.0	0.0	0.0	0.0	0.00	0.0	0.00	2.9	0.00
9	6883.	-132.	-2.17	2.83	1028.92	0.7	0.0	0.0	0.0	0.0	0.00	0.0	0.00	2.3	0.00
10	6953.	-155.	-2.20	2.93	1028.92	0.6	0.0	0.0	0.0	0.0	0.00	0.0	0.00	1.7	0.00
11	7023.	-178.	-2.23	3.03	1028.92	0.5	0.0	0.0	0.0	0.0	0.00	0.0	0.00	1.1	0.00
12	7093.	-201.	-2.26	3.13	1028.92	0.4	0.0	0.0	0.0	0.0	0.00	0.0	0.00	0.5	0.00
13	7163.	-224.	-2.29	3.23	1028.92	0.3	0.0	0.0	0.0	0.0	0.00	0.0	0.00	-0.1	0.00
14	7233.	-247.	-2.32	3.33	1028.92	0.2	0.0	0.0	0.0	0.0	0.00	0.0	0.00	-0.7	0.00
15	7303.	-270.	-2.35	3.43	1028.92	0.1	0.0	0.0	0.0	0.0	0.00	0.0	0.00	-1.3	0.00

WAVE ENERGY IN THE BREAKER ZONE = 0.000000 JOULES

TOTAL LONGSHORE CURRENT ENERGY = 0.000000 JOULES

TOTAL POSITIVE LONGSHORE CURRENT ENERGY = 0.000000 JOULES

TOTAL NEGATIVE LONGSHORE CURRENT ENERGY = 0.000000 JOULES

APPENDIX 1 - RELEVANT BOOM DATA AND DUTY

CIRCULARITY TEST

BOOM BEING AT HOUR 1 ON JULY 4, 1974

STORM - JAW METHOD: PRESSURE AT CENTER OF BOOM = 1000.0 MILLIBARS
PRESSURE AT 1A GUST INKINGING BOOM = 1000.0 MILLIBARS
MAXIMUM PRESSURE EXCEEDED IN STORM = 1022.9 MILLIBARS

LENGTH OF MAJOR HALF AXIS = 3.1 KILOMETERS
LENGTH OF MINOR HALF AXIS = 1.0 KILOMETERS
ORIENTATION OF MAJOR AXIS = 100 DEGREES FROM NORTH

STORM VELOCITY = 400 KILOMETERS/HOUR STORM AZIMUTH = 90

SHORE - POSITION COORDINATES - X = 1000, Y = 0 KILOMETERS

SHORE LATITUDE = 43, INSHORE AZIMUTH = 90, DEGREE
NEARSHORE SLOPE = 0.333, OFFSHORE SLOPE = 0.1, KILOMETERS

BOOM	X	Y	X1	Y1	DATE	WIND	DIR	DIR	DIR	EFFECT	WAVE	WAVE	BREAKER	WAVE
	KM	KM	KM	KM	MB	DEG	M/S	M/S	M/S	WIND	WAVE	WAVE	WAVE	WAVE
1	400	500	1.1	1.15	1022.8	196.2	0.0	0.0	0.0	0.0	0.0	0.0	0.0	0.0
2	500	500	1.1	1.06	1022.8	196.5	0.0	0.0	0.0	0.0	0.0	0.0	0.0	0.0
3	500	500	1.1	0.97	1022.8	196.6	0.0	0.0	0.0	0.0	0.0	0.0	0.0	0.0
4	500	500	1.1	0.88	1022.8	196.6	0.0	0.0	0.0	0.0	0.0	0.0	0.0	0.0
5	500	500	1.1	0.80	1022.8	196.6	0.0	0.0	0.0	0.0	0.0	0.0	0.0	0.0
6	500	500	1.1	0.71	1022.8	196.7	0.0	0.0	0.0	0.0	0.0	0.0	0.0	0.0
7	500	500	1.1	0.62	1022.8	196.7	0.0	0.0	0.0	0.0	0.0	0.0	0.0	0.0
8	500	500	1.1	0.53	1022.8	196.7	0.0	0.0	0.0	0.0	0.0	0.0	0.0	0.0
9	500	500	1.1	0.44	1022.8	196.7	0.0	0.0	0.0	0.0	0.0	0.0	0.0	0.0
10	500	500	1.1	0.35	1022.8	196.8	0.0	0.0	0.0	0.0	0.0	0.0	0.0	0.0
11	500	500	1.1	0.26	1022.8	196.8	0.0	0.0	0.0	0.0	0.0	0.0	0.0	0.0
12	500	500	1.1	0.17	1022.8	196.8	0.0	0.0	0.0	0.0	0.0	0.0	0.0	0.0
13	500	500	1.1	0.08	1022.8	196.7	0.0	0.0	0.0	0.0	0.0	0.0	0.0	0.0
14	500	500	1.1	0.00	1022.8	196.6	0.0	0.0	0.0	0.0	0.0	0.0	0.0	0.0
15	500	500	1.1	-0.08	1022.8	196.6	0.0	0.0	0.0	0.0	0.0	0.0	0.0	0.0
16	500	500	1.1	-0.17	1022.8	196.6	0.0	0.0	0.0	0.0	0.0	0.0	0.0	0.0
17	500	500	1.1	-0.26	1022.8	196.6	0.0	0.0	0.0	0.0	0.0	0.0	0.0	0.0
18	500	500	1.1	-0.35	1022.8	196.6	0.0	0.0	0.0	0.0	0.0	0.0	0.0	0.0
19	500	500	1.1	-0.44	1022.8	196.6	0.0	0.0	0.0	0.0	0.0	0.0	0.0	0.0
20	500	500	1.1	-0.53	1022.8	196.7	0.0	0.0	0.0	0.0	0.0	0.0	0.0	0.0
21	500	500	1.1	-0.62	1022.8	196.7	0.0	0.0	0.0	0.0	0.0	0.0	0.0	0.0
22	500	500	1.1	-0.71	1022.8	196.7	0.0	0.0	0.0	0.0	0.0	0.0	0.0	0.0
23	500	500	1.1	-0.80	1022.8	196.8	0.0	0.0	0.0	0.0	0.0	0.0	0.0	0.0
24	500	500	1.1	-0.88	1022.8	196.8	0.0	0.0	0.0	0.0	0.0	0.0	0.0	0.0
25	500	500	1.1	-0.97	1022.8	196.7	0.0	0.0	0.0	0.0	0.0	0.0	0.0	0.0
26	500	500	1.1	-1.06	1022.8	196.6	0.0	0.0	0.0	0.0	0.0	0.0	0.0	0.0
27	500	500	1.1	-1.15	1022.8	196.6	0.0	0.0	0.0	0.0	0.0	0.0	0.0	0.0
28	500	500	1.1	-1.24	1022.8	196.6	0.0	0.0	0.0	0.0	0.0	0.0	0.0	0.0
29	500	500	1.1	-1.33	1022.8	196.6	0.0	0.0	0.0	0.0	0.0	0.0	0.0	0.0
30	500	500	1.1	-1.42	1022.8	196.6	0.0	0.0	0.0	0.0	0.0	0.0	0.0	0.0
31	500	500	1.1	-1.51	1022.8	196.6	0.0	0.0	0.0	0.0	0.0	0.0	0.0	0.0
32	500	500	1.1	-1.60	1022.8	196.6	0.0	0.0	0.0	0.0	0.0	0.0	0.0	0.0
33	500	500	1.1	-1.69	1022.8	196.6	0.0	0.0	0.0	0.0	0.0	0.0	0.0	0.0
34	500	500	1.1	-1.78	1022.8	196.6	0.0	0.0	0.0	0.0	0.0	0.0	0.0	0.0
35	500	500	1.1	-1.87	1022.8	196.6	0.0	0.0	0.0	0.0	0.0	0.0	0.0	0.0
36	500	500	1.1	-1.96	1022.8	196.6	0.0	0.0	0.0	0.0	0.0	0.0	0.0	0.0
37	500	500	1.1	-2.05	1022.8	196.6	0.0	0.0	0.0	0.0	0.0	0.0	0.0	0.0
38	500	500	1.1	-2.14	1022.8	196.6	0.0	0.0	0.0	0.0	0.0	0.0	0.0	0.0
39	500	500	1.1	-2.23	1022.8	196.6	0.0	0.0	0.0	0.0	0.0	0.0	0.0	0.0
40	500	500	1.1	-2.32	1022.8	196.6	0.0	0.0	0.0	0.0	0.0	0.0	0.0	0.0
41	500	500	1.1	-2.41	1022.8	196.6	0.0	0.0	0.0	0.0	0.0	0.0	0.0	0.0
42	500	500	1.1	-2.50	1022.8	196.6	0.0	0.0	0.0	0.0	0.0	0.0	0.0	0.0
43	500	500	1.1	-2.59	1022.8	196.6	0.0	0.0	0.0	0.0	0.0	0.0	0.0	0.0
44	500	500	1.1	-2.68	1022.8	196.6	0.0	0.0	0.0	0.0	0.0	0.0	0.0	0.0
45	500	500	1.1	-2.77	1022.8	196.6	0.0	0.0	0.0	0.0	0.0	0.0	0.0	0.0
46	500	500	1.1	-2.86	1022.8	196.6	0.0	0.0	0.0	0.0	0.0	0.0	0.0	0.0
47	500	500	1.1	-2.95	1022.8	196.6	0.0	0.0	0.0	0.0	0.0	0.0	0.0	0.0
48	500	500	1.1	-3.04	1022.8	196.6	0.0	0.0	0.0	0.0	0.0	0.0	0.0	0.0
49	500	500	1.1	-3.13	1022.8	196.6	0.0	0.0	0.0	0.0	0.0	0.0	0.0	0.0
50	500	500	1.1	-3.22	1022.8	196.6	0.0	0.0	0.0	0.0	0.0	0.0	0.0	0.0
51	500	500	1.1	-3.31	1022.8	196.6	0.0	0.0	0.0	0.0	0.0	0.0	0.0	0.0
52	500	500	1.1	-3.40	1022.8	196.6	0.0	0.0	0.0	0.0	0.0	0.0	0.0	0.0
53	500	500	1.1	-3.49	1022.8	196.6	0.0	0.0	0.0	0.0	0.0	0.0	0.0	0.0
54	500	500	1.1	-3.58	1022.8	196.6	0.0	0.0	0.0	0.0	0.0	0.0	0.0	0.0
55	500	500	1.1	-3.67	1022.8	196.6	0.0	0.0	0.0	0.0	0.0	0.0	0.0	0.0
56	500	500	1.1	-3.76	1022.8	196.6	0.0	0.0	0.0	0.0	0.0	0.0	0.0	0.0
57	500	500	1.1	-3.85	1022.8	196.6	0.0	0.0	0.0	0.0	0.0	0.0	0.0	0.0
58	500	500	1.1	-3.94	1022.8	196.6	0.0	0.0	0.0	0.0	0.0	0.0	0.0	0.0
59	500	500	1.1	-4.03	1022.8	196.6	0.0	0.0	0.0	0.0	0.0	0.0	0.0	0.0
60	500	500	1.1	-4.12	1022.8	196.6	0.0	0.0	0.0	0.0	0.0	0.0	0.0	0.0
61	500	500	1.1	-4.21	1022.8	196.6	0.0	0.0	0.0	0.0	0.0	0.0	0.0	0.0
62	500	500	1.1	-4.30	1022.8	196.6	0.0	0.0	0.0	0.0	0.0	0.0	0.0	0.0
63	500	500	1.1	-4.39	1022.8	196.6	0.0	0.0	0.0	0.0	0.0	0.0	0.0	0.0
64	500	500	1.1	-4.48	1022.8	196.6	0.0	0.0	0.0	0.0	0.0	0.0	0.0	0.0
65	500	500	1.1	-4.57	1022.8	196.6	0.0	0.0	0.0	0.0	0.0	0.0	0.0	0.0
66	500	500	1.1	-4.66	1022.8	196.6	0.0	0.0	0.0	0.0	0.0	0.0	0.0	0.0
67	500	500	1.1	-4.75	1022.8	196.6	0.0	0.0	0.0	0.0	0.0	0.0	0.0	0.0
68	500	500	1.1	-4.84	1022.8	196.6	0.0	0.0	0.0	0.0	0.0	0.0	0.0	0.0
69	500	500	1.1	-4.93	1022.8	196.6	0.0	0.0	0.0	0.0	0.0	0.0	0.0	0.0
70	500	500	1.1	-5.02	1022.8	196.6	0.0	0.0	0.0	0.0	0.0	0.0	0.0	0.0
71	500	500	1.1	-5.11	1022.8	196.6	0.0	0.0	0.0	0.0	0.0	0.0	0.0	0.0
72	500	500	1.1	-5.20	1022.8	196.6	0.0	0.0	0.0	0.0	0.0	0.0	0.0	0.0
73	500	500	1.1	-5.29	1022.8	196.6	0.0	0.0	0.0	0.0	0.0	0.0	0.0	0.0
74	500	500	1.1	-5.38	1022.8	196.6	0.0	0.0	0.0	0.0	0.0	0.0	0.0	0.0
75	500	500	1.1	-5.47	1022.8	196.6	0.0	0.0	0.0	0.0	0.0	0.0	0.0	0.0
76	500	500	1.1	-5.56	1022.8	196.6	0.0	0.0	0.0	0.0	0.0	0.0	0.0	0.0
77	500	500	1.1	-5.65	1022.8	196.6	0.0	0.0	0.0	0.0	0.0	0.0	0.0	0.0
78	500	500	1.1	-5.74	1022.8	196.6	0.0	0.0	0.0	0.0	0.0	0.0	0.0	0.0
79	500	500	1.1	-5.83	1022.8	196.6	0.0	0.0	0.0	0.0	0.0	0.0	0.0	0.0
80	500	500	1.1	-5.92	1022.8	196.6	0.0	0.0	0.0	0.0	0.0	0.0	0.0	0.0
81	500	500	1.1	-6.01	1022.8	196.6	0.0	0.0	0.0	0.0	0.0	0.0	0.0	0.0
82	500	500	1.1	-6.10	1022.8	196.6	0.0	0.0	0.0	0.0	0.0	0.0	0.0	0.0
83	500	500	1.1	-6.19	1022.8	196.6	0.0	0.0	0.0	0.0	0.0	0.0	0.0	0.0
84	500	500	1.1	-6.28	1022.8	196.6	0.0	0.0	0.0	0.0	0.0	0.0	0.0	0.0
85	500	500	1.1	-6.37	1022.8	196.6	0.0	0.0	0.0	0.0	0.0	0.0	0.0	0.0
86	500	500	1.1	-6.46	1022.8	196.6	0.0	0.0	0.0	0.0	0.0	0.0	0.0	0.0
87	500	500	1.1	-6.55	1022.8	196.6	0.0	0.0	0.0	0.0				

CIRCULAR STORM TEST

RUN BEGINS AT HOUR 1 ON JULY 4, 1976

STORM - BAROMETRIC PRESSURE AT CENTER OF LOW = 1000.0 MILLIBARS
PRESSURE AT LARGEST ENCIRCLING ISOBAR = 1020.0 MILLIBARS
MAXIMUM PRESSURE INCLUDED IN STORM = 1022.9 MILLIBARS

LENGTH OF MAJOR HALF AXIS = 300.0 KILOMETERS
LENGTH OF MINOR HALF AXIS = 200.0 KILOMETERS
ORIENTATION OF MAJOR AXIS = 0.0 DEGREES FROM NORTH

STORM VELOCITY = 40. KILOMETERS/HOUR STORM AZIMUTH = 90.

SHORE - POSITION COORDINATES - X = 1000.0 Y = 0.0 KILOMETERS

SHORE LATITUDE = 43. ANSHORE AZIMUTH = 90. DEGREES
NEARSHORE SLOPE = 0.033 ANSHORE FETCH = 1000. KILOMETERS

HOUR	X	Y	X1	Y1	BARO. PRESS.	WIND ANGLE	SURF. WIND	UNSH WIND	ALSH WIND	EFFECT. WIND	WAVE H	WAVE T	BREAKER H	WAVE ANGLE	LSC VELOC.
	KM	KM	RAD	RAD	MB	DEG	M/S	M/S	M/S	M/S	M	SEC	M	DEG	CM/SEC
1	480.	200.	0.44	1.15	1022.8	273.9	0.1	0.0	-0.1	0.1	0.00	0.0	0.00	-30.2	-0.7
2	520.	200.	0.44	1.06	1022.8	275.9	0.3	0.0	-0.3	0.2	0.00	0.1	0.00	-31.2	-1.9
3	560.	200.	0.44	0.97	1022.7	278.2	0.7	0.1	-0.7	0.5	0.00	0.3	0.00	-31.7	-4.2
4	600.	200.	0.44	0.88	1022.5	280.7	1.5	0.2	-1.5	1.1	0.02	0.5	0.00	-31.4	-8.2
5	640.	200.	0.44	0.80	1022.3	283.3	2.8	0.5	-2.8	2.1	0.05	0.9	0.03	-31.2	-14.4
6	680.	200.	0.44	0.71	1021.9	286.3	5.0	1.4	-4.8	3.8	0.13	1.4	0.08	-30.9	-23.4
7	720.	200.	0.44	0.62	1021.2	289.8	8.0	2.7	-7.5	6.3	0.29	2.4	0.19	-30.4	-35.8
8	760.	200.	0.44	0.53	1020.1	294.1	11.9	4.9	-10.9	9.6	0.57	2.9	0.41	-29.6	-51.3
9	800.	200.	0.44	0.44	1019.0	299.3	16.3	7.9	-14.2	13.3	0.99	3.8	0.77	-28.3	-68.3
10	840.	200.	0.44	0.35	1017.5	305.6	20.3	11.8	-18.5	17.5	1.55	4.8	1.30	-26.3	-84.3
11	880.	200.	0.44	0.26	1016.3	313.3	23.7	16.3	-21.2	21.2	2.22	5.7	1.79	-23.3	-95.0
12	920.	200.	0.44	0.17	1014.7	322.5	26.6	20.8	-23.9	24.4	2.93	6.6	2.79	-19.4	-97.4
13	960.	200.	0.44	0.08	1013.4	333.0	27.0	24.6	-22.5	26.6	3.64	7.3	3.63	-14.3	-84.9
14	1000.	200.	0.44	0.00	1013.4	344.3	28.0	27.0	-21.5	27.6	4.28	8.0	4.39	-8.4	-56.5
15	1040.	200.	0.44	-0.08	1013.8	355.5	27.5	27.5	-20.0	27.5	4.79	8.5	4.98	-2.3	-16.9
16	1080.	200.	0.44	-0.17	1014.7	36.1	26.2	26.2	-18.0	26.1	5.13	8.9	5.36	3.3	-24.0
17	1120.	200.	0.44	-0.26	1016.0	45.3	23.7	22.9	-16.2	23.4	5.30	9.1	5.49	8.1	-11.0
18	1160.	200.	0.44	-0.35	1017.5	53.0	20.3	18.7	-14.9	19.7	4.51	8.4	4.59	12.0	-3.3
19	1200.	200.	0.44	-0.44	1019.0	59.3	16.3	14.2	-12.9	15.6	3.03	6.9	3.02	17.1	11.0
20	1240.	200.	0.44	-0.53	1020.2	64.5	12.1	10.0	-10.0	10.9	1.79	5.3	1.75	22.5	20.0
21	1280.	200.	0.44	-0.62	1021.2	68.8	8.4	6.5	-6.2	7.4	0.91	3.8	0.87	28.4	34.0
22	1320.	200.	0.44	-0.71	1021.9	72.3	5.4	4.0	-3.6	4.9	0.38	2.4	0.36	33.6	37.5
23	1360.	200.	0.44	-0.79	1022.3	75.2	3.2	2.2	-2.3	2.9	0.12	1.4	0.11	37.1	22.0
24	1400.	200.	0.44	-0.88	1022.6	77.5	1.7	1.2	-1.3	1.5	0.00	0.3	0.00	39.4	5.7
1	1440.	200.	0.44	-0.97	1022.7	79.3	0.9	0.5	-0.5	0.9	0.00	0.0	0.00	40.0	0.0
2	1480.	200.	0.44	-1.06	1022.8	80.7	0.4	0.2	-0.3	0.3	0.00	0.0	0.00	40.0	0.0
3	1520.	200.	0.44	-1.15	1022.8	81.8	0.1	0.1	-0.1	0.1	0.00	0.0	0.00	40.0	0.0
1	480.	100.	0.42	1.15	1022.8	259.1	0.2	-0.0	-0.2	0.1	0.00	0.0	0.00	-30.2	-1.3
2	520.	100.	0.42	1.06	1022.7	260.5	0.5	-0.0	-0.5	0.3	0.00	0.2	0.00	-31.1	-2.0
3	560.	100.	0.42	0.97	1022.6	262.1	1.1	-0.1	-1.1	0.7	0.00	0.2	0.00	-31.6	-5.0
4	600.	100.	0.42	0.88	1022.3	264.0	2.2	-0.2	-2.2	1.4	0.04	0.6	0.01	-31.9	-9.0
5	640.	100.	0.42	0.80	1021.9	266.2	4.1	-0.2	-4.1	2.8	0.07	1.1	0.01	-31.1	-14.1
6	680.	100.	0.42	0.71	1021.0	268.8	6.9	-0.2	-6.9	4.5	0.10	1.6	0.02	-30.4	-19.3
7	720.	100.	0.42	0.62	1019.6	272.6	11.0	0.4	-11.0	7.4	0.30	2.4	0.08	-28.6	-24.4
8	760.	100.	0.42	0.53	1017.8	279.9	16.0	1.6	-15.4	11.2	0.73	3.3	0.25	-26.4	-36.0
9	800.	100.	0.42	0.44	1015.3	289.7	21.7	4.0	-21.3	15.4	1.26	4.3	0.51	-23.4	-46.0
10	840.	100.	0.42	0.35	1012.5	286.3	26.9	7.0	-25.8	21.7	1.96	5.1	0.97	-19.4	-50.0
11	880.	100.	0.42	0.26	1009.5	294.1	30.5	12.4	-27.8	24.4	2.70	6.3	1.69	-13.4	-51.0
12	920.	100.	0.42	0.17	1006.9	305.6	30.3	17.1	-24.6	25.1	3.45	7.1	2.47	-7.4	-126.1
13	960.	100.	0.42	0.08	1005.2	322.5	28.5	22.5	-21.2	25.4	4.06	7.8	2.97	-1.4	-114.0
14	1000.	100.	0.42	0.00	1004.5	344.3	27.3	26.3	-19.7	27.1	4.57	8.1	3.49	3.3	-58.2
15	1040.	100.	0.42	-0.08	1005.2	36.1	25.3	23.3	-18.0	25.1	5.08	8.7	3.98	8.1	-24.7
16	1080.	100.	0.42	-0.17	1006.9	43.0	20.3	21.9	-16.0	24.7	5.28	9.2	4.24	12.0	-31.4
17	1120.	100.	0.42	-0.26	1009.5	49.3	16.3	14.3	-14.3	15.9	3.90	8.5	3.40	17.1	-30.0
18	1160.	100.	0.42	-0.35	1012.5	53.0	12.1	10.1	-10.1	10.9	2.71	7.4	2.41	22.5	-20.0
19	1200.	100.	0.42	-0.44	1015.3	57.5	8.4	6.4	-6.4	6.9	1.79	5.3	1.75	28.4	-34.0
20	1240.	100.	0.42	-0.53	1017.8	60.7	5.4	4.4	-4.4	4.9	0.91	3.8	0.87	33.6	-37.5
21	1280.	100.	0.42	-0.62	1019.6	62.7	3.2	2.2	-2.3	2.9	0.38	2.4	0.36	37.1	-22.0
22	1320.	100.	0.42	-0.71	1021.2	64.1	1.7	1.2	-1.3	1.5	0.12	1.4	0.11	39.4	-5.7
23	1360.	100.	0.42	-0.79	1021.8	65.1	0.9	0.5	-0.5	0.9	0.00	0.0	0.00	40.0	0.0
24	1400.	100.	0.42	-0.88	1022.3	65.9	0.4	0.2	-0.3	0.3	0.00	0.0	0.00	40.0	0.0
1	1440.	100.	0.42	-0.97	1022.6	67.5	0.2	0.1	-0.1	0.1	0.00	0.0	0.00	40.0	0.0
2	1480.	100.	0.42	-1.06	1022.7	67.5	0.1	0.0	-0.1	0.0	0.00	0.0	0.00	40.0	0.0
3	1520.	100.	0.42	-1.15	1022.8	67.3	0.0	0.0	-0.1	0.0	0.00	0.0	0.00	40.0	0.0
1	480.	0.	0.00	1.15	1022.8	241.4	0.2	-0.1	-0.2	0.1	0.00	0.0	0.00	-26.6	-1.4
2	520.	0.	0.00	1.06	1022.7	241.4	0.5	-0.2	-0.5	0.3	0.00	0.1	0.00	-27.3	-2.0
3	560.	0.	0.00	0.97	1022.6	241.4	1.1	-0.3	-1.1	0.6	0.00	0.2	0.00	-27.6	-5.0
4	600.	0.	0.00	0.88	1022.3	241.4	2.2	-0.4	-2.2	1.2	0.02	0.5	0.00	-27.7	-9.0
5	640.	0.	0.00	0.80	1021.9	241.4	4.1	-0.4	-4.1	2.3	0.05	0.9	0.01	-27.1	-14.1
6	680.	0.	0.00	0.71	1021.0	241.4	6.9	-0.4	-6.9	3.4	0.10	1.6	0.02	-26.4	-19.3
7	720.	0.	0.00	0.62	1018.8	241.4	10.2	-0.4	-10.2	5.1	0.27	2.4	0.08	-25.1	-24.4
8	760.	0.	0.00	0.53	1016.5	241.4	13.9	-0.4	-13.9	7.0	0.38	2.9	0.19	-23.4	-36.0
9	800.	0.	0.00	0.44	1013.4	241.4	17.1	-0.4	-17.1	9.6	0.57	3.4	0.34	-19.4	-46.0
10	840.	0.	0.00	0.35	1009.5	241.4	18.8	-0.4	-18.8	10.9	0.74	3.9	0.57	-13.4	-50.0
11	880.	0.	0.00	0.26	1006.9	241.4	18.1	-0.4	-18.1	10.9	0.86	4.0	0.66	-7.4	-51.0
12	920.	0.	0.00	0.17	1003.5	241.4	14.4	-0.4	-14.4	10.9	0.77	3.5	0.59	-1.4	-54.0
13	960.	0.	0.00	0.08	1000.8	241.4	8.0	-0.3	-8.0	9.0	0.27	1.8	0.17	-2.6	-32.0
14	1000.	0.	0.00	-0.00	999.0	241.4	0.0	0.0	0.0	0.0	0.00	0.0	0.00	20.0	0.0
15	1040.	0.	0.00	-0.08	1000.8	241.4	13.1	0.4	13.1	10.9	0.28	2.4	0.19	20.0	0.0
16	1080.	0.	0.00	-0.17	1003.5	241.4	17.1	0.4	17.1	10.9	0.51	3.0	0.34	25.0	0.0
17	1120.	0.	0.00	-0.26	1006.9	241.4	19.9	0.4	19.9	10.9	0.67	3.4	0.44	29.0	0.0
18	1160.	0.	0.00	-0.35	1009.5	241.4	19.9	0.4	19.9	10.9	0.74	3.6	0.49	32.0	0.0
19	1200.	0.	0.00	-0.44	1013.4	241.4	19.9	0.4	19.9	10.9	0.77	3.6	0.49	32.0	0.0
20	1240.	0.	0.00	-0.53	1017.8	241.4	19.9	0.4	19.9	10.9	0.77	3.6	0.49	32.0	0.0
21	1280.	0.	0.00	-0.62	1019.6	241.4	16.7	0.4	16.7	10.9	0.68	3.2	0.44	28.0	0.0
22	1320.	0.	0.00	-0.71	1021.2	241.4	11.2	0.3	11.2	9.8	0.43	2.0	0.28	20.0	0.0
23	1360.	0.	0.00	-0.79	1021.8	241.4	6.0	0.2	6.0	9.0	0.28	1.4	0.19	10.0	0.0
24	1400.	0.	0.00	-0.88	1022.3	241.4	3.0	0.1	3.0	8.0	0.11	0.7	0.07	5.0	0.0
1	1440.	0.	0.00	-0.97	1022.6	241.4	2.0	0.0	2.0	7.0	0.05	0.4	0.03	4.0	0.0
2	1480.	0.	0.00	-1.06	1022.7	241.4	1.0	0.0	1.0	6.0	0.02	0.2	0.01	3.0	0.0
3	1520.	0.	0.00	-1.15	1022.8	241.4	0.0	0.0	0.0	5.0	0.00	0.0	0.00	2.0	0.0

800-762-2269 • Fax 800-762-2270

LENGTH OF MAJOR AXIS = 300.0 KILOMETERS
 LENGTH OF MINOR AXIS = 300.0 KILOMETERS
 INCLINATION OF MAJOR AXIS = 0.0 DEGREES FROM NORTH

1. $\theta = 90^\circ$ (1) $\theta = 0^\circ$ (2) $\theta = 45^\circ$ (3) $\theta = 135^\circ$ (4) $\theta = 225^\circ$

Distance from base of cliff to top of hill = 1000 ft

SHORE AZIMUTH = 67 DEGREES
AVERAGE FLIGHT = 100 KILOMETERS

[illegible]

CIRCULAR STORM TEST

RUN BEGINS AT HOUR 1 ON JULY 4, 1976

STORY - BAROMETRIC PRESSURE AT CENTER OF LOW = 1000.0 MILLIBARS
PRESSURE AT LARGEST ENCIRCLING ISOBAR = 1020.0 MILLIBARS
MAXIMUM PRESSURE INCLUDED IN STORM = 1022.9 MILLIBARS

LENGTH OF MAJOR HALF AXIS = 300.0 KILOMETERS
LENGTH OF MINOR HALF AXIS = 300.0 KILOMETERS
ORIENTATION OF MAJOR AXIS = 0.0 DEGREES FROM NORTH

STORM VELOCITY = 40. KILOMETERS/HOUR STORM AZIMUTH = 90.

SHORE - POSITION COORDINATES - X = 1000.0 Y = 0.0 KILOMETERS

SHORE LATITUDE = 43. ONSHORE AZIMUTH = 90. DEGREES
NEARSHORE SLOPE = 0.033 AVERAGE FETCH = 1000. KILOMETERS

HOUR	X	Y	X1	Y1	BARO. PRESS.	WIND ANGLE	SURF. WIND	ONSH WIND	ALSH WIND	EFFECT. WIND	WAVE H	WAVE T	BREAKER H	ANGLE	LSC VELOC.
	KM	KM	RAD	RAD	MB	DEG	M/S	M/S	M/S	M/S	M	SEC	M	DEG	CM/SEC
1	480.	-400.	-0.89	1.15	1022.8	191.4	0.0	-0.0	-0.0	0.0	0.00	0.0	0.00	-2.4	-0.0
2	520.	-400.	-0.89	1.06	1022.8	189.1	0.0	-0.0	-0.0	0.0	0.00	0.0	0.00	-4.4	-0.0
3	560.	-400.	-0.89	0.97	1022.8	186.7	0.0	-0.0	-0.0	0.0	0.00	0.0	0.00	-2.2	-0.0
4	600.	-400.	-0.89	0.88	1022.8	183.9	0.0	-0.0	-0.0	0.0	0.00	0.0	0.00	-1.9	-0.0
5	640.	-400.	-0.89	0.80	1022.8	180.9	0.1	-0.1	-0.0	0.0	0.00	0.0	0.00	-0.4	-0.0
6	680.	-400.	-0.89	0.71	1022.8	177.6	0.3	-0.3	0.0	0.1	0.00	0.0	0.00	1.1	0.0
7	720.	-400.	-0.89	0.62	1022.7	173.9	0.5	-0.4	0.0	0.1	0.00	0.1	0.00	3.0	0.0
8	760.	-400.	-0.89	0.53	1022.7	169.9	0.7	-0.7	0.1	0.2	0.00	0.1	0.00	5.2	0.7
9	800.	-400.	-0.89	0.44	1022.6	165.5	1.0	-1.0	0.2	0.3	0.00	0.2	0.00	7.5	1.4
10	840.	-400.	-0.89	0.35	1022.5	160.8	1.4	-1.3	0.4	0.5	0.00	0.3	0.00	9.9	2.4
11	880.	-400.	-0.89	0.26	1022.4	155.7	1.7	-1.6	0.7	0.8	0.00	0.4	0.00	12.5	3.7
12	920.	-400.	-0.89	0.17	1022.3	150.3	2.0	-1.8	1.0	0.7	0.01	0.4	0.01	15.1	5.3
13	960.	-400.	-0.89	0.08	1022.2	144.7	2.2	-1.8	1.3	0.8	0.01	0.5	0.01	17.7	6.9
14	1000.	-400.	-0.89	0.00	1022.2	139.0	2.3	-1.7	1.5	0.9	0.02	0.5	0.01	20.2	8.4
15	1040.	-400.	-0.89	-0.08	1022.2	133.3	2.2	-1.5	1.6	0.9	0.02	0.6	0.02	22.4	9.1
16	1080.	-400.	-0.89	-0.17	1022.3	127.7	2.0	-1.2	1.6	0.9	0.02	0.6	0.01	24.1	10.0
17	1120.	-400.	-0.89	-0.26	1022.4	122.3	1.7	-0.9	1.5	0.8	0.02	0.6	0.01	24.2	9.4
18	1160.	-400.	-0.89	-0.35	1022.5	117.3	1.4	-0.6	1.2	0.7	0.01	0.5	0.01	23.5	8.0
19	1200.	-400.	-0.89	-0.44	1022.6	112.5	1.0	-0.4	1.0	0.5	0.01	0.4	0.00	26.7	6.3
20	1240.	-400.	-0.89	-0.53	1022.7	108.1	0.7	-0.2	0.7	0.4	0.00	0.3	0.00	27.5	4.6
21	1280.	-400.	-0.89	-0.62	1022.7	104.1	0.5	-0.1	0.5	0.3	0.0	0.2	0.00	27.9	3.1
22	1320.	-400.	-0.89	-0.71	1022.8	100.4	0.3	-0.0	0.3	0.2	0.00	0.1	0.00	28.7	1.9
23	1360.	-400.	-0.89	-0.79	1022.8	97.1	0.2	-0.0	0.1	0.1	0.00	0.0	0.00	28.6	1.0
24	1400.	-400.	-0.89	-0.88	1022.8	94.1	0.1	-0.0	0.1	0.0	0.00	0.0	0.00	31.8	0.4
1	1440.	-400.	-0.89	-0.97	1022.8	91.4	0.0	-0.0	0.0	0.0	0.00	0.0	0.00	0.0	0.0
2	1480.	-400.	-0.89	-1.06	1022.8	88.9	0.0	0.0	0.0	0.0	0.00	0.0	0.00	0.0	0.0
3	1520.	-400.	-0.89	-1.15	1022.8	86.6	0.0	0.0	0.0	0.0	0.00	0.0	0.00	0.0	0.0
1	480.	-500.	-1.11	1.15	1022.8	185.1	0.0	-0.0	-0.0	0.0	0.00	0.0	0.00	-2.4	-0.0
2	520.	-500.	-1.11	1.06	1022.8	182.8	0.0	-0.0	-0.0	0.0	0.00	0.0	0.00	-1.3	-0.0
3	560.	-500.	-1.11	0.97	1022.8	180.3	0.0	-0.0	-0.0	0.0	0.00	0.0	0.00	-0.1	-0.0
4	600.	-500.	-1.11	0.88	1022.8	177.6	0.0	-0.0	0.0	0.0	0.00	0.0	0.00	1.1	0.0
5	640.	-500.	-1.11	0.80	1022.8	174.7	0.0	-0.0	0.0	0.0	0.00	0.0	0.00	2.5	0.0
6	680.	-500.	-1.11	0.71	1022.8	171.6	0.0	-0.0	0.0	0.0	0.00	0.0	0.00	4.0	0.1
7	720.	-500.	-1.11	0.62	1022.8	168.2	0.0	-0.0	0.0	0.0	0.00	0.0	0.00	5.6	0.0
8	760.	-500.	-1.11	0.53	1022.8	164.6	0.1	-0.1	0.0	0.0	0.00	0.0	0.00	7.4	0.1
9	800.	-500.	-1.11	0.44	1022.8	160.8	0.1	-0.1	0.0	0.0	0.00	0.0	0.00	9.3	0.3
10	840.	-500.	-1.11	0.35	1022.8	156.7	0.2	-0.2	0.0	0.0	0.00	0.0	0.00	11.4	0.7
11	880.	-500.	-1.11	0.26	1022.8	152.5	0.2	-0.2	0.1	0.1	0.00	0.0	0.00	13.4	1.1
12	920.	-500.	-1.11	0.17	1022.8	148.1	0.3	-0.2	0.1	0.1	0.00	0.0	0.00	15.5	1.6
13	960.	-500.	-1.11	0.08	1022.8	143.6	0.3	-0.3	0.2	0.1	0.00	0.1	0.00	17.5	1.9
14	1000.	-500.	-1.11	0.00	1022.8	139.0	0.3	-0.2	0.2	0.1	0.00	0.1	0.00	19.4	2.3
15	1040.	-500.	-1.11	-0.08	1022.8	134.4	0.3	-0.2	0.2	0.1	0.00	0.1	0.00	20.9	2.6
16	1080.	-500.	-1.11	-0.17	1022.8	129.9	0.3	-0.2	0.2	0.1	0.00	0.1	0.00	21.6	2.8
17	1120.	-500.	-1.11	-0.26	1022.8	125.5	0.2	-0.1	0.2	0.1	0.00	0.1	0.00	23.0	2.4
18	1160.	-500.	-1.11	-0.35	1022.8	121.3	0.2	-0.1	0.2	0.1	0.00	0.1	0.00	24.3	2.2
19	1200.	-500.	-1.11	-0.44	1022.8	117.2	0.1	-0.0	0.1	0.0	0.00	0.0	0.00	25.5	1.8
20	1240.	-500.	-1.11	-0.53	1022.8	113.4	0.1	-0.0	0.1	0.0	0.00	0.0	0.00	26.1	1.5
21	1280.	-500.	-1.11	-0.62	1022.8	109.8	0.0	-0.0	0.0	0.0	0.00	0.0	0.00	26.9	1.2
22	1320.	-500.	-1.11	-0.71	1022.8	106.4	0.0	-0.0	0.0	0.0	0.00	0.0	0.00	27.9	0.9
23	1360.	-500.	-1.11	-0.79	1022.8	103.3	0.0	-0.0	0.0	0.0	0.00	0.0	0.00	29.4	0.6
24	1400.	-500.	-1.11	-0.88	1022.8	100.4	0.0	-0.0	0.0	0.0	0.00	0.0	0.00	30.4	0.4
1	1440.	-500.	-1.11	-0.97	1022.8	97.7	0.0	-0.0	0.0	0.0	0.00	0.0	0.00	0.0	0.0
2	1480.	-500.	-1.11	-1.06	1022.8	95.2	0.0	-0.0	0.0	0.0	0.00	0.0	0.00	0.0	0.0
3	1520.	-500.	-1.11	-1.15	1022.8	92.9	0.0	-0.0	0.0	0.0	0.00	0.0	0.00	0.0	0.0

Unclassified Distribution List

OFFICE OF NAVAL RESEARCH 2 COPIES
GEOGRAPHY PROGRAMS
CODE 462
ARLINGTON, VIRGINIA 22217

DEFENSE DOCUMENTATION CENTER 12 COPIES
CAMERON STATION
ALEXANDRIA, VIRGINIA 22314

DIRECTOR, NAVAL RESEARCH LAB 6 COPIES
ATTENTION TECHNICAL INFORMATION OFFICER
WASHINGTON, D. C. 20375

DIRECTOR
OFFICE OF NAVAL RESEARCH BRANCH OFFICE
1030 EAST GREEN STREET
PASADENA, CALIFORNIA 91101

DIRECTOR
OFFICE OF NAVAL RESEARCH BRANCH OFFICE
219 SOUTH DEARBORN STREET
CHICAGO, ILLINOIS 60604

DIRECTOR
OFFICE OF NAVAL RESEARCH BRANCH OFFICE
495 SUMMER STREET
BOSTON, MASSACHUSETTS 02210

COMMANDING OFFICER
OFFICE OF NAVAL RESEARCH BRANCH OFFICE
BOX 39
FPO NEW YORK 09510

CHIEF OF NAVAL RESEARCH
ASST. FOR MARINE CORPS MATTERS
CODE 100M
OFFICE OF NAVAL RESEARCH
WASHINGTON, D. C. 22217

CHIEF OF NAVAL RESEARCH
OCEAN SCIENCE AND TECHNOLOGY GROUP
CODE 480
OFFICE OF NAVAL RESEARCH
WASHINGTON, D. C. 22217

OFFICE OF NAVAL RESEARCH
OPERATIONAL APPLICATIONS DIVISION
CODE 200
ARLINGTON, VIRGINIA 22217

OFFICE OF NAVAL RESEARCH
SCIENTIFIC LIAISON OFFICER
SCRIPPS INSTITUTION OF OCEANOGRAPHY
LA JOLLA, CALIFORNIA 92038

DIRECTOR, NAVAL RESEARCH LABORATORY
ATTN LIBRARY, CODE 2628
WASHINGTON, D. C. 20375

COMMANDER
NAVAL OCEANOGRAPHIC OFFICE
ATTN. LIBRARY CODE 1600
WASHINGTON, D. C. 20374

NAVAL OCEANOGRAPHIC OFFICE
CODE 3001
WASHINGTON, D. C. 20374

CHIEF OF NAVAL OPERATIONS
OP 987P1
DEPARTMENT OF THE NAVY
WASHINGTON, D. C. 20350

OCEANOGRAPHER OF THE NAVY
HOFFMAN II BUILDING
200 STUVAL STREET
ALEXANDRIA, VIRGINIA 22322

NAVAL ACADEMY LIBRARY
U. S. NAVAL ACADEMY
ANNAPOLIS, MARYLAND 21402

COMMANDING OFFICER
NAVAL COASTAL SYSTEMS LABORATORY
PANAMA CITY, FLORIDA 32401

LIBRARIAN
NAVAL INTELLIGENCE
SUPPORT CENTER
4301 SUTLAND ROAD
WASHINGTON, D. C. 20390

COMMANDING OFFICER
NAVAL CIVIL ENGINEERING LABORATORY
PORT HUENEME, CALIFORNIA 93041

OFFICER IN CHARGE
ENVIRONMENTAL PREDICTION
RESEARCH FACILITY
NAVAL POST GRADUATE SCHOOL
MONTEREY, CALIFORNIA 93940

DR. WARREN C. THOMPSON
DEPT OF METEOROLOGY & OCEANOGRAPHY
U.S. NAVAL POST GRAD. SCHOOL
MONTEREY, CALIFORNIA 93940

DIRECTOR
AMPHIBIOUS WARFARE BOARD
U.S. ATLANTIC FLEET
NAVAL AMPHIBIOUS BASE
NORFOLK, LITTLE CREEK, VIRGINIA 23520

COMMANDER, AMPHIBIOUS FORCE U. S. PACIFIC FLEET FORCE METEOROLOGIST COMPHIRPAC CODE 25 5 SAN DIEGO, CALIFORNIA 92155	MINISTERIALDIREKTOR DR. F. WEVER RUE/FU BUNDESMINISTERIUM DER VERTEIDIGUNG HARDTHOEHE D-5300 BUNN, WEST GERMANY
COMMANDING GENERAL MARINE CORPS DEVELOPMENT AND EDUCATIONAL COMMAND QUANTICO, VIRGINIA 22134	OBERRREGIERUNGSRAT DR. JAEGER RUE/FU BUNDESMINISTERIUM DER VERTEIDIGUNG HARDTHOEHE D-5300 BUNN, WEST GERMANY
DR. A. L. SLAFKOSKY SCIENTIFIC ADVISOR COMMANDANT OF THE MARINE CORPS (CODE AX) WASHINGTON, D. C. 20380	MR. TAGE STRARUP DEFENCE RESEARCH ESTABLISHMENT OSTERBRUGADES KASERNE DK-2100 KOBENHAVN O, DENMARK
DEFENSE INTELLIGENCE AGENCY DIAAP-10A WASHINGTON, D. C. 20301	PROF. DR. RER. NAT. H.G. GIERLOFF-EMDEN INSTITUT F. GEOGRAPHIE UNIVERSITAET MUENCHEN LUISENSTRASSE 37/III D-800 MUENCHEN 2, WEST GERMANY
DIRECTOR COASTAL ENGINEERING RESEARCH CENTER U.S. ARMY CORPS OF ENGINEERS KINGMAN BUILDING FORT BELVOIR, VIRGINIA 22060	PROF. DR. EUGEN SEIBOLD GEOL.-PALAEONTOLOG. INSTITUT UNIVERSITAET KIEL ULSHAUSENSTRASSE 40-60 D-2300 KIEL, WEST GERMANY
CHIEF, WAVE DYNAMICS DIVISION USAE-WES P. O. BOX 631 VICKSBURG, MISSISSIPPI 39180	DR. R. KUESTER GEOL.-PALAEONTOLOG. INSTITUT UNIVERSITAET KIEL ULSHAUSENSTRASSE 40-60 D-2300 KIEL
COMMANDANT U.S. COAST GUARD ATTN: GECV/61 WASHINGTON, D. C. 20591	PROF. DR. FUEHRHOETER LEHRSTUHL F. HYDROMECHANIK U. KUESTENWASSERBAU TECHNISCHE HOCHSCHULE BRAUNSCHWEIG BEETHOVENSTRASSE 51A D-3300 BRAUNSCHWEIG, WEST GERMANY
OFFICE OF RESEARCH AND DEVELOPMENT XDS/62 U.S. COAST GUARD WASHINGTON, D.C. 20591	PROF. DR. WALTER HANSEN DIREKTOR D. INSTITUTS F. MEERESKUNDE UNIVERSITAET HAMBURG HEIMHUEDERSTRASSE 71 D-2000 HAMBURG 13, WEST GERMANY
NATIONAL OCEANOGRAPHIC DATA CENTER X0764 ENVIRONMENTAL DATA SERVICES NOAA WASHINGTON, D. C. 20235	PROF. DR. KLAUS HASSELMANN INSTITUT F. GEOPHYSIK UNIVERSITAET HAMBURG SCHLUETERSTRASSE 22 D-2000 HAMBURG 13, WEST GERMANY
CENTRAL INTELLIGENCE AGENCY ATTENTION OCR/DO-PUBLICATIONS WASHINGTON, D. C. 20505	
DR. DONALD SWIFT MARINE GEOLOGY AND GEOPHYSICS LABORATORY AUMI - NOAA 15 RICKENHACKER CAUSEWAY MIAMI, FLORIDA 33149	

DR. JOHN T. KUD HENRY KRUMB SCHOOL OF MINES SEELEY W. MIDD BUILDING COLUMBIA UNIVERSITY NEW YORK, NEW YORK 10027	PROF. DR. NILS JERLOV INSTITUTE FOR PHYSICAL OCEANOGRAPHY KOBENHAVNS UNIVERSITET HARALDSGADE 6 DK-2200 KOBENHAVN, DENMARK
DR. EDWARD B. THORNTON DEPARTMENT OF OCEANOGRAPHY NAVAL POSTGRADUATE SCHOOL MONTEREY, CALIFORNIA 93940	DR. J. B. MATTHEWS COASTAL OCEANOGRAPHY GROUP BEDFORD INSTITUTE OF OCEANOGRAPHY DARTMOUTH, NOVA SCOTIA CANADA
PROF. C. A. M. KING DEPARTMENT OF GEOGRAPHY UNIVERSITY OF NOTTINGHAM NOTTINGHAM, ENGLAND	IR. H. J. SCHOFEMAKER WATERLOOPKUNDIG LABORATORIUM TE DELFT 61 RAAM, DELFT NETHERLANDS
DR. DOUGLAS L. INMAN SCRIPPS INSTITUTE OF OCEANOGRAPHY LA JOLLA, CALIFORNIA 92037	IR. M. W. VAN BATENBERG PHYSISCH LABORATORIUM TNO OUDE WAALSDORPER WEG 63, DEN HAAG NETHERLANDS
DR. DONN S. GORSLINE DEPARTMENT OF GEOLOGY UNIVERSITY OF SOUTHERN CALIFORNIA LOS ANGELES, CALIFORNIA 90007	MR. H. G. TORNATORE ITT AVIONICS 9140 OLD ANNAPOLIS ROAD COLUMBIA, MARYLAND 21043
DR. WILLIAM W. WOOD DEPARTMENT OF GEOSCIENCES PURDUE UNIVERSITY LAFAYETTE, INDIANA 47907	DR. ROBERT L. MILLER DEPARTMENT OF GEOPHYSICAL SCIENCES UNIVERSITY OF CHICAGO CHICAGO, ILLINOIS 60637
DR. ALAN W. NIEDORODA DIRECTOR, COASTAL RESEARCH CENTER UNIVERSITY OF MASSACHUSETTS AMHERST, MASSACHUSETTS 01002	COASTAL STUDIES INSTITUTE LOUISIANA STATE UNIVERSITY BATON ROUGE, LOUISIANA 70803
DR. RENNO M. BRENNINKMEYER, S. J. DEPT. OF GEOLOGY AND GEOPHYSICS BOSTON COLLEGE CHESTNUT HILL, MASSACHUSETTS 02167	DR. HERNARD LE MEHAUTE TETRA TECH, INC. 630 NORTH ROSEMEAD BOULEVARD PASADENA, CALIFORNIA 91107
DR. OMAR SHEMDIN JPL-CALTECH MAIL STOP 183-501 4800 OAK GROVE DRIVE PASADENA, CALIFORNIA 91103	DR. RICHARD A. DAVIS, JR. DEPARTMENT OF GEOLOGY UNIVERSITY OF SOUTH FLORIDA TAMPA, FLORIDA 33620
DR. LESTER A. GERHARDT RENNSELAER POLYTECHNIC INSTITUTE TROY, NEW YORK 12181	DR. WILLIAM T. FOX DEPARTMENT OF GEOLOGY WILLIAMS COLLEGE WILLIAMSTOWN, MASSACHUSETTS 01267
MR. FRED THOMSON ENVIRONMENTAL RESEARCH INSTITUTE P.O. BOX 618 ANN ARBOR, MICHIGAN 48107	DR. WILLIAM S. GAITHER DEAN, COLLEGE OF MARINE STUDIES ROBINSON HALL UNIVERSITY OF DELAWARE NEWARK, DELAWARE 19711

DR. J. A. DRACUP
ENVIRONMENTAL DYNAMICS, INC.
1609 WESTWOOD BOULEVARD, SUITE 202
LOS ANGELES, CALIFORNIA 90024

DR. THOMAS K. PEUCKER
SIMON FRASER UNIVERSITY
DEPARTMENT OF GEOGRAPHY
BURNABY 2, B. C., CANADA

DR. BRUCE HAYDEN
DEPARTMENT OF ENVIRONMENTAL SCIENCES

(14) TTR-141

SECURITY CLASSIFICATION OF THIS PAGE (When Data Entered)

REPORT DOCUMENTATION PAGE		READ INSTRUCTIONS BEFORE COMPLETING FORM
1. REPORT NUMBER [REDACTED]	2. GOVT ACCESSION NO. AD A087858	3. RECIPIENT'S CATALOG NUMBER
4. TITLE (and Subtitle) Coastal Storm Model.	5. TYPE OF REPORT & PERIOD COVERED Technical Report, No. 14 April 1976	6. PERFORMING ORG. REPORT NUMBER
7. AUTHOR(s) William T. Fox Richard A. Davis, Jr.	8. CONTRACT OR GRANT NUMBER(s) N00014-69-C-151	
9. PERFORMING ORGANIZATION NAME AND ADDRESS Williams College Williamstown, Massachusetts 01267	10. PROGRAM ELEMENT, PROJECT, TASK AREA & WORK UNIT NUMBERS 388-092	
11. CONTROLLING OFFICE NAME AND ADDRESS Geography Programs, Code 462 Office of Naval Reserach Arlington, VA 22217	12. REPORT DATE April 1976	13. NUMBER OF PAGES 122
14. MONITORING AGENCY NAME & ADDRESS (if different from Controlling Office) (12) 131	15. SECURITY CLASS. (of this report) Unclassified	15a. DECLASSIFICATION/DOWNGRADING SCHEDULE
16. DISTRIBUTION STATEMENT (of this Report) Unlimited		
17. DISTRIBUTION STATEMENT (of the abstract entered in Block 20, if different from Report)		
18. SUPPLEMENTARY NOTES		
19. KEY WORDS (Continue on reverse side if necessary and identify by block number) Computer simulation models Coastal storms Waves Beaches Longshore currents Fourier Analysis		
20. ABSTRACT (Continue on reverse side if necessary and identify by block number) A mathematical simulation model of a coastal storm has been programmed to forecast or hindcast wave and longshore current conditions at a coastal site. Storm parameters for the model are based on the size, shape intensity and path of the storm as derived from weather maps. An elliptical form is used to model the size and shape of the storm which are controlled by varying the length and orientation of the major and minor axes. Storm intensity is a function of the barometric pressure gradient which is modeled by an		

DD FORM 1 JAN 73 1473

EDITION OF 1 NOV 68 IS OBSOLETE
S/N 0102-014-6601

Unclassified

SECURITY CLASSIFICATION OF THIS PAGE (When Data Entered)

111111 2111

Unclassified

SECURITY CLASSIFICATION OF THIS PAGE(When Data Entered)

20. Abstract continued

inverted normal curve through the storm center. The storm path is based on actual storm positions for the hindcast mode, and on projected positions assuming constant speed and direction for the forecast mode. The location, shoreline orientation and nearshore bottom slope provide input data for each coastal site.

For each storm position, the geostrophic wind speed and direction are computed at the shore site as a function of barometric pressure gradient and latitude. The geostrophic wind is converted into surface wind speed and direction by applying corrections for frictional effects over land and sea. The surface wind speed, fetch and duration are used to compute the wave period, breaker height and breaker angle at the shore site. The longshore current velocity is computed as a function of wave period, breaker height and angle and nearshore bottom slope.

The model was tested by comparing hindcast output with observed data for several coastal locations. Forecasts were made for actual storms and for hypothetical circular and elliptical shaped storms.

Unclassified

SECURITY CLASSIFICATION OF THIS PAGE(When Data Entered)